BULLETIN

OF

The Geological Society of America

VOLUME 71 NUMBER 7

DETROIT PUBLIC LIBRARY
JUL 29 1960
TECHNOLOGY DEPARTMENT

July 1960

PUBLISHED MONTHLY BY THE SOCIETY

COUNCIL

President

HOLLIS D. HEDBERG, Princeton University, Princeton, N. J.

Past President

MARLAND P. BILLINGS, Cambridge, Massachusetts

Vice-President

THOMAS B. NOLAN, Washington, D. C.

Secretary

FREDERICK BETZ, JR., 419 West 117 Street, New York 27, N. Y.

Treasurer

J. EDWARD HOFFMEISTER, University of Rochester, Rochester 20, N. Y.

Councilors

(Term expires 1960)

H. H. HESS
Princeton, N. J.

HAROLD N. FISK
Houston, Texas

C. O. SWANSON
Trail, British Columbia, Canada

C. C. ALBRITTON, JR.
Dallas, Texas

(Term expires 1961)

JOHN C. FRYE
Urbana, Ill.

CHARLES F. PARK, JR.
Stanford, Calif.

ROBERT P. SHARP
Pasadena, Calif.

E. F. OSBORN
University Park, Pa.

(Term expires 1962)

NORMAN D. NEWELL
New York, N. Y.

GEORGE P. WOOLLARD
Madison, Wis.

VINCENT C. KELLEY
Albuquerque, N. M.

HAROLD L. JAMES
Menlo Park, Calif.

COMMITTEE ON PUBLICATIONS

LAUREN A. WRIGHT, *Chairman*
WILLIAM C. KRUMBEIN
E. N. GODDARD

Conferees

FREDERICK BETZ, JR., *Editor-in-Chief*
AGNES CREAGH, *Managing Editor*

MARCIA VAN METER, *Senior Editorial Assistant*
BARBARA FLYNN, *Junior Editorial Assistant*

MORGAN GUARANTY TRUST COMPANY OF NEW YORK
Bankers and Custodians

PRICE WATERHOUSE & COMPANY
Auditors

HUGH SATTERLEE
Counsel

Bulletin
of
The Geological Society of America

VOLUME 71 July 1960 NUMBER 7

CONTENTS

	Pages
Paleomagnetic observations in the United States: New evidence for polar wandering and continental drift. By D. W. Collinson and S. K. Runcorn	915–958
Wind direction in the western United States in the Late Paleozoic. By N. D. Opdyke and S. K. Runcorn	959–972
Classification of volcanic breccias. By Richard V. Fisher	973–982
Sediments of the Gulf of California. By John V. Byrne and K. O. Emery	983–1010
Chemical composition of sandstones. By G. V. Middleton	1011–1026
Petrology and structure of the Cockeysville formation (pre-Silurian) near Baltimore, Maryland. By Philip W. Choquette	1027–1052
Biogeochemical prospecting for manganese in northeast Tennessee. By F. Donald Bloss and Robert L. Steiner	1053–1066
Photographic study of some deep-sea floor environments in the eastern Pacific. By Carl J. Shipek	1067–1074
Models and methods for analysis of the mode of formation of fossil assemblages. By Ralph Gordon Johnson	1075–1086
Submarine topography in the Gulf of Alaska. By William M. Gibson	1087–1108
Short Notes	
Unusual structure associated with rock creep in the Black Hills, South Dakota. By James J. Norton and Jack A. Redden	1109–1112
Late Pleistocene marine terraces on Santa Rosa Island, California. By Phil C. Orr	1113–1120

Subscription $15.00 per year.

Printing Office: Mt. Royal & Guilford Aves., Baltimore 2, Md.

Communications for publications should be addressed to The Geological Society of America, Dr. Frederick Betz, Jr., Secretary, 419 West 117 Street, New York, N. Y.

Please give notice of change of address 4 weeks in advance. Claims for nonreceipt of the Bulletin of a given month must be sent to the Secretary of the Society before the end of the second succeeding month.

Second-class Postage paid at Baltimore, Md.
Accepted for mailing at special rate of postage provided for in Section 1103
Act of October 3, 1917, authorized on July 8, 1918.

PAPERS IN PRESS FOR FORTHCOMING ISSUES

TECTONOPHYSICAL INVESTIGATIONS. By V. V. Beloussov

ACOUSTIC-REFLECTION STUDIES OF THE CONTINENTAL SHELF AND SLOPE OFF SOUTHERN CALIFORNIA. By D. G. Moore

GRAVITY MEASUREMENTS ON THE SALMON GLACIER AND ADJOINING SNOW FIELD, BRITISH COLUMBIA, CANADA. By R. D. Russell, J. A. Jacobs, and F. S. Grant

EVOLUTION OF THE NEW HAMPSHIRE SHORE LINE. By Sherwood D. Tuttle

CORRELATION PROBLEMS OF WISCONSIN DRIFTS IN ILLINOIS, INDIANA, MICHIGAN, AND OHIO. By James H. Zumberge

GEOLOGY OF THE WABUSH LAKE AREA, SOUTHWESTERN LABRADOR AND EASTERN QUEBEC, CANADA. By Gordon Gastil and David M. Knowles

MORRISON, CLOVERLY, AND SYKES MOUNTAIN FORMATIONS, NORTHERN BIGHORN BASIN, WYOMING AND MONTANA. By Ralph Moberly, Jr.

CENOZOIC GEOLOGY IN THE VICINITY OF CARLIN, NEVADA. By Jerome Regnier

SPECTROGRAPHIC DETERMINATION OF TRACE ELEMENTS IN LAKE WATERS OF NORTHERN MAINE. By M. Dean Kleinkopf

MEMOIR IN PRESS

MORPHOLOGY, CLASSIFICATION, AND LIFE HABITS OF THE PRODUCTOIDEA (BRACHIOPODA). By Helen Muir-Wood and G. Arthur Cooper

Comprehensive revision of the Productoidea. Includes all genera described in the world literature, plus new families and genera, and their stratigraphic range and geographic distribution. New information and interpretations of shell structure and other features. The authors propose a new classification for Productoidea. Extensive bibliography and illustrations of almost all genera.

About 500 pages, 8 figures, 135 photographic collotype plates. Expected date of issue, September

Price will be about $10 for Fellows and Members of GSA and about $15 for all others.

TREATISE ON INVERTEBRATE PALEONTOLOGY

PART I—MOLLUSCA 1 (Chitons, Scaphopods, Gastropods) will be issued early in August.

Retail price:	Pre-Publication (before August 10)	$6.00
	Post-Publication	$7.00
Special price to GSA Fellows and Members		
	Pre-Publication (before August 10)	$5.00
	Post-Publication	$5.50

RECENTLY ISSUED MEMOIRS

(See back cover of this issue for further listings.)

77. RELATION OF ORE DEPOSITION TO DOMING IN THE NORTH AMERICAN CORDILLERA. By Edward Wisser. List price, $4.00. Special price to Fellows and Members of GSA, $2.50
78. MOLLUSCAN FAUNAS OF THE FLAGSTAFF FORMATION OF CENTRAL UTAH. By Aurèle La Rocque. List price, $4.50. Special price to Fellows and Members of GSA, $3.00
79. ROCK DEFORMATION. By David Griggs and John Handin, *Editors*. List price, $12.00. Special price to Fellows and Members of GSA, $7.50
80. STILLWATER IGNEOUS COMPLEX: A QUANTITATIVE MINERALOGICAL STUDY. By Harry H. Hess. List price, $5.50. Special price to Fellows and Members of GSA, $3.50

BULLETIN OF THE GEOLOGICAL SOCIETY OF AMERICA
VOL. 71, PP. 915-968, 27 FIGS. JULY 1960

POLAR WANDERING AND CONTINENTAL DRIFT: EVIDENCE FROM PALEOMAGNETIC OBSERVATIONS IN THE UNITED STATES

BY D. W. COLLINSON AND S. K. RUNCORN

ABSTRACT

Further studies of the paleomagnetic directions of red sandstones and siltstones of various geological ages in the United States are described. Usually the directions of magnetization of samples from a formation at one site are grouped symmetrically about a mean direction. From such a mean direction the position of the pole for that geological age can be calculated. There are, however, magnetically unstable formations in which the directions of magnetization are distributed approximately in the plane containing the present dipole field at the site and the original direction of the magnetic field. This planar distribution is the result of a superposition of a secondary magnetization on the original one. The former is thought to be a viscous or chemical magnetization acquired in the last 1,000–1,000,000 years.

Pole positions calculated from mean directions at different sites are consistent for the same formation and for different formations of the same geological age.

The study confirms the general trend of the polar-wandering curve for North America obtained by Runcorn (1956a), which lies around the northern Pacific Ocean: the pole being in the central tropical Pacific in late Precambrian time, moving across to the tropical western Pacific in the early Paleozoic and to Asia in the late Paleozoic and early Mesozoic. The data also show that the polar-wandering curve for North America is displaced westward relative to that for Europe, as Runcorn (1956b) showed, and provide an estimate for the amount of drift between the two continents since Mesozoic time, which is of the order of 30° in longitude.

CONTENTS

TEXT

	Page
Introduction	916
Acknowledgments	917
Statistical treatment of paleomagnetic directions	918
Conventions used throughout the paper	919
Precambrian formations	919
Lower Paleozoic formations	920
Upper Paleozoic formations	921
Triassic formations	922
Jurassic and Tertiary formations	922
Conclusions	923
Polar-wandering curves	923
Comparison with results of other workers	925
Evidence for continental drift	926
Evidence relating to reversals of the geomagnetic field	926
References cited	927

ILLUSTRATIONS

Figure	Page
1. Bass limestone (Precambrian)	932
2. Hakatai shales (Precambrian)	932
3. Shinumo quartzite (Precambrian)	933
4. Bonito Canyon quartzite (Precambrian)	933
5. Belt series (Precambrian)	934
6. Belt series (Precambrian)	934
7. Belt series (Precambrian)	935
8. Belt series (Precambrian)	935
9. Belt series (Precambrian)	936
10. Tapeats sandstone (Cambrian)	936
11. Bright Angel shale (Cambrian)	937
12. Lodore formation (Cambrian)	937
13. Juniata beds (Ordovician)	938
14. Deadwood formation (Mississippian)	938
15. Naco sandstone (Pennsylvanian)	939
16. Supai formation (Permian)	941
17. Moenkopi formation (Lower Triassic)	943
18. Chugwater formation (Triassic)	945
19. Mean directions of magnetization of Chugwater formation before dip correction	950
20. Mean directions of magnetization of Chugwater formation after dip correction	950
21. Newark group (Upper Triassic)	951
22. Chinle formation (Upper Triassic)	953
23. Kayenta formation (Lower Jurassic)	955
24. Carmel formation (Jurassic)	956
25. Duchesne River formation (Tertiary)	956
26. Pole positions and paths based on British and North American rocks	957
27. Pole positions for late Paleozoic and early Mesozoic times	958

Table	Page
1. Directions of magnetization, statistics, and pole positions	928
2. Longitudes of pole positions derived from European and American rocks of the same age	930
3. Calculated rate of polar wandering	930
4. Sequence of alternations of magnetization in Chugwater and Moenkopi formations	931

Introduction

In this paper we describe paleomagnetic observations on red beds of various geological ages in North America. This is an extension of the paleomagnetic survey described by Runcorn (1956a), in which it was established, by observations on rocks from Arizona and Utah, that the axis of the mean geomagnetic dipole (with which the axis of rotation is thought to coincide) has moved since the late Precambrian, along a roughly circular path around the northern half of the present Pacific Ocean at a rate of about ⅓° per million years. Runcorn (1956b) showed that there is a systematic difference between the polar-wandering paths inferred from American and British results, which is best interpreted by assuming that continental drift of North America westward relative to Europe took place in post-Triassic time. The considerably extended paleomagnetic survey reported in this paper supports these conclusions.

Samples of well-bedded, fine-grained red sandstones and siltstones were collected, mainly on the Colorado Plateau where no severe tectonic movements have occurred since the deposition of the sandstones. Apart from samples which fragmented during cutting or which were too weakly magnetized to be measured, the directions of magnetization of all the samples are recorded in the figures and tables of this paper. No experiments on modifying the observed magnetizations, *e.g.*, by demagnetization, are reported here, and the only correction made to the observations is that for the local geological dip at the site—the usual assumptions being made that the bedding planes were initially horizontal and that tectonic movements caused inappreciable rotation of the beds about the vertical. The measurements were carried out by the method described by Collinson, Creer, Irving and Runcorn (1957). With the astatic magnetometer used at Newcastle it has been possible to determine directions of magnetization of 10-cc specimens to accuracies within 1°–3° for intensities of magnetization as low as 3.10^{-7} emu/cc. Only about 30 discs from the whole collection had intensities too weak to be measured.

The theory of the sampling technique has been described by Runcorn (1957) and by Watson and Irving (1957), who show that a sufficiently accurate mean direction of magnetization of a rock formation (and therefore an accurate pole position) can be obtained by measurements on a comparatively small number of rock samples (10 to 20) provided these are well distributed stratigraphically. Consequently the normal procedure followed in making the collections was to sample at random intervals through the full thickness of a particular formation at one or more localities. The observed scatter of the directions of magnetization of a set of samples spanning a small fraction of a geological period is not usually greater than that to be expected from the geomagnetic secular variation (up to about 30° from the mean). Thus the random deviations between the directions of the field at the times of deposition and the present directions of magnetization of the corresponding samples may be assumed to be smaller, *i.e.*, only a few degrees. If the time spanned is of the order of a geological period, however, it is possible that superposed on the scatter due to the secular variation is that due to the movement of the axis of rotation, which may not be, over a span of a few million years, the smooth path inferred from the overall survey of the geological column. The scatter due to this cause could be of the order of 20°.

Runcorn (1956a) and Creer (1957) showed that the observations on red sandstones fall into two broad groups: (1) directions of magnetization symmetrically distributed around their mean, to which the statistical methods by Fisher (1953) may reasonably be applied, and (2) directions of magnetization scattered along a great circle through the direction of the present axial dipole field. This conclusion is again verified by the results reported in this paper. The simplest hypothesis to explain this result is to suppose that the directions of group (1) are coincident, apart from errors discussed in the previous paragraph, with the directions of the field at the time of deposition of the rock samples. It is reasonable to suppose that these rocks have been unaffected by the changing geomagnetic field since their original magnetization; they are therefore termed stable. On the other hand, group (2) appears to consist of rocks the magnetizations of which are the vector resultants of stable magnetizations acquired in the geomagnetic field at the time of deposition and secondary magnetizations acquired in the latter part of Cenozoic time in the present geomagnetic field. They are therefore termed partially stable rocks. Occasionally the effect of this secondary magnetization is so strong relative to the primary magnetization that no estimate of the latter is possible.

The directions of magnetization of lavas are

sometimes greatly scattered (Cox, 1957; Creer, 1958) but are still symmetrical about a mean direction, from which it may be inferred that the secondary magnetization acquired by them is randomly directed. For instance, a viscous magnetization acquired during the unoriented storage of specimens between collection and measurement would be a reasonable explanation of the effects. Demagnetization by alternating fields of the order of 100 gauss removes this secondary magnetization, and the directions of magnetization become much more closely grouped. In red sandstones and siltstones no such large but symmetrical dispersion of directions has been observed. The planar distribution must therefore arise from a comparatively stable secondary magnetization lying along the direction of the present dipole field. This could be a viscous magnetization with a longer time constant than that of the lavas—the red sandstones contain hematite grains, while the lavas contain magnetite.

There are, however, other processes by which some samples of the red sandstones might have acquired this secondary magnetization. The samples collected from outcrops will have been exposed at the surface for at least some thousands of years. During this time the following processes might have occurred:

(1) A component of thermo-remanent magnetization might have been acquired through the daily heating and cooling.

(2) Water from desert storms and the heat might have caused some of the hematite grains to form iron hydroxides and carbonates and thus to lose their original magnetization. These unstable compounds might eventually form hematite again, which would then become remagnetized by the process of "chemical magnetization". It is possible that this process could occur also through the circulation of ground water and consequently affect rocks at depth.

It appears that this secondary magnetization is more frequently observed in the Western United States than in Europe (*cf.* results given by Creer, Irving, and Runcorn 1957) and could therefore be the effect of the desert climate on surface outcrops. In any case, the secondary magnetization of the red sandstones must have been acquired when the rocks were *in situ* and since the beginning of the Pleistocene, when the geomagnetic field last acquired its present polarity.

At various times mechanisms have been suggested by which the directions of magnetization of a group of samples from a rock formation could have become systematically different from the corresponding directions of the geomagnetic field at the times of their formation. The preferential settling of elongated or discoidal iron-oxide grains either horizontally or in the direction of water currents is a bias which might be introduced at the time of formation of the rock. Irreversible changes of magnetization by the process of magnetostriction caused by stress due to tectonic activity or deep burial; "chemical magnetization" occurring through the gradual change of maghemite, a common constituent of the red soils which may go to form red beds, to hematite long after deposition of the beds; or a partial thermo-remanent magnetization due to the fall of temperature after deep burial are examples of biases which could occur at any time between the formation of the rock and the present. The change in the direction of magnetization resulting from recent fields, which was discussed in the previous paragraph, is the only one of such effects for which clear evidence exists.

A further factor must be considered: If an appreciable proportion of the magnetized grains are elongated along their direction of magnetization, compaction subsequent to the magnetization process appears capable of reducing the angle of inclination. If the magnetization of the sediment occurred during deposition through the alignment of the magnetized iron-oxide grains by the geomagnetic field, an appreciable error would result only if (1) the degree of compaction were larger than, say, 5 to 10 per cent, which would not be expected in a sandstone, although possibly in a shale; and (2) the iron-oxide particles were sufficiently large to interlock with the other grains. If, on the other hand, the heavy minerals were smaller than the other grains, which is usually true in sandstones, the magnetized particles would be free to rotate, especially if the sediment were water-logged. Thus it would appear that the geomagnetic field will retain the power to orient the magnetized grains until the final stages of compaction. On the other hand chemical magnetization will occur only after the bulk of the water is squeezed out from the pores of the sediment, *i.e.*, after compaction had been substantially completed. To examine whether such effects do, in fact, bias the determinations of the mean field directions, comparisons between different formations of the same age collected in different places is necessary.

ACKNOWLEDGMENTS

The field work was carried out during the summers of 1955 and 1956 in co-operation with

Dr. N. D. Opdyke, except for the Belt series which was sampled in the summer of 1957 with the help of Mr. H. R. Eisenbeis. The preparation of the rock specimens, coring, and cutting into discs was done by W. Rutherford, and the magnetic measurements and computation were made with the able assistance of A. Major, P. Dewell, and W. Rutherford in the Physics Department of King's College, Newcastle upon Tyne. This research was made possible by generous support from the Penrose Bequest of The Geological Society of America, from the Museum of Northern Arizona, Flagstaff, and from the Department of Scientific and Industrial Research, London.

We have been most fortunate in the help and advice which we have received from American geologists, particularly Mr. L. F. Brady, Dr. R. C. Gutschick, Dr. J. W. Harshbarger, Dr. J. F. Lance, and Dr. E. D. McKee.

We are grateful to the Superintendents of the Grand Canyon and Glacier National Parks for permission to collect rocks in the parks.

Statistical Treatment of Paleomagnetic Directions

The statistical methods used in this paper follow the treatment of Fisher (1953), who assumes that the population from which a sample of directions of magnetization is drawn is such that the probability of a direction making an angle between θ and $\theta+d\theta$ with the true direction is proportional to exp (κ cos θ).$d\theta$. Fisher shows that if each direction is represented by a unit vector the direction of the vector mean is the best estimate of the true direction. He also shows that a cone of confidence can be described about this mean direction which will contain the true direction at any assigned probability, the semi-angle α of the cone of confidence for a probability of 95 per cent being usually calculated. The parameter κ is a measure of the scatter, termed the precision, which is larger as the directions are more tightly grouped. For large κ the distribution becomes approximately Gaussian with a standard deviation in degrees equal to $88/\kappa^{\frac{1}{2}}$ (Runcorn, 1957).

It has been argued (*e.g.*, Blackett, 1956) that the application of such statistical methods to this subject gives an undue impression of accuracy. This point of view seems to rest on the following grounds: (1) The cone of confidence derived from the scatter of a set of observations does not include systematic errors, and it may be misleading to direct the attention of the reader to the random error in the mean direction when it may be smaller than the systematic error. (2) The analysis is based on the assumption that the directions are distributed with a frequency proportional to exp (κ cos θ), which implies assumptions about the physical cause of the scatter (Wilson, 1959). (3) Where small samples are used the divergence between the actual distribution and the theoretical one for an infinite population will be obvious by inspection.

We think that criticism (1) is mistaken because an exact statistical method is a powerful means of determining a systematic bias if one exists. This is carried out by comparing mean directions taken from two or more sets of results obtained from different localities in the same formation and testing whether the differences could arise from the finite number of samples used. The studies of the Chugwater formation in the different localities and the upper and lower parts of the Supai discussed in this paper are examples of this method of searching for systematic errors.

Objection (2) is not well founded. Runcorn (1956c) shows that if the three rectangular components of the magnetization of a series of rock samples are each distributed according to the Gauss-error function with the same standard deviations, then the directions of magnetization are distributed with a frequency proportional to exp(κ cos θ), assigning unit intensity to each sample. As the Gaussian distribution is approached where the errors are the result of a large number of independent errors, positive or negative, Fisher's distribution would appear to be appropriate to discuss the scatter of magnetization of samples, each containing a very large number of magnetized particles. Because the magnetization of the sample is weak there can be no interaction between the particles—all act independently. Further, as in Gaussian statistics, the calculations made prove to be rather insensitive to the exact form of the probability-distribution function.

Objection (3) might be raised to all modern statistical work which, having been developed largely for use in the nonphysical sciences, allows exactly for the effect of a small sample. There can be no merit in collecting larger and larger numbers of samples unless these are used effectively, *i.e.*, by an exact statistical method, and the size of the sample is simply determined by the accuracy required in the mean direction, which depends on the use to be made of the observations. The sample size used in this paper proves to be adequate in

view of the doubt which exists of the age relationships of the rocks examined.

Conventions Used Throughout The Paper

The directions of magnetization of discs cut from samples collected from a certain section of a rock formation are plotted on a stereographic projection. Points on the lower hemisphere of the projection, *i.e.*, representing directions with positive (downward) angles of inclination, are represented by full dots. Points on the upper hemispheres of the projection, *i.e.*, representing directions with negative (upward) angles of inclination, are represented by open circles. Directions from discs cut from the same core are connected together by a full line, and directions from cores from the same rock sample are connected by a broken line. The samples are numbered from the bottom of the section upward: missing numbers represent samples either too weakly magnetized to be measured or too fragile to be satisfactorily cut to shape.

The direction which the geomagnetic field would have at the site if the earth's field were that of a dipole orientated along the present geographical axis is plotted on each stereographic projection by a square (full for sites in the present northern hemisphere).

For each set of directions at one section, the mean direction is calculated and plotted as a star. From this calculation is omitted the occasional result which is erratically displaced from the main group. The center of the star is a dot if the direction has a positive angle of inclination and an open circle if the direction has a negative angle of inclination. Described around the mean point is the 95 per cent circle or cone of confidence of radius α. Samples from some formations in which the bedding planes were easily recognizable were cored so that the axes of the cores are perpendicular to these bedding planes. The declination and inclination of the magnetization of the discs cut from these cores were thus automatically corrected for tectonic dip. The mean directions of magnetization plotted for these formations therefore can be taken as estimates of the geomagnetic field at the times of deposition. This procedure is indicated by an asterisk in the column in Table 1 headed Geological Dip. In all other cases the points on the projections give the directions of magnetization in space today, *i.e.*, the plane of the projection is the horizontal at the site. The declination and inclination given in Table 1 is corrected for local geological dip, and this corrected mean is indicated on the stereograms by a full or open triangle, according to whether the inclination is positive or negative respectively.

Where secondary magnetization is appreciable, so that the distribution of directions of magnetization is planar, the primary direction must be estimated. A point on the great circle lying near the end of the planar distribution farthest from the present dipole field is indicated by a cross on the stereograms. If the strata are flat lying this is the estimate of the primary direction. Where the rock strata are tilted and the plane of projection is the present horizontal, the planar distribution passes through the present dipole field, and the direction indicated by a cross must be corrected in the usual way for the geological dip. This point, denoted by an open or full triangle, is then the estimated primary direction of magnetization.

In Table 1, S is the number of samples collected, N denotes the number of discs cut, and N' the number used in the statistics, R is the vector sum of these N' directions (each being assigned unit length), κ the precision, and D and I the angles of declination and inclination of the vector mean direction.

Unless otherwise stated the term "pole" is always used to mean the geographical pole or pole of rotation for the geological period under discussion.

Corresponding to the 95 per cent cone of confidence for a mean direction of magnetization is a 95 per cent oval of confidence for the corresponding pole positions. In Table 1 are given the semi axes ($d\psi$, $d\chi$) of this oval along and perpendicular respectively to the great circle joining the site to the pole position.

We now proceed to describe the measurements through the geological column (Table 1).

Precambrian Formations

In the Western United States upper Precambrian (Algonkian) unmetamorphosed red beds, which have been little affected by serious tectonic movements, are prominent in the Grand Canyon series and in the Belt series.

UNKAR GROUP OF THE GRAND CANYON SERIES (ALGONKIAN) (FIGS. 1-3): The lowest formation of this group, exposed in the Canyon of the Colorado River, is the Bass limestone, a brown limestone which proves to have sufficient remanent magnetization for measurement. This formation was sampled near the Kaibab Trail south of the Colorado River.

Lying conformably on the Bass limestone is

the Hakatai shale, a series of red shales, which was sampled north of the Colorado River 4.3 miles from Kaibab Bridge, just west of the Kaibab Trail, north of Phantom Ranch.

The Shinumo quartzite conformably overlies the Hakatai shale and is a hard compact fine-grained purplish quartzite. It was sampled near the Kaibab Trail south of the Colorado River.

The results show possible slight effects of recent secondary magnetization. Thus the original mean direction of magnetization of the Hakatai shale is likely to have had a more southerly declination and a smaller angle of inclination than the mean of the observed directions.

BONITO CANYON QUARTZITE (PRECAMBRIAN) (Fig. 4): The Bonito Canyon quartzite of Precambrian age was sampled east of Fort Defiance. Assuming it to have been deposited under water the well-marked ripple-marked surface was taken as the original horizontal. The quartzite rests unconformably below the Supai formation, and its age has been discussed recently by Lance (1959), who concludes that it is older than the Grand Canyon series.

BELT SERIES (ALGONKIAN) (Figs. 5-9): The Belt series consists of a thick series of limestones, red shales, and argillites (Clapp and Deiss, 1931) which crop out mainly in Montana, where the collections reported in this paper were made. An illitic shale from the Siyeh formation of this series has recently been satisfactorily dated at 750 million years by Goldich, Baadsgaard, Edwards, and Weaver (1959).

The lowest group of the Belt series sampled was the Ravalli group in Glacier National Park, in which the Appekunny formation and the overlying Grinnell formation can be sampled easily along the road west from St. Mary's. Above these lies the Siyeh limestone at the top of which is several hundred feet of sandy and shaly beds, mostly red, which are probably correlated with the much thicker Spokane formation of the Piegan group. These were sampled at McDonald Creek. The Spokane is fully exposed in Prickly Pear Canyon, north of Helena, where it was sampled along Highway 91.

The Missoula group, possibly correlating in part with the Piegan group farther east, was sampled near Missoula, where it rests conformably on the Wallace limestone. Lowest in the section is the Miller Peak formation which was sampled in Donovan Creek, off Highway 10, east of Missoula, Montana. Above it, possibly unconformably, lies the Hellgate formation, on which the McNamara formation rests conformably. This was sampled at McNamara's Landing on State Highway 20 in Blackfoot Canyon.

Lower Paleozoic Formations

Fine-grained and undisturbed red beds of Early Paleozoic age are rare in the Western United States, but the formations sampled are described.

TAPEATS SANDSTONES (CAMBRIAN) (Fig. 10): A few feet of red sandstones was found in the Tapeats sandstones in a creek bed south and west of Peach Springs, Arizona (Wood, 1956, Ph.D. Thesis, Univ. Arizona). The Tapeats sandstone can be traced almost continuously from this area northward along Peach Springs Draw to the Grand Canyon, where McKee (1945) studied the Cambrian rocks. The upper 100 feet of the Tapeats sandstone becomes finer-grained as the base of the overlying Bright Angel formation is approached, cross-bedding becomes less evident or absent, and beds of red or of yellowish-gray shaly siltstone, 6 inches to 2 feet thick, alternate with beds of light-brown to black sandstone of similar thickness. A few of the beds of the shaly siltstone are light greenish gray.

A Cambrian pole position, based on an incomplete preliminary examination of these results, was quoted by Day and Runcorn (1955) but was withdrawn in the survey of British and American paleomagnetic results by Creer, Irving, and Runcorn (1957).

BRIGHT ANGEL SHALE (CAMBRIAN) (Fig. 11): The Bright Angel shale of the Tonto group of Cambrian age of the Grand Canyon region, lying conformably below the Muav limestone and above the normally coarse-grained Tapeats sandstone, has been sampled in the Grand Wash cliffs near the Diamond Bar Ranch, Arizona, where it includes some red sandstones, as described by McKee (1945). Starting from the lower contact with the Tapeats sandstone 260 feet was sampled.

LODORE FORMATION (CAMBRIAN?) (Fig. 12): The Lodore formation was sampled along Highway 44 between Manila and Vernal, Utah, on the north flank of the Uinta Mountains, where the beds dip steeply beneath a massive Madison limestone exposure. Samples 12 and 13 are excluded from the statistical analysis. Although Williams (1953) gives the age of this formation as Cambrian, the basis for this appears to be lithological rather than paleontological.

These Cambrian results present an interesting example of secondary magnetization.

The meaning of directions of magnetization of the Bright Angel shale and the Tapeats sandstone becomes evident when they are considered in conjunction with the Lodore formation. Although the two former are considerably scattered, the directions lie roughly about the great circle between the present dipole field and the southwest group of directions of the Lodore formation, and appear to be the result of secondary magnetizations along the present field obscuring the original directions of magnetization.

JUNIATA RED BEDS (UPPER ORDOVICIAN) (FIG. 13): The Juniata red beds of Late Ordovician age were sampled on the Pennsylvania Turnpike 2.5 miles east of Bedford, Pennsylvania, where a highway cut exposes upper Ordovician and lower Silurian sandstones in the western limb of the Friend's Cove anticline. Cores were taken perpendicular to the bedding planes of the Juniata beds, which were overturned. This exposure is much faulted, and the unusually large scatter of the results may be caused by the complex stress pattern.

Comparing these early Paleozoic pole positions and the one obtained by Graham (1949) for the Silurian, it appears that they follow a smooth path in continuation with the late Precambrian path already described. However, it would seem to be more reasonable to postulate a very late Precambrian or at least a very early Cambrian age for the Lodore formation at this locality.

UPPER PALEOZOIC FORMATIONS

DEADWOOD FORMATION (CARBONIFEROUS-MISSISSIPPIAN?) (FIG. 14): The Deadwood formation in Wyoming is usually regarded as Cambrian in age. The outcrop of the upper part of this formation in the area 35 miles northeast of Rawlins, Wyoming, which consists of red-bed deposits, has been dated by Finnell (1951, Master's Thesis, Univ. Wyoming) as probably Mississippian, from the discovery of a fragment of a bone of a member of the family Cochliodontidae. The Madison limestone of Mississippian age lies conformably above the Deadwood formation in this area. Comparison of the paleomagnetic directions of this formation and those of the Supai formation support Finnell's suggestion of a late Paleozoic age for this formation in this particular area.

NACO LIMESTONE (CARBONIFEROUS-PENNSYLVANIAN) (FIG. 15): Sandstone layers in the Naco limestone were sampled in Fossil Creek near Pine, Arizona, at a locality described by Jackson (1952).

SUPAI FORMATION (PERMIAN) (FIG. 16): The Supai formation was sampled in Oak Creek Canyon, Arizona. The lower part (members B and C) was sampled on a butte 1 mile northwest of Sedona (Fig. 16 C). The upper part (member A) was sampled up to the Fort Apache limestone (samples 30–46) above Oak Creek bridge on the west side of the canyon, and above the Fort Apache limestone (samples 47–50) on a butte near the old road from Sedona to Flagstaff (Fig. 16 B).

The Supai formation was also sampled at Hunter's Point where it is tilted on the south flank of the Fort Defiance uplift (Fig. 16 A).

There seems to be some evidence that in the thickest formations studied, such as the Supai formation in Oak Creek Canyon, there is a systematic difference in magnetization between the upper and lower parts. This is clearly shown on Figures 16 B and 16 C. We do not know, as yet, the cause of changes of magnetization within one formation or between outcrops of the same formation in different localities. However, Runcorn (1957) argues that, because the sediments of a given formation at different sites cannot be exactly contemporaneous, the discrepancies found may result from motion of the pole of rotation during the time represented by the deposits. The average movement of the pole of rotation throughout geological time is about ½° per million years. It is not unreasonable to suppose that for short times the pole can move at a rate of 1° per million years. Consequently, polar movements of the order of 20° can take place in a part of one geological period. Thus the change of the mean direction of magnetization through a formation may arise from this cause. Other causes of discrepancy between the mean directions of magnetization of samples collected in different parts of a formation can be suggested, but at this stage we merely wish to point out that there is a possibility that these discrepancies may represent time differences. It is known that the Defiance uplift was a positive area in the late Paleozoic, and it seems reasonable to suggest that the Supai exposures at Hunter's Point are correlated with the upper rather than the lower Supai exposures in Oak Creek Canyon. Thus the agreement between the mean direction in Figures 16 A and B appears to support the above argument.

Triassic Formations

MOENKOPI FORMATION (EARLY AND MEDIAL TRIASSIC AGE) (FIG. 17): The Moenkopi formation of the Colorado Plateau consists of interfingered marine and continental beds. In Arizona and Utah the continental beds predominate; they consist of red claystones, siltstones, and sandstones, which accumulated on mud flats and deltas. The most recent monograph on this formation is by McKee (1954).

The Moenkopi was sampled at the following sites: (A) Capitol Reef National Monument, Utah; (B) Sand Canyon, Dinosaur National Monument, Colorado; (C) Split Mountain, Dinosaur National Monument, Colorado; (D) Vernal, Utah; (E) Poverty Tank, 5 miles west of Cameron, Arizona; (F) Echo cliffs, 8 miles south of the Navajo Bridge, Arizona (section 10 of Figure 5 and section 8 of Figure 6 respectively of the northwest-southeast series of sections of the Moenkopi formation given by McKee, 1954).

CHUGWATER FORMATION (TRIASSIC) (FIG. 18): This formation was sampled from the following sites in Wyoming: (A) Red Mountain, Albany County; (B) Rawlins, Carbon County; (C) east of Thermopolis, Hot Springs County; (D) north of Lander, Fremont County; (E) Dinwoody Lakes in Wind River Range, Fremont County; (F) Fort Washakie in Wind River Range, Fremont County; (G) a butte north of Shell, Big Horn County; (H) Sheep Mountain, north of Greybull, Bighorn County; (I) north of Alcova Reservoir, Natrona County; (J) Troublesome Creek, Carbon County.

For the sections where opposed directions of magnetization were found, the means of the two mean directions from the opposite groups were used to calculate the pole. This procedure should eliminate small components of secondary magnetization. Thus on the corresponding figures the great circle has been drawn through the present dipole field direction and this final mean axis, the circles terminating at the latter.

These results are in agreement with the angles of declination determined from seven bore-hole cores from the Chugwater formation near Speas dome and east of Alcova, which lay between 4° and 48° east of south. The orientation of the bore-hole cores was obtainable in this case because the beds dipped in a direction known from the general geological structure in the region. This information has been kindly made available by the Pan-American Oil Company of Tulsa, Oklahoma.

Figures 19 and 20 show the mean directions of magnetization of the various opposed groups of the Chugwater formation at the different localities before and after correction for local geological dip. It will observed that the points are better grouped after correction. This, of course, is an argument in favor of the hypothesis that, apart from a small component of viscous magnetization along the present dipole field, the magnetization is an original one. In many cases the circles of confidence do not overlap. There is therefore some suggestion of systematic difference between the directions of magnetization of the Chugwater formation at different localities which, as in the case of the Supai formation discussed above, could result from age differences between the sections.

NEWARK GROUP (UPPER TRIASSIC) (FIG. 21): An exposure of the basal Brunswick formation of the Newark series of the Triassic red beds of eastern North America (McLaughlin, 1950) was sampled in the Delaware River valley south of Frenchtown, New Jersey. These results have been discussed by Du Bois, Irving, Opdyke, Runcorn, and Banks (1957).

CHINLE FORMATION (UPPER TRIASSIC) (FIG. 22): The Chinle formation of Late Triassic age described by Harshbarger, Repenning, and Irwin (1957) was sampled in the Moab area and in the Colorado National Monument at the following sites: (A) Colorado National Monument, (B) Colorado National Monument, (C) along the highway north of Moab, (D) east of Moab on the south side of the Colorado River. It will be seen that the results at sites A and B are more consistent with a Jurassic than with a Triassic age.

Jurassic and Tertiary Formations

In these formations directions of magnetization are found which are little different from those of the present dipole field.

KAYENTA FORMATION (LOWER JURASSIC) (FIG. 23): The Kayenta formation has been described by Harshbarger, Repenning, and Irwin (1957). Collections were made at the following sites: (A) East of Kanab, Arizona; (B) in the Navajo National Monument, Arizona; (C) in the Echo Cliffs at the Gap, Arizona; (D) the type locality north of Kayenta, Arizona.

CARMEL FORMATION (JURASSIC) (FIG. 24): The Carmel formation was sampled south of Moab, Utah.

TERTIARY RED BEDS IN UTAH (FIG. 25): Tertiary red beds in the Duchesne River formation were sampled near Roosevelt, Utah. A few samples of gray marine sandstones of Pliocene age from the eastern Los Angeles basin, California, were measured. The local geological dip of the beds was between 45° and 55°. Their directions of magnetization in space at the present time were found to be close to that of the present geomagnetic field. (The mean was N. 17° W. + 51°; *cf.* present dipole field N. 0° + 53°.) These rocks were probably tilted in the last million years, so that these sandstones have a negligible stable component of magnetization. Gray, white, and green sandstones often seem to have a weak and unstable magnetization in contrast to the red sandstones on which paleomagnetic surveys have usually been based. Miller and Folk (1955) have noticed that red sandstones show a relative abundance of iron oxide compared to white, gray, and green sandstones. This fact alone probably accounts for the much stronger magnetization found in red sandstones. The greater stability of the magnetization of the red sandstones is probably due to the presence of hematite which has a much higher coercive force than does the magnetite present in the white, gray, and green sandstones.

CONCLUSIONS

Polar-Wandering Curves

Figures 26 and 27 show the positions of the poles calculated by the authors quoted above, by Runcorn (1956a), and from the data presented in this paper. Where it is clear that the distribution is substantially free from secondary magnetization, a pole position is calculated directly from the vector mean direction. The presence of secondary magnetization obscures the original directions of magnetization to a varying degree. However, even if the secondary magnetization has an extremely important effect, as in the Chinle formation, the great circles for rocks of the same age coincide. Runcorn (1956b) shows that for flat-lying rocks it is possible to determine exactly from the position of the great circle the longitude of the pole position at that geological time. Its latitude, however, in the absence of an experimental method of removing the secondary magnetization, may only be roughly estimated. Whether the rock strata are flat lying or not, an estimated pole is calculated: if flat lying, from the point on the great circle near the end of the distribution farthest from the present dipole field, indicated by a cross on the stereograms; if tilted, from this estimated direction after correction for geological dip, indicated by a triangle on the stereograms. The corresponding pole position is then plotted.

Figure 26 gives the mean pole positions for different formations except that the Hakatai shale poles for the two different sites are plotted. It also shows that the poles from successively older geological periods, with the exception of the Mississippian poles, lie progressively farther from the present pole along a reasonably smooth path. We consider this to be a most significant fact, from which the inference may be drawn that the paleomagnetic directions record a phenomenon which changes gradually with geological time. It is therefore more reasonable to explain it primarily by a geophysical change affecting the earth as a whole rather than by the local geological and mineralogical processes, which were discussed in the introduction to this paper. It is therefore concluded that the major part of the magnetization of these red beds was acquired parallel to the geomagnetic field about the time of their deposition.

The pole positions of the upper Precambrian formations are grouped together near the equator in the central Pacific (Fig. 26). There is some evidence that they are spread in the overall direction of the polar-wandering curve, and the differences could reflect the long period of time represented by these rocks. The age of the Siyeh formation quoted above indicates that this period could be 100-200 million years, and, if the overall rate of polar wandering is taken as about 0.3° per million years, then the observed spread in the pole positions is explicable. The inference that the Grand Canyon series and the Belt series are contemporaneous is in agreement with the conclusions of geologists who have studied these formations. The considerable divergence between the pole positions determined by Runcorn (1956a) and Doell (1955) for the Hakatai shales on the south side of the Colorado River, which are in good agreement, and those determined in this paper for the other formations in the Grand Canyon series at the same site and the Hakatai shales on the north side of the Colorado River is puzzling. The discrepancy in latitude can be reduced by assuming a component of secondary magnetization. If this were allowed for, the north magnetic pole would be moved southward (Runcorn, 1956b).

The directions of magnetization of samples from the Grinnell formation (Fig. 6) and the Spokane formation from Prickly Pear Canyon (Fig. 8) are distributed with a slight spread in the direction of the present dipole field. This suggests that their vector means require a small correction for secondary magnetization in the latter direction. In Figure 26 arrows are drawn from pole positions A.6 and A.8, calculated from the vector mean directions in Figure 6 and Figure 8, respectively, to pole positions, corrected by the usual method for these effects. All the late Precambrian pole positions then come very close together, except for the Hakatai shales on the south rim of the Canyon.

Figure 26 shows that the poles for the Belt series and for the Grand Canyon series lie on the polar-wandering curve in order of their stratigraphical positions, except for that of the McNamara formation (pole A.9b), which, stratigraphically, is the youngest of the Belt rocks and might, therefore, be expected to lie west of the other poles instead of to the east. The question of whether the sampled section of this formation is really older than the sampled sections of the other formations of the Belt series in spite of its apparent stratigraphic position or whether in fact the pole moved back on its path during these times must be left open. The similar anomaly of pole A.7 is not, perhaps, of significance in view of the small number of samples available.

The Bonito Canyon quartzite has a pole near those of the Belt and Grand Canyon series. This result is therefore evidence against the older Precambrian age that Lance (1959) suggests, unless the Bonito Canyon quartzite acquired its present magnetization long after its formation, possibly as a result of slight metamorphism. Allowance for a possible small component of secondary magnetization would move the south magnetic pole computed for this formation (which is the pole plotted on Fig. 26) northward, closer to the main group of the late Precambrian poles.

So far it has been assumed that the directions of magnetization of a series of samples taken from a certain rock series are scattered randomly about a mean direction, which corresponds to a definite pole position. It is necessary now to consider what modification arises if the rock series spans a sufficient time for a small motion of the pole to take place, which to a first approximation can be regarded as occurring along an element of a great circle. Suppose we now assume that a number of sets of samples are collected from the rock series, but that each set is differently distributed in time. If the number of measurements in each set is sufficient to reduce to negligible amounts the effect of the random scatter on the mean directions from each set of samples, then the pole positions calculated from the mean directions will not coincide but will be scattered along the path of the pole during the time considered. In the sampling of a rock series cropping out in different places, it is inevitable that collections of samples from different localities will be weighted differently with respect to the time spanned by the whole rock series. But it is clear that the mean pole position determined from the pole positions calculated from the different localities will tend to approximate the pole position corresponding to the mean of the time interval covered by the entire rock formation.

Figure 27 shows the pole positions determined by the authors quoted above, by Runcorn (1956a), and in this paper from the various localities for the Carboniferous, Permian, and Triassic. The scatter of the Triassic poles appears to be slightly greater in the general direction of the polar movement and may possibly be partly due to time differences between the various sections. Pole positions for the two Chinle localities A and B are not shown because they lie close to the present pole.

In this paper the circles of confidence of the mean directions of magnetization have been calculated giving each disc unit weight. Whether this is entirely desirable depends on which of the possible causes of dispersion of directions of magnetization is most important in a particular set of observations. Dispersion due to the geomagnetic secular variation is likely to be present in most of the collections discussed in this paper, for Runcorn (1957) has shown, by order-of-magnitude arguments, that discs of sandstone were deposited in times short compared with the time scale of the geomagnetic secular variation. However, this is unlikely to be true in limestones in which the rate of deposition may be comparable with that of ocean sediments, *i.e.*. 1 mm/1000 years. Confirmation of this is given by the directions of magnetization of the Bass limestone (Fig. 1). They are slightly distributed along a great circle due to secondary magnetization along the present dipole field, but they are, however, scattered through only a few degrees perpendicular to the great circle.

The errors of collection, cutting, and measurement are of the order of 1°–3°. Consequently, it appears that in the limestone the geomagnetic secular variation is smoothed out even in a single disc.

Therefore unless many pairs of sandstone discs are exactly contemporaneous (to within a few years) the procedure followed in calculating the circles of confidence of the mean direction of magnetization and the ovals of confidence of the pole positions appears to be realistic.

The polar-wandering path from North American rocks given by Runcorn (1956a) and the one which we suggest on the basis of the new information do not differ significantly. The one determined from the data in this paper lies farther south in the early Paleozoic and Precambrian.

It is interesting to determine from Figure 26 the rate of polar movement relative to North America. Table 3 gives the angular distance between successive poles, the approximate time interval between them, using the time scale given by Holmes (1944, p. 105), and the calculated rate of polar movement. The rate is roughly constant, the mean rate being about 0.3° per million years in agreement with that given by Creer, Irving, and Runcorn (1957).

Comparisons with Results of Other Workers

The results described in this paper are consistent with those obtained by most other workers.

Howell and Martinez (1956; 1957) sampled concretions in the Barnett formation of Mississippian age in the Llano uplift in Texas. From seven localities with southeast magnetization and one locality with a northwest magnetization they estimated the pole positions at 41° N., 128° E., and 42° N., 142° E. respectively. From the Point Peak member of the Wilberns formation in the same area Howell and Martinez (1957) also obtained a Cambrian pole position at 0° N., 158° E. In each of these formations secondary magnetizations were found, and the quoted results roughly allow for this. These results agree quite well with those given by Runcorn (1956a) and in this paper.

Doell (1955) sampled all the major sedimentary formations of the Grand Canyon but found that only the Hakatai shales and Supai shales are strongly and consistently magnetized. For the Hakatai shales it is necessary to allow for the small local geological dip (Creer, Irving, and Runcorn, 1957). Doell's Algonkian pole position is at 13° N., 127° W., and his Permian pole at 39° N., 115° E., which agree reasonably well with those given by Runcorn (1956a)—31° N., 150° W., and 26° N., 121° E. respectively, from nearly the same sites. Doell states that his Precambrian results were badly scattered, the angle of the circle of confidence being 18°. The Supai results obtained by Runcorn (1956a) show some effect of secondary magnetization, but the pole position given was not corrected to allow for this, *i.e.*, it was simply computed from the vector mean direction. If rough allowance is made for this the direction of magnetization is given by D = S. 40° E. and I = +12°, corresponding to a pole position at 33° N., 120° E.

Du Bois (1957) has determined poles for the Keweenawan rocks around Lake Superior. Those for the Freda and Nonesuch shales, the magnetic stability of which can be demonstrated, and the Jacobsville sandstone (9°N. 169°E., 14°S. 170°W., respectively) fall close to the main group of the Grand Canyon series. The poles for the Portage Lake and Copper Harbor formation (25°N. 170°W., and 30°N 176°E., respectively) are also in rough agreement with the results of this paper on the Precambrian but are closer in longitude than in latitude. However, the pole of the Chequamegon (69°S. 133°E.), which is the stratigraphically highest formation in the Keweenawan series, has such a high latitude that it is possible that it has a high degree of secondary magnetization.

Thus, apart from some instances of secondary magnetization along the present dipole field direction, the mean directions of magnetization of red sandstones of the same geological age from different sites give concordant results; the discrepancies are of the order which could result from differences in age. This result conflicts with the conclusion implied by some results of Kintzinger (1957), who determined the magnetization of samples of the Moenkopi and the Dinosaur Canyon member of the Moenave formation near Marble Canyon, Arizona. He found a direction of magnetization for the Moenkopi of D = N. 35° W. and I = +35° in reasonable accord with the results given above. Runcorn (1956a) gives a determination of the direction of magnetization of the Moenkopi formation which is significantly different from those of this paper and from Kintzinger's determination, but he stated that the great scatter and the inhomogeneous

character of the particular strata sampled made the determination of dubious accuracy. However, Kintzinger's results on the Dinosaur Canyon member and those of Graham (1955) on the Chinle from New Mexico, which he quotes, give a declination well to the east of north with a positive angle of inclination, for which there is no parallel in Triassic rocks of the Western United States. The cause of this anomaly is not known, although these results of Kintzinger and Graham are based on very few samples.

Evidence for Continental Drift

Runcorn (1956b) shows that the polar-wandering path calculated from North American results lies to the west of that calculated from Europe. This conclusion is confirmed by the results of this paper (Fig. 26).

He argued that the discrepancy between the polar-wandering paths for North America and Europe could not be explained as a systematic difference in the amount of secondary magnetization in the British and American rocks, because this component would not affect the longitude of the pole positions, and therefore a relative shift of North America westward of about 24° with respect to Europe since Mesozoic time was postulated. Table 2 shows that the differences of longitude between the British and American poles, calculated from the results in this paper, are greater than the 24° determined from the earlier data by Runcorn (1956b) and closer to that suggested by Du Bois (1957). If, prior to middle Mesozoic time, the continents of Europe and North America were very much nearer and possibly in contact the discrepancy between the two polar-wandering paths would be negligible. But these paths are similar in shape only to a first approximation. In particular the kinks in both curves at the end of the Paleozoic seem real and may be associated with the beginning of the postulated continental displacement of North America westward relative to Europe. To infer, in detail, the relative movements of the two continents through geological time we must await more detailed paleomagnetic surveys in each continent. Even then the fact that three angles are required to specify the position of a continent relative to the earth's axis at any time, whereas paleomagnetic observations supply only two, gives rise to an indeterminacy that must be resolved by geological considerations.

Evidence Relating to Reversals of the Geomagnetic Field

The following explanations of the opposed directions of magnetization found in many formations have been suggested:

(1) At irregular intervals in the earth's history, of the order of millions of years, the geomagnetic field reversed its polarity as a result of changes in the magnetohydrodynamic interactions in the fluid core of the earth. The actual reversal of the field would occupy a short time (of the order of thousands of years), and during this interval the axial symmetry of the field about the earth's axis of rotation would be lost.

(2) Because of the complex mineralogy of the iron oxides they contain, certain rocks have the property of becoming magnetized antiparallel to the geomagnetic field at the time of their formation.

Were the alternations between opposed directions of magnetization sufficiently well spread in the geological column, it would be a simple matter to test whether or not reversals of the geomagnetic field have really occurred by correlation over large distances, for if (2) happens frequently we should not find the same sign of magnetization at different places in rocks of the same age. The following considerations from the present study are relevant to this discussion:

(1) So far extensive measurements of rocks of Permian age in North America and Europe have given magnetization of one sign only (positive, *i.e.*, the south magnetic pole near Asia on the convention of Creer, Irving, and Runcorn).

(2) In Triassic time both European and American rocks show more than one reversal of magnetization. Table 4 shows the sequence of reversals of magnetization at the various sites of the Chugwater and Moenkopi formations. The western exposures of the Chugwater formation in Wyoming all show three or four zones of opposed magnetization which may correspond. On the other hand each of the eastern and northern exposures shows only one zone, in each case positive (except for the single negative sample at Shell). This suggests that the time spanned by the western exposures is longer than that by the eastern exposures. Red Mountain section in the south was among the most extensively sampled sections and shows four zones. The Utah exposures of the Moenkopi formation are all of positive sign,

except for the single uppermost sample in Sand Canyon, and the Arizona exposures show three or four successive reversals. Thus it can be concluded that closely related sections which are likely to cover similar time intervals show the same number of alternations of magnetization.

This evidence from rather widely scattered localities appears to us to be easier to reconcile with explanation (1) than with (2).

References Cited

Blackett, P. M. S., 1956, Lectures on rock magnetism: Jerusalem, Weizmann Science Press, 131 p.

Clapp, C. H., and Deiss, C. F., 1931, Correlation of Montana Algonkian formations: Geol. Soc. America Bull., v. 42, p. 673–696

Collinson, D. W., Creer, K. M., Irving, E., and Runcorn, S. K., 1957, The measurement of the permanent magnetization of rocks: Royal Soc. Philos. Trans. A, v. 250, p. 73–82

Cox, A., 1957, Remanent magnetization of lower to middle Eocene basalt flows from Oregon: Nature, v. 179, p. 685–686

Creer, K. M., 1957. The remanent magnetization of

Page 927, column 1, Creer 1958 reference, *for* South Africa, *read* South America

[illegible] Preliminary paleomagnetic measurements from South Africa: Ann. de Geophys., v. 14, p. 373–390

Creer, K. M., Irving, E. and Runcorn, S. K., 1957, Geophysical interpretation of paleomagnetic directions from Great Britain: Royal Soc. Philos. Trans. A, v. 250, p. 144–156

Day, A. A., and Runcorn, S. K., 1955, Polar Wandering—some geological, dynamical and paleomagnetic aspects: Nature, v. 176, p. 422–426

Doell, R. R., 1955, Paleomagnetic study of rocks from the Grand Canyon of the Colorado River: Nature v. 176, p. 1167

Du Bois, P. M., 1957, Comparison of paleomagnetic results for selected rocks of Great Britain and North America: Adv. in Physics, v. 6, p. 177–186

Du Bois, P. M., Irving, E., Opdyke, N. D., Runcorn, S. K., and Banks, M. R., 1957, The geomagnetic field in Upper Triassic times in the United States: Nature, v. 180, p. 1186–1187

Fisher, R. A., 1953, Dispersion on a sphere: Royal Soc. Philos. Proc. A, v. 217, p. 295

Goldich, S. S., Baadsgaard, H., Edwards, G. and Weaver, C. E., 1959, Investigations in radioactivity—dating of sediments: Am. Assoc. Petroleum Geologists Bull. v. 43, p. 654–662.

Graham, J. W., 1949, The stability and significance of magnetism in sedimentary rocks; Jour. Geophys. Research, v. 54, p. 131–167

——1955, Evidence of polar shift since Triassic times: Jour. Geophys. Research, v. 60, p. 329–347

Harshbarger, J. W., Repenning, C. A. and Irwin, J. H., 1957, Stratigraphy of the uppermost Triassic and the Jurassic rocks of the Navajo Country: U. S. Geol. Survey Prof. Paper 291

Holmes, A., 1944, Principles of physical geology: London, Nelson, 532 p.

Howell, L. G., and Martinez, J. D., 1956, Paleomagnetism of chemical sediments: Nature, v. 178, p. 204

——1957, Polar wandering as indicated by rock magnetism: Geophysics, v. 22, p. 384–397

Jackson, R. L., 1952, Pennsylvanian-Permian facies of the Supai formation in central Arizona: Ariz. Geol. Soc. Guidebook, S. Arizona Excursion

Kintzinger, P. R., 1957, Paleomagnetic survey of Triassic rocks from Arizona: Geol. Soc. America Bull., v. 68, p. 931–932

Lance, J. F., 1959, Precambrian rocks of northern Arizona: New Mexico Geol. Soc. 9th Field Conf. Handbook, p. 66–70

McKee, E. D., 1945, Cambrian history of the Grand Canyon region: Carnegie Inst. Washington Pub. 563, pt I

——1954, Stratigraphy and history of the Moenkopi formation of Triassic age: Geol. Soc. America Mem. 61, 133 p.

Miller, D. N., and Folk, R. L., 1955, Occurrence of detrital magnetite and ilmenite in red sedi[illegible]ice of red gists Bull., v. 39, p. 338–345

McLaughlin, D. B., 1950, A suggested correlation of Triassic areas of the eastern United States: Pa. Acad. Sci. Proc., v. 24, p. 161–169

Nairn, A. E. M., 1960, Paleomagnetic results from Europe: Jour. Geology, v. 68, p. 285–306

Runcorn, S. K., 1956a, Paleomagnetic survey in Arizona and Utah; Preliminary results: Geol. Soc. America Bull., v. 67, p. 301–316

——1956b, Paleomagnetic comparisons between Europe and North America: Geol. Assoc. Canada Proc., v. 8, p. 77–85

——1956c, Field observations of rock magnetism: Intern. Geol. Cong. Proc., Mexico City

——1957, The sampling of rocks for paleomagnetic comparison between the continents: Adv. in Physics, v. 6, p. 169–176

Watson, G. S., and Irving, E., 1957, Statistical methods in rock magnetism: Royal Astron. Soc., Mon. Not. Geophys. Suppl., v. 7, p. 290–299

Williams, N. C., 1953, Late Precambian and early Paleozoic geology of Western Uinta Mountains, Utah: Am. Assoc. Petroleum Geologists Bull., v. 37, p. 2734–2742

Wilson, R. L., 1959, Remanent magnetism of late Secondary and early Tertiary British rocks: Philos. Mag., v. 4, p. 750–755

Museum of Northern Arizona, Flagstaff, Arizona, and the Department of Physics, King's College, Newcastle upon Tyne, England

Manuscript Received by the Secretary of the Society, August 15, 1958

TABLE 1.—DIRECTIONS OF MAGNETIZATION, STATISTICS, AND POLE POSITIONS

Fig. No.	Formation	Geol. Age	Locality	Township and Range	Lat.	Long.	Thickness sampled (ft.)	Geol. Dip		S	N	N'	R	D	I	α	κ	Pole position		$d\psi$	$d\chi$
								Str.	Dip									Lat.	Long.		
25	Duchesne River	T	Roosevelt	S22, T. 6 S., R. 1 W.	40° N.	110° W.	50	—	—	24	85	85	78.9	N. 2° E.	+65°	5°	13.8	83° N.	99° W.	6°	8°
24	Carmel	J	Moab	S22, T. 27 S., R. 22 E.	39° N.	109° W.	50	—	—	9	31	31	28.0	N. 11° W.	+63°	9°	10.0	80° N.	160° W.	11°	14°
23 (A)	Kayenta	J	Kanab	S33, T. 43 S., R. 7 W.	37° N.	113° W.	100	—	—	10	39	33	30.15	N. 4° E.	+53°	9°	11.6	85° N.	23° E.	9°	13°
23 (B)	Kayenta	J	Navajo Nat. Mon.	S20, T. 38 N., R. 14 E.	37° N.	111° W.	200	—	—	7	27	27	23.2	N. 25° W.	+50°	11°	6.9	—	—	—	—
23 (C)	Kayenta	J	Echo Cliffs	S32, T. 34 N., R. 9 E.	37° N.	112° W.	140	—	—	14	43	43	40.8	N. 14° E.	+43°	6°	13.7	73° N.	19° E.	5°	7°
23 (D)	Kayenta	J	Kayenta	S2, T. 38 N., R. 19 E.	37° N.	110° W.	50	N. 49° E.	16° S.	8	43	43	38.9	N. 20° E.	+50°	6°	13.5	72° N.	6° W.	6°	8°
22 (B)	Chinle	Tr	Colorado Nat. Mon.		39° N.	109° W.	50	N. 60° W.	3° NE.	7	31	31	28.79	N. 34° E.	+60°	7°	13.6	—	—	—	—
22 (A)	Chinle	Tr	Colorado Nat. Mon.		39° N.	109° W.	100	—	—	6	29	29	27.96	N. 4° W.	+66°	5°	25.4	—	—	—	—
22 (D)	Chinle	Tr	Moab	S20, T. 25 S., R. 22 W.	39° N.	109° W.	140	—	—	10	60	60	20.48	N. 59° E. S. 20° E.	+73° −10°	—	—	48° S. 50° N.	114° E. 114° E.	—	—
22 (C)	Chinle	Tr	Moab	S20, T. 25 S., R. 22 W.	39° N.	109° W.	220	N. 46° W.	20° SW.	14	39	39	25.56	S. 20° E. S. 24° E.	+44° −7°	—	—	23° S. 49° N.	90° E. 109° E.	—	—
21	Newark	Tr	Frenchtown		41° N	75° W	100	N. 45° E.	10° NW.*	20	78	70	69.19	N 6° E	+28°	3°	86.3	64° N	92° E.	2°	3°
18 (A)	Chugwater	Tr	Red Mtn.	S15, T. 12 N., R. 76 W.	41° N.	106° W.	160	N. 73° E.	13° S.	18	75	16	15.48	N. 25° W.	+15°	6°	30.0	47° N.	116° E.	3°	5°
												52	47.72	S. 29° E.	−6°	6°	11.7				
18 (B)	Chugwater	Tr	Rawlins	S22, T. 23 N., R. 88 W.	42° N.	107° W.	90	N. 66° W.	8° NE.	9	33	12	11.75	N. 32° W.	+12°	4°	43.1	46° N.	121° E.	3°	5°
												21	20.22	S. 31° E.	−19°	6°	25.3				
18 (C)	Chugwater	Tr	Thermopolis	S21, T. 42 N., R. 94 W.	44° N.	108° W.	400	N. 75° W.	10° NE.	6	33	18	17.68	N. 28° W.	+16°	5°	56.0	52° N.	103° E.	4°	7°
												15	13.94	S. 10° E.	−19°	11°	13.2				
18 (D)	Chugwater	Tr	Lander	S4, T. 31 N., R. 99 W.	43° N.	109° W.	320	N. 43° W.	18° NE.	10	49	12	11.89	N. 16° W.	+27°	4°	55.0	47° N.	100° E.	4°	8°
												37	32.34	S. 23° E.	+15°	9°	7.7				
18 (E)	Chugwater	Tr	Dinwoody Lakes	S24, T. 5 N., R. 6 W.	43° N.	109° W.	220	N. 45° W.	15° NE.	10	42	20	19.37	N. 21° W.	+25°	6°	30.2	52° N.	111° E.	3°	5°
												22	20.76	S. 26° E.	−20°	7°	17.0				
18 (F)	Chugwater	Tr	Fort Washakie	S26, T. 15, R. 2 W.	43° N.	109° W.	120	N. 39° W.	11° NE.	11	53	25	23.94	N. 14° W.	+14°	6°	22.5	44° N.	105° E.	3°	5°
												28	27.20	S. 34° E.	+6°	5°	33.6				
18 (G)	Chugwater	Tr	Shell	S24, T. 53 N., R. 90 W.	45° N.	108° W.	100	—	—	5	21	5	—	N. 20° W.	+36°	—	—	—	—		
												16	14.99	S. 25° E.	−23°	7°	16.0	56° N.	113° E.	4°	8°
18 (H)	Chugwater	Tr	Sheep Mtn.	S2, T. 53 N., R. 94 W.	45° N.	108° W.	70	N. 52° W.	20° SW.	9	38	35	33.43	S. 32° E.	−6°	3°	58.0	40° N.	115° E.	2°	3°
18 (I)	Chugwater	Tr	Alcova Res'vr.	S14, T. 30 N., R. 83 W.	43° N.	107° W.	90	N. 36° W.	11° E.	10	48	48	34.2	S. 28° E.	−18°	8°	9.75	49° N.	118° E.	4°	8°
18 (J)	Chugwater	Tr	Troublesome Creek	S20, T. 25 N., R. 81 W.	42° N.	107° W.	90	N. 68° E.	28° S.	9	43	43	38.71	S. 46° E.	−12°	7°	10.0	36° N.	135° E.	4°	7°
17 (A)	Moenkopi	Tr	Capitol Reef	S16, T. 29 N., R. 6 E.	38° N.	111° W.	70	—	—	10	39	39	30.65	S. 41° E.	+24°	—	—	26° N.	114° E.	—	—
														S. 29° E.	−6°			46° N.	114° E.		
17 (B)	Moenkopi	Tr	Sand Canyon	S19, T. 15, R. 7 E.	40° N.	109° W.	100	—	—	8	30	27	24.48	S. 33° E.	−7°	9°	10.5	43° N.	118° E.	5°	9°

*Reversed

17 (A)	Moenkopi	T_R	Capitol Reef	S16, T. 29 N., R. 6 E.	38° N.	111° W.	70	—	—	10	39	39	30.65	S. 41° E. S. 29° E.	+24° −6°	—	—	26° N. 46° N.	114° E. 114° E.	—	—
17 (B)	Moenkopi	T_R	Sand Canyon	S10, T. 15, R. 7 E.	40° N.	109° W.	100	—	—	8	30	27	24.48	S. 32° E.	−7°	9°	10.5	43° N.	118° E.	5°	9°
17 (C)	Moenkopi	T_R	Split Mtn.		40° N.	109° W.	100	—	—	5	23	23	22.20	S. 24° E.	−4°	6°	27.5	46° N.	105° E.	3°	6°
17 (D)	Moenkopi	T_R	Vernal	S35, T. 25, R. 21 E.	41° N.	109° W.	50	N. 39° E.	15° E.	9	41	38	35.96	S. 22° E.	−4°	6°	17.7	46° N.	104° E.	3°	6°
17 (E)	Moenkopi	T_R	Poverty Tank	S21, T. 29 N., R. 9 E.	36° N.	111° W.	120	N. 65° E.	4° N.	11	30	27	25.80	N. 23° W.	+36°	7°	21.7	64° N.	127° E.	5°	8°
17 (F)	Moenkopi	T_R	Echo Cliffs	S2, T. 39 N., R. 7 E.	37° N.	112° W.	320	—	—	22	48	42	39.53	N. 11° W.	+28°	6°	16.6	66° N.	95° E.	4°	6°
16 (A)	Supai	P	Hunter's Point	S2, T. 27 N., R. 6 W.	36° N.	109° W.	100	N. 3° W.	25° E.	7	24	24	23.29	S. 16° E.	+5°	5°	32.0	49° N.	96° E.	3°	5°
16 (B)	Supai	P	Oak Creek Canyon	S1, T. 18 N., R. 6 E.	35° N.	112° W.	480	—	—	14	32	32	29.54	S. 19° E.	+10°	8°	12.6	46° N.	96° E.	4°	8°
16 (C)	Supai	P	Oak Creek Canyon	S5, T. 17 N., R. 6 E.	35° N.	112° W.	350	—	—	16	57	55	52.86	S. 39° E.	+18°	4°	25.0	33° N.	116° E.	2°	4°
15	Naco limestone	C_P	Fossil Creek	S29, T. 12 N., R. 7 E.	34° N.	112° W.	150	—	—	9	20	20	19.12	S. 55° E.	+16°	7°	21.6	23° N.	130° E.	4°	7°
14	Deadwood	C_M	Rawlins	S17, T. 21 N., R. 87 W.	42° N.	107° W.	50	S. 46° W.	12° SE.	7	34	34	31.88	S. 29° E.	−14°	7°	15.5	47° N.	117° E.	4°	7°
13	Juniata	O	Bedford		40° N.	79° W.	1500	N. 39 E.	75° SE.*	12	60	56	47.18	S. 49° E.	+26°	8°	6.2	20° N.	153° E.	5°	9°
12	Lodore	€	Vernal	S18, T. 6 N., R. 19 E.	41° N.	110° W.	200	S. 88° W.	28° N.*	11	38	26	24.20	N. 59° E.	+4°	8°	13.9	23° S.	174° W.	4°	7°
												7	6.76	S. 54° W.	+13°	13°	25.0				
11	Bright Angel Shales	€	Diamond Bar Ranch	S8, T. 28 N., R. 16 W.	36° N.	114° W.	260	—	—	20	44	—	—	—	—	—	—	—	—	—	—
10	Tapeats	€	Peach Spring	S3, T. 25 N., R. 11 W.	36° N.	114° W.	10	—	— —	15	47	—	—	—	—	—	—	—	—	—	—
9b	McNamara	A	Blackfoot canyon	S10, T. 13 N., R. 17 W.	47° N.	114° W.	84	N. 75° W.	22° N.*	20	62	53	51.29	N. 26° E.	−43°	4°	30.0	14° S.	138° W.	3°	5°
9a	Miller Peak	A	Donovan Creek	S26, T. 13 N., R. 18 W.	47° N.	114° W.	65	N. 35° W.	41° SW.*	14	23	23	21.90	S. 54° W.	+30°	7°	20.0	11° S.	166° W.,	4°	8°
8	Spokane	A	Prickly Pear Canyon	S3, T. 13 W., R. 4 W.	47° N.	112° W.	400	N. 68° E.	10° NW.	39	72	71	67.16	S. 52° W.	+55°	4°	18.2	5° N.	152° W.	4°	6°
7	Spokane	A	McDonald Creek		49° N.	114° W.	50	N. 46° W.	19° NE.	5	19	19	17.92	S. 26° W.	+39°	8°	9.9	16° S.	139° W.	6°	10°
6	Grinnell	A	Glacier Park		49° N.	114° W.	70	N. 44° W.	16° SW.*	16	44	44	41.1	S. 45° W.	+48°	6°	14.8	2° S.	152° W.	5°	8°
5	Appekunny	A	Glacier Park		49° N.	114° W.	110	N. 38° W.	16° SW.	15	39	38	36.40	S. 43° W.	+29°	6°	14.6	15° S.	156° W.	4°	7°
4	Bonito Canyon quartzite	A	Fort Defiance, Ariz.		36° N.	109° W.	100	N. 15° W.	20° SW.*	16	75	74	70.10	N. 31° E.	−25°	4°	18.7	33° S.	146° W.	2°	4°
3	Shinumo quartzite	A	Grand Canyon		36° N.	112° W.	100	N. 28° E.	10° SE.	14	61	61	50.65	N. 72° W. S. 66° W.	+65° +33°	—	—	37° N. 7° S.	166° W. 173° W.	—	—
2	Hakatai shales	A	Grand Canyon		36° N.	112° W.	36	N. 57° W.	8° NE.	14	44	41	37.82	N. 69° W. S. 65° W.	+58° +31°	—	—	36° N. 9° S.	177° W. 174° W.	—	—
1	Bass limestone	A	Grand Canyon		36° N.	112° W.	300	N. 28° E.	10° SE.	14	45	43	41.19	S. 52° W. S. 45° W.	+52° +34°	5°	23.2	6° S. 21° S.	154° W. 158° W.	3°	6°

S—Number of samples collected; N—Number of discs measured; N′—Number of discs used in the determination of the mean direction; R—Vector sum of the N′ directions (each assigned unit length); D—Mean declination; I—Mean inclination; α—Semi-angle of cone of confidence; κ—Precision (see text); $d\psi$, d_X—Semi-axes of the oval of confidence around each pole position.

An asterisk in the "Geological Strike and dip" column indicates that the samples were cored perpendicular to the bedding plane. No entry in the same column indicates that the beds are flat-lying.

TABLE 2.—LONGITUDES OF POLE POSITIONS DERIVED FROM EUROPEAN AND AMERICAN ROCKS OF THE SAME AGE

The longitudes for European rocks are the mean values for each age determined by various workers.

	European rocks Longitude	American rocks		Difference in longitude
		Formation	Longitude	
Triassic	147° E.	Chugwater	114° E.	+33°
		Moenkopi	110° E.	+37°
Permian	169° E.	Supai	104° E.	+65°
		Supai (Runcorn, 1956a)	119° E.	+50°
		Supai (Doell, 1955)	115° E.	+54°
Carboniferous	150° E.	Naco ss. (Runcorn, 1956a)	117° E.	+33°
		Naco ss. (C_D)	130° E.	+20°
		Deadwood (C_M)	117° E.	+33°
Cambrian	173° E.	Wilberns (Howell and Martinez, 1957)	158° E.	+15°
		Lodore	174° W.	−13°
Pre-Cambrian	123° W.	Hakatai shales (Doell, 1955)	127° W.	+4°
		Hakatai shales (Runcorn, 1956a)	150° W.	+27°
		Hakatai shales	174° W.	+51°
		McNamara	138° W.	+15°
		Miller Peak	166° W.	+43°
		Spokane (Prickly Pear Canyon)	152° W.	+29°
		Spokane (McDonald Creek)	139° W.	+16°
		Appekunny	156° W.	+33°
		Grinnell	152° W.	+29°
		Shinumo quartzite	173° W.	+50°
		Bonito Canyon quartzite	146° W.	+23°
		Bass limestone	158° W.	+35°

TABLE 3.—CALCULATED RATE OF POLAR WANDERING

Geological periods	Time interval in millions of years	Angular distance in degrees	Rate of movement in degrees per million years
Upper Triassic–Tertiary	150	28	0.2
Lower Triassic–Upper Triassic	30	10	0.3
Permian–Lower Triassic	30	12	0.4
Pennsylvanian–Permian	25	17	0.7
Silurian–Pennsylvanian	100	21	0.2
Ordovician–Silurian	25	14	0.6
Cambrian–Ordovician	90	20	0.2

TABLE 4.—SEQUENCE OF ALTERNATIONS OF MAGNETIZATION IN CHUGWATER AND MOENKOPI FORMATIONS

Chugwater Formation

A (Red Mtn.)		B (Rawlins)		C (Thermopolis)		D (Lander)		E (Dinwoody Lakes)		F (Fort Washakie)		G (Shell)		H (Sheep Mtn.)		I (Alcova Resvr.)		J (Troublesome Creek)	
Samples	Sign	Samples	Sign	Samples	Sign	Samples	Sign	Samples	Sign	Samples	Sign	Samples	Sign	Samples	Sign	Samples	Sign	Samples	Sign
12–18	+ve									10–11	−ve								
10–11	−ve	10	−ve	6	+ve	7–10	+ve	9–10	+ve	9	+ve								
3–9	+ve	3–9	+ve	3–5	−ve	5–6	−ve	7–8	−ve	6–8	−ve								
1	−ve	1–2	−ve	1–2	+ve	1–4	+ve	3–6	+ve	1–5	+ve	2–6	+ve	1–10	+ve	1–10	+ve	19–27	+ve
								1–2	−ve			1	−ve						

Moenkopi Formation

A (Capitol Reef)		B (Sand Canyon)		C (Split Mtn.)		D (Vernal)		E (Poverty Tank)		F (Echo Cliffs)	
Samples	Sign	Samples	Sign	Samples	Sign	Samples	Sign	Samples	Sign	Samples	Sign
		8	−ve					13–15	−ve	24	+ve
2–10	+ve	1–7	+ve	1–6	+ve	1–9	+ve	12	+ve	11–23	−ve
								1–11	−ve	8–10	+ve
										3–7	−ve

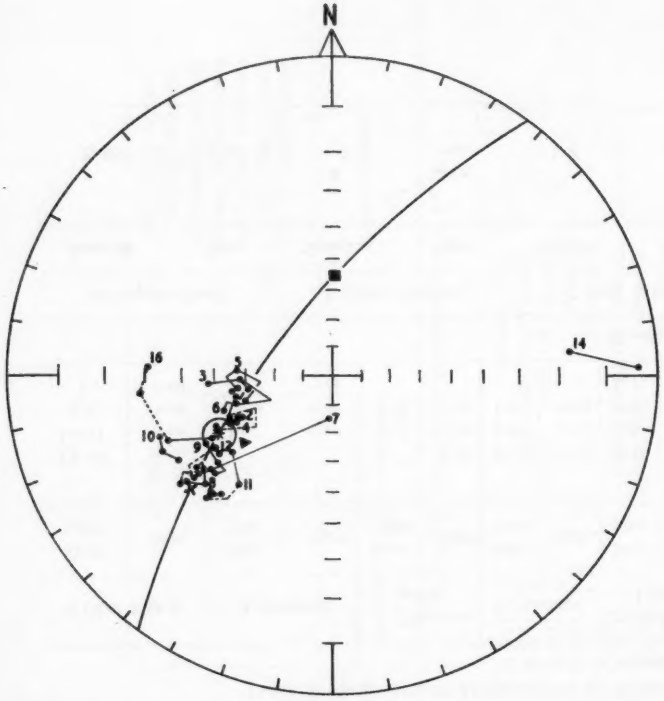

FIGURE 1

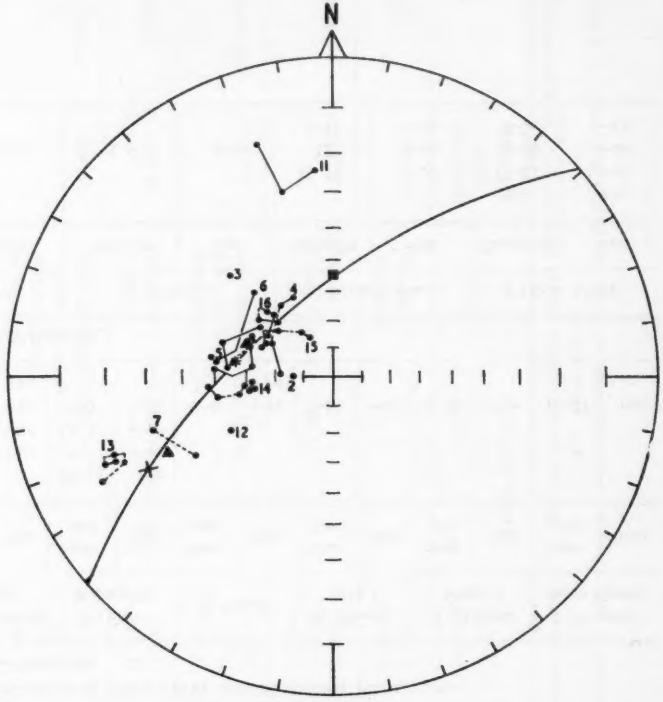

FIGURE 2

FIGURE 1.—BASS LIMESTONE (ALGONKIAN) FROM KAIBAB TRAIL, S. RIM OF GRAND CANYON
FIGURE 2. HAKATAI SHALES (ALGONKIAN) FROM KAIBAB TRAIL, N. RIM OF GRAND CANYON

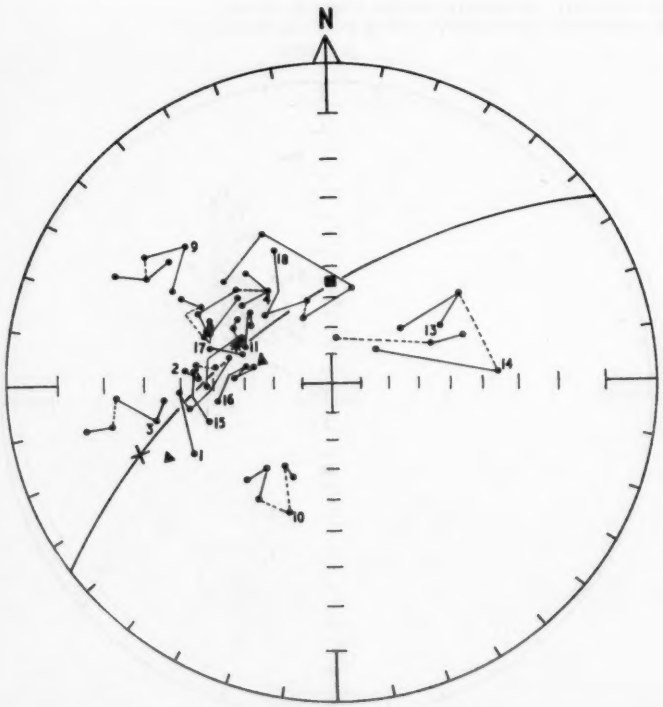

FIGURE 3

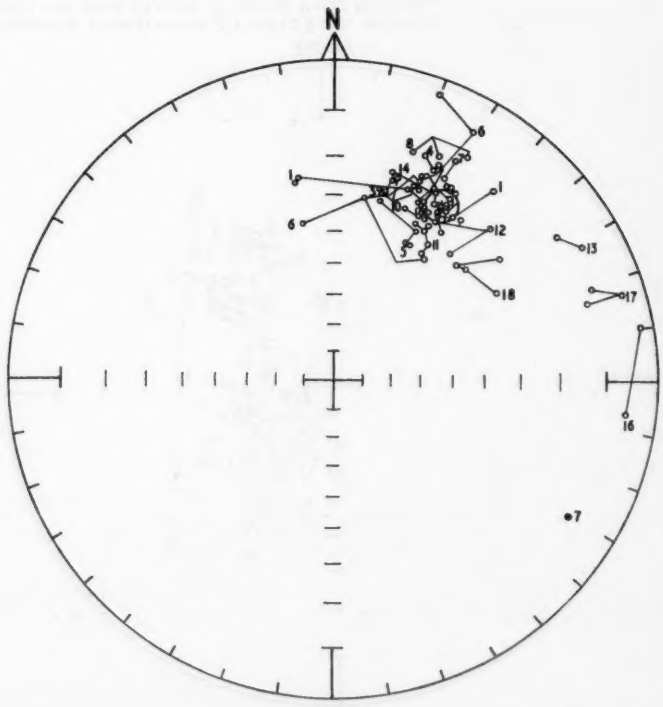

FIGURE 4

FIGURE 3.—SHINUMO QUARTZITE (ALGONKIAN) FROM KAIBAB TRAIL, S. RIM OF GRAND CANYON
FIGURE 4.—BONITO CANYON QUARTZITE (PRECAMBRIAN) FROM BLUE CREEK, FORT DEFIANCE, ARIZONA

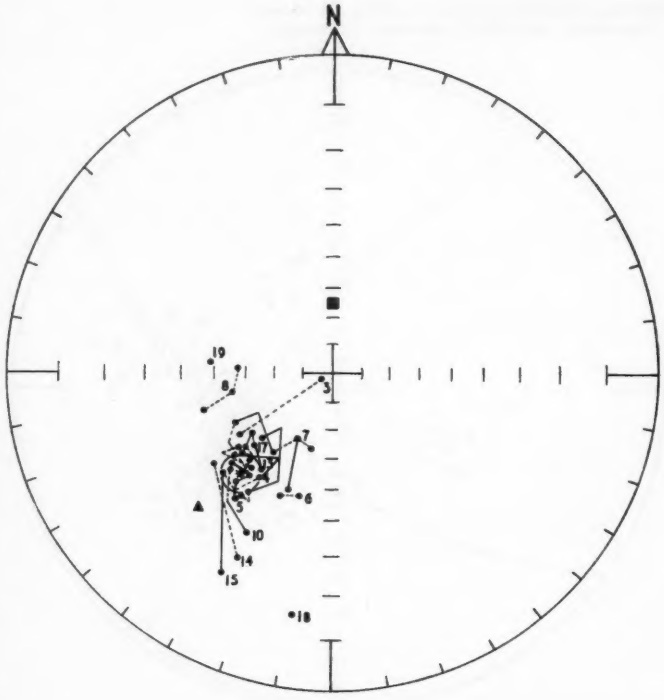

FIGURE 5

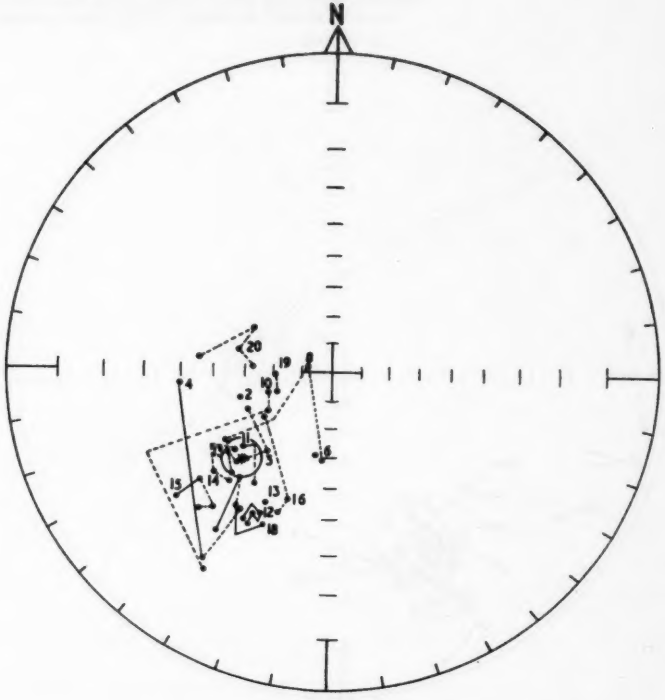

FIGURE 6

FIGURE 5.—BELT SERIES (ALGONKIAN): APPEKUNNY FORMATION FROM GLACIER NATIONAL PARK, MONTANA
FIGURE 6.—BELT SERIES (ALGONKIAN): GRINNELL FORMATION FROM GLACIER NATIONAL PARK, MONTANA

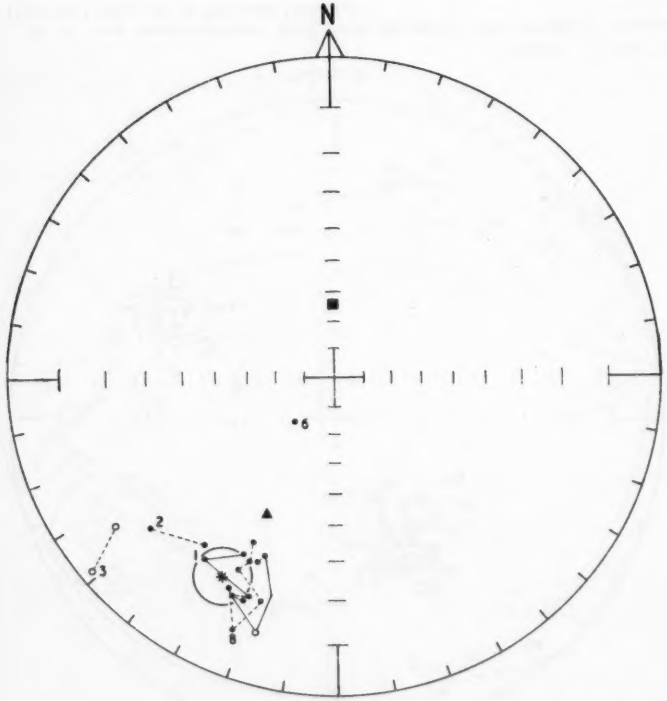

FIGURE 7

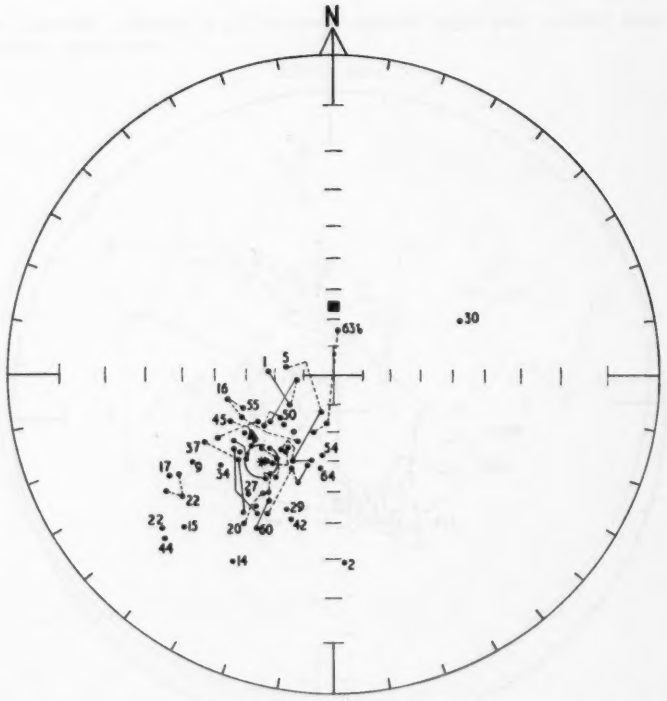

FIGURE 8

FIGURE 7.—BELT SERIES (ALGONKIAN): SPOKANE FORMATION FROM MCDONALD CREEK, MONTANA
FIGURE 8.—BELT SERIES (ALGONKIAN): SPOKANE FORMATION FROM PRICKLY PEAR CANYON, MONTANA

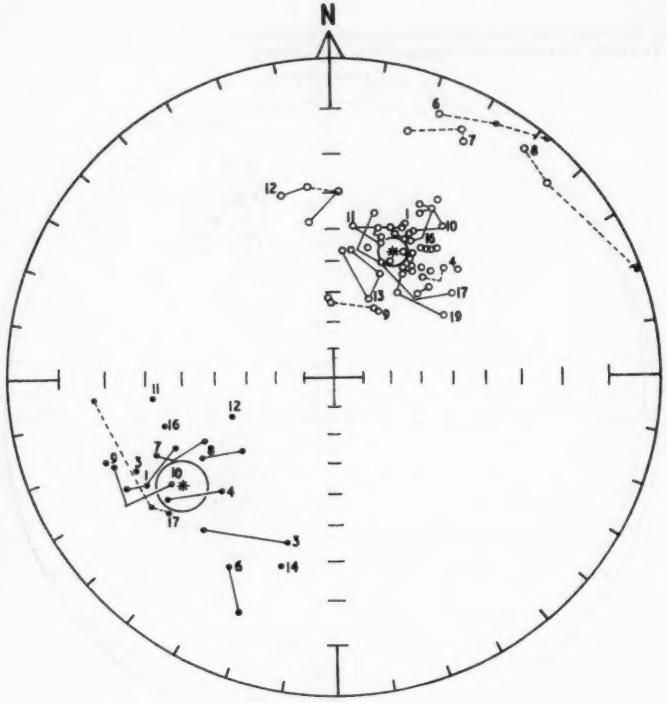

FIGURE 9

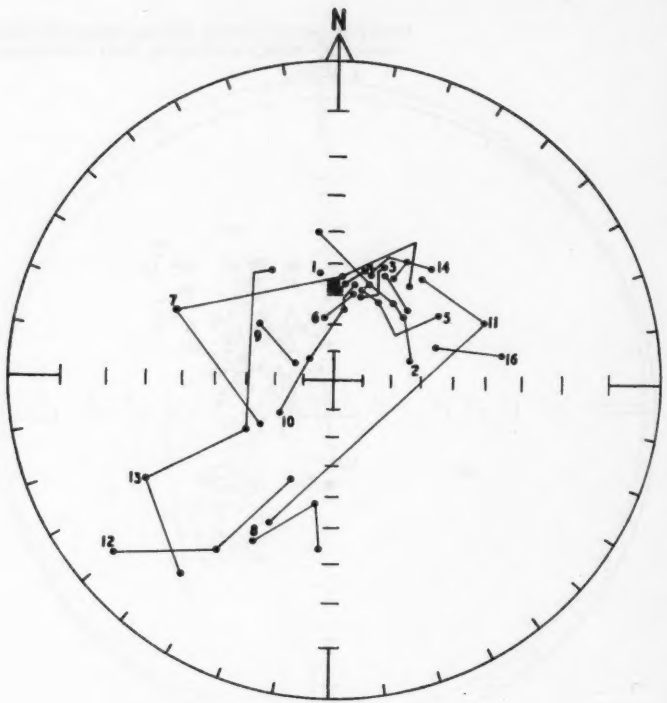

FIGURE 10

FIGURE 9.—BELT SERIES (ALGONKIAN)

N. E. −ve magnetizations: McNamara formation from Blackfoot Canyon, Missoula, Montana. S. W. +ve magnetizations: Miller Peak formation from Donovan Creek, east of Missoula, Montana.

FIGURE 10.—TAPEATS SANDSTONE (CAMBRIAN) FROM PEACH SPRINGS, ARIZONA

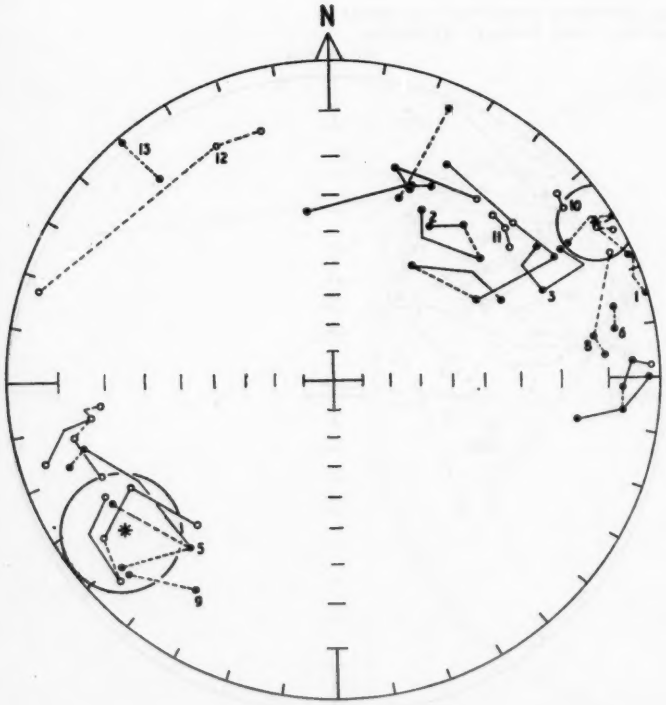

FIGURE 11

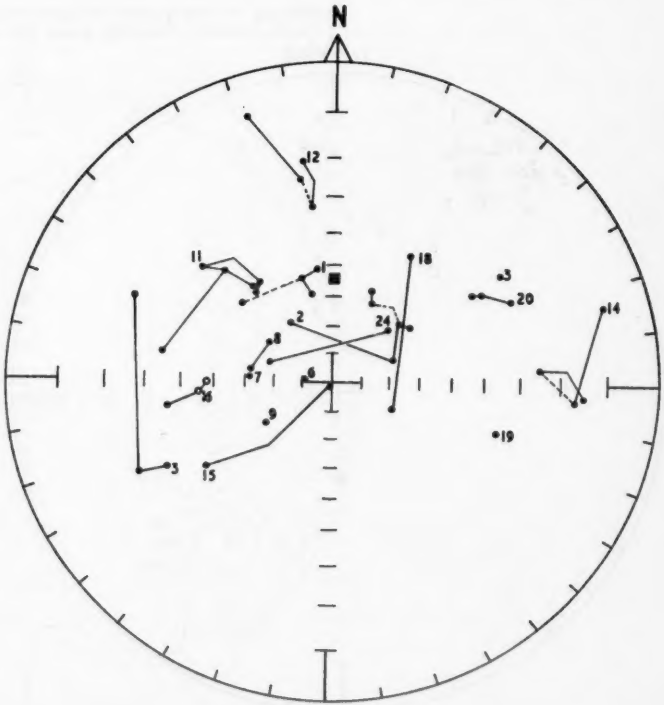

FIGURE 12

FIGURE 11.—BRIGHT ANGEL SHALE (CAMBRIAN) FROM DIAMOND BAR RANCH, ARIZONA
FIGURE 12.—LODORE FORMATION (CAMBRIAN) FROM UINTA MOUNTAINS, UTAH

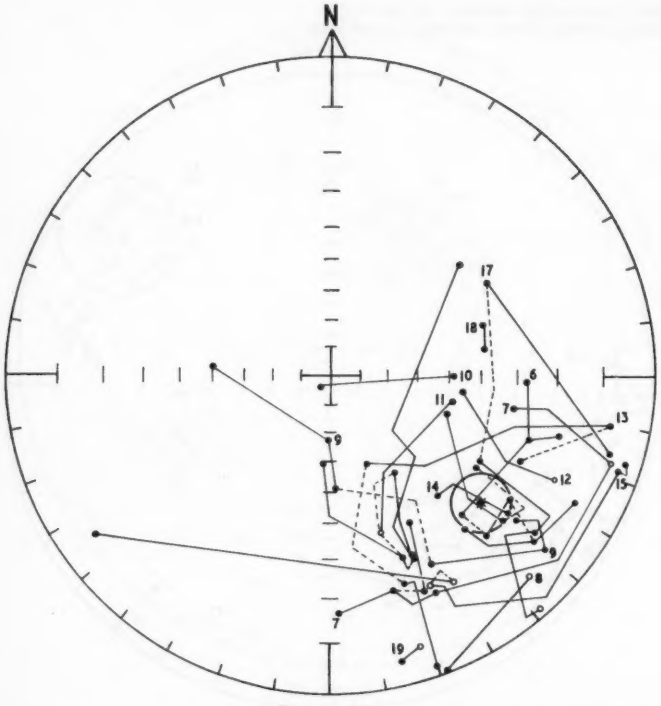

FIGURE 13

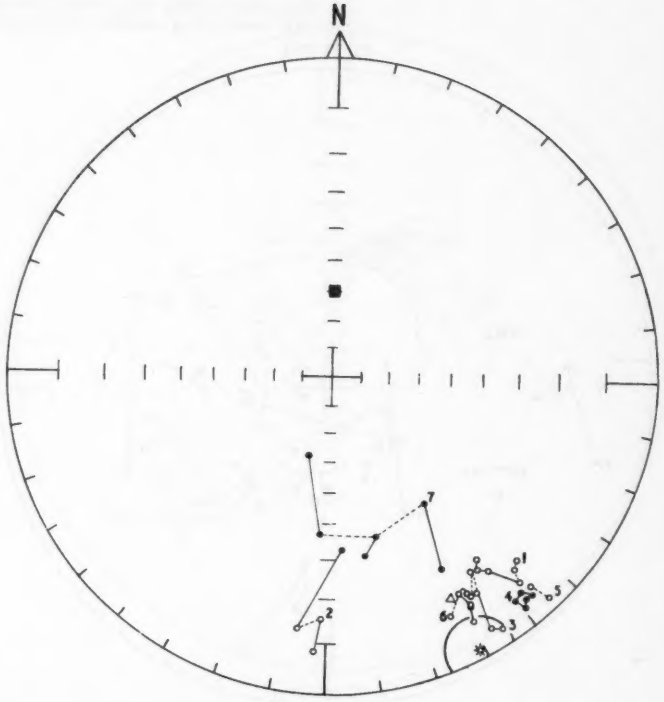

FIGURE 14

FIGURE 13.—JUNIATA BEDS (ORDOVICIAN) FROM BEDFORD, PENNSYLVANIA
FIGURE 14.—DEADWOOD FORMATION (MISSISSIPPIAN) FROM RAWLINS, WYOMING

FIGURE 15.—NACO SANDSTONE (PENNSYLVANIAN) FROM COLORADO PLATEAU

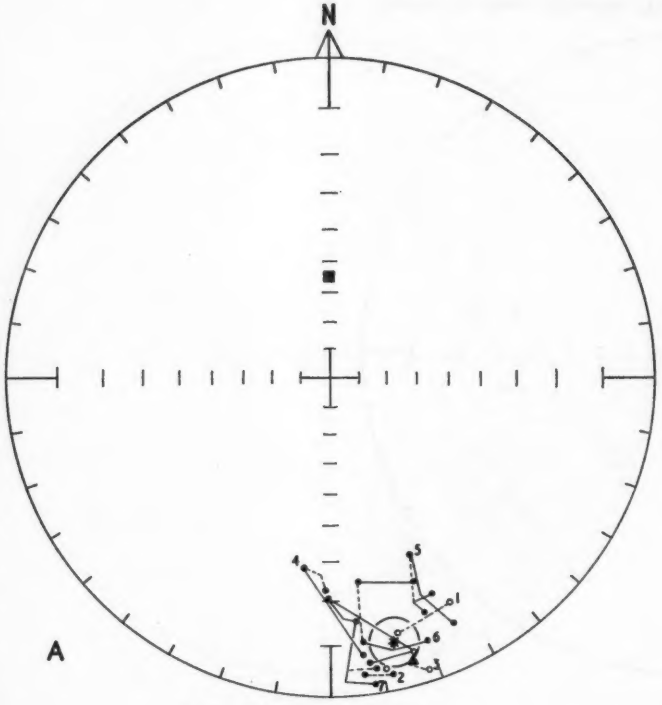

A. Hunter's Point, Colorado Plateau.

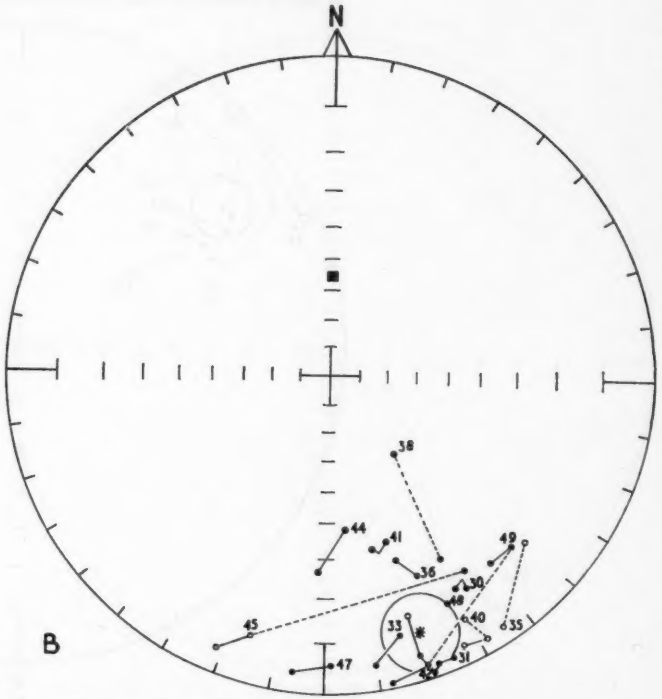

B. Upper part of section, Oak Creek Canyon, Colorado Plateau.

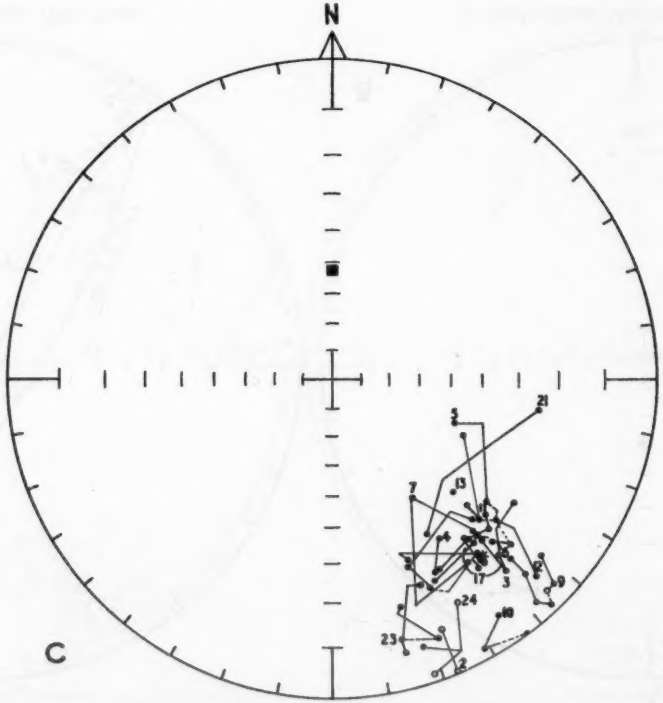

C. Lower part of section, Oak Creek Canyon, Colorado Plateau.

FIGURE. 16—SUPAI FORMATION (PERMIAN)

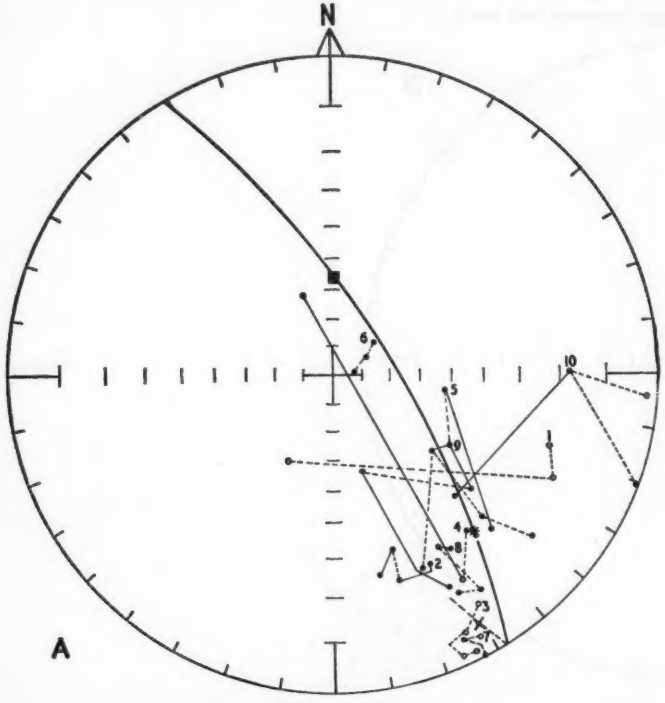

A. Capitol Reef National Park, Utah.

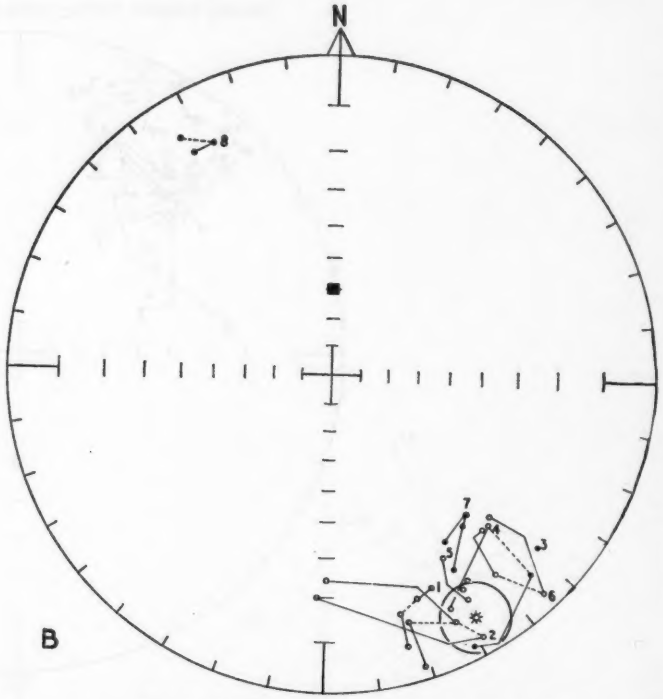

B. Sand Canyon, Dinosaur National Park.

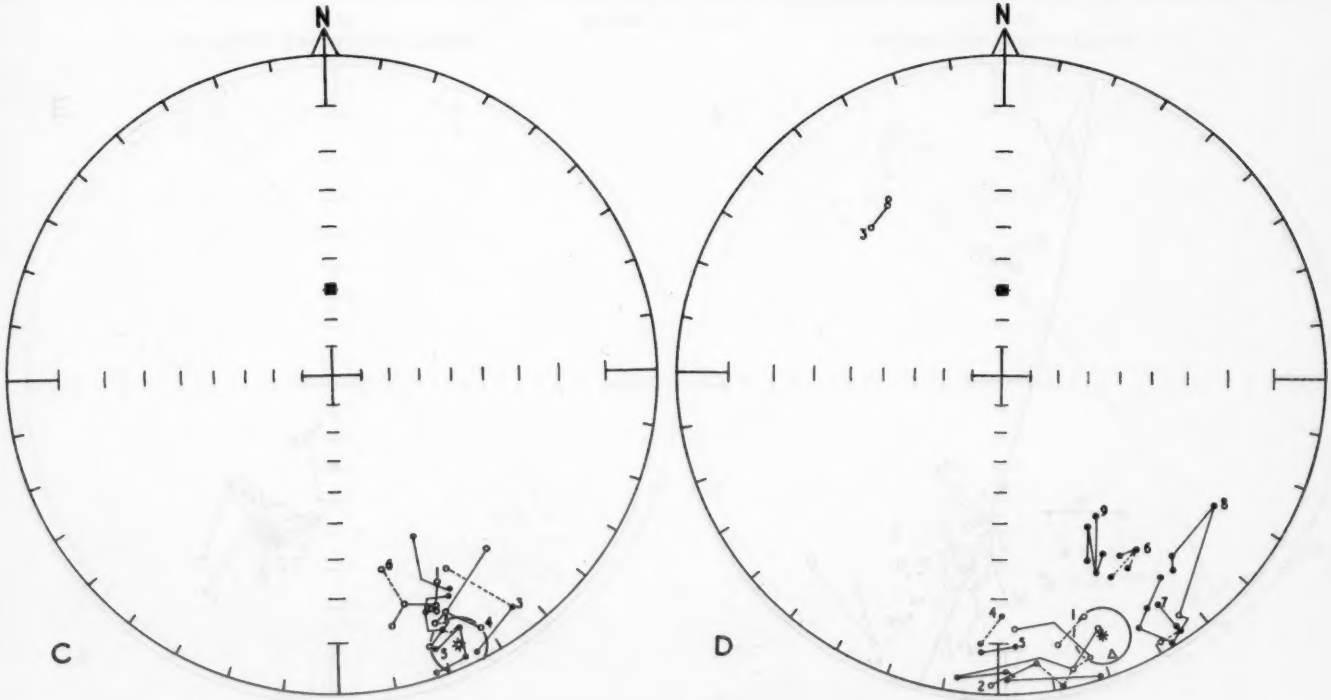

C. Split Mountain, Colorado.

D. Vernal, Utah.

FIGURE 17.—MOENKOPI FORMATION (LOWER TRIASSIC)

(*Continued on next page*)

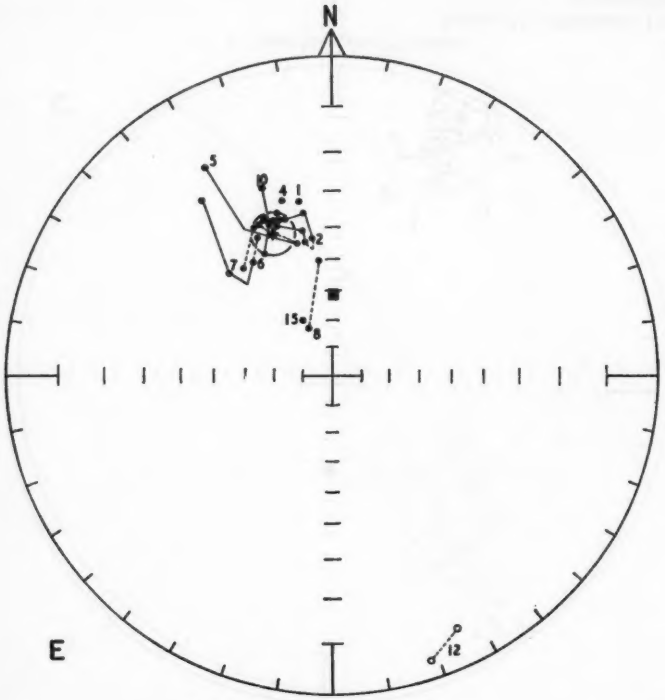

E. Poverty Tank, Colorado Plateau.

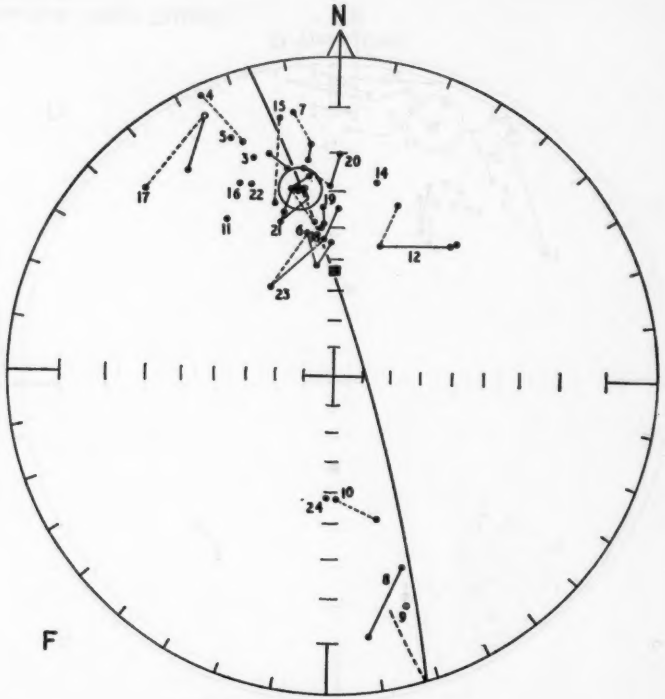

F. Echo Cliffs, Colorado Plateau.

FIGURE 17. (*Cont'd.*)

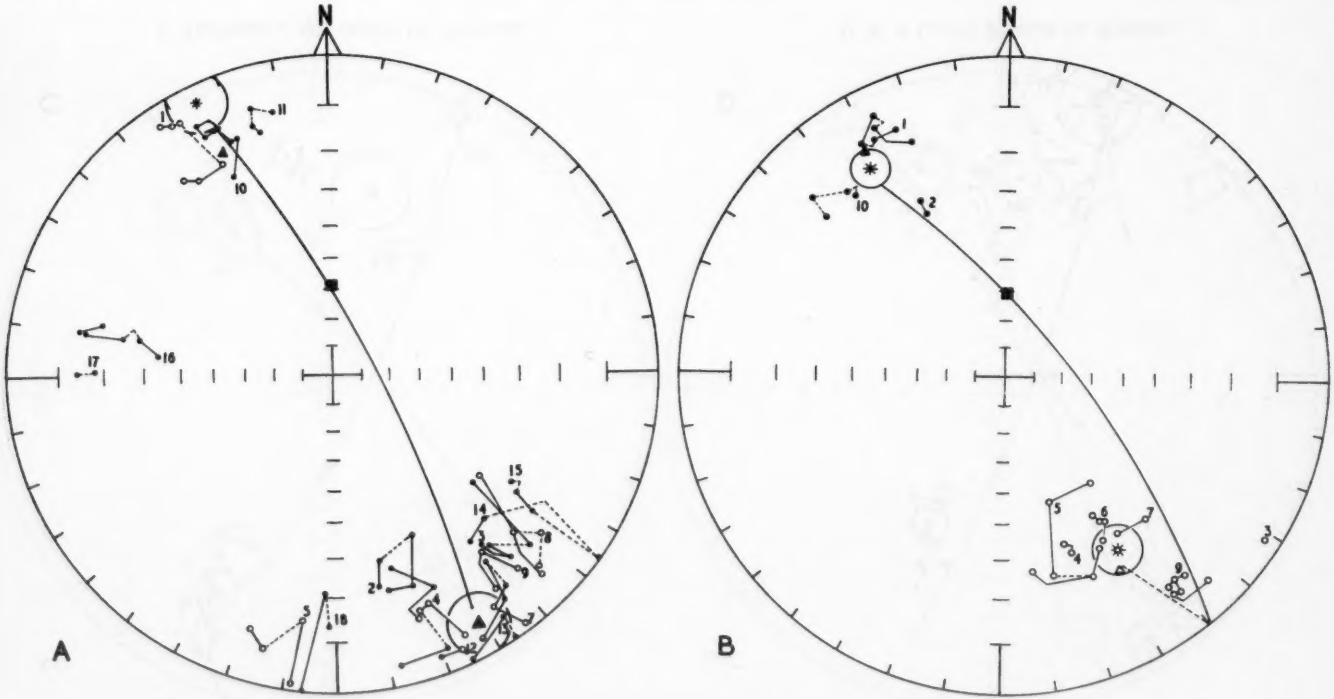

A. Red Mountain, Albany Co. Wyoming.

B. Rawlins, Wyoming.

FIGURE 18.—CHUGWATER FORMATION (TRIASSIC)

(*Continued on following pages*)

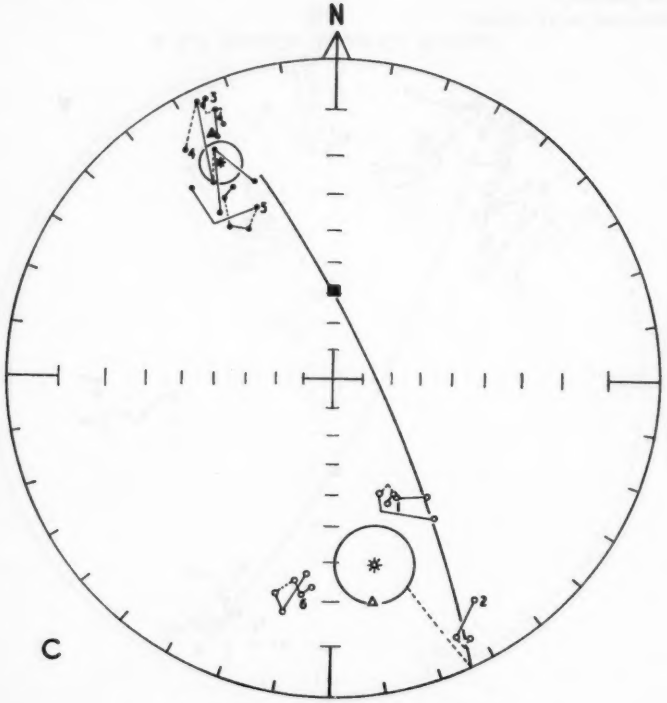

C. Thermopolis, Hot Springs Co., Wyoming.

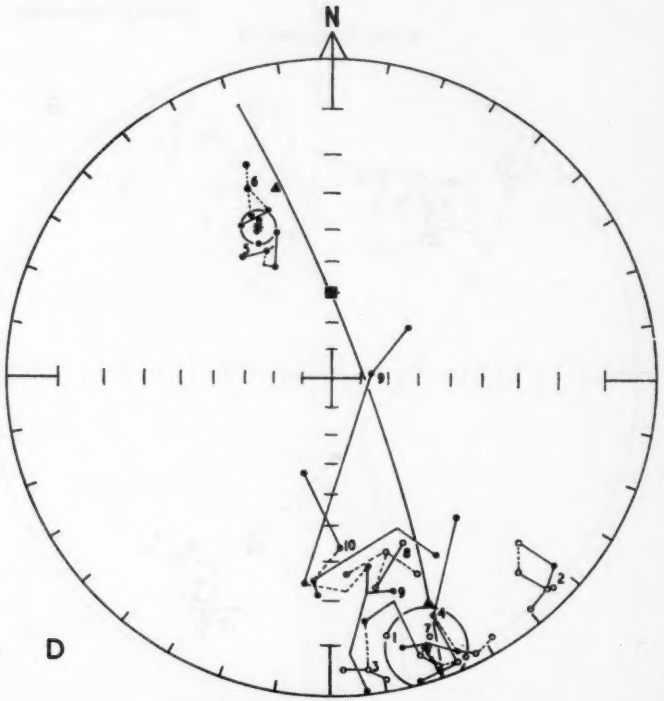

D. N. of Lander, Fremont Co. Wyoming.

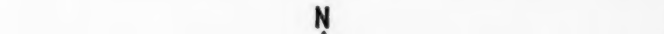

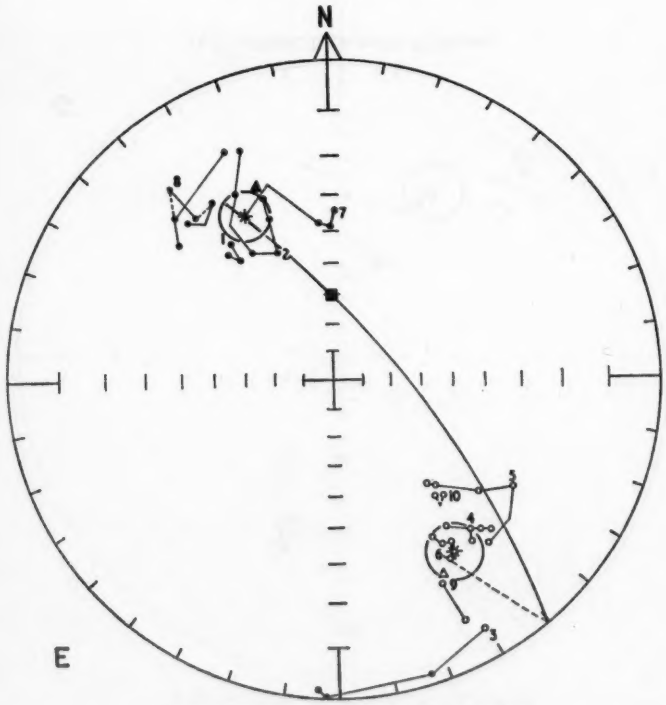

E. Dinwoody Lakes, Fremont Co. Wyoming.

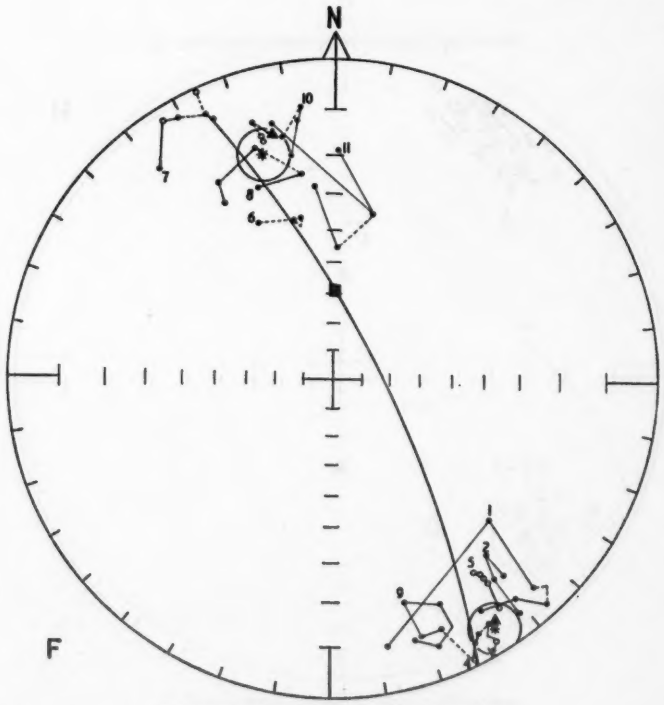

F. Fort Washakie, Fremont Co. Wyoming.

FIGURE 18 (*Cont'd.*)

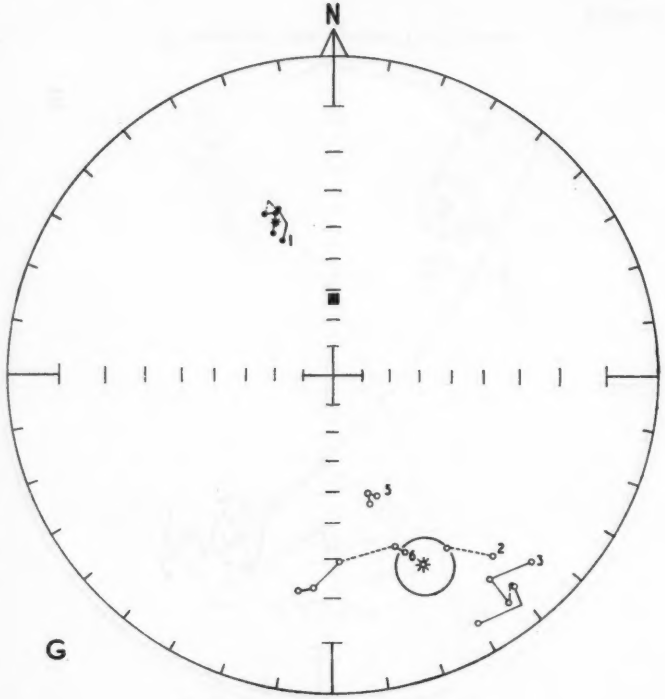

G. N. of Shell, Bighorn Co. Wyoming.

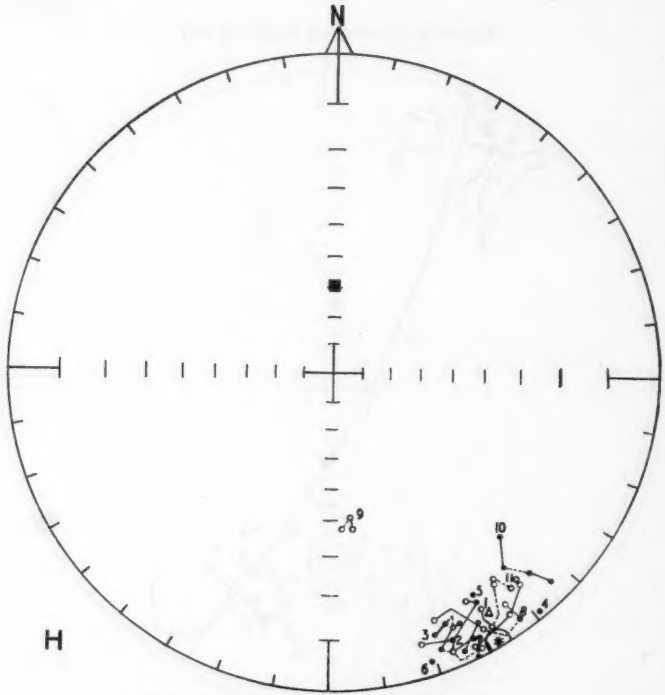

H. Sheep Mountain, N. of Greybull, Wyoming.

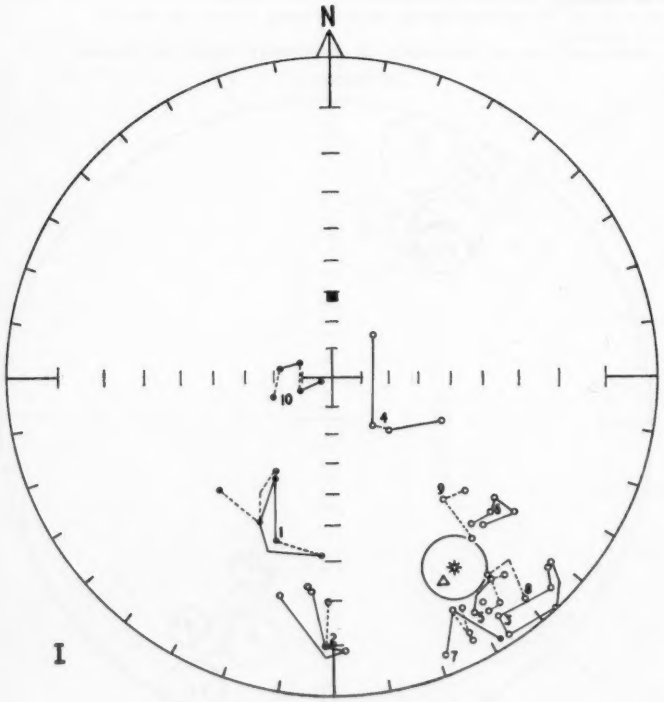

I. Alcova Reservoir, N. of Rawlins, Wyoming.

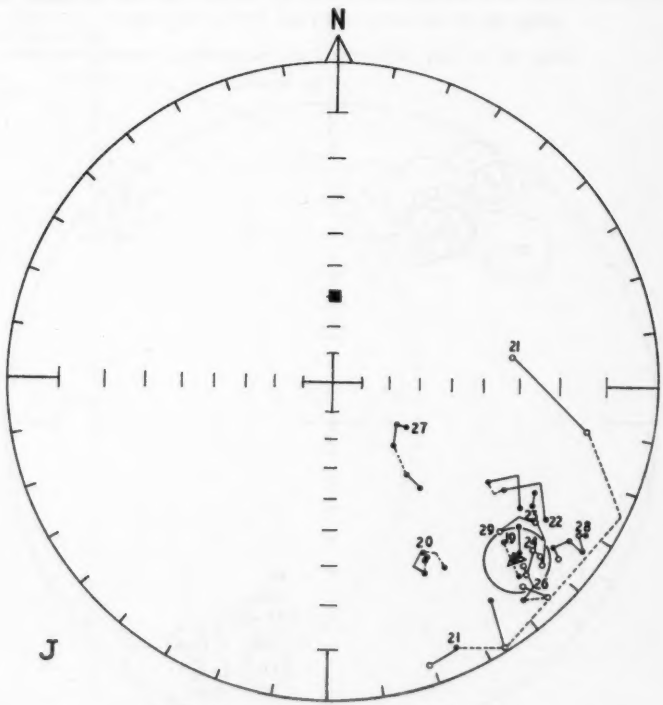

J. Troublesome Creek, Carbon Co. Wyoming.

FIGURE 18. (*Cont'd.*)

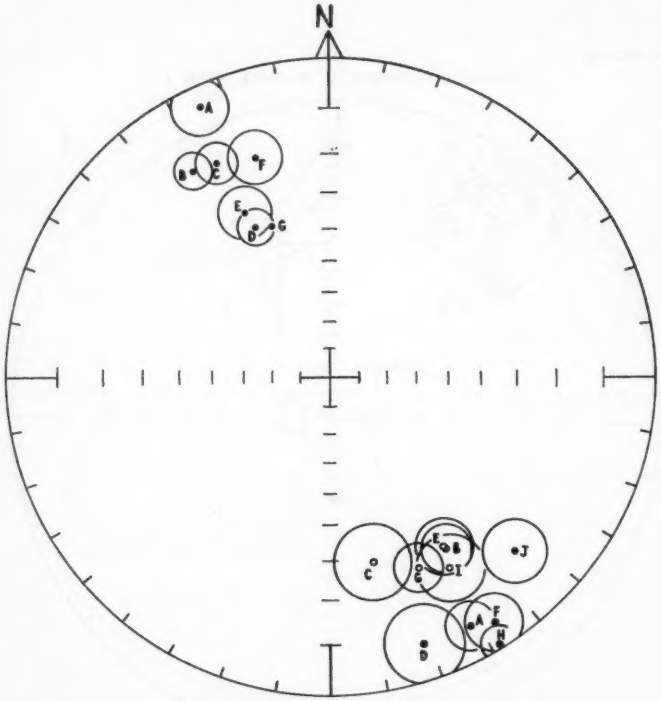

FIGURE 19

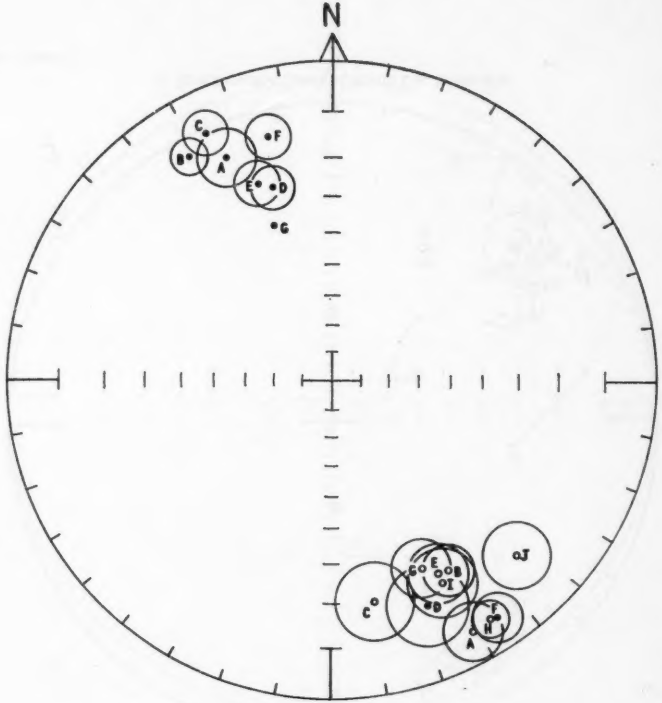

FIGURE 20

FIGURE 19.—MEAN DIRECTIONS OF MAGNETIZATION OF CHUGWATER FORMATION BEFORE CORRECTION FOR GEOLOGICAL DIP OF THE BEDS
Symbols as in Figure 18

FIGURE 20.—MEAN DIRECTIONS OF MAGNETIZATION OF CHUGWATER FORMATION AFTER CORRECTION FOR GEOLOGICAL DIP OF THE BEDS
Symbols as in Figure 18

Symbols as in Figure 18

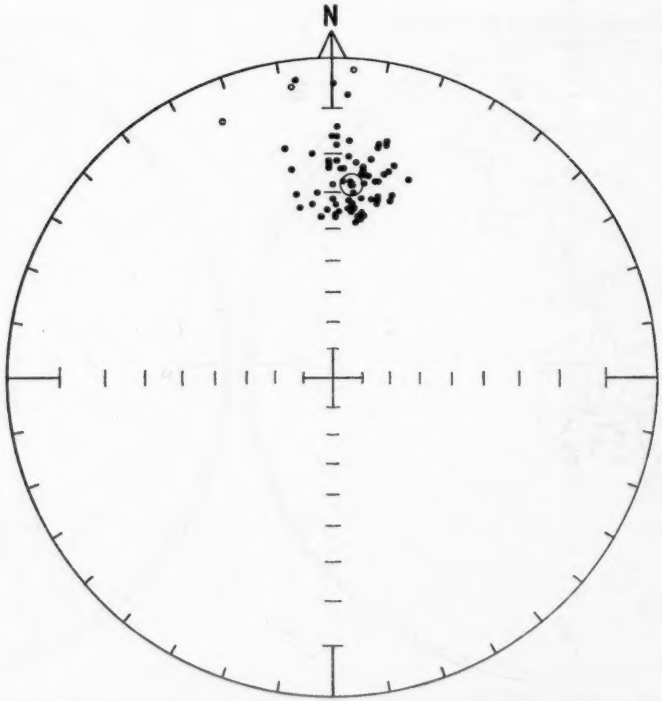

FIGURE 21.—NEWARK GROUP (TRIASSIC) FROM FRENCHTOWN, NEW JERSEY

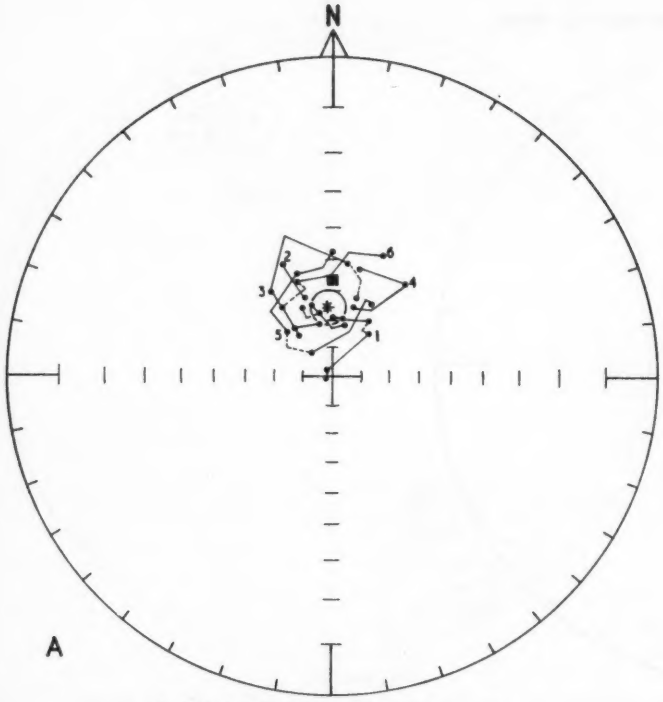

A. Site I at Colorado National Monument

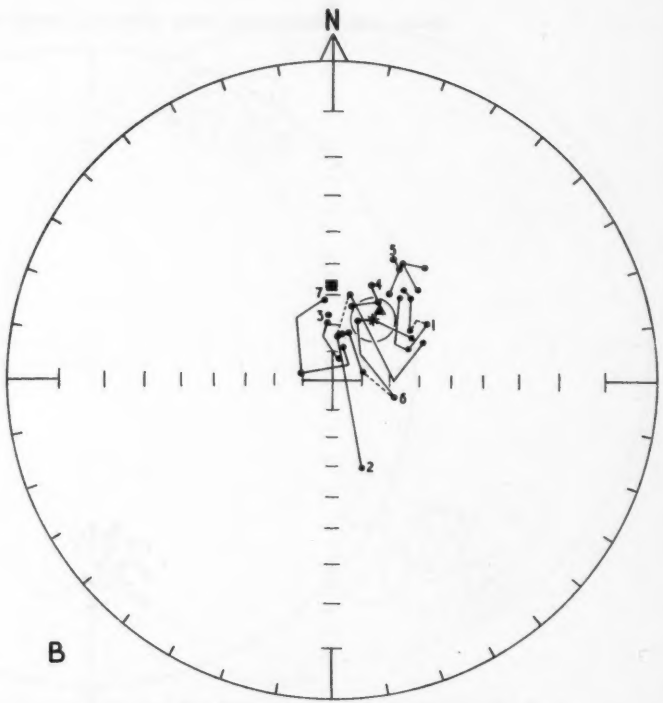

B. Site II at Colorado National Monument

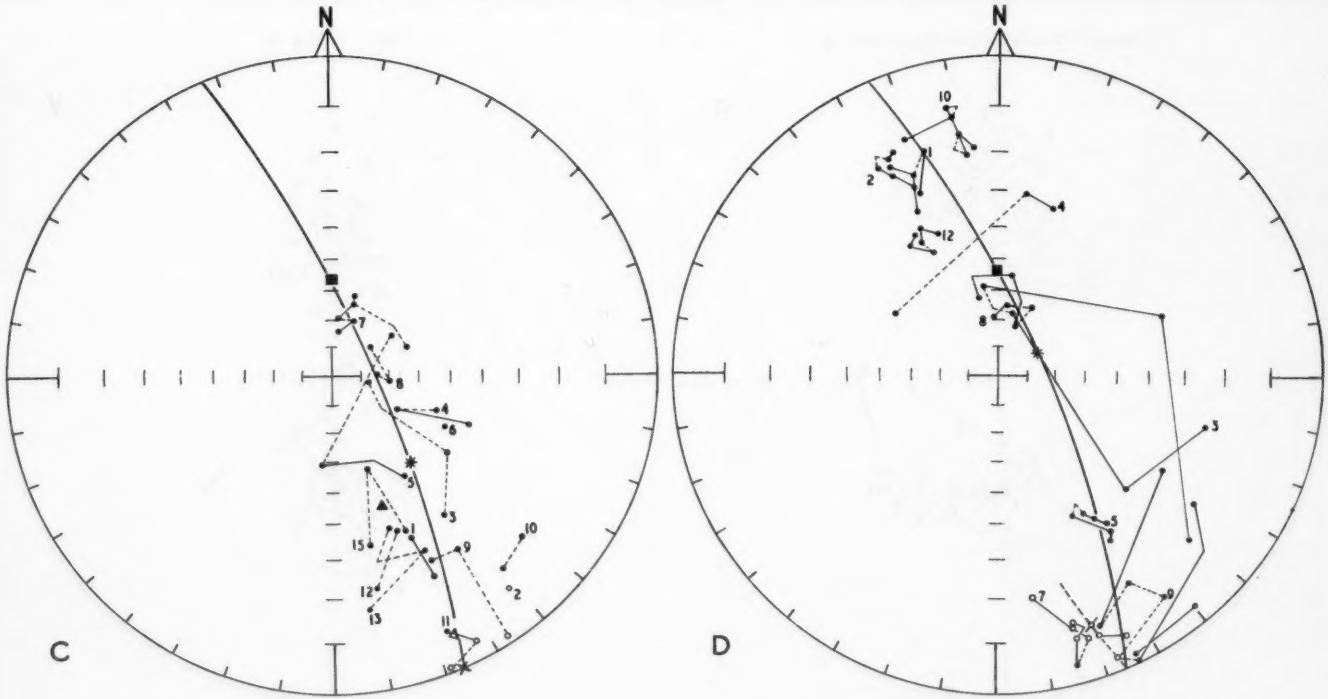

C. North of Moab, Utah

D. East of Moab, Utah

FIGURE 22.—CHINLE FORMATION (UPPER TRIASSIC)

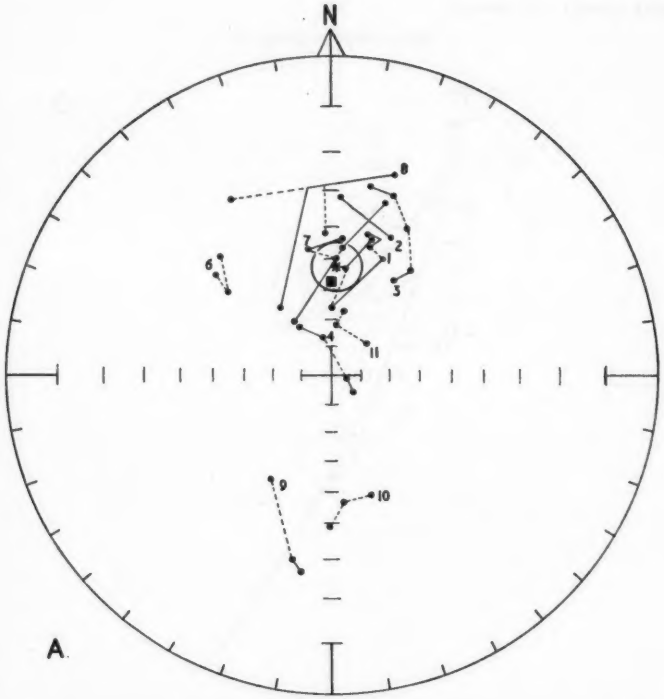

A. Kanab, Utah

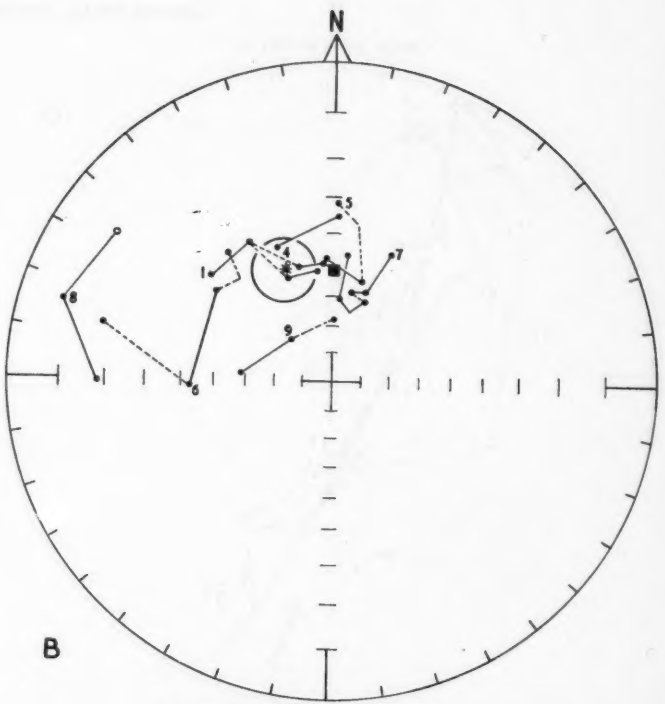

B. Navajo National Monument, Arizona

C. Echo Cliffs, Colorado Plateau

D. Kayenta, Arizona

FIGURE 23.—KAYENTA FORMATION (LOWER JURASSIC)

FIGURE 24
FIGURE 24.—CARMEL FORMATION (JURASSIC) FROM MOAB, UTAH
FIGURE 25.—DUCHESNE RIVER FORMATION (TERTIARY) FROM ROOSEVELT, UTAH

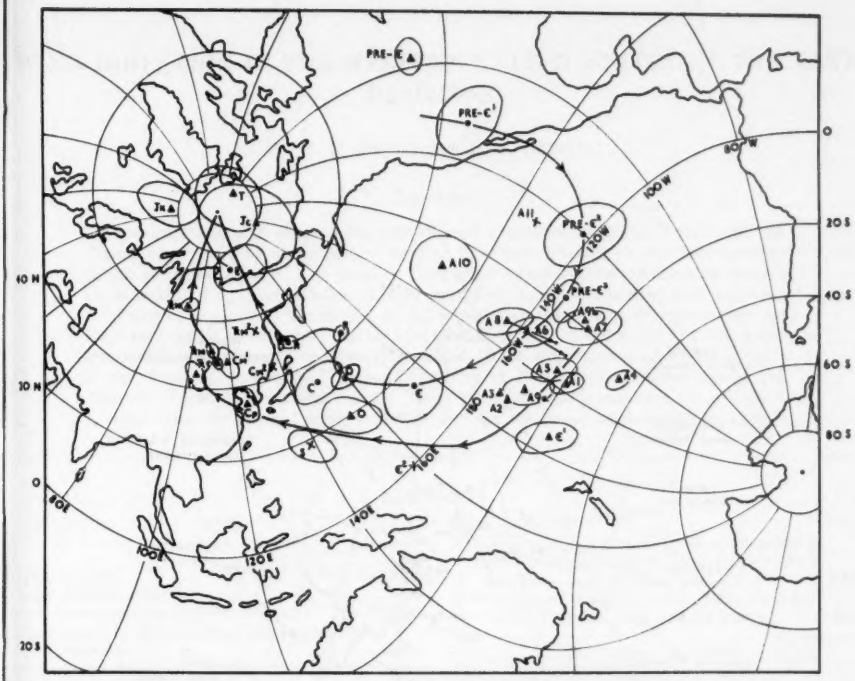

FIGURE 26.—POLE POSITIONS AND PATHS BASED ON BRITISH AND AMERICAN ROCKS

British rocks——●——. American rocks——▲——.

Poles determined from British rocks are those given by Creer, Irving, and Runcorn (1957), but the Triassic and Permian poles are slightly modified on the basis of data by Nairn (1960).

Poles determined from American rocks are as follows:

J_K mean of Kayenta poles (Jurassic)
J_C Carmel pole (Jurassic)
$\bar{K}M^1$ mean of Moenkopi poles (Triassic)
$\bar{K}M^2$ Moenkopi pole (Kintzinger 1957)
$\bar{K}C$ mean of Chugwater poles (Triassic)
$\bar{K}N$ Newark formation (Upper Triassic)
C_m^1 Deadwood formation (Mississippian?)
C_m^2 Barnett formation (Howell and Martinez, 1957) (Mississippian)
A 10 Hakatai shales (Runcorn, 1956a)
A 11 Hakatai shales (Doell, 1955)
Pre-ϵ Michigan dykes (Graham's data quoted by Creer, Irving, and Runcorn, 1957)

Algonkian poles A1–9 and all other poles: as in Table 1 and the figures of this paper.

Projection is oblique Mercator's, with pole at 0° N., 112° E., giving a uniform scale for angular distance near polar-wandering paths.

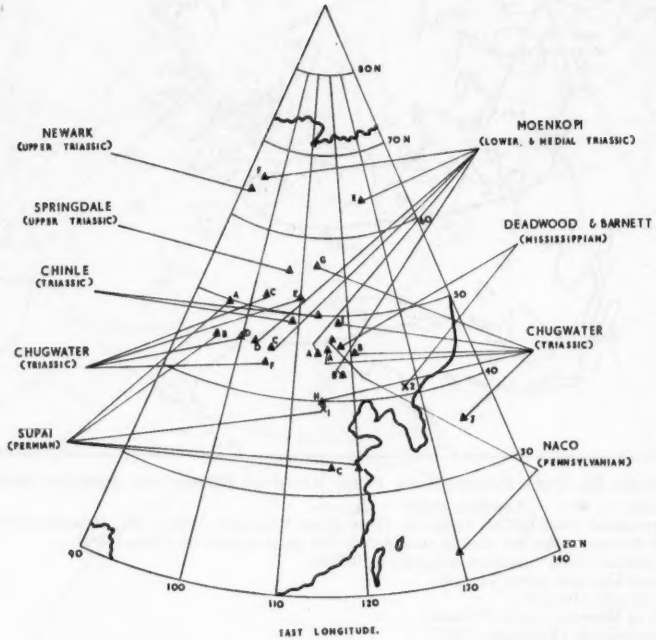

FIGURE 27.—POLE POSITIONS FOR TRIASSIC, PERMIAN, AND CARBONIFEROUS ROCKS

Letters on the Moenkopi, Chugwater, and Supai pole positions refer to localities listed in the text of this paper. Other pole positions denoted by a triangle represent pole positions determined in this paper and in Runcorn (1956a). Pole positions determined by a cross refer to other authors as follows: (1) Doell (1955); (2) Howell and Martinez (1957). (Stereographic polar projection)

BULLETIN OF THE GEOLOGICAL SOCIETY OF AMERICA
VOL. 71, PP. 959-972, 4 FIGS., 2 PLS. JULY 1960

WIND DIRECTION IN THE WESTERN UNITED STATES IN THE LATE PALEOZOIC

BY N. D. OPDYKE AND S. K. RUNCORN

ABSTRACT

From paleomagnetic surveys the latitude and orientation of Great Britain and the United States relative to the axis of rotation have been inferred for successive periods in the geological column. The question then arises whether these positions agree with those indicated by paleoclimatic studies. Assuming that a trade-wind belt has been a feature of the general circulation of the atmosphere throughout geological time, an important test is to determine the ancient wind directions by the study of eolian sandstones. Determinations of the directions of dip of the large-scale cross-stratified parts of the Tensleep, Casper, and Weber formations of Permo-Pennsylvanian age in the Western United States are described. These sandstones are considered to be eolian, in which case the inferred wind directions and the results of paleomagnetism agree.

CONTENTS

TEXT

	Page
Introduction	959
Acknowledgments	960
General circulation of the atmosphere	960
Stratigraphy of the Tensleep, Casper, and Weber formations	960
General description of the cross-stratification	962
Technique of field measurements	964
Statistical analysis of the results	966
Geophysical interpretation of results	968
References cited	970

ILLUSTRATIONS

Figure	Page
1. Mean directions of the paleowind at various outcrops of the Tensleep, Casper, and Weber formations	961
2. Histogram of directions of dip of cross-strata	964
3. Histogram of angles of dip of cross-strata in the Tensleep, Weber, and Casper sandstones	968
4. Positions of equators and poles in Carboniferous, Permian, and Triassic times	969

Plate	Facing page
1. Planar cross-stratification in the Weber sandstone and Tensleep sandstone	962
2. Planar cross-stratification and trough cross-stratification in the Weber sandstone	963

TABLES

Table	Page
1. Wind-direction data for Tensleep, Casper, and Weber formations of the western United States	967
2. Wind-direction data for two outcrops of the Nugget formation of Wyoming	969

INTRODUCTION

Creer, Irving, and Runcorn (1954; 1957) and Runcorn (1956a; 1956b) have discussed the directions of magnetization of samples of rocks of different ages in Great Britain and the United States. They show that in late Tertiary and Quaternary times the mean geomagnetic axis, determined by averaging over times longer than several thousand years, coincides with the present geographical axis. Durham (1952) has shown that the geographic latitude of North America remained unchanged during the Tertiary. As the longest free decay time of the geomagnetic field is a few thousand years, this coincidence of the mean geomagnetic axis with the geographical axis over a much longer time is thought to be a permanent property of the earth. In earlier geological periods the geomagnetic axis moved over the earth's surface in a curved path at an average rate of about 0.3° per million years; consequently it has been postulated that the geographical pole has wandered similarly. Better agreement is obtained between the paths based on rocks from Europe and from North America if it is assumed that the two continents were about 24° closer in pre-Jurassic time than they are today. This,

and data from other continents, seems to imply that continental drift has occurred.

Runcorn (1954), Elsasser (1955), and Bullard and Gellman (1954) have suggested that the coincidence of the mean geomagnetic and the geographic axes is the consequence of the important influence of the rotation of the earth upon fluid motions in the core. A further and perhaps more clear-cut argument that the mean geomagnetic and rotational axes have always been coincident has been given by Creer, Irving, and Runcorn (1957) and Runcorn (1959). The core and mantle are not coupled sufficiently tightly for them to rotate at exactly the same speed. Thus, for an observer on the earth's surface, nonaxial components of the field, if present, will be averaged out over times long compared to the period of relative rotation of the core and mantle. The mean geomagnetic field is symmetrical about the axis of rotation. Further considerations show that the mean field is a dipole oriented along the geographical axis.

Thus paleomagnetic measurements give the positions of the geographical poles for different geological periods relative to the localities from which the rocks were collected. The question arises whether the positions of the poles so determined agree with those based on paleoclimatic considerations. Because these latter have usually been based on qualitative evidence, we were led to consider whether the determination of the direction of the wind from observations of the directions of dip of the cross-strata in eolian sandstones could be used to test the hypothesis of polar wandering. In the hydrodynamics of the atmosphere, as in the earth's core, the Coriolis force plays a decisive role because of the large length scales. It seems likely therefore that the general planetary circulation of the atmosphere throughout geological time will consist of an equatorial easterly trade-wind zone, a mid-latitude westerly zone, and a polar zone. The wind pattern will therefore be symmetrical about the axis of rotation, wherever this happens to be on the earth's surface, with only minor asymmetries produced by the topography of the globe and world-wide climatic changes.

In this paper we attempt to determine the wind direction in Utah, Colorado, and Wyoming in Permo-Pennsylvanian time from observations on the large-scale cross-stratified parts of the Tensleep, Casper, and Weber sandstones, which we believe to be of eolian origin. These data, along with data obtained for Permian time in Arizona by Reiche (1938) and in England by Shotton (1937; 1956), are considered in relation to the positions of North America and Europe relative to the axis of rotation in late Paleozoic time determined by paleomagnetic studies.

Acknowledgments

The field work for this paper was carried out during the collection of specimens for paleomagnetic research, made possible by generous support from the Penrose Bequest of The Geological Society of America and from the Department of Scientific and Industrial Research, London. We are grateful to Drs. E. D. McKee, S. H. Knight, D. L. Blackstone, D. W. Boyd, J. W. Harshbarger, and Prof. T. S. Westoll for much discussion and advice.

General Circulation of the Atmosphere

At present between about 20° N, Lat. and 20° S, Lat., except in the monsoon belt in India, trade winds blow with more or less constancy depending on the topography. Over the oceans the trade winds are remarkably constant (Crowe, 1951). In continental areas we have much less information, and it appears that the wind pattern is somewhat less consistent.

The theory of the general circulation of the atmosphere has not yet been fully developed, but the trade winds are a direct consequence of the rising of air heated by the sun in the equatorial region and the deflection by the Coriolis force of the air moving in to take its place. Although the heat flow and the temperature difference between the equatorial and polar regions, and the angular velocity of the earth may have changed during geological time it is reasonable to suppose that a trade-wind zone has always existed, although its range in latitude may have varied, and, of course, if polar wandering and continental drift occurred, the relative positions of the zone and the continents would have varied.

Stratigraphy of the Tensleep, Casper, and Weber Formations

The upper parts of the Casper formation of southeast Wyoming (Darton, 1908), the Tensleep formation of Wyoming (Darton, 1904; 1908; P. C. Wilson, 1956, Ph.D. thesis, Univ. Wash.), and the Weber formation of Utah (King, 1876) contain conspicuously cross-stratified units of pure quartzose sand. Their environments of deposition have previously

FIGURE

FIGURE 1.—MEAN DIRECTIONS OF THE PALEOWIND AT VARIOUS OUTCROPS OF THE TENSLEEP, CASPER, AND WEBER FORMATIONS (WITH REICHE'S DATA ON THE COCONINO SANDSTONE FOR COMPARISON)

been little studied, but the authors consider that they are likely to be of eolian origin.

Figure 1 shows the areal distribution of the three formations. They crop out as massive white, pink, or buff to gray sandstones locally cemented by silica or calcium carbonate. The lower beds of the formations include limestone, dolomite, gypsum, and shale beds and lenses. The total carbonate in the formations increases as the axis of the depositional basins are approached in eastern Wyoming and central Utah.

The Tensleep formation ranges in thickness from 240 to 450 feet; individual sandstone units range from 1 to 180 feet thick. The massive cross-stratified sandstone units usually occur in the upper part of the formation. The lower portion of the Tensleep contains variable amounts of limestone, dolomite, and shale.

The Tensleep formation appears to be middle Pennsylvanian (Desmoinian), on the basis of a microfauna 175 feet below the top of the formation at Wind River Canyon (Branson, 1939), at the top of the formation at Shell Canyon (Pierce, 1947), and 238 feet below the top of the formation northeast of Lander (Hollingsworth, quoted by Agatson, 1954, p. 528). Recently in the southern part of the Bighorn Mountains a Lower Permian microfauna has been recovered from the topmost part of the formation (Verville, 1957), indicating that the Tensleep may range into the Permian, although the forms are poorly preserved and could have been introduced into the Tensleep by the resorting of the sand by the incoming Phosphoria sea. The Tensleep is overlain disconformably by the Permian Phosphoria formation and is underlain conformably by the Pennsylvanian Amsden formation.

The Casper formation is dominantly sandstone along the west side of the Laramie and Shirley basins and mainly sandstone and arkose (Fountain arkose) in the southern Laramie basin. It ranges between 230 and 500 feet in thickness; limestone is common in the lower part of the formation in those areas.

The cross-stratified part of the Casper formation, termed the Upper Division by Agatson (1954), has been placed in the Lower Permian on the evidence of both micro- and macrofauna at the base of the Upper Casper formation. The Casper is underlain conformably by the Fountain arkose and succeeded by the Permian Opeche and Satanka shales. Knight (1929) mapped the cross-strata in an outcrop of the Casper formation south of Laramie and concluded that it was laid down in a shallow sea. This view was disputed by Twenhofel (1950) on the grounds that the large-scale cross-stratified units which Knight describes are not likely to be of marine origin.

The Weber formation throughout the eastern part of the Uinta Mountains is a massive, cross-stratified sandstone up to 1200 feet in thickness. Love *et al.* (1949) placed it in the Upper Pennsylvanian and Lower Permian, but further data are given by Bissell and Childs (1958). Around White Rock, Utah, the formation conformably overlies the Morgan formation which contains a Des Moines fauna (Middle Pennsylvanian), but the top of the Weber sandstone is Wolfcampian in age. The Weber sandstone underlies the Permian Park City beds. At the type section in Weber Canyon, Utah, Desmoinesian fossils have been found, but from the Utah–Colorado line eastward the Weber sandstone is probably entirely Wolfcampian. Untermann and Untermann (1954) have suggested that the Weber formation is in part eolian.

General Description of the Cross-Stratification

The cross-stratification of these sandstones is of two general types, following the classification of McKee and Weir (1953). The first type is planar cross-stratification—*i.e.*, the lower bounding surface of sets of cross-strata is a planar surface of erosion (Pl. 1). This type is characterized by the following properties:

(1) The large-scale sets of cross-strata are truncated by nearly horizontal surfaces.

(2) The cross-laminated units between successive planar surfaces range in thickness from 6 inches to 30 or 40 feet—*i.e.*, up to large scale in the McKee and Weir classification.

(3) The truncating surfaces are not strictly

Plate 1.—PLANAR CROSS-STRATIFICATION IN THE WEBER SANDSTONE AND TENSLEEP SANDSTONE

Figure 1.—Weber sandstone in Brush Creek Gorge (looking from the southwest)
Figure 2.—Weber sandstone in Brush Creek Gorge (looking from the south)
Figure 3.—Tensleep sandstone in Tensleep Canyon (looking from the west)

FIGURE 1

FIGURE 2

FIGURE 3

PLANAR CROSS-STRATIFICATION IN THE WEBER SANDSTONE AND TENSLEEP SANDSTONE

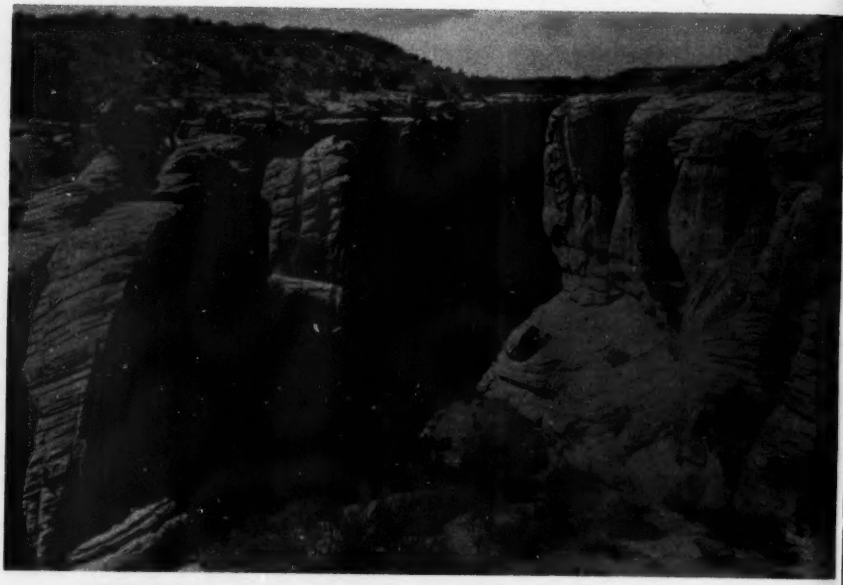

FIGURE 1

FIGURE 2

PLANAR CROSS-STRATIFICATION AND TROUGH CROSS-STRATIFICATION IN THE WEBER SANDSTONE

horizontal but in places are gently concave upward.

(4) The truncating surfaces are local, for two sections about 2 miles apart do not contain the same number of surfaces. Large sand grains are sometimes present on these surfaces.

(5) In the well-developed cross-stratified parts of these sandstones no sign of channeling by aqueous erosion has been recorded.

(6) The variation in the direction and amount of dip on the bedding planes in one set of cross-strata is negligible. The angles of dip range up to 33°—the angle of repose of dry sand.

Thus these features can best be explained by the interaction of eolian deflation and deposition, with deflation and deposition proceeding in adjacent areas. Such a phenomenon could be caused by short-period climatic cycles such as those today in the Great Plains region with alternate fixation and rejuvenation of the sand area accompanied by an increase in sand supply (Melton, 1940). The thickness of the units would be partially controlled by the amount of sand being brought into the area. As deflation proceeds, sand above a certain size would be left behind on the surface of the deflation planes causing a lag of accumulation which would explain the larger grains often found on these surfaces. H. W. Peirce of the Arizona Bureau of Mines suggests that one of the factors controlling the position of the deflation plane is the fluctuating ground-water table which would limit the depth to which erosion proceeds. The dune forms responsible for the cross-lamination would be transverse dunes. The great consistency in direction of dip within the cross-stratified units seems to support this contention. In areas of the Great Plains where deep sand has been reactivated, transverse dunes are the most prominent forms (Melton, 1940).

The second type of cross-stratification observed in these sandstones is trough cross-stratification—*i.e.*, the lower bounding surfaces of the sets are curved surfaces of erosion. Knight (1929) termed this type festoon bedding (Pl. 2, fig. 2). The shape of the sets is lenticular with concave cross-laminae of large scale. Knight (1929) recorded one cross-stratum 100 feet in height with a dip of 33° and at least 1000 feet in width. This type of bedding is similar to the cross-bedding in the Permian sands of Great Britain, described by Shotton (1937) and interpreted by him as barchan dunes—the result of eolian deposition.

These two types of cross-stratification are the common forms in the other sandstones of the western part of the United States which have large-scale cross-laminated sets, particularly the Navajo sandstone of Jurassic age, the Wingate sandstone of Triassic age, and the Coconino sandstone of Permian age. These sandstones, because of the cross-lamination and the sorting and texture of the particles, have been interpreted as of eolian origin, in the case of the Navajo and Wingate sandstones, by Harshbarger, Repenning, and Irwin (1957), and in the case of the Coconino sandstone by McKee (1934) and Reiche (1938).

The textural features of the cross-stratified units of the Tensleep and Weber also support the eolian origin of the cross-lamination. Twenty-eight specimens from four widely separated localities in the Tensleep (Sinks of the Popo Agie, Wind River Canyon, Hyettesville, Tensleep Canyon) collected for textural analysis are fine-grained and well sorted (average coefficient of sorting 1.20, range 1.11–1.28; median 123 microns, range 92–142). Specimens collected from three localities in the Weber (Manila, Brush Creek Gorge, Skull Creek) indicate that the Weber is fine-grained (average md. = 159 microns, range 103–256) and well sorted (average coefficient of sorting 1.23, range, 1.09–1.48; Pettijohn, 1957). Individual grains from the three formations show pitting and frosting. Those textural features are consistent with eolian deposition although this textural work should be extended.

Heaton (1950) believes that the sand forming the Tensleep, Casper, and Weber formations came from the west because the sands thicken westward. The cross-bedding information (Fig. 1) makes this hypothesis untenable. It would seem that the southwestward thickening is due to moving of the sand into this area by the wind and accumulation in great thicknesses along the edge of the gently subsiding Cordilleran geosyncline. Some of the sand was

PLATE 2.—PLANAR CROSS-STRATIFICATION AND TROUGH CROSS-STRATIFICATION IN THE WEBER SANDSTONE

FIGURE 1.—Weber sandstone in Brush Creek Gorge (looking from the east)

FIGURE 2.—Weber sandstone in Sand Canyon (looking from the north)

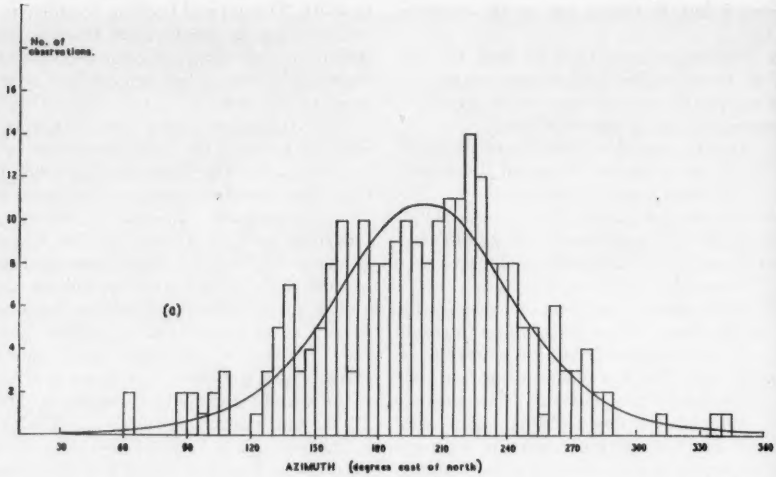

a, Tensleep sandstone

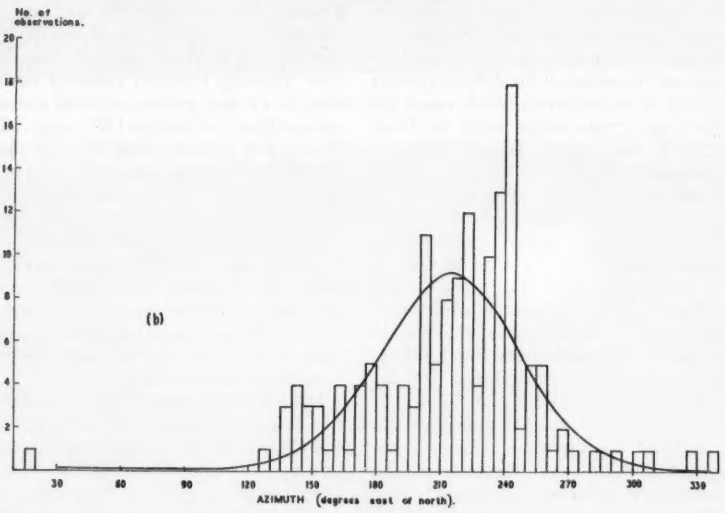

b, Weber sandstone

FIGURE 2.—HISTOGRAM OF DIREC

possibly derived from the beaches of the Permo-Pennsylvanian sea of eastern and northeastern Wyoming, some from the eolian erosion of the Fountain fan. The northern part of the ancestral Rockies may have been the ultimate source but could not have been the direct source since the direction of transport was southwestward, whereas the ancestral Rockies lay south and southwest of the Casper and Tensleep formations. The possibility that some of the sand may have been derived from as far away as the Canadian Shield cannot be excluded.

TECHNIQUE OF FIELD MEASUREMENTS

In the localities visited the sandstones are friable and either weather along the cross-laminae or, when struck with a hammer, split

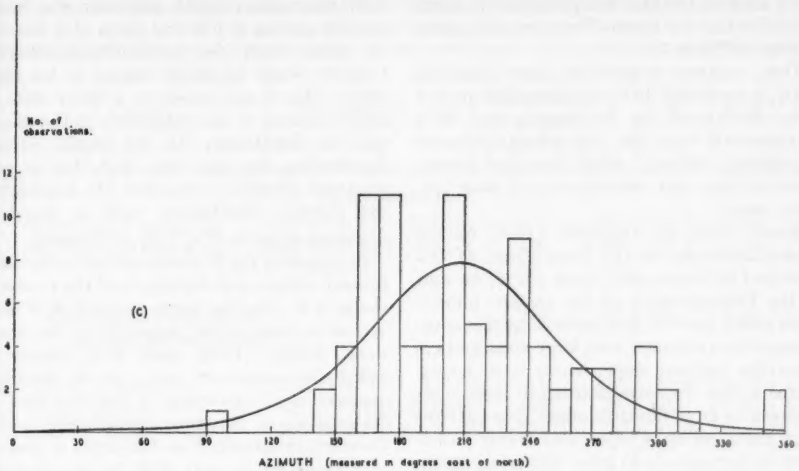

c, Casper sandstone (authors' measurement)

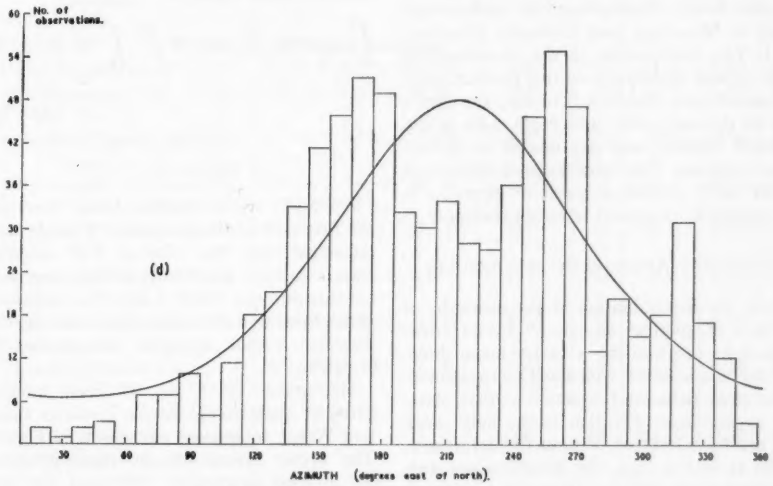

d, Casper sandstone (Knight's measurements)

TION OF DIP OF CROSS-STRATA

along them. The azimuths of the lines of greatest dip on these surfaces and the angles of inclination were therefore easily determined with an accuracy of a few degrees. The readings were corrected, where necessary, for structural dip. Each individual reading was taken from separate cross-stratified sets and consequently given equal weight in the statistical treatment. About 30 readings were made at each locality (McKee, 1940; Kiersch, 1950). The scatter of the results therefore represents the effects of curvature of dunes and changes in wind pattern. Figure 2 shows histograms of all the observations. The direction and magnitude of the vector means of the azimuths of the directions of dip of the cross-strata were computed for each locality, each azimuth representing a unit vector. A map giving the direction of the vector

mean for each locality, interpreted as the mean wind direction for Permo-Pennsylvanian times, is given in Figure 1.

Thus, contrary to previous work (Agatson, 1954), it was found that cross-laminated units of these formations dip consistently and in a southwesterly direction, from which is inferred an entirely different wind direction (northeasterly) from that characteristic of these latitudes today.

Recent work by Pettijohn (1957) on the cross-stratification of the Precambrian of Ontario and by Potter and Siever (1956) on that of the Pennsylvanian of the eastern interior basin shows that the flow patterns of the paleocurrents are consistent over large areas and are down the regional slope, which is to be expected as the cross-stratification in these cases is shown to be of fluviatile origin. The patterns from the Tensleep, Casper, and Weber formations do not appear to have this relationship. The major positive topographic element of the late Pennsylvanian and early Permian was the ancestral Rocky Mountains of the southeastern corner of Wyoming and Colorado (Agatson, 1954). The distribution of the cross-bedding seems to bear no relation to this positive area; the paleocurrent direction is toward the southwest on the east, west, and north sides of the ancestral Rockies, and not related to the regional tectonics. This orientation of directional pattern with respect to positive elements is best explained as a result of eolian transport.

Statistical Analysis of the Results

From the determination of the azimuths of the lines of greatest dip on N sets of cross-strata from one locality, a vector mean direction can be calculated, which will be an estimate of the mean paleowind direction at that place. The vector mean direction is the only mean that can be calculated without indeterminacy, where, as in this case, the directions are scattered over about 180°. Assuming this hypothesis and the principle of maximum likelihood, it can be shown that the probability-distribution function $P(\theta)$ of azimuths making angle θ with the mean is given by the normalized expression

$$P(\theta) = \frac{1}{2\pi I_0(K)} \exp (K \cos \theta) \qquad (1)$$

where $I_0(K)$ is the modified Bessel function of the first kind of zero order, and K can be conveniently termed the precision.

Were the dunes exactly similar in shape with their axes parallel, and azimuths measured at random at different parts of a number of dunes, then the probability-distribution function would be simply related to the dune shape. This is not, however, a likely state of affairs because of the irregularity of the dunes, and the distribution (1), the circular normal distribution, fits the data well. For closely clustered directions, equation (1) approaches the normal distribution with a standard deviation equal to $57\sqrt{1/K}$ (in degrees).

In general if the N directions are represented by unit vectors and the length of the resultant vector is R, then the vector strength R/N is an inverse measure of the dispersion of the directions. Reiche (1938) used R/N, which he called the consistency ratio, as an empirical measure of the grouping of the directions in his analysis of the cross-stratification in the Coconino sandstone. Now the center of gravity of N points on the unit circle lies at a distance R/N from its center. But by equation (1) this distance is also equal to

$$\int_0^{\pi} \cos\theta \exp (K \cos\theta)\, d\theta \Big/ \int_0^{\pi} \exp (K \cos\theta)\, d\theta = I_1(K)/I_0(K)$$

$$\therefore I_1(K)/I_0(K) = R/N$$

where $I_1(K)$ is the modified Bessel function of the first kind of the first order. Thus K can be estimated from the value of R/N calculated from a sample, and Court (1952) gives tables for this purpose. Table 1 lists the localities at which measurements were taken, and the mean direction, vector strength, and estimated K are given.

Histograms (in 5° or 10° class intervals) fitted by equation (1) for the Tensleep, Casper, and Weber formations are given in Figure 2. The vector means for the three formations are in good agreement: they and the corresponding vector-strengths derived values of K are shown in Table 1. For comparison all the observations of Knight (1929) are plotted in Figure 2d, and these results, as well as those for his two localities separately, are given in Table 1. Although the mean direction is close to our value for this formation, the dispersions of his observations are greater (*i.e.*, K is less). The reason for this is that we measured azimuth only on cross-strata of dip greater than 20°, because the attitude of deposition of these would be more likely to be dictated by the

TABLE 1.—WIND-DIRECTION DATA FOR THE TENSLEEP, CASPER, AND WEBER FORMATIONS OF THE WESTERN UNITED STATES

Ref. to Fig. 1.	Locality	Township and range	Mean azimuth of dip (east of north)	N	R	R/N	K
		Casper Sandstone					
1.	Sand Creek,* Albany Co.	S1, 12, T. 12 N., R. 75 W.	236°	388	177.3	0.46	1.04
2.	Red Buttes, *Albany Co.	S1, 2, 11–14, T. 14 N., R. 73 W.	199°	424	228.6	0.54	1.29
	All Knight's observations on the Casper sandstone:		214°	812	362.4	0.45	1.00
3.	Alcova, Natrona Co.	S16, 17, T. 30 N., R. 83 W.	211°	32	23.0	0.72	2.14
4.	Casper, Natrona Co.	S6, 7, T. 32 N., R. 80 W.	192°	29	25.4	0.88	4.48
5.	Laramie, Albany Co.	S16–18, R. 72 W., T. 15 N.	225°	26	14.5	0.56	1.36
	All the author's observations on the Casper sandstone:		207°	87	61.0	0.70	2.03
		Tensleep Sandstone					
6.	Flat Top Mountain	S8, 9, T. 23 N., R. 78 W.	186°	30	21.6	0.72	2.14
7.	Troublesome Creek, Carbon Co.	S20, T. 25 N., R. 81 W.	153°	29	14.1	0.49	1.13
8.	Tensleep Canyon, Washakie Co.	S1, 12, T. 47 N., R. 88 W.	207°	31	28.0	0.90	4.87
9.	Hyettesville, Big Horn Co.	S10, 15, 16, T. 50 N., R. 89 W.	226°	31	26.5	0.85	3.68
10.	Copper Hill, Hot Springs Co.	S13, 14, T. 41 N., R. 94 N.	211°	30	24.0	0.80	2.87
11.	Dinwoody Lakes, Fremont Co.	S1, 2, T. 4 N., R. 6 W.	195°	31	15.8	0.51	1.19
12.	Sinks of the Pope Agie, Fremont Co.	S7, 8, T. 32 N., R. 100 W.	196°	31	24.8	0.80	2.75
13.	Lander, Fremont Co.	S32, 30, 19, T. 31 N., R. 99 W.	195°	26	22.8	0.88	4.45
	All observations on the Tensleep sandstone:		200°	239	168.8	0.70	2.01
		Weber Sandstone					
14.	Manila, Utah	S3, T. 2 N., R. 19 E.	249°	30	25.1	0.84	3.48
15.	Skull Creek, Colo.	S30, T. 2 S., R. 22 E.	202°	37	32.7	0.88	4.48
16.	Brush Creek Gorge, Utah	S24, T. 2 S., R. 21 E.	226°	32	26.4	0.83	3.30
17.	Sand Canyon, Colo.	S18, T. 6 N., R. 103 W.	204°	32	25.5	0.80	2.87
18.	Split Mountain, Dinosaur Nat. Mon.	S14, T. 4 S., R. 23 E.	203°	30	24.8	0.83	3.30
	All observations on the Weber sandstone:		216°	161	127.2	0.79	2.75

* Calculated from the observations of Knight (1929)

wind alone, rather than the local irregularities of the surface on which the dunes were being built. Thus Knight finds that the maximum

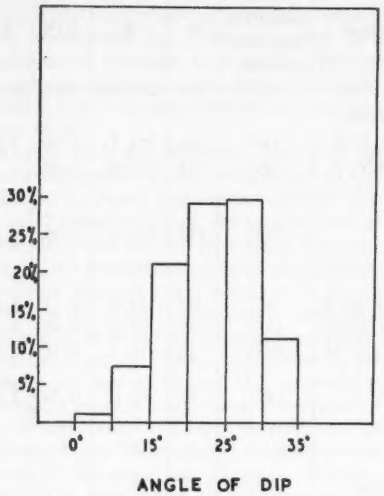

FIGURE 3.—HISTOGRAM OF ANGLES OF DIP OF CROSS-STRATA IN THE TENSLEEP, WEBER, AND CASPER SANDSTONES

number of his readings, 31.8 per cent for the Red Buttes locality and 30.4 per cent for the Sand Creek locality, occur within the interval 20°–25° of dip, whereas for our results (Fig. 3) the corresponding figure is 28 per cent for dips of 25°–30°. Mean directions at the various localities are all reasonably close to each other except that from Troublesome Creek. At this locality the geological tilt is considerable, and a number of faults converge, which makes the determination of the dip of the cross strata subject to error.

GEOPHYSICAL INTERPRETATION OF RESULTS

Figure 4 shows the equators in relation to North America and Europe for Carboniferous, Permian, and Triassic time based on paleomagnetic measurements. North America and Europe are moved 24° closer together (Runcorn, 1956b) by rotating one continent with respect to the other about the present pole, but this change in the paleogeography does not materially affect the argument of this section. The winds determined by Shotton for the British Permian and those for the North American Pennsylvanian both become northeast winds within a belt 0°–20° N. of the equator at that time. A possible explanation of these paleowind results is that they represent the trade winds of late Paleozoic time in Great Britain and in western United States.

If, notwithstanding the paleomagnetic data, these continents and the poles were in their present relationship in late Paleozoic times, there seem to be two alternative explanations of the data:

(1) The paleowinds were not planetary winds but resulted from local geography.

(2) In late Paleozoic time the trade-wind belt extended over a greater range of latitude to include the Western United States and Great Britain.

A number of reasons argue against these alternatives. To the first explanation there are two main objections: (1) The wind directions over nearly 1000 miles in Permo-Pennsylvanian time are substantially constant. The minor variations may plausibly be the result of local geography, but a wind pattern constant over an area of this order is most easily explained as arising from planetary causes. (2) The pattern persists over a long period of geological time. Poole (1957) shows that the Wingate eolian sandstone of Triassic age and the Navajo eolian sandstone of Jurassic age on the Colorado plateau both indicate a north wind. Results for the equivalent in Wyoming of the Navajo formation, the Nugget formation, are shown in Table 2; they are in agreement with Poole's results. Only in the Chuska sandstone (Tertiary) of Arizona (Wright, 1956) is a wind found similar to the present prevailing winds (*i.e.*, southwest winds). This again is consistent with the paleomagnetic data which show that in Tertiary time North America was in approximately the same position, relative to the pole, as it occupies today.

The second possibility that the trade-wind belt spread over latitudes up to 55° cannot be excluded. However, the Permian winds in Great Britain are east winds relative to the present geographical meridian with very little suggestion of a north component. This would appear to be incompatible with a trade wind and implies that the orientation of Great Britain relative to the earth's axis of rotation was not the same as at present. This of course is what the paleomagnetic angle of declination for Permian time indicates.

The Carboniferous, Permian, and Triassic equators in Figure 4 are based on a survey of

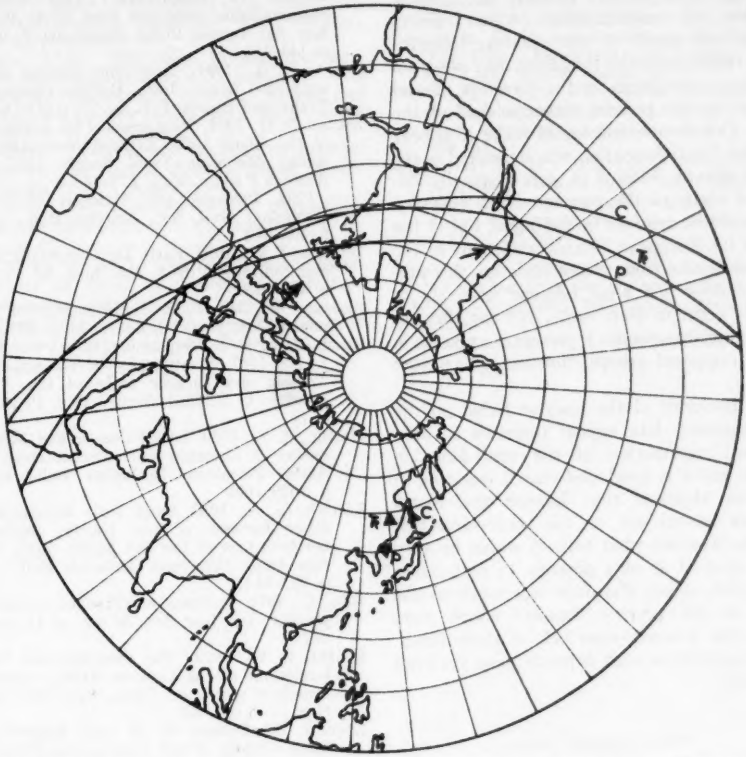

FIGURE 4.—POSITIONS OF EQUATORS AND POLES IN CARBONIFEROUS, PERMIAN, AND TRIASSIC TIME

TABLE 2.—WIND-DIRECTION DATA FOR TWO OUTCROPS OF THE NUGGET FORMATION OF WYOMING

Locality	Township and range	Mean azimuth of dip (east of north)	N	R	R/N	K
1. Lander, Fremont Co.....	S23, 24, 25, T. 31 N., R. 99 W.	175°	47	31.06	0.66	1.79
2. Manila.....	S6, T. 2 N., R. 20 E.	198°	30	25.9	0.86	3.91

European and North American paleomagnetic data from these periods (Creer, Irving, and Runcorn, 1957). The results from the European Permian and Triassic would place most of Europe north of the equator at this time. If North America and Europe are moved 24° closer to each other as indicated by a comparison of the polar-wandering paths from the two continents then most of North America is north of the equators derived from Europe. Collinson and Runcorn (1960) show that results from the Carboniferous and Triassic of North America also place southwestern United States in the northern hemisphere. However,

the Supai formation of Permian age gives a direction of magnetization which places Arizona just south of the equator. Unfortunately results from this formation may possess a secondary component in the direction of and induced by the present magnetic field of the earth. This component would make it appear that the Supai formation was deposited south of the equator even if it were originally deposited north of the equator. This difficulty cannot yet be resolved in the Supai, but in the case of the European Triassic and many of the Triassic results from North America this ambiguity does not arise because reversals of polarity occur in these rocks, and the effect of a secondary component if present is opposite in the two opposed groups, thus cancelling itself out.

The positions of the equator based on the paleomagnetic data appear therefore to offer the best explanation of the wind-direction results, and it is concluded that it was only in the late Mesozoic that Europe and North America moved out of the trade-wind belt into the westerly-wind belt. It would be very satisfactory if it were possible to find eolian sandstones of late Paleozoic age much to the north of the present deposits which were within the westerly-wind belt of those times. Unfortunately no such deposits have yet been reported.

References Cited

Agatson, R. S., 1954, Pennsylvanian and Permian of northern and eastern Wyoming: Am. Assoc. Petroleum Geologists Bull., v. 38, p. 508–583

Bissell, H. J., and Childs, Orlo E., 1958, The Weber formation in Utah and Colorado: Rocky Mountain Assoc. of Petroleum Geologists 1958 Guidebook, p. 26–30

Branson, C. C., 1939, Pennsylvania formations of central Wyoming; Geol. Soc. America Bull., v. 50, p. 1199–1226

Bullard, E. C., and Gellman, H., 1954, Homogeneous dynamos and terrestrial magnetism; Roy. Soc. London Philos. Trans. A, v. 247, p. 213–278.

Collinson, D. W., and Runcorn, S. K., 1960, Polar wandering and continental drift: new evidence from paleomagnetic observations in the United States: Geol. Soc. America Bull., v. 71, p. 915–958

Court, A., 1952, New statistical techniques in geophysics; p. 45–85 *in* Landsberg, H.E., *Editor*, Advances in Geophysics, v. 1, New York, Academic Press, p. 362

Creer, K. M., Irving E., and Runcorn, S. K., 1954, The direction of the geomagnetic field in remote epochs in Great Britain; Jour. Geomagnetism and Geoelectricity, v. 6, p. 163–168

—— 1957, Paleomagnetic investigations in Great Britain, VI: Geophysical interpretation of paleomagnetic directions from Great Britain; Roy. Soc. London Philos. Trans., ser. A, v. 250, p. 144–156

Crowe, P. R., 1951, Wind and weather in the equatorial zone; Inst. British Geographers Trans. and Papers, Pub. no. 17, p. 23–76

Darton, N. H., 1904, Comparison of the stratigraphy of the Black Hills, Bighorn Mountains and Rocky Mountain Front Range; Geol. Soc. America Bull., v. 15, p. 379–448

—— 1908, Paleozoic and Mesozoic of Central Wyoming: Geol. Soc. America Bull., v. 19, p. 403–470

Durham, J. W., 1952, Early Tertiary marine fauna and continental drift: Am. Jour. Sci., v. 250, p. 321–343

Elsasser, W. M., 1955, Hydromagnetism I, A review: Am. Jour. Physics, v. 23, p. 590–609

Harshbarger, J. W., Repenning, C. A., and Irwin, J. H., 1957, Stratigraphy of the uppermost Triassic and Jurassic rocks of the Navajo country: U. S. Geol. Survey Prof. Paper 291, p. 74

Heaton, R. L., 1950, Late Paleozoic and Mesozoic history of Colorado and adjacent areas: Am. Assoc. Petroleum Geologists Bull., v. 34, p. 1659–1698

Kiersch, G. A., 1950, Small scale structures and other features of the Navajo sandstone, northern part of the San Rafael Swell, Utah: Am. Assoc. Petroleum Geologists Bull., v. 34, p. 923–942

King, C., 1876, Paleozoic subdivisions on the 40th parallel: Am. Jour. Sci., 3d ser., v. 11, p. 475–482

Knight, S. H., 1929, The Fountain and Casper formations of the Laramie Basin, a study in genesis of sediments: Univ. Wyo. Pub. in Sci. Geol., v. 1, p. 1–82

Love, J. D., Denson, N. M., and Botinelly, T., 1949, Geology of the Glendo area, Wyoming: U. S. Geol. Survey Prelim. Chart 29, Oil and Gas Invest. Ser.

McKee, E. D., 1934, The Coconino sandstone—its history and origin: Carnegie Inst. Washington Pub. 440, p. 77–115

—— 1940, Three types of cross-lamination in Paleozoic rocks of northern Arizona: Am. Jour. Sci., v. 238, p. 811–824

McKee, E. D., and Weir, G. W., 1953, Terminology for stratification and cross-stratification in sedimentary rocks: Geol. Soc. America Bull., v. 64, p. 381–390

Melton, F. A., 1940, A tentative classification of sand dunes; Its application to dune history of the southern High Plains: Jour. Geology, v. 48, p. 113–173

Pettijohn, F. J., 1957, Sedimentary rocks: New York, Harper and Bros., p. 718

Pierce, W. G., 1947, Bighorn Basin guide book: Wyoming Geol. Assoc., p. 35

Poole, F. G., 1957, Paleowind directions in late Paleozoic and early Mesozoic time on the Colorado Plateau as determined by cross strata (Abstract), Geol. Soc. Am. Bull., v. 68, p. 1870

Potter, P. E., and Siever, R., 1956, Sources of basal Pennsylvanian sediments in the eastern interior basin 3, some methodological implications: Jour. Geology, v. 64, p. 447–455

Reiche, P., 1938, An analysis of cross laminations in the Coconino sandstone: Jour. Geology, v. 46, p. 905–932

Runcorn, S. K., 1954, The earth's core: Am. Geophys. Union Trans., v. 35, p. 49–63

— 1956a, Paleomagnetic survey in Arizona and Utah: Preliminary results: Geol. Soc. America Bull., v. 67, p. 301–316

— 1956b, Paleomagnetic comparisons between Europe and North America: Geol. Assoc. Canada Proc., v. 8, p. 77–85

— 1959, On the theory of the geomagnetic secular variation: Ann. de. Geophys., v. 15, p. 87–92

Shotton, F. W., 1937, The Lower Bunter sandstones of North Worcestershire and East Shropshire: Geol. Mag., v. 74, p. 5

— 1956, Some aspects of the New Red Desert in Britain: Liverpool and Manchester Geol. Jour., v. I, p. 450–466

Twenhofel, W. H., 1950, Principles of sedimentation (2nd ed.): New York, McGraw-Hill, p. 673

Untermann, G. E., and Untermann, B. R., 1954, The Uinta Mountains and vicinity: Utah Geol. Min. Survey Reprint 43, 11 p.

Verville, G. J., 1957, Wolfcampian fusulinids from the Tensleep sandstone in the Bighorn Mountains, Wyoming: Jour. Paleontology, v. 31, p. 349–352

Wright, H. E., Jr., 1956, Origin of the Chuska sandstone, Arizona and New Mexico: A structural and petrographic study of a Tertiary Eolian sediment: Geol. Soc. America Bull., v. 67, p. 413–434

Museum of Northern Arizona, Flagstaff, Arizona; Geology and Physics Departments, King's College, Newcastle upon Tyne, England

Manuscript Received by the Secretary of the Society, August 15, 1958

BULLETIN OF THE GEOLOGICAL SOCIETY OF AMERICA
VOL. 71, PP. 973-982 JULY 1960

CLASSIFICATION OF VOLCANIC BRECCIAS

By Richard V. Fisher

Abstract

Volcanic breccias are grouped into three major categories based upon process of fragmentation: *autoclastic*, *pyroclastic*, and *epiclastic*. Autoclastic volcanic breccias result from internal processes acting during movement of semisolid or solid lava; they include *flow breccia* and *intrusion breccia*. Pyroclastic breccia is produced by volcanic explosion and includes *vulcanian breccia*, *pyroclastic flow breccia*, and *hydrovolcanic breccia*. Epiclastic volcanic breccias result from transportation of loose volcanic material by epigene geomorphic agents, or by gravity, and include *laharic breccia*, *water-laid volcanic breccia*, and *volcanic talus breccia*. Other volcanic breccia terms are discussed.

The rock types mentioned heretofore may also be designated by prefixing compositional terms as in *basaltic block breccia* and *andesitic vulcanian breccia*. The term volcanic breccia is used as a general term applying to all coarse-grained rocks composed of angular volcanic fragments.

CONTENTS

TEXT

	Page
Introduction	973
Acknowledgments	974
Proposed classification	974
Discussion	974
Autoclastic volcanic breccia	974
General statement	974
Flow breccia	974
Volcanic intrusion breccia	975
Pyroclastic breccia	976
General statement	976
Vulcanian breccia	976
Pyroclastic flow breccia	976
Hydrovolcanic breccia	977
Miscellaneous types	977
Epiclastic volcanic breccia	978
General statement	978
Laharic breccia	978
Water-laid volcanic breccia	978
Volcanic talus breccia	979
Miscellaneous types	979
References cited	979

Introduction

The classification proposed herein is intended as a classificatory guide; as a systematic collection of terms needed to relate volcanic breccias genetically; and as an attempt to bring together the ever-growing body of information about volcanic breccias. It should be regarded as a progress report subject to addition, subtraction, or partial or complete rejection, depending upon its usefulness as information continues to accumulate.

Volcanic breccias originate in different ways. They may form on the surface or beneath the surface. Fragments may form during volcanic explosion or during movement of a lava flow, or they may be formed by epigene geomorphic agents acting upon unconsolidated volcanic debris as well as upon solid lava, and all the types may be mixed together.

Since there is such diversity, volcanic breccias cannot be considered only as pyroclastic rocks. Wentworth and Williams (1932, p. 30–33) define volcanic breccia as a pyroclastic rock composed of volcanic fragments which are solidified before aerial flight and deposition. This definition narrowly restricts volcanic breccia in meaning; therefore the present author defined it as "...a rock composed predominantly of angular volcanic fragments greater than 2 mm in size set in a subordinate matrix of any composition and texture, or with no matrix: or of fragments other than volcanic set in a volcanic matrix (Fisher, 1958, p. 1072)." Thus origin is not a factor in the definition.

Many terms for volcanic breccia are in general use, for example, water-laid breccia (C. E. Stearns, 1953, p. 467), explosion breccia (H. T. Stearns and Macdonald, 1942, p. 23), explosive breccia (Rouse, 1937, p. 1267), welded breccia (Erickson, 1953, p. 1370),

autobreccia (Shelton, 1955), vent breccia (H. T. Stearns and Macdonald, 1942, p. 24), throat breccia (Gilluly, 1946, p. 46–47), vent agglomerate (Appledorn and Wright, 1957, p. 458). The proposed classification attempts to systematize such terms.

The review of pyroclastic classifications given by Wentworth and Williams (1932) shows that volcanologists are, in general, interested in classifying pyroclastic ejecta and their mode of origin rather than the resultant rocks and their characteristics, as is attempted in the present paper. The reader is referred to Wentworth and Williams for a review of previous classifications.

Papers reporting volcanic breccias are numerous, therefore references cited in this paper are for the most part limited to papers which discuss origin, nomenclature, or criteria.

Acknowledgments

The writer greatly appreciates the helpful discussions of volcanic breccias with his colleagues Robert W. Webb and Bruce O. Nolf. Special thanks are due Ray E. Wilcox for long and instructive discussions on the general field of pyroclastic rocks. G. O. Macdonald and H. T. Stearns critically reviewed the manuscript and offered appreciated advice.

Proposed Classification

The volcanic breccias are divided into three major types according to the mechanism of fragmentation: *autoclastic*, *pyroclastic*, and *epiclastic*. Autoclastic volcanic breccias contain fragments broken and incorporated during movement of liquid, semisolid, and/or solid lava, such as flow and volcanic intrusion breccias. Pyroclastic breccias contain fragments explosively produced, transported, and deposited. Epiclastic volcanic breccias contain fragments produced by any process of rock fragmentation and transported by any epigene geomorphic agent such as mudflows, running water, glaciers, and sea waves or by gravity (mass wasting).

Volcanic breccias are grouped here primarily on the basis of the type of fragmentation; secondary bases depend upon general usage. Volcanic breccias to be discussed are classified as follows:

- Autoclastic
  - Flow breccia
  - Volcanic intrusion breccia
    - Peperite breccia
    - Friction breccia
- Pyroclastic
  - Vulcanian breccia
  - Pyroclastic flow breccia
  - Hydrovolcanic breccia
- Epiclastic
  - Laharic breccia
  - Water-laid volcanic breccia
  - Volcanic talus breccia

These types can further be designated according to rock composition. Thus there are basaltic block breccias, andesitic laharic breccias, *etc.* The term volcanic breccia may be applied to any of the types given heretofore if they are being referred to in a general way or if their specific origin is unknown.

Discussion

Autoclastic Volcanic Breccia

General statement.—Autoclastic volcanic breccia forms by fragmentation of semisolid and/or solid lava during confinement beneath the surface or by relatively slow movement of unconfined lava flows, rather than by explosive disruption. Grouped here are flow breccia and volcanic intrusion breccia.

Flow breccia.—Flow breccia forms by fragmentation of an advancing and congealing lava flow. Two types of flow breccia are recognized in active volcanic regions: aa and block (Finch, 1933; Jones, 1943) which are definitively discussed by Macdonald (1953). Aa flows are characterized by jagged and spinose surfaces which may be covered with loose fragments. *Aa breccia* is proposed for breccia formed by aa lava flows. Block lava flows are characterized by generally smooth polyhedral blocks. *Block breccia* is proposed for breccia formed from block lava.

Breccias similar to those produced by flow form by collapse or sinking of crusts in a lava lake (H. T. Stearns and Macdonald, 1947, p. 20–21) and if recognized could be termed "collapse breccia."

Several accounts of ancient flow breccia appear in the literature (Dings and Robinson, 1957, p. 32; Kelley, 1946, p. 299; Rouse, 1937, p. 1281; Shelton, 1955, p. 55). Williams (1932b) describes lavas of "block type" from Lassen Volcanic National Park, and Wells (1956) states that "blocky flow breccias" occur in the Roxy formation in southern Oregon. H. T. Stearns reports aa breccia on Tutuila, Samoan Islands (1944, p. 1289 and Pl. 2, fig. 1), and H. T. Stearns, Macdonald, and Swartz (1940, p. 40) report an aa breccia dike on the Island of Lanai.

Huffington (1943, p. 1028) has applied the term flow conglomerate to volcanic flows which have incorporated rounded sedimentary and/or volcanic rocks. But what if the incorporated fragments are angular? Flow breccia, the logical counterpart of flow conglomerate, cannot be used for such a rock; therefore this writer recommends that the term flow conglomerate be abandoned. Alvir (1929) uses the term volglomerate. However, to nomenclaturally separate flows with incorporated foreign fragments from those which contain autoclastic fragments, this author suggests the terms xenolithic flow breccia or xenolithic flow conglomerate. Xenolithic flow breccias are reported by H. T. Stearns and Macdonald (1946, p. 147; 1942, p. 303).

Volcanic intrusion breccia.—Volcanic intrusion breccia forms by movement of liquid, semisolid, or solid lava under confinement within the lithosphere by (1) internal brecciation within a moving solid or semisolid igneous mass, (2) brecciation along the solidified flanks of an intrusion by friction, (3) brecciation and commingling with the material which the lava intrudes, (4) explosions caused by ground water coming in contact with magma, or (5) possibly by the process of fluidization (D. L. Reynolds, 1954).

Volcanic intrusion breccia is a special type of intrusion breccia. Intrusion breccias formed by plutonic intrusions are excluded from the present discussion, although all transitions from "plutonic" to "volcanic" phenomena may exist. A nomenclatural problem is also encountered where volcanic processes cause brecciation of nonvolcanic basement rock as in the case of carbonatite pipes of Mbeya (Fick and van der Heyde, 1959), the Bell-Domingo breccia (Gabelman, 1953; Peters, 1953), and others, although just what constitutes a "volcanic process" might be debated. Here, a volcanic process is considered to be a process related to near-surface igneous activity within vents which reach the earth's surface.

Volcanic intrusion breccia can apply to any volcanic breccia which shows crosscutting relationships, although the special types, *peperite breccia* (*pépérite*), and *friction breccia* may or may not show such features.

Various ideas on the origin of breccia pipes are given by Gates (1959), including accounts by Thompson (1950), Locke (1926), Burbank (1941), Tyrrell (1928), E. B. Bailey *et al.* (1924), Richey (1932; 1940), Lovering and Goddard (1950), Rust (1937), Anderson, Scholz, and Strobell (1955), and Tweto (1951). Gates concludes that the breccia pipes described by him originated by a complex process involving streaming gases, rock bursts, and collapse stoping, along with abrasion, attrition, and wedging, perhaps with many repeated episodes, which formed a complex association of intrusion phenomena.

D. L. Reynolds (1954) described fluidization, a process causing brecciation and rounding of fragments by streaming gases. She discusses breccias (both volcanic and nonvolcanic) formed by this process, such as the Swabian tuff pipes (Cloos, 1941), the breccias of Sudbury (Yates, 1938; Fairbairn and Robson, 1942), and the Tertiary agglomerate vents of Northern Ireland (Richey, 1932; D. L. Reynolds, 1951).

There are many reports of intrusion breccias (Appledorn and Wright, 1957; Curtis, 1954; Durrell, 1944; Hay, 1954; Klepper, Weeks, and Ruppel, 1957; Rouse, 1937; Williams, 1936; Eckel *et al.*, 1949; Gregory, 1951; Lovering and Tweto, 1953, and others).

The formation of intrusion breccia is generally ascribed to violent explosions, although Curtis (1954) has described a mechanism for quiet brecciation (autobrecciation) where breccia formed beneath the surface, flowed onto the surface, and grades into epiclastic volcanic breccias. Likewise, Hay (1954) indicates that intrusive volcanic breccia in the Absaroka volcanic field may be the result of quiet intrusion.

Peperite breccia (*pépérite*) results from shallow intrusion of fluid magma into unconsolidated or poorly consolidated sediments or rocks. Peperite breccia has been described from Marysville Buttes, California (Williams, 1929, p. 166–175), and from near Los Angeles, California (Macdonald, 1939). Intrusion breccia similar to *pépérite* is described by Klepper *et al.* (1957) in the Elkhorn Mountains volcanic rocks of Montana.

Friction breccia forms within differentially rising solid or semisolid magma or between a body of magma and its wall rock. It may be composed entirely of solidified magma fragments or of admixed solidified magma fragments and wall-rock fragments and may have a matrix of dense-textured congealed magma and/or fragmental material formed by attrition.

H. T. Stearns and Macdonald (1947, p. 20) use the term friction breccia for volcanic rocks brecciated by faulting; such breccias should be termed volcanic fault breccia to distinguish between brecciation by primary movement of magma and secondary movement of faulting.

Friction breccia may be caused by the rise of plug domes. Lacroix (1904) has described the plug dome of Mont Pelée. Williams (1932a) gives a general account of domes including plug domes.

Autobrecciation as described by Curtis (1954) is a brecciation process which may occur in volcanic pipes; the material may be extruded onto the surface and move outward as a viscous brecciating flow. This type of extrusion may cause dry avalanches similar to the extrusion at Semeru, Java, in 1885 where lava rose to the edge of the crater without explosion, spilled over the edge, and caused an avalanche. If a crater is filled with water, lahars may result.

Hay (1954, p. 611) describes small, irregular breccia dikes that terminate upward into fine-grained bedded layers but do not extend downward into underlying "tuff-breccia". These might be termed "volcanic clastic dikes". H. T. Stearns (1944, p. 1291 and Fig. 3, p. 1293) describes a clastic dike composed of tuff formed by infilling of ash.

Vent breccia (H. T. Stearns and Macdonald, 1942, p. 24) should be used only if a vent can be recognized. The term throat breccia has also been used to describe breccia within the central core of an intrusive plug (Gilluly, 1946, p. 47–48; Stearns, Macdonald, and Swartz, 1940, p. 46–47).

Pyroclastic Breccia

General statement.—Pyroclastic breccias are formed by explosions and ejection of liquid and/or solid fragments from volcanic sources, and may be divided into three main types: *vulcanian breccia*, *pyroclastic flow breccia*, and *hydrovolcanic breccia*.

The terms explosion breccia (H. T. Stearns and Macdonald, 1946, p. 16) and explosive breccia (Rouse, 1937, p. 1267) are both in use but are more general than pyroclastic breccia, which is preferred by this author.

Wentworth and Williams (1932, p. 25–26) have defined the term agglomerate in two ways:

(1) In their list of suggested usage, definition of terms (p. 45), they define it as follows:

> Agglomerate.—Contemporaneous pyroclastic rocks containing a predominance of rounded or subangular fragments greater than 32 mm. in diameter, lying in an ash or tuff matrix and usually localized within volcanic necks . . . or at a short distance therefrom. The form of the fragments is in no way determined by the action of running water, as in volcanic conglomerates, but is a primary feature determined during actual eruption.

(2) In the table of pyroclastic rock names (p. 51), they use agglomerate as follows (no a direct quote): Fragments (greater than 3 mm) are of material chiefly plastic at the time of eruption and have forms, surface markings, or internal structures assumed in response to forces acting during flight (bombs of any variety), or to forces acting at the time of detachment, or after landing (driblets). The lithified material is termed agglomerate. In the first sense it is broadly defined to include any fragment (regardless of composition or degree of original plasticity) rounded by volcanic action. In the second sense it is narrowly restricted, mainly to particles which were plastic at the time of eruption. Since a term is needed for pyroclastic rocks composed of large, rounded (in distinction to angular) explosion debris, the first definition is preferred. Agglomerate is used in this broad sense by Fick and van der Heyde (1959, p. 859–861) where agglomerate fragments are altered basement gneiss. *Agglutinate* (G. W. Tyrrell *in* Wentworth and Williams, 1932, p. 26) may be considered as a special type of agglomerate.

Vulcanian explosions and the class of explosions which includes *nuées ardentes* produce angular accidental and accessory as well as liquid essential fragments. Lithified pyroclastic deposits composed dominantly of large angular fragments are pyroclastic breccias; if the dominant fragments are large and rounded, the rock is agglomerate.

Vulcanian breccia.—Vulcanian breccia is composed of angular, accessory, essential, or accidental blocks greater than 32 mm produced by vulcanian (or ultravulcanian) explosion.

Tuff breccia (Norton, 1917, p. 170) is a widely used term but is commonly used as a substitute for volcanic breccia as defined by Wentworth and Williams; this use is not recommended because tuff breccia implies a pyroclastic origin. Volcanic breccia as defined by Fisher (1958) is a more suitable general name for breccias of unknown origin. Lapilli-breccia has been used for mixtures of lapilli and larger-grained fragments (Appledorn and Wright, 1957, p. 457).

Pyroclastic flow breccia.—Grouped here are breccias produced by extrusions of solid-liquid-gas mixtures. Williams (1956) recognizes three major types: (1) *Pelean type*, which may result from explosions through flanks of a dome (*nuées ardentes d'explosion dirigée* of Lacroix), or by the collapse of a dome without attendent explosion (*nuée ardente d'avalanche* of Lacroix);

(2) *Krakatoan type*, initiated by vertical low-pressure explosions through craters (*nuées ardentes d'explosions vulcaniennes* of Lacroix); and (3) *fissure type*, initiated by low-pressure upwelling of effervescing magma through fissures. The fissure type is most widespread and develops typical textures and structures of "welded tuff" deposits. Williams uses the term glowing avalanche for these types, but descriptions of such phenomena show that not all "flows" glow, nor are they necessarily avalanches. A suitable term in place of glowing avalanche is pyroclastic flow (Williams, 1941, p. 379). If, in some cases, the material is transported by avalanche, it may be termed pyroclastic avalanche. By suffixing breccia, lapilli, or tuff, as in *pyroclastic flow breccia*, *pyroclastic flow tuff*, *etc.*, one indicates the general origin and grade-size limits. If recognizable, specific types may be given specific names, such as "Peléan breccia" (Mathews, 1952a).

The term ignimbrite (Marshall, 1935) was first used to describe acidic rocks of supposed *nuée ardente* origin, although the term welded tuff (Iddings, 1909, p. 331) has precedence and is most commonly used in the United States for rocks of the same type.

Use of the term welded tuff, however, is not without difficulty, as noted by Mathews (1952a). The "welded tuffs" described by him were too coarse-grained to be tuff and were not welded, so he proposed the terms Peléan tuff-breccia or glowing-avalanche debris. Both these terms, however, are restricted only to the types produced by *nuée ardente*.

Erickson (1953) has described a rock he considers to be welded breccia. The argument against this term is the same as for welded tuff, *i.e.*, breccia formed by pyroclastic flow may not be welded.

The literature on pyroclastic flows is extensive (Anderson and Flett, 1903; Enlows, 1955; Escher, 1933; Gilbert, 1938; Lacroix, 1904; 1930; Perret, 1937; Williams, 1956; and many others). Williams (1956, p. 59–65) gives a brief resumé of the various types as well as criteria for the recognition of their products, and Enlows (1955) gives a detailed review of criteria for their recognition.

Hydrovolcanic breccia.—Hydrovolcanic breccias originate by steam explosions as the result of hot lava coming in contact with water or ice, as in phreatic explosions (H. T. Stearns and Macdonald, 1946, p. 16–17; Williams, 1941, p. 380) and steam explosions resulting from lava flowing from land into water, from non-ice areas onto or against ice, or from lava extruded beneath water or ice.

Primary structural features of lava flowing into water are described by Fuller (1931) and by Hoffman (1933).

Peacock (1926) has ascribed the origin of palagonite-breccia and pillow basalt ("globular basalt") of Viðey, Iceland, to subglacial activity. Subglacial eruptions are a known phenomenon (Barth, 1950; Nielson, 1937).

Noe-Nygaard (1940) postulates that the Palagonite-System of Iceland was partly formed beneath or in the immediate vicinity of ice caps.

Mathews (1952b, p. 553–554) divides volcanic products into four classes dependent upon position with regard to glacial ice as follows: (1) volcanic products laid down beneath the ice (subglacial); (2) volcanic products surrounded on all sides, but not covered by ice at the time of eruption (intraglacial); (3) volcanic products deposited partly or entirely on the surface of the ice (supraglacial); and (4) volcanic products deposited against the margin of the ice. Mathews also gives criteria suggesting proximity of ice during extrusion (p. 553).

Greenwood (1956, p. 167–177) discusses evidence for a Cretaceous submarine eruption causing a local laharic breccia.

Phreatovolcanic breccia is used here for breccia formed by contact of hot lava or magma with ground water or by contact of hot lava with surface water which has seeped underground. Williams (1941, p. 380) calls attention to three types caused by (1) sudden access of surface water to "hot rocks" at depth (Soeoh, Sumatra, Stehn, 1934), (2) influx of ground water into central conduits following drainage of lava below the water table (Kilauea, 1924, H. T. Stearns and Clark, 1930; Jaggar, 1947), and (3) absorption of ground water and consequent crystallization of magmas (Lassen Peak, 1914–1917, Day and Allen, 1925).

Miscellaneous types.—Vent agglomerate is agglomerate located within a vent (Williams, 1926, p. 234–235) and is a pyroclastic rock. *Vent breccia* is composed of angular debris in vents but is not necessarily pyroclastic in origin, for, as pointed out by H. T. Stearns and Macdonald (1942, p. 23, 167–170), vents may be filled by volcanic debris derived from the sides of vents by collapse, explosion, landslide, or washing by water.

An unusual pyroclastic deposit is described

by H. T. Stearns, Bryan, and Crandall (1939, p. 34–35); the clasts are chiefly river gravel, and consequently the deposit looks water-laid. The deposit was apparently formed by phreatic explosions through gravel and sand.

Pseudoagglomerate or *pseudobreccia* are appropriate terms for rocks superficially resembling agglomerate or breccia. Williams (1932b) describes solfatarized andesite which resembles coarse agglomerate. Weathered block lavas may be agglomeratelike in appearance where chemical action has altered the blocks along their interstices. Goodspeed and Coombs (1937) describe a pseudobreccia which resembles dacite flow breccia, but they believe on the basis of microscopic evidence that the breccia originated by recrystallization replacement of a sandy shale. Incomplete replacement left remnants of the clastic rock in the form of fragments.

Epiclastic Volcanic Breccia

General statement.—Epiclastic volcanic breccia contains fragments produced by any type of rock fragmentation which are transported by epigene geomorphic agents or by gravity transfer.

Laharic breccia.—The word lahar comes from the Indonesian word for volcanic materials transported by water and is defined by Van Bemmelen (1949, p. 191) as "a mudflow, containing debris and angular blocks of chiefly volcanic origin. . . ."

Laharic breccias may form by mudflow carrying, dispersing, and depositing coarse- and fine-grained volcanic particles and/or admixed nonvolcanic material. Mudflows grade from extremely viscous to fluid; therefore there are all gradations between laharic and water-laid volcanic breccias.

Volcanic mudflows may originate, according to C. A. Anderson (1933, p. 252–258), as a result of (1) eruptions through crater lakes, causing the melting of ice and snow, following heavy rains or accompanied by heavy rains, and (2) without eruptions with the collapse of the dam of a crater lake, by heavy rains falling on unconsolidated ejecta, and by the rapid melting of ice and snow. Also, they may form when *nuées ardentes* enter streams (Williams, 1956, p. 61–62). Lacroix (1906, p. 668) believes that the unstable condition of loose material on a steep volcanic cone and the consequent rapid denudation is more important than eruptions as a cause of lahars. Greenwood (1956, p. 167–177) reports a submarine laharic breccia.

Lahars have been studied in detail by Kemmerling (1921). Crandall and Waldron (1956) have described a Recent volcanic mudflow from the slopes of Mt. Rainier, Washington. Fisher (1960) has discussed criteria for the recognition of laharic breccias.

Laharic breccia is proposed for volcanic breccias formed by lahars, regardless of initial cause.

Water-laid volcanic breccia.—Water-laid volcanic breccia is composed of angular to subangular volcanic rocks that originate from any volcanic region undergoing rapid erosion. The source material may be pyroclastic debris; fragments may originate from volcanic flows undergoing weathering and erosion. Water-laid volcanic breccias may therefore originate in either active or nonactive volcanic regions and may be transported and deposited in stream channels or deposited in any standing body of water, continental or marine. Such volcanic breccias are true sedimentary rocks.

Many examples of water-laid volcanic breccia are found in the literature, although many of the deposits are referred to as pyroclastic deposits—a use not recommended. Coarse-grained marine "pyroclastic" rocks interbedded with limestone are reported from the Lesser Antilles by Christman (1953, p. 71). "Sedimentary breccia" composed of rocks and minerals derived from lava flows, graywacke, and shale in Alaska is described by Cady *et al.* (1955, p. 47). "Water-laid breccia" (volcanic breccia) is used by C. E. Stearns (1953) for detrital volcanic material deposited by streams on ancient coalesced alluvial fans. A well-bedded fanglomerate deposit from the Island of Hawaii is reported by H. T. Stearns and Macdonald (1946, p. 166). Wells (1956) reports water-laid volcanic rocks in the southern Cascades of Oregon.

Flood deposits may be initiated by subglacial extrusions that generate great quantities of water. In Iceland these floods are known as *jokulhlaup*. Barth (1950, p. 10) reported discharge rates as high as 50,000 m^3/sec. for these floods (as compared with a discharge rate of 10,000 m^3/sec. for the Amazon River).

The fragments of water-laid volcanic breccia, depending upon the length of transportation, either in a stream, lake, or ocean, may show the effects of wear. Thus there is every gradation between volcanic breccia and conglomerate. Also, where pyroclastic flows issue into streams, lahars may result, and, with increasing distance of transportation, will grade into

volcanic gravels, sands, silts, and clays (Williams, 1956, p. 61–62).

Some authors use "volcanic conglomerate" for volcanic breccias deposited by water, regardless of fragment rounding. Lacroix advocated such a use. It is preferable to restrict *volcanic conglomerate* to deposits formed predominantly of large rounded water-worked volcanic fragments. T. L. Bailey (1926, p. 109) sets the lower size limit of volcanic conglomerate at 1 mm, but to be consistent within commonly accepted size limits for conglomerate, 2 mm is recommended (Fisher, 1958).

Volcanic breccia-conglomerate or volcanic conglomerate-breccia are terms suitable for transitional phases of water-laid coarse-grained volcanic rocks containing approximately equal amounts of both angular and rounded particles.

Volcanic talus breccia.—Volcanic talus breccia is composed of angular volcanic fragments, with or without matrix, formed by mass transfer. These breccias form in active or in old volcanic regions.

In areas of active volcanism, talus breccia accumulates around the lower slopes of volcanic cones and within craters by avalanche or landslide due to oversteepening of slopes. Such processes on Vesuvius are described by Perret (1924). Talus breccia (*breches d'ecroulement*, Lacroix, 1906, p. 636) also forms by the protrusion of domes and spines Williams (1932a).

Talus breccia developed within upper Pliocene(?) volcanic rocks in Idaho is described by H. T. Stearns and Isotoff (1956, p. 27). H. T. Stearns and Macdonald (1942) interpret some vent breccias on the Island of Maui, Hawaii, in part as talus breccia which developed in inactive craters. Earthquakes were a cause of volcanic landslides and talus accumulations on the Island of Hawaii in 1868 and 1929 (H. T. Stearns and Macdonald, 1946, p. 51) and on the Island of Maui in 1938 (H. T. Stearns and Macdonald, 1942, p. 60).

Miscellaneous types.—Epiclastic volcanic breccias may form in nearly any of the ways shown in the classifications of Norton (1917) and J. H. Reynolds (1928). One type which has received some attention is produced by glaciation of volcanic regions (Byers *et al.*, 1947; Mathews, 1947; 1951a; 1951b, 1952a; 1952b; Simons and Mathewson, 1955; H. T. Stearns, 1945). Volcanic breccia formed by glaciation (glacial volcanic breccia) is similar to all glacial breccias except in its composition of fragments.

References Cited

Alvir, A. D., 1929, A geological study of the Angat-Novaliches region: Philippine Jour. Sci., v. 40, no. 3, p. 359–419

Anderson, C. A., 1933, The Tuscan formation of northern California: Univ. Calif. Dept. Geol. Sci. Bull., v. 23, p. 215–276

Anderson, C. A., Sholz, E. A., and Strobell, J. D., Jr., 1955, Geology and ore deposits of the Bagdad area, Yavapai county, Arizona: U. S. Geol. Survey Prof. Paper 278, 103 p.

Anderson, T., and Flett, J. S., 1903, Report on the recent eruptions of the Soufrière in St. Vincent in 1902: Royal Soc. London Philos. Trans., A, v. 200, pt. 1, p. 353–553

Appledorn, C. R., and Wright, H. E., Jr., 1957, Volcanic structures in the Chuska Mountains, Navajo reservation, Arizona-New Mexico: Geol. Soc. America Bull., v. 68, p. 445–468

Bailey, E. B., *et al.*, 1924, The Tertiary and post Tertiary geology of Mull, Loch Aline and Obine: Geol. Survey Scotland Mem., 445 p.

Bailey, T. L., 1926, The Gueydan, a new Middle Tertiary formation from the southwestern coastal plain of Texas: Univ. Texas Bull. no. 2645, 187 p.

Barth, T. F. W., 1950, Volcanic geology, hot springs and geysers of Iceland: Carnegie Inst. Washington Pub. 587, 174 p.

Burbank, W. S., 1941, Structural control of ore deposition in the Red Mountains, Sneffels, and Telluride districts of the San Juan Mountains, Colorado: Colo. Sci. Proc., v. 14, p. 141–261

Byers, F. M., Jr., Hopkins, O. M., Weir, K. L., and Fisher, B., 1947, Volcanic investigations on Umnak Island, 1946: U. S. Geol. Survey Alaska Volcano Investigation, Rept. no. 2, Progress of Investigations in 1946, pt. 3, p. 19–53

Cady, W. M., Wallace, R. E., Hoare, J. M., and Webber, E. J., 1955, The central Kuskokwim region, Alaska: U. S. Geol. Survey Prof. Paper 268, 132 p.

Christman, R. A., 1953, Geology of St. Bartholomew, St. Martin, and Anguilla, Lesser Antilles: Geol. Soc. America Bull., v. 64, p. 65–96

Cloos, H., 1941, Bau und Tätigkeit von Tuffschloten. Untersuchungen an dem Schwäbischen vulkan: Geol. Rundschau, v. 32, p. 709–800

Crandell, D. R., and Waldron, H. H., 1956, A recent mudflow of exceptional dimensions from Mt. Rainier, Washington: Am. Jour. Sci., v. 254, p. 349–362

Curtis, G. H., 1954, Mode of origin of pyroclastic debris in the Mehrten formation of the Sierra Nevada: Univ. Calif., Dept. Geol. Sci. Bull., v. 29, p. 453–502

Day, A. L., and Allen, E. T., 1925, The volcanic activity and hot springs of Lassen Peak: Carnegie Inst. Washington Pub. no. 360, 190 p.

Dings, M. G., and Robinson, C. S., 1957, Geology and ore deposits of the Garfield quadrangle, Colorado: U. S. Geol. Survey, Prof. Paper 289, 110 p.

Durrell, Cordell, 1944, Andesite breccia dikes near Blairsden, California: Geol. Soc. America Bull., v. 55, p. 255–272

Eckel, E. B., Williams, J. S., Galbraith, F. W., *et al.*, 1949, Geology and ore deposits of the La Plata district, Colorado: U. S. Geol. Survey Prof. Paper 219, 179 p.

Enlows, H. E., 1955, Welded tuffs of Chiricahua National Monument, Arizona: Geol. Soc. America Bull., v. 66, p. 1215–1246

Erickson, R. L., 1953, Stratigraphy and petrology of the Tascotal Mesa quadrangle, Texas: Geol. Soc. America Bull., v. 64, p. 1353–1386

Escher, B. G., 1933, On a classification of central eruptions: Leidsche Geol. Meded., Deel VI, Afl., I, p. 45–48

Fairbairn, H. W., and Robson, G. M., 1942, Breccia at Sudbury, Ontario: Jour. Geology, v. 50, p. 1–33

Fick, L. J., and van der Heyde, C., 1959, Additional data on the geology of the Mbeya Carbonatite: Econ. Geology, v. 54, p. 842–872

Finch, R. H., 1933, Block lava: Jour. Geology, v. 41, p. 769–770

Fisher, R. V., 1958, Definition of volcanic breccia: Geol. Soc. America Bull., v. 69, p. 1071–1073

—— 1960, Criteria for recognition of laharic breccias, southern Cascade Mountains, Washington: Geol. Soc. America Bull., v. 71, p. 127–132

Fuller, R. E., 1931, The aqueous chilling of lava on the Columbia River basalt: Am. Jour. Sci., ser. 5, v. 21, p. 281–300

Gabelman, J. W., 1953, Definition of a mineral belt in south central Colorado: Econ. Geology, v. 48, p. 177–210

Gates, Olcott, 1959, Breccia pipes in the Shoshone Range, Nevada: Econ. Geology, v. 54, p. 790–815

Gilbert, C. M., 1938, Welded tuff in eastern California: Geol. Soc. America Bull., v. 49, p. 1829–1861

Gilluly, J., 1946, The Ajo mining district, Arizona: U. S. Geol. Survey Prof. Paper 209, 112 p.

Goodspeed, G. E., and Coombs, H. A., 1937, Replacement breccias of the lower Keechelus: Am. Jour. Sci., v. 34, p. 12–23

Greenwood, R., 1956, Submarine volcanic mudflows and limestone dikes in the Grayson formation (Cretaceous) of central Texas: Gulf Coast Assoc. Geol. Soc. Trans., v. 6, p. 167–177

Gregory, H. E., 1951, The geology and geography of the Paunsaugunt region, Utah: U. S. Geol. Survey Prof. Paper 226, 116 p.

Hay, R. L., 1954, Structural relationships of tuff breccia in Absaroka Range, Wyoming: Geol. Soc. America Bull., v. 65, p. 605–620

Hoffman, M. G., 1933, Structural features in the Columbia River lavas of central Washington: Jour. Geology, v. 41, p. 184–195

Huffington, R. M., 1943, Geology of the northern Quitman Mountains, Trans-Pecos, Texas: Geol. Soc. America Bull., v. 54, p. 987–1048

Iddings, J. P., 1909, Igneous rocks: New York, John Wiley and Sons, v. I, 464 p.

Jaggar, T. A., 1947, Origin and development of craters: Geol. Soc. America Mem. 21, 508 p.

Jones, A. F., 1943, Classification of lava surfaces: Am. Geophys. Union Trans., 24*th* Ann. Mtg., pt. 1, p. 265–268

Kelley, V. C., 1946, Geology, ore deposits, and mines of the Mineral Point, Poughkeepsie, and Upper Uncompaghre districts, Ouray, San Juan, Hinsdale counties, Colorado: Colo. Sci. Soc. Proc., v. 14, p. 287–466

Kemmerling, G. L., 1921, De witbarsting van der G. Keloet inden nacht van den 19den op den 20sten Mei 1919: Dienst v. h. Mijnwezen Ned. O. Ind. Vulk. Med. No. 2, 120 p.

Klepper, M. R., Weeks, R. A., and Ruppel, E. T., 1957, Geology of the southern Elkhorn Mountains, Jefferson and Broadwater counties, Montana: U. S. Geol. Survey Prof. Paper 292, 82 p.

Lacroix, A., 1904, La Montagne Pelée et ses éruptions: Paris, Masson et Cie, editeurs, 662 p.

—— 1906, Contribution a l'étude des brèches et conglomérats volcaniques: Bull. Soc. Geol. France, ser. 4, v. 6, p. 635–685

—— 1930, Remarques sur les matériaux de projection des volcans et sur la genèse des roches pyroclastiques qu'ils constituent: Jubilee Vol. 1830–1930, Centennaire de la Société Géologique de France, Tome II, p. 421–472

Locke, A., 1926, The formation of certain ore bodies by mineralization stoping: Econ. Geology, v. 21, p. 431–453

Lovering, T. S., and Goddard, E. N., 1950, Geology and ore deposits of the Front Range, Colorado: U. S. Geol. Survey Prof. Paper 223, 319 p.

Lovering, T. S., and Tweto, O. 1953, Geology and ore deposits of the Boulder County tungsten district, Colorado: U. S. Geol. Survey Prof. Paper 245, 199 p.

Macdonald, G. A., 1939, An intrusive peperite at San Pedro Hill, California: Univ. Calif., Dept. Geol. Sci. Bull., v. 24, p. 329–338

—— 1953, Pahoehoe, aa and block lava: Am. Jour. Sci., v. 251, p. 169–191

Marshall, P., 1935, Acid rocks of the Taupo Rotorua volcanic district: Royal Soc. New Zealand Trans., v. 64, p. 328–366

Mathews, W. H., 1947, "Tyuas", flat-topped volcanoes in northern British Columbia: Am. Jour. Sci., v. 245, p. 560–570

—— 1951a, Historic and prehistoric fluctuations of alpine glaciers in the Mount Garibaldi map-area, southwestern British Columbia: Jour. Geology, v. 59, p. 357–380

—— 1951b, The Table, a flat topped volcano in southern British Columbia: Am. Jour. Sci., v. 249, p. 830–841

—— 1952a, Mount Garibaldi, a supraglacial Pleistocene volcano in southwestern British Columbia: Am. Jour. Sci., v. 250, p. 81–103

—— 1952b, Ice-dammed lavas from Clinker Mountain, southwestern British Columbia: Am. Jour. Sci., v. 250, p. 553–565

Nielson, B., 1937, A volcano under an ice cap, Vatnajökull, Iceland, 1934–1936: Geog. Jour., London, v. 40, p. 6–23

Noe-Nygaard, A., 1940, Subglacial activity in ancient and recent times: K. Dansk. Geog. Selsk., Folia Geog. Danica, v. 1, no. 2, 67 p.

Norton, W. H., 1917, Studies for students: A classification of breccias: Jour. Geology, v. 25, p. 160–194

Peacock, M. A., 1926, The geology of Viðey, southwest Iceland: Royal Soc. Edinburgh Trans., v. 54, p. 441–465

Perret, F. A., 1924, The Vesuvius eruption of 1906: Carnegie Inst. Washington Pub. no. 339, 151 p.

—— 1937, The eruption of Mont Pelée, 1929–1932: Carnegie Inst. Washington Pub. no. 458, 125 p.

Peters, W. C., 1953, Definition of a mineral belt in south central Colorado; discussion: Econ. Geology, v. 48, p. 599–600

Reynolds, D. L., 1951, The geology of Slieve Gullion, Foughill and Carrickcarnan: an

actualistic interpretation of a Tertiary gabbro-granophyre complex: Royal Soc. Edinburgh Trans., v. 62, pt. 1, p. 85–143
—— 1954, Fluidization as a geological process, and its bearing on the problem of intrusive granites: Am. Jour. Sci., v. 252, p. 577–614
Reynolds, J. H., 1928, Breccias: Geol. Mag., v. LXV, no. 3, p. 97–107
Richey, J. E., 1932, The Tertiary ring complex of Slieve Gullion: Geol. Soc. London Quart. Jour., v. 88, p. 776–849
—— 1940, Association of explosive brecciation and plutonic intrusions in the British Tertiary igneous province: Bull. Volcanologique, ser. 2, tome 7, p. 157–175
Rouse, J. T., 1937, Genesis and structural relationships of the Absaroka volcanic rocks, Wyoming: Geol. Soc. America Bull., v. 48, p. 1257–1296
Rust, G. W., 1937, Preliminary notes on explosive volcanism in southeastern Missouri: Jour. Geology, v. 45, p. 48–75
Shelton, J. S., 1955, Glendora volcanic rocks, Los Angeles Basin, California: Geol. Soc. America Bull., v. 66, p. 45–90
Simons, F. S., and Mathewson, D. E., 1955, Geology of Great Sitkin Island, Alaska: U. S. Geol. Survey, Bull. 1028-B, 43 p.
Stearns, C. E., 1953, Tertiary geology of the Galisteo-Tonque area, New Mexico: Geol. Soc. America Bull., v. 64, p. 459–508
Stearns, H. T., 1944, Geology of the Samoan Islands: Geol. Soc. America Bull., v. 55, p. 1279–1332
—— 1945, Glaciation of Mauna Kea, Hawaii: Geol. Soc. America Bull., v. 56, p. 267–274
Stearns, H. T., and Clark, W. O., 1930, Geology and water resources of the Kau district, Hawaii: U. S. Geol. Survey Water Supply Paper 616, p. 29–191
Stearns, H. T., and Isotoff, A., 1956, Stratigraphic sequence in the Eagle Rock volcanic area near American Falls, Idaho: Geol. Soc. America Bull., v. 67, p. 19–34
Stearns, H. T., and Macdonald, G. A., 1942, Geology and ground-water resources of the Island of Maui, Hawaii: Hawaii Div. Hydrography Bull. 7, 344 p.
—— 1946, Geology and ground-water resources of the Island of Hawaii: Hawaii Div. Hydrography Bull. 9, 363 p.
—— 1947, Geology and ground-water resources of the Island of Molokai, Hawaii: Hawaii Div. Hydrography Bull. 11, 113 p.
Stearns, H. T., Bryan, L. L., and Crandall, Lynn, 1939, Geology and water resources of the Mud Lake Region, Idaho: U. S. Geol. Survey Water Supply Paper 818, 125 p.
Stearns, H. T., Macdonald, G. A., and Swartz, J. H., 1940, Geology and ground-water resources of the islands of Lanai and Kahoolawe, Hawaii: Hawaii Div. Hydrography, Bull. 6, 177 p.
Stehn, C. E., 1934, Die semivulkanischen Explosionen des Pematang Bata in der Soeoh-Senke (Süd Sumatra) in Jahre 1933: Natuurk. Tijdschr. voor Ned.-Indië, v. 94, p. 46–69
Thompson, G. A., Jr., 1950, Structural geology of the Terlingua quicksilver district, Texas: U. S. Geol. Survey Open File Report 55
Tweto, Ogden, 1951, Form and structure of sills near Pando, Colorado: Geol. Soc. America Bull., v. 62, p. 507–532
Tyrrell, G. W., 1928, The geology of Arran: Geol. Survey Scotland Mem., 292 p.
Van Bemmelen, R. W., 1949, The geology of Indonesia, v. 1A: The Hague, Martinus Nijhoff, 732 p.
Wells, F. G., 1956, Geology of the Medford quadrangle, Oregon-California: U. S. Geol. Survey Map GQ 89
Wentworth, C. K., and Williams, H., 1932, The classification and terminology of the pyroclastic rocks: Nat. Research Council, Rept. Comm. Sedimentation, Bull. 89, p. 19–53
Williams, H., 1926, Notes on the characters and classification of pyroclastic rocks: Geol. Soc. Liverpool, Proc., v. 14, p. 223–248
—— 1929, Geology of the Marysville buttes, California: Univ. Calif. Dept. Geol. Sci. Bull., v. 18, p. 103–220
—— 1932a, The history and character of volcanic domes: Univ. Calif., Dept. Geol. Sci. Bull., v. 21, p. 51–146
—— 1932b, Geology of Lassen Volcanic National Park: Univ. Calif., Dept. Geol. Sci. Bull., v. 21 p. 195–385
—— 1936, Pliocene volcanoes of the Navajo-Hopi country: Geol. Soc. America Bull., v. 47, p. 111–172
—— 1941, Volcanology: Geol. Soc. America Fiftieth Anniv. Vol., p. 367–390
—— 1956, Glowing avalanche deposits of the Sudbury basin: Ontario Dept. Mines, 65th Ann. Rept. v. LXV, pt. 3, p. 57–89
Yates, A. B., 1938, The Sudbury intrusive: Royal Soc. Canada Trans., 3d ser., v. 32, p. 151–172

UNIVERSITY OF CALIFORNIA, GOLETA, CALIFORNIA
MANUSCRIPT RECEIVED BY THE SECRETARY OF THE SOCIETY, FEBRUARY 16, 1959

Introductio
Physiograp
Borderin
Islands
Gulf floo
Climate an
Sediments
General
Texture
Composi
Genera
Detrit
Clay
Authig
Calcar
Organi
Organi
Sulfur
Miscella
Rate of
Conclusion
Origin o
Lithofaci
Diatoma
References

Figure
1. Physio
Mex

BULLETIN OF THE GEOLOGICAL SOCIETY OF AMERICA
VOL. 71, PP. 983–1010, 14 FIGS., 2 PLS. JULY 1960

SEDIMENTS OF THE GULF OF CALIFORNIA

BY JOHN V. BYRNE AND K. O. EMERY

ABSTRACT

The Gulf of California is an elongate trough bordered by highlands on the west and mostly by lowlands on the east. Fault scarps divide its floor into a succession of closed basins separated by ridges, some of which are capped by islands. Water flows into the open sea along the east side and leaves along the west side after partial evaporation. About half of the runoff from land reaching the gulf enters at its head via the Colorado River, but dilution of the gulf water is not evident. Winter upwelling caused by northwesterly winds brings high-nutrient (including high-silica) water to the surface where diatoms and other phytoplankton flourish so abundantly that they discolor the water. On death, the siliceous frustules fall to the bottom forming diatomaceous muds in the middle third of the gulf. High-organic matter in the muds is also a result of high production in surface waters and of anaerobic conditions within the sediments, although not in the water above them. Sediments of the northern third of the gulf are deltaic, and those of the southern third are normal marine green muds. Sands and gravels composed of shell debris and detritus from land are concentrated along the shores and in channels between islands where tidal currents are swift. The physiography and geological history indicate that the gulf is a taphrogeosyncline. Its sediments should form chiefly shale and graywacke, facies considered typical of geosynclines, although climatic and oceanographic factors may be more responsible for their deposition than are tectonic factors.

CONTENTS

TEXT

	Page
Introduction	984
Physiography and areal geology	984
Bordering lands	984
Islands	986
Gulf floor	986
Climate and oceanography	988
Sediments	992
General	992
Texture	993
Composition	995
General	995
Detrital sand and silt	995
Clay	998
Authigenic minerals	998
Calcareous material	998
Organic silica	999
Organic matter	999
Sulfur constituents	999
Miscellaneous properties	1003
Rate of deposition	1004
Conclusions and geological significance	1005
Origin of gulf	1005
Lithofacies of gulf	1006
Diatomaceous muds	1006
References Cited	1008

ILLUSTRATIONS

Figure	Page
1. Physiographic provinces of northwestern Mexico	985
2. Generalized bathymetric chart of the gulf	987
3. Regional sections across the Gulf of California	988
4. Basins of the Gulf of California	989
5. Properties of gulf water	990
6. Temperature and salinity sections	991
7. Areas in which phytoplankton blooms have been observed	993
8. Distribution of median diameters of surface sediments	994
9. Distribution of sediment types	996
10. Average composition of sediment types of Figure 9	997
11. Distribution of calcium carbonate (acid-soluble material) and organic silica (mostly diatoms) in surface sediments	1000
12. Distribution of organic nitrogen (micro-Kjeldahl) in surface sediments as compared with contours of percentage of clay	1001
13. Some properties of diatomaceous mud in a core	1003
14. Probable lithofacies to be expected of present surface sediments	1007

Plate	Facing page
1. Rocket view of region	998
2. Laminated diatomaceous sediments	999

TABLES

Table	Page
1. Properties of basin waters	992
2. Average parameters of sediment types	1002
3. Properties of diatomaceous sediments	1008

Introduction

The Gulf of California was the first part of the eastern Pacific Ocean to be explored by Europeans. In 1533, only 12 years after the fall of Mexico City, Hernando Cortez sent an ill-fated expedition north from Acapulco, but on reaching the area of La Paz most of the members were killed in an Indian attack. Two years later, interested by pearls brought to him by the survivors, Cortez himself made a short trip to La Paz. During the next few years more detailed explorations of the gulf were ordered by Cortez, and two, under Francisco de Ulloa in 1539 and Hernando de Alarcón in 1540, succeeded in reaching the head of the gulf by ship. Nevertheless, 80 years later the belief became current that the gulf was open to the north—a strait that separated an island 2500 km long from the mainland. Not until 1701 was the true form of the gulf re-established, this time by Eusebio Francisco Kino, a Jesuit priest, who traveled by land. Another Jesuit, Fernando Consag, charted the head of the gulf by boat in 1721, invalidating once and for all the notion that Baja California is an island.

The main result of the early Spanish expeditions was the mapping of shore lines. The underwater form of the gulf was not studied in any detail until 1873–1875 when it was sounded by two U. S. Navy ships under the command of admiral-to-be George Dewey. His maps form almost the entire basis for navigational charts of the region published before 1940.

With the development of southern California came increased interest in the scientific problems of the nearby gulf. Cruises throughout the gulf chiefly for biological collecting were organized by the U. S. Fish Commission in 1889 (Townsend, 1901), by the California Academy of Sciences in 1921 (Slevin, 1923), and by the Allan Hancock Foundation of the University of Southern California in 1936, 1937, and 1940. The first information concerning the oceanography and sediments was obtained by two expeditions of Scripps Institution of Oceanography (University of California) in 1939 and 1940. Emery was a member of the second of these cruises, which was under the leadership of F. P. Shepard and Roger Revelle—a research project financed jointly by The Geological Society of America and Scripps Institution. Data presented in this report were obtained chiefly from the two Scripps Expeditions supplemented by some material from the Hancock Expeditions. Most of them were assembled by Byrne in 1957 as a doctoral dissertation, portions of which are summarized here. Appreciation is expressed to Allan Hancock Foundation for providing laboratory facilities, to the Humble Division of the Humble Oil and Refining Company for financial aid, to S. C. Rittenberg for previously unpublished chemical measurements, and to F. P. Shepard, T. van Andel, G. A. Rusnak, J. C. Griffiths, and F. J. Pettijohn for critical review of the manuscript.

Physiography and Areal Geology

Bordering Lands

Figure 1, modified from Ordóñez (1936) and Beal (1948), summarizes the physiography of the land areas near the gulf. Seven physiographic provinces border the gulf, four on the west, one on the north, and two on the east.

The Southern Cape province west of the gulf consists of highly metamorphosed sediments intruded by crystalline rocks and locally overlain by Miocene and Pliocene sediments. The only major break in the mountainous backbone of the peninsula is the narrow Isthmus of La Paz, a lowland floored by sediments and separated probably by faults from adjacent mountain ranges. North of the isthmus and bordering most of the southern half of the western coast of the gulf is the South-Central Peninsula province, a westward-tilted volcanic tableland which has a precipitous eastern slope down to the gulf. Miocene to Recent volcanic flows and pyroclastics are locally overlain by thick Pliocene to Recent marine and nonmarine sediments, mostly clastic. Farther north, the Northern Peninsula province is also a westward-tilted fault block, which has a very steep eastern slope and elevations at its top locally higher than 3000 m. However, the top surface of this province was cut by erosion across a batholith of Middle Cretaceous age.

At its northern end the gulf is limited by the Colorado Desert, consisting of the delta of the Colorado River and a trough (Imperial Valley) that contains the Salton Sea (Pl. 1). The trough, which has a surface more than 84 m below sea level, is a structural and topographic continuation of the gulf that extends about 250 km beyond the gulf's present northern limit. The delta that bars the ocean from the Salton Sea is almost flat and has a drainage divide only about 10 m. above sea level (Longwell, 1954) and a thickness of more than 6000 m of Pliocene to Recent deltaic sediments (Tarbet, 1951; Dibblee, 1954). Bordering the west side of the delta are the Cocopah Mountains, on the west

side of which is a lowland that seasonally contains water, the Laguna Salada (Pl. 1).

The eastern coast of the gulf is bordered by only two provinces. At the north is the Sonoran Desert, which grades almost imperceptibly into the Colorado Desert farther north. The province consists of broad plains of alluvium through which protrude mountain ranges of Paleozoic and Mesozoic sedimentary, metamorphic, intrusive, and volcanic rocks. The coastal area is low and sandy except for a few rocky points such as one near Guaymas, the largest town bordering the gulf. Farther south, the gulf is bordered by the Pacific Coastal Plain (Fig. 1), a gently sloping alluvial surface broken only by a few volcanic hills. The plain contains many tidal inlets and swamps, covered mostly by mangroves. Inland from both the Sonoran Desert and the Pacific Coastal Plain provinces are the mountains of the Sierra Madre Occidental which reach elevations of more than 2000 m and supply much alluvium to westward-flowing streams. Streams from the Central Plateau east of the Sierra Madre Occidental are blocked from the gulf, as are streams from the Western Cape province of Baja California so that these two provinces need not be considered in discussions of gulf sedimentation.

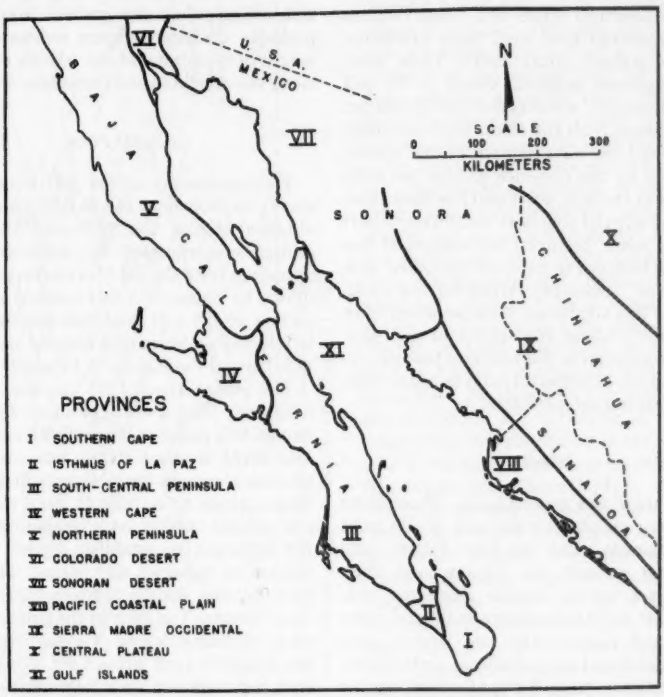

FIGURE 1.—PHYSIOGRAPHIC PROVINCES OF NORTHWESTERN MEXICO
Modified from Ordóñez (1936) and Beal (1948)

Sediments brought to the gulf are controlled largely by the nature of the bordering provinces, The chief source of stream-borne sediments, at least until Hoover Dam was completed in 1935, was the Colorado River. Because of its low gradient across the delta, the river carries fine-grained sediments, mostly fine sands, silts, and clays. The Colorado River, which drains 68 per cent of the area tributary to the gulf, is estimated to have contributed prior to construction of Hoover Dam about 50 per cent of the total amount of stream-borne detrital sediment annually brought to the gulf. Streams draining into the northern part of the eastern side are seasonal but are capable of bringing coarse sediments, sands, and gravels. Many

streams entering southeast of Guaymas are large and permanent but debouch through mangrove swamps that intercept much of the coarser part of the load that otherwise would reach the gulf itself. Streams on the west coast contribute sand and gravel as a result of their seasonal torrential flow, very steep gradients, and coarse-grained source rocks. Thus, most of the fine-grained sediment comes to the gulf at its northern end, whereas most of the coarser sediment comes from the sides. Some sediment is contributed by wave erosion of the shores, as indicated by the presence of high sea cliffs along most of the west coast and low ones along most of the alluvial shores of the northern part of the east coast; however, the amount of this sediment is believed to be small compared with stream-borne sediment. Wind-derived sediment is far less significant because winds blow predominantly along the length of the gulf. Organic production in the waters is the only remaining source of sediment, and in some areas it is the most important source.

Islands

Islands are of two general kinds. Those along the southern mainland coast and at the front of the Colorado delta are low offshore sand islands that protect the lagoons and their swamps from waves. Islands along the peninsular coast and the northern mainland coast are high and rugged. The two largest ones, Tiburón and Angel de la Guarda, reach elevations of 1200 m or more. Except for local sand or gravel beaches, the shores are sea cliffs. Most of these islands lie atop submarine ridges and are structurally complicated by faults and folds. Details of their stratigraphy and structure are given in studies by Hanna (1927), Anderson (1950), and Durham (1950). Islands off the Southern Cape province (Fig. 1) consist of granite overlain by Miocene volcanic and Pliocene sedimentary rocks. The same lithology characterizes the next few islands to the north. The other islands off the South-Central Peninsula province consist of Miocene to Recent volcanic rocks and commonly Pliocene to Recent marine and fluvial sedimentary rocks; thus they have a stratigraphy similar to that of the adjacent peninsula. Two of these islands, Coronado and Tortuga, are volcanic cones, but the shapes of the others are largely controlled by faults. Islands off the Northern Peninsula province are similar to that province in that each has outcrops of granitic and metamorphic rocks overlain by Miocene volcanic and Pliocene to Recent sedimentary rocks.

The small size of the islands and the seasonal nature of their streams permit little stream-borne sediment to reach the gulf, and most of that sediment is coarse-grained. Marine erosion probably contributes more sediment per unit length of coast around the islands than it does along the mainland and peninsular shores.

Gulf Floor

The topography of the gulf is mapped primarily on data from the 28,000 echo soundings obtained during the 1939 and 1940 Scripps cruises supplemented by scattered lead-line soundings from the old Navy surveys. Contours drawn by Shepard (1950) provide an excellent picture of the gulf floor; the interested reader is referred to Shepard's contour maps for details beyond those given in Figure 2.

The gulf is about 1100 km long and tapers irregularly from a width of about 250 km at its mouth to a point at its northern end. The median depth is about 460 m, but, instead of exhibiting a smooth southeasterly deepening, the floor appears to contain 11 deep closed basins and several smaller ones. Sounding density is not sufficient to establish beyond doubt the closure of some of the basins. Three basins have bottom depths between 3200 and more than 3300 m. The floor of the gulf is revealed to have the same degree of gross irregularity as the adjacent land areas (Fig. 3), though the land has more fine-scale irregularities produced by stream erosion. The general impression provided by the cross sections of Figure 3 is that the gulf occupies the western edge of a westward-tilted mainland fault block where it abuts against the eastern edge of another westward-tilted fault block that forms the peninsula. Modification of the simple blocks by secondary faulting and by erosion and deposition has only partly obscured the general structure.

A shelf borders most of the gulf. Although existing soundings are not spaced closely enough to be certain of the precise depths of the shelf break, the mean of 56 crossings of the shelf break is 125 m, nearly the same as the 132-m average depth of the shelf break throughout the world (Shepard, 1948, p. 143). There appears to be no significant departure from the mean except between Guaymas and Angel de la Guarda Island where a greater depth may have resulted from gulfward prograding of the Colorado delta. This part of the shelf is also

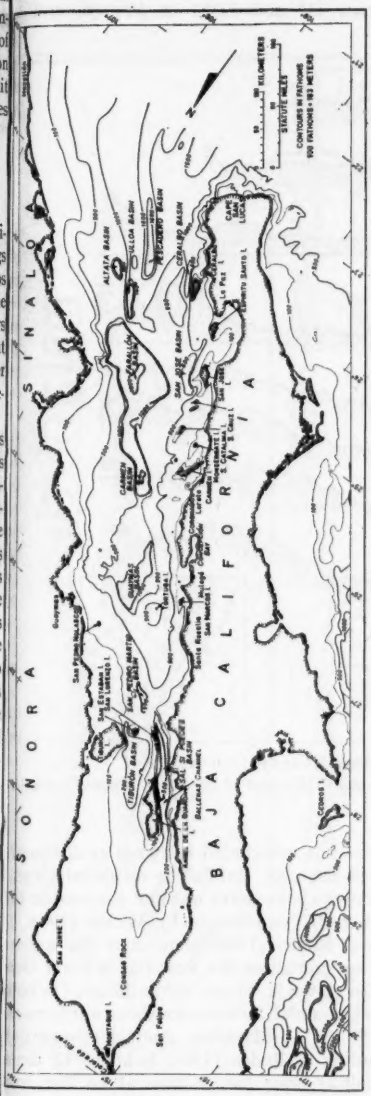

FIGURE 2.—GENERALIZED BATHYMETRIC CHART OF THE GULF
Redrawn from the more detailed chart of Shepard (1950)

the widest of the gulf. Farther southeast on the mainland side the shelf is only moderately wide, averaging about 30 km. In contrast, the shelf is narrow around islands and along most of the peninsula side of the gulf, averaging about 5 km except within broad embayments where it is wider. Although too few rock samples are available to provide a critical test, the presence of the widest shelf off the Colorado delta suggests an origin there through deposition. Elsewhere it is probably due to erosion perhaps accompanied by some deposition.

Beyond the shelves are slopes that lead down into the basins of the gulf. A few may be of depositional origin—where they front wide shelves and are of low declivity. An example is the shelf north of Tiburón Island, where the slope is only about 0.5°. Elsewhere, the slopes are much steeper, with a mean declivity of about 13°. Commonly these slopes are straight, related to fault structures on the adjacent land, and form a sharp angle with the adjacent basin floor. As shown by Shepard (1950) these characteristics are indicative of fault origin. Supporting this suggestion is the fact that the gulf is well-known for its great seismic activity (Gutenberg and Richter, 1949).

Submarine canyons locally have cut into the shelves and slopes of the gulf, as elsewhere in the world; however, the only canyons recognized to date are near the mouth of the gulf. Four canyons fringe the tip of the peninsula, and one is just within the gulf on the mainland side (Shepard, 1950). Inadequate sounding lines suggest the presence of still other canyons near the mouth of the gulf and possibly of smaller ones farther within the gulf.

Most interesting as sites of sediment deposition are the basins that form the deepest areas of the gulf. The 11 larger basins may be grouped into two categories: long narrow basins, which trend northwesterly parallel to the gulf itself, and broad flatter-floored basins that trend more northerly (Fig. 4). Outstanding examples of the first type are Ceralbo and southern Sal si Puedes basins; the only two good examples of the second type are Guaymas and Farallón basins. According to Shepard (1950, p. 18), the broad basins may have been produced by the pulling apart of offsets on right-lateral strike-slip faults, whereas the narrow ones are more like grabens between splinter faults. The basin bottoms apparently are not so flat as those off southern California, which probably indicates less filling by sediments. The general trend toward deeper basins from the head to the mouth

of the gulf does not appear to be merely a reflection of less filling in basins at greater distances from the Colorado delta, because the sills (low points on basin rims) and the tops of

(Aw) at both sides of the mouth. Mean air temperatures near the entrance range between 20° and 28°C., but the range increases northward to between 14° and 31°C. at Mulegé, and to

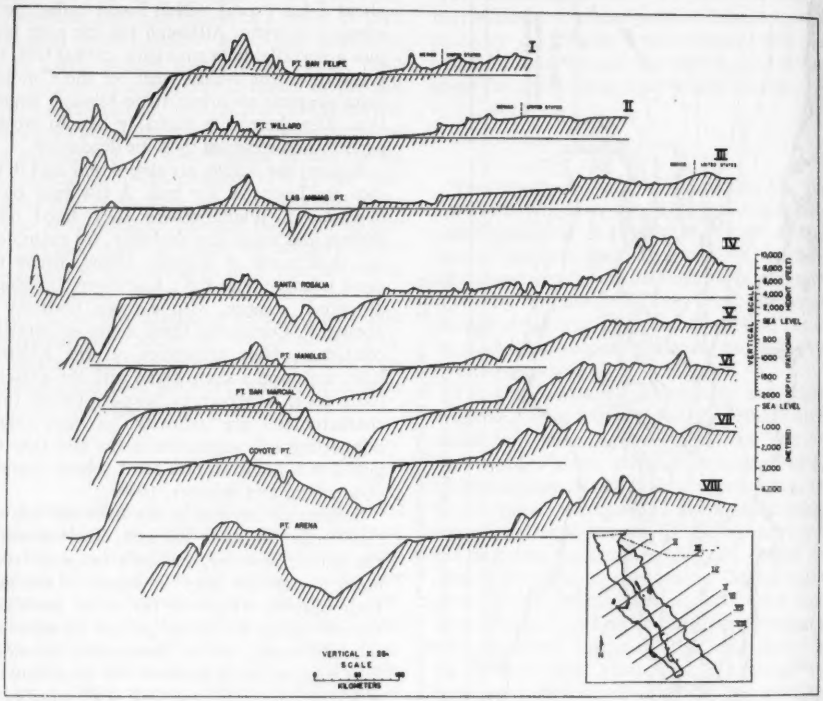

FIGURE 3.—REGIONAL SECTIONS ACROSS THE GULF OF CALIFORNIA

The sections are drawn from the continental slope on the west to the crest of the Sierra Madre Occidental on the east.

islands and banks also are generally lower or deeper southeastward. The general southeastward deepening of all three points can only be a product of diastrophism. Of interest with respect to sedimentation is the fact that the bottoms of the basins are as much as 1585 m (865 fathoms) deeper than their sills (Fig. 4), though the average is much less, about 665 m (365 fathoms).

CLIMATE AND OCEANOGRAPHY

The gulf with its great length ranges from a desert climate—BWh according to Köppen-Geiger classification (Goode, 1943, p. 20–21)—at the north, through dry steppe (BSshv) and mild (Cw) in the middle, to tropical savanna

greater but unrecorded extremes at the north end of the gulf. Rainfall is restricted largely to winter at the north end and summer at the south end. Compilations by Wilson (1955, p. 9) and Roden (1958) show that the annual average rainfall on the west side is lower than on the east side, 12 cm versus 30 cm. On both sides the rainfall increases southeastward, reaching 85 cm at Mazatlán. Annual evaporation according to Roden (1958) is about 12 times rainfall at Guaymas, 9 times at La Paz, and 2.5 times at Mazatlán; average excess of evaporation over rainfall throughout the whole gulf is about 250 cm. At this rate, the average excess of water lost by evaporation over direct rainfall is about 0.017 million m^3/sec., or 5.4 × 10^{11} m^3/year. This is about 17 times the annual

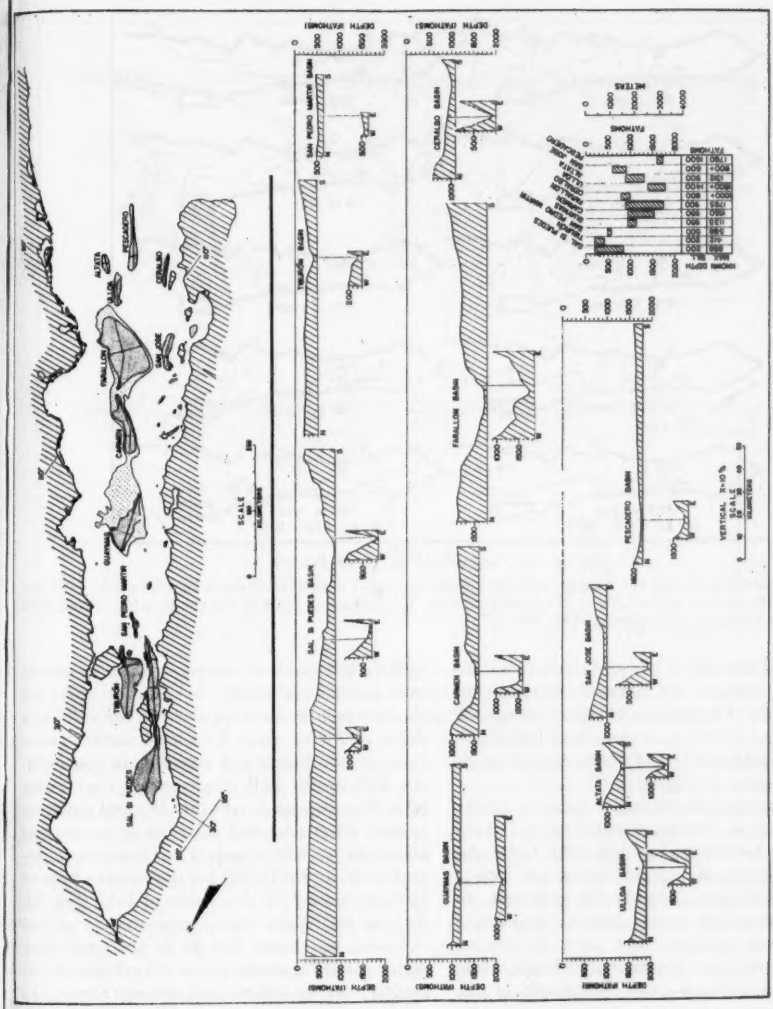

FIGURE 4.—BASINS OF THE GULF OF CALIFORNIA

The sections across the basins were made along lines shown on the insert map. A comparison of basin-bottom and sill depths is given at the lower right.

runoff into the gulf by all streams including the former Colorado River. Winds are mostly of low velocity (1.5 to 6.0 m/sec.), northwesterly throughout the gulf in winter and southeasterly in the southern half of the gulf during summer and in the northern half for part of the summer. Winter gales (Chubascos) of up to 30 m/sec. occur during winter, and occasional hurricanes from the southeast (Los Cordonazos) of up to 45 m/sec. occur during the fall.

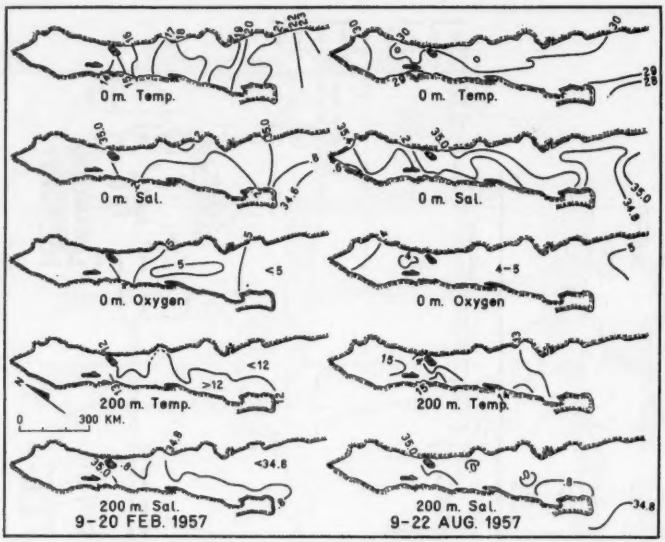

FIGURE 5.—PROPERTIES OF GULF WATER

Values measured during the winter (left) and summer (right) cruises of Scripps Institution in 1957 are mapped at the surface and at 200 m. Temperature is in °C., salinity in ‰, and oxygen in ml/L. From data of Marine Research Committee (1958a; 1958b)

The oceanography of the gulf is known chiefly from cruises by Scripps Institution of Oceanography in 1939 (Sverdrup and staff, 1943) and in 1957 (Marine Research Committee, 1958a; 1958b). Additional information collected by other organizations applies only to local areas, mostly shore stations. The data show that during winter the surface-water temperature decreases northward from the mouth of the gulf, and during the summer it increases northward (Fig. 5), more or less paralleling the regional variation of air temperature. Low temperatures of winter are largely due to upwelling induced by the northwesterly winds of winter that blow the surface water away from the head of the gulf and particularly from the area just south of Tiburón and Angel de la Guarda islands. Salinity of surface waters increases northward in all seasons; the greatest increase is indicated for summer according to data from four cruises made in 1957. The high salinity is a result of the excess of evaporation over rainfall and runoff. No dilution effect by the Colorado River is apparent in the gulf. At a depth of 200 m, away from local surface variations, the isotherms and isohalines in the southern half of the gulf clearly show that water from the open sea moves into the gulf along its eastern coast and that salty water moves out along its western coast. This movement, reported by Roden (1958) for the winter cruise of 1939, is verified by the cruises of 1957 (Fig. 5). Taking 34.6 ‰ as the average salinity of the inflowing water and 35.1 ‰ for the outflowing water, Roden computed from the salt and water budget that the inflow must average about 1.19 million m^3/sec. and the outflow about 1.17. This flow is about 1200 times the average annual addition of water to the gulf by runoff of streams.

Viewed in vertical section (Fig. 6) the water of the gulf exhibits a sharp decrease in temperature and increase in salinity between 0 and 150 m. Downbowing of isohalines at the head of

the gulf indicates production there of highly saline water. Upbowing of isohalines and isotherms shown by cross sections of the gulf (Sverdrup, 1940) indicates local upwelling of thus denser water that is deeper than the sill, just as is true of basins off southern California (Emery, 1954). However, the relatively high temperature in Guaymas Basin (Table 1) and

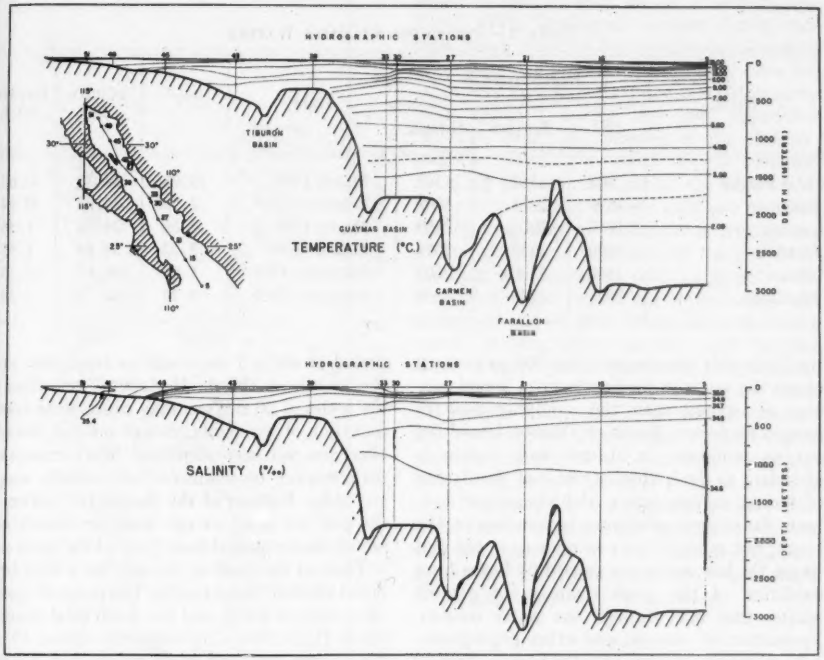

FIGURE 6.—TEMPERATURE AND SALINITY SECTIONS
Based on data reported by Sverdrup and staff (1943)

deep water at several points along the eastern side of the gulf due to removal of surface water by wind push. At depths greater than 150 m the change of temperature and salinity is more gradual (Fig. 6). Carmen and Farallón basins contain water that is within 0.1°C. and 0.02 ‰ salinity of being isothermal and isohaline at depths below a level about 200 m deeper than their sills. Sal si Puedes Basin, however, exhibits not only a progressive change with depth but also changes between the surveys of 1939 and 1957. For other basins only few data are available. In general the deeper the sill, the lower the temperature, the higher the salinity, and the higher the oxygen content (Table 1). If this relationship were more nearly exact and if the basin waters were isothermal and isohaline, it would mean that the sills act as submerged dams, blocking off the colder and saltier and the changes with depth and time in Sal si Puedes Basin indicate that the water in these basins is partly derived from the north where salty water sinks owing to increased density after part of it had evaporated. South of these basins the water does not appear to be dense enough to sink to the floors of other basins; instead, it flows out of the gulf at intermediate depths, and sea water from greater depths flows into the gulf to fill the basins as far north as Carmen Basin. The water that is trapped in each basin remains until it becomes mixed with overlying water, but the duration of entrapment is not long, as shown by its lack of stagnation: free dissolved oxygen is never absent from it.

In most places oxygen in the surface waters ranges between 4 and 6 ml/L, but in a few places it reaches concentrations of 9 ml/L, far above saturation, owing to intensive photo-

synthetic activity by phytoplankton. Below 30 m oxygen decreases, reaching a minimum of less than 0.1 ml/L between depths of 150 and 900 m. At greater depth the oxygen again increases to values as much as 2 ml/L. Because the basin sills are deeper than 900 m in most places the water in the basins has a higher content of oxygen than the overlying zone of oxygen minimum. North of Tiburón Island the oxygen minimum is absent, and oxygen is abundant to the bottom, a result of the sinking of former surface water of high oxygen content. An oxygen minimum is common in the ocean, but rarely is it as extreme as in the gulf where the low values are caused by losses from oxidation of the great quantity of organic matter that falls through the water column. Production of diatoms and other phytoplankton greater than normal for the ocean is typical of the surface waters of the gulf owing to upwelling at its head caused by winter's northwesterly winds and to upwelling near projecting points on both sides caused by winds at any time of year. Theory suggests that upwelling should be most intense along the western coast during winter's northwesterly winds and along the eastern coast during summer's southeasterly winds, but seasonal observations are incomplete. The upwelled water is cold, salty, and high in silica and probably in other nutrients. The high production of phytoplankton (mostly diatoms and dinoflagellates) associated with the upwelling often causes the water to become red in large irregular patches (Fig. 7). That Ulloa encountered upwelled water during his visit in 1539 is indicated by his name for the gulf, "Ancón de San Andreas y Mar Bermejo"—San Andres Bay and Vermilion Sea—"because it is that color and we arrived there on the day of San Andres."

Irregularities in the isobaric surfaces computed from the temperature and salinity measurements of the 1939 Scripps Expedition led to the suggestion by Sverdrup (1940) of internal waves as the cause. Later confirmed on a theoretical basis by Munk (1941), the waves have a period of about 7 days and an amplitude near the mouth of 100 m. Horizontal velocities at the nodes of 20 cm/sec. may cause some transportation of sediments, though no such bottom effect has yet been identified. More important with respect to sediments are surface waves and tides. Because of the short fetch, waves in the gulf are small except near the mouth and are of shorter period than those of the open sea.

Table 1.—Properties of Basin Waters

Basin	Depth—meters			Date	T°C.	Salinity ‰	Oxygen ml/L
	Sill	Bottom	Sample				
Sal si Puedes	365	1570	1269	March 1939	10.98	34.76	0.62
Guaymas	1650	2075	1707	February 1957	2.99	34.65	0.59
Carmen	1650	2850	2430	March 1939	2.56	34.62	1.28
Farallón	1650	3230	2014	March 1939	2.32	34.65	1.51
Ulloa	2560	3300+	2805	February 1957	1.90	34.67	2.39
Pescadero	2925	3220	3050	February 1957	1.91	34.72	2.20

Tides at the head of the gulf have long been noted for their great height. The range of spring tides there is 9.6 m, and the mean tidal range is 6.6 m (U. S. Navy Hydrographic Office, 1951). This range decreases southeastward to a mean of 2.2 at Guaymas and 0.7 m at Mazatlán. The great tidal range near the head of the gulf is reflected in strong tidal currents between the islands northwest of Guaymas; however, the swiftest current is in the Colorado River estuary where the velocity often exceeds 4.5 m/sec. Frequently this current is accompanied by a tidal bore having a height of about 1 m. Interaction with the flow of the river formerly produced a bore 3 m high that was capable of considerable erosion of the deltaic channels (Sykes, 1937).

Sediments

General

About 310 samples of the underwater sediments are available from the gulf. Of these, 175 were collected in shallow-water dredging operations of Allan Hancock Foundation, but washing during collection and subsequent biological picking introduced a bias that permits their

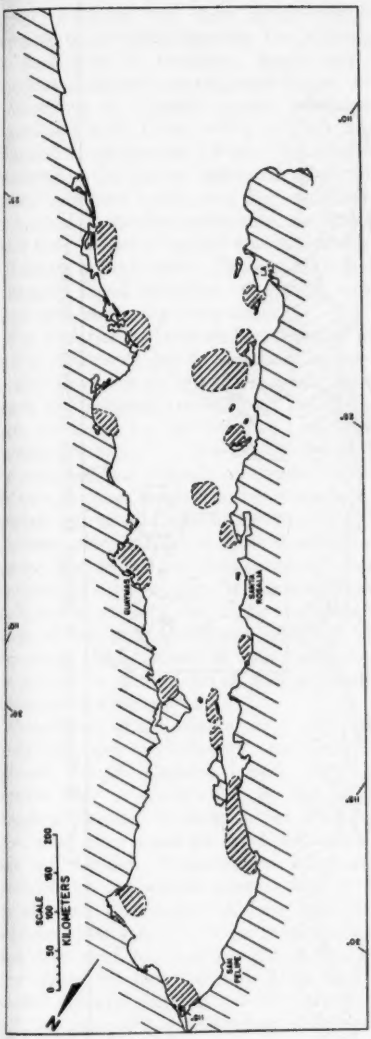

FIGURE 7.—AREAS IN WHICH PHYTOPLANKTON BLOOMS HAVE BEEN OBSERVED

use only for general typing. Those collected by Scripps Institution comprise 30 large snapper samples and 105 cores having lengths up to 5.1 m. Because of shortening during the process of coring, the material actually represents thicknesses at least as great as 7.5 m (Emery and Dietz, 1941). Inadequate storage during wartime years resulted in considerable losses of core samples and data, so that many cores can serve only as spot surface samples. Most cores were obtained during the 1940 expedition (Revelle, 1950), but samples of the 1939 expedition present a more nearly uniform sampling pattern throughout the region. Although the samples average only one per 1600 km² of area, they are sufficient to portray the general pattern of sediments in the gulf when the data are combined with bathymetric information. Reporting of the properties of the sediments and of their relationship to source rocks, oceanographic factors, and tectonic theory constitutes the main basis of this study.

Analyses of grain size were made on about 525 samples (many are for sections at different depths in cores). Percentages of acid-soluble material (considered to be calcium carbonate) and of organic nitrogen were run on 420 samples. Percentages of water content, heavy minerals, shells, foraminiferal tests, and diatoms and measurements of other parameters, such as density, color, and grain shape were made on varying numbers of the samples.

Texture

Most measurements of the grain-size distribution of samples before treatment with acid were made at Scripps Institution; sieves were used for sand fractions and the standard pipette method (Twenhofel and Tyler, 1941, p. 55) for silt and clay fractions. The results were plotted as cumulative curves from which median and quartile grain sizes were obtained. On the basis of grain size of its sediments the gulf can be divided into four provinces. Most of the southern two-thirds has sediment with median diameters finer than 4 microns and thus of clay size (Fig. 8). In the vicinity of Tiburón and Angel de la Guarda islands the sediment is much coarser, to 425 microns, and thus is mostly of silt and sand size. Immediately north of these islands the sediment is again fine-grained, but farther north it coarsens to about 90 microns (very fine sand) off the mouth of the Colorado River. Near shore throughout most of the gulf the sediment is coarse but is incompletely sampled. Cores in areas of fine-

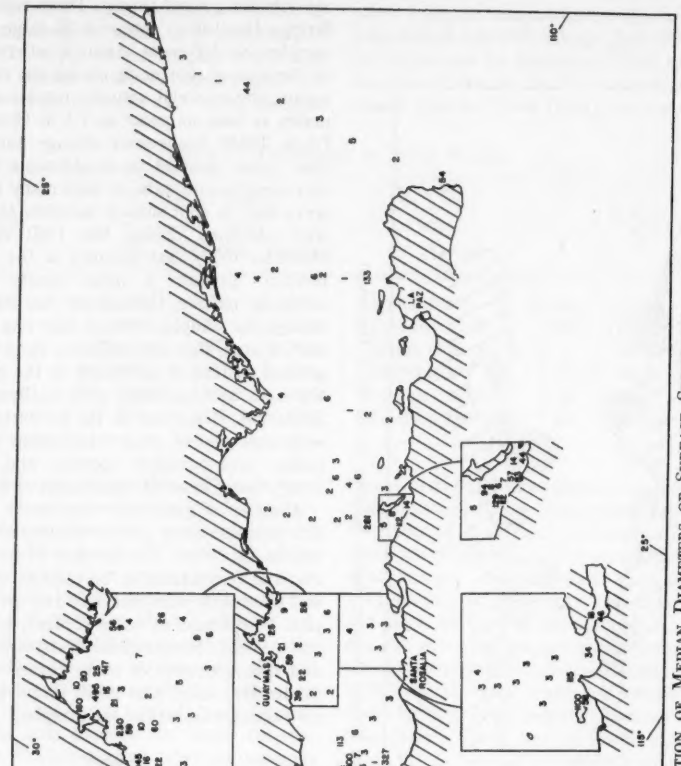

FIGURE 8.—DISTRIBUTION OF MEDIAN DIAMETERS OF SURFACE SEDIMENTS

grained sediment exhibit little change of median diameter with depth; but one core (lat. 26°38′; long. 110°00′), which has sediment mostly between 2 and 3 microns in grain diameter, contains two sand layers—possibly emplaced by turbidity currents. Two others on the east side of Pescadero Basin and in Guaymas Basin also contain sand layers.

According to Trask's sorting coefficients (Twenhofel and Tyler, 1941, p. 111) most sediments range between 1.5 and 8.0; low values characterize the coarser sediments where winnowing has been active, and high coefficients are typical of the finer sediments, particularly those that consist of mixed fine detrital clays and coarse organic debris. There appears to be systematic areal variation of sorting coefficients with increasing water depth.

The variation of both median diameter and sorting coefficients can be visualized by use of descriptive names for types of sediment, where names are assigned according to the proportions of sand (> 62 microns), silt (4–62 microns), and clay (< 4 microns). By use of the compositional triangle of Shepard (1954), the samples were assigned sediment names and grouped into areas of similar sediment (Fig. 9). The results are parallel to those of median diameter (Fig. 8) but are more easily visualized. The predominant sediment is silty clay (Table 2); however, the silty clay in the southern two-thirds of the gulf is different from the silty clay north of the islands in that most of the silt content is in the form of diatom frustules instead of detrital grains.

Complexity of the areas of sand, silty sand, sandy silt, and sand-silt-clay near Guaymas, Tiburón Island, Carmen Island, and Concepción Bay is partly due to the greater sampling density in those areas. Elsewhere most near-shore areas are left blank owing to lack of samples. Fragmentary information provided by old washed samples and by the known wave and current activity near shore indicates that most of these areas must be floored by sand. Much of the sand is deposited near shore by the Colorado River and by smaller streams that enter both sides of the gulf, but some of it is shell debris. Coarse sediment in the channels between islands is mostly shell concentrate left from winnowing by tidal currents. Finer sediments far from shore are the result of deposition in areas of quiet water.

Composition

General.—The chief clue to the origin of a sediment is its composition. In the gulf, as elsewhere, the bulk of the sediments can be classed as detrital, organic, and authigenic. Relict and residual sediments also are probably present in minor amounts, but their accurate identification and mapping require more detailed information than is yet available in the gulf. Authigenic sediments are limited chiefly to a few glauconite grains; the dominant origins of the sediments are detrital and organic. For simplicity in discussion, detrital sediments are best subdivided into sand-silt and clay groups because of differences in mineralogy and techniques of study. The organic sediments of the gulf are subdivided into three groups: calcium carbonate, silica, and organic matter. Organic matter is the least abundant of these constituents and must be determined chemically. The other materials, detrital sands and silts (> 4 microns), clays (< 4 microns), foraminiferal tests, shells, and diatoms, vary in relative proportions in the different textural types of sediment in the gulf (Fig. 10). In some types, such as sand and gravel, the coarse texture is a result of the presence of shell concentrates. In contrast, the fine texture of silty clay, an indication of slow deposition in areas far from shore in the gulf, allows diatom frustules to be far more abundant than in coarser sediments where rapid deposition masks them. Thus, texture, composition, and rate of deposition are closely interrelated.

Detrital sand and silt.—By means of a heavy liquid, carbon tetrabromide, the detrital grains of sand and silt size were separated into light- and heavy-mineral components. The light minerals that form the bulk of this fraction consist of quartz, orthoclase, and plagioclase, identified by etching with hydrofluoric acid and selective stains (Twenhofel and Tyler, 1941, p. 131). The quartz-orthoclase-plagioclase ratios show considerable variation with type of sediment (Table 2) and area. Averages (*see* Table 2 for method of notation) for several areas are as follows:

vicinity of Carmen Island	20–25–10
north of Concepción Bay	29–4–10
near Guaymas	128–39–10
near Tiburón Island	47–23–10
in Ballenas Channel	205–31–10
near Colorado delta	425–45–10

The high ratio of quartz to total feldspar near the delta probably indicates selective destruction of feldspars during weathering and long transportation by the river. Low percentages of quartz (average quartz/feldspar ratio = 1.7) elsewhere reflect the geology of nearby land

FIGURE 9.—DISTRIBUTION OF SEDIMENT TYPES
According to the nomenclature diagram proposed by Shepard (1954)

masses and indicate an arkosic character of the sands. In keeping with the mineralogy, the low degree of roundness (0.15 to 0.50) and of sphericity (0.70 to 0.85) is suggestive of mild heavy-mineral content. Every sample has at least one mineral which might be assigned to each of the above source rocks. Basaltic hornblende, derived from volcanic rocks, is present

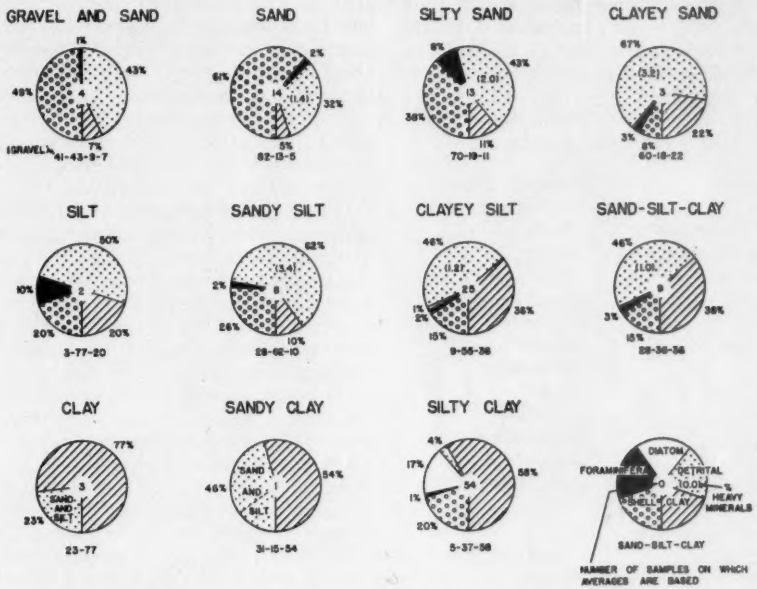

FIGURE 10.—AVERAGE COMPOSITION OF SEDIMENT TYPES OF FIGURE 9

Detrital refers only to detrital sand and silt (coarser than 4 microns), whereas clay refers to inorganic grains finer than 4 microns and probably also of detrital origin.

conditions of transportation for most of the sand and lack of polycyclic material.

Heavy minerals range between 1 and 7 per cent and average 1.6. About 45 heavy-mineral species were identified, but the average suite consists of between 14 and 19 minerals. Hornblende, augite, and basaltic hornblende are by far the most abundant heavy minerals. Most of the minerals and especially the more abundant ones are only moderately stable according to the classifications of Milner (19 2, p. 499) and Reiche (1950). These are the species expected to accompany highly feldspathic light minerals in sediments. They are indicative of provenance from all types of igneous and metamorphic rocks. Each mineral was assigned a probable source, such as acid, intermediate, or basic igneous rock, or metamorphic rock (Milner, 1952, p. 229–357). Each sample was then analyzed to determine from which type of source it was chiefly derived as indicated by its in almost every sample; volcanic glass was also noted in many of the samples. The volcanic content of the heavy-mineral fractions is particularly high near Tiburón Island and in the sediments of Ballenas Channel. Sediments near the mouth of the gulf and in the deeper parts of the area south of Carmen Island contain chiefly minerals having an acid igneous and metamorphic derivation. Near Carmen Island the volcanic and basic igneous minerals increase markedly, the acid igneous minerals almost disappear, and the metamorphic minerals decrease. Along the shore north of Concepción Bay the minerals are mainly of intermediate and basic igneous and volcanic origin. The Guaymas area is marked by metamorphic and volcanic minerals, as well as by minerals having an acid igneous origin in the southern part of the area and ones of basic igneous origin in the north. The area near Tiburón Island shows a concentration of metamorphic, basic igneous, and

volcanic minerals. These same mineral types appear in the sediment of Ballenas Channel, in addition to minerals originating in intermediate igneous rocks. Samples near the Colorado delta contain minerals representative of all types of igneous and metamorphic rocks but have a low percentage of volcanic constituents. Thus, the composition of heavy minerals is closely related to the kinds of rock that constitute the various physiographic provinces of Figure 1.

Heavy minerals that occur in gulf sediments are (in order of decreasing abundance):

Hornblende	Volcanic glass
Augite	Collophane
Basaltic hornblende	Rutile
Sphene (titanite)	Zircon
Magnetite	Andalusite
Hematite	Apatite
Ilmenite	Diopside
Leucoxene	Olivine
Topaz	Sillimanite
Hypersthene	Fluorite
Epidote	Limonite
Garnet	Tourmaline
Biotite	Chlorite
Glauconite	Staurolite

Present but rare are:

Actinolite	Monazite
Axinite	Pyrite
Barite	Spodumene
Clinozoisite	Tremolite
Dolomite	Vesuvianite
Dumortierite	Wollastonite
Enstatite	Xenotime
Glaucophane	Zoisite
Kyanite	

Clay.—The clay-size fraction of most sediment is high, attaining a maximum of 82 per cent in deep water near Mazatlán. Except near shore, all samples contain more than 20 per cent clay. Grim, Dietz, and Bradley (1949) studied the clay mineralogy of 32 samples from 22 cores that are representative of most of the gulf. A sample from near the mouth of the gulf is similar to others from the deep Pacific Ocean in which montmorillonite and illite are about equally abundant and kaolinite less abundant. Samples from farther north in the gulf have higher percentages of kaolinite, so that these three kinds of clay minerals are about equally abundant. There is no indication of variation in clay mineralogy at depth within the cores or of difference between the 1.0-micron, 0.1-micron, and the −0.1-micron fractions on which the studies were made. Chemical analyses showed that the SiO_2/R_2O_3 ratio is variable, probably because of variations in the percentages of finely comminuted diatom debris in the clay-size fractions.

Authigenic minerals.—Glauconite is present in many of the samples but is not very abundant in any of them. It occurs mainly as a filling of foraminiferal tests, and all stages of filling and replacement were noted. There is no correlation between the presence of glauconite and the grain size or the sand-silt-clay ratio of the sediment. Most of the samples containing glauconite were collected from water less than 600 m deep, although one sample is from 1400 m and three are from water deeper than 2300 m. Collophane was noted only in the heavy-mineral fractions, and it has the appearance of being detrital. Emery and Dietz (1950) indicated the presence of small phosphorite nodules containing Miocene Foraminifera at two locations in the gulf; this again suggests a detrital origin of the collophane.

Calcareous material.—The fraction of the sediments soluble in dilute hydrochloric acid consists of shell fragments, foraminiferal tests, and some algal debris; calcareous precipitates were not detected. All this material is assumed to be calcium carbonate, though minor amounts of magnesium carbonate are probably also present. Acid-soluble fractions range from 1 to 89 per cent. All samples in which calcium carbonate is more than half of the sample by

PLATE 1.—ROCKET VIEW OF REGION STUDIED

Large dark area at left is head of Gulf of California north of Angel de la Guarda Island. Small dark area at middle right is Salton Sea. The gray area between them is the delta of the Colorado River; extending from its head toward the right is the Colorado River and toward the lower right corner is the Gila River. The ridge at the far side of the delta is the Cocopah Mountains that separate the delta from Laguna Salada, a playa lake basin. Note the long fairly straight fault scarp bordering the far side of gulf and Salton Sea that extends far beyond the sea toward Los Angeles (the smoggy area above the Salton Sea). Blocks of the Basin and Range Province are well shown by alternating dark and light patches throughout most of the region. Photograph by K-25 camera (infra-red film) mounted in the Navy's Viking 12 rocket at elevation of 232 km. Official USN photograph.

ROCKET VIEW OF REGION

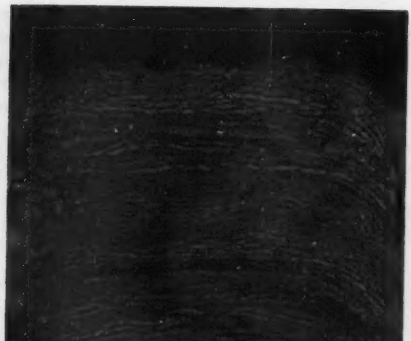

FIGURE 1

FIGURE 2

FIGURE 3

LAMINATED DIATOMACEOUS SEDIMENTS

weight are coarse-grained and have median diameters greater than 62 microns. Figure 11 presents the distribution of calcium carbonate throughout the surface sediments of the gulf but does not distinguish between shell material and foraminiferal tests. Most samples with high calcium carbonate caused by shell debris are from close to shore in relatively shallow water. Large shell reefs with associated corals occur near the south end of the peninsula. Samples that contain more than 5 per cent foraminiferal tests were collected in depths between 100 and 1000 m. Moderately high percentages of tests occur only in sand, silty sand, clayey silt, and sand-silt-clay. Few were found in samples from the deep basins of the gulf.

Organic silica.—By far the most organic silica in the sediments is in the form of diatom frustules, though small percentages of broken radiolarians and sponge spicules are also present. Great difficulty was experienced in attempts to make quantitative separations of the frustules by heavy liquids and mechanical means. The only practicable method discovered was that of washing the samples through screens having openings of 62 and 44 microns and estimating by binocular microscope the percentage of frustules in each size fraction. The highest percentage was found usually in the middle fraction—between 44 and 62 microns. As shown by Figures 11 and 12, percentages in total samples range from 0 to 48 and are greatest in silty clay sediments. Comparison of Figures 2 and 11 shows that highest concentrations occur in the middle third of the gulf, not necessarily in the basins, but on their gentle side slopes as well. The lateral distribution of diatoms is undoubtedly greater than shown in Figure 11, but lack of samples from the areas near all the observed plankton blooms prevents precise outlining of the area of diatom distribution. Figure 7 shows the areas in which phytoplankton blooms have been observed by Allen (1923; 1938), Cupp and Allen (1938), Gilbert and Allen (1943), Osorio Tafall (1943), and U. S. Navy Hydrographic Office (1951). These localities probably represent only a small percentage of all the areas in which blooms have occurred. Even though phytoplankton blooms occur in near-shore areas, currents locally are such that the diatoms cannot settle to the bottom but must be winnowed away to areas of quieter water.

More than 31 genera and 67 species of diatoms have been reported by Allen (1923; 1938), Cupp and Allen (1938), and Gilbert and Allen (1943) from the waters of the gulf, but most of the frustules remaining in the sediments are of *Thalassiothrix longissima*, *Coscinodiscus* sp., and *Pseudoeunotia doliolus*. Resolution of silica accounts for the destruction of many of the diatoms; however, the massive character of *Coscinodiscus* sp. probably explains its concentration in the sediments. General resistance to solution of silica also results from the high content of dissolved silica in the water owing to upwelling. The presence of diatoms at great depth in cores as well as at the surface demonstrates that similar conditions have existed for thousands of years. Generally the diatoms are dispersed throughout the sediment, but in several cores, particularly in the Guaymas area, high concentrations of diatoms in layers give the sediment a banded or laminated appearance.

Organic matter.—The content of organic matter is known from 420 Kjeldahl analyses for nitrogen made at Scripps Institution on samples collected in 1939. Values as great as 0.6 per cent by dry weight were found in surface sediments, corresponding roughly to 10 per cent total organic matter. Such high values are rare in marine sediments. There seems to be no definite areal pattern to the percentages of organic nitrogen except that values at the northern end of the gulf are generally lower than those at the southern end (Fig. 12). A typical inverse relationship exists between the organic nitrogen content and the grain size of the sediment (Table 2). Correlation of high organic content with fineness of the sediment is common and is caused by the similarity in settling velocity of organic debris and clays, as well as adsorption of organic matter by clay minerals.

Sulfur constituents.—For several cores of laminated diatomaceous muds S. C. Rittenberg

---

PLATE 2.—LAMINATED DIATOMACEOUS SEDIMENTS

FIGURE 1.—Diatom mud (silty clay) 85–89 cm deep in sediment off Guaymas (Lat. 27°51′; Long. 111°26′; 585 m). Bending of layers at side is due to frictional drag against wall of core tube. ×1.3.

FIGURE 2.—Valmonte diatomite (Late Miocene) from Palos Verdes Hills in southern California. ×1.3.

FIGURE 3.—Thin section of diatom mud 275 cm deep in sediment off Guaymas (Lat. 26°17′; Long. 111°13′; 631 meters). Note thick layer of haphazardly oriented large diatoms. ×285.

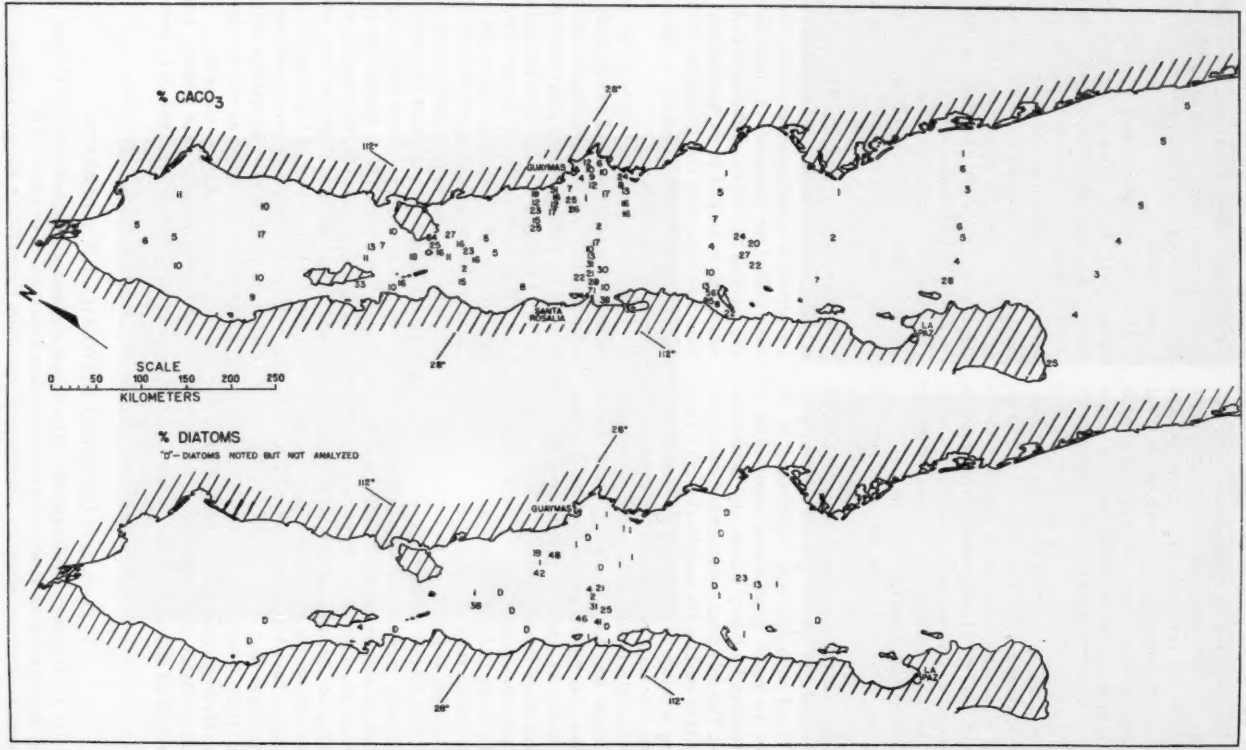

FIGURE 11.—DISTRIBUTION OF CALCIUM CARBONATE (ACID-SOLUBLE MATERIAL) AND ORGANIC SILICA (MOSTLY DIATOMS) IN SURFACE SEDIMENTS

FIGURE 11.—DISTRIBUTION OF CALCIUM CARBONATE (ACID-SOLUBLE MATERIAL) AND ORGANIC SILICA (MOSTLY DIATOMS) IN SURFACE SEDIMENTS

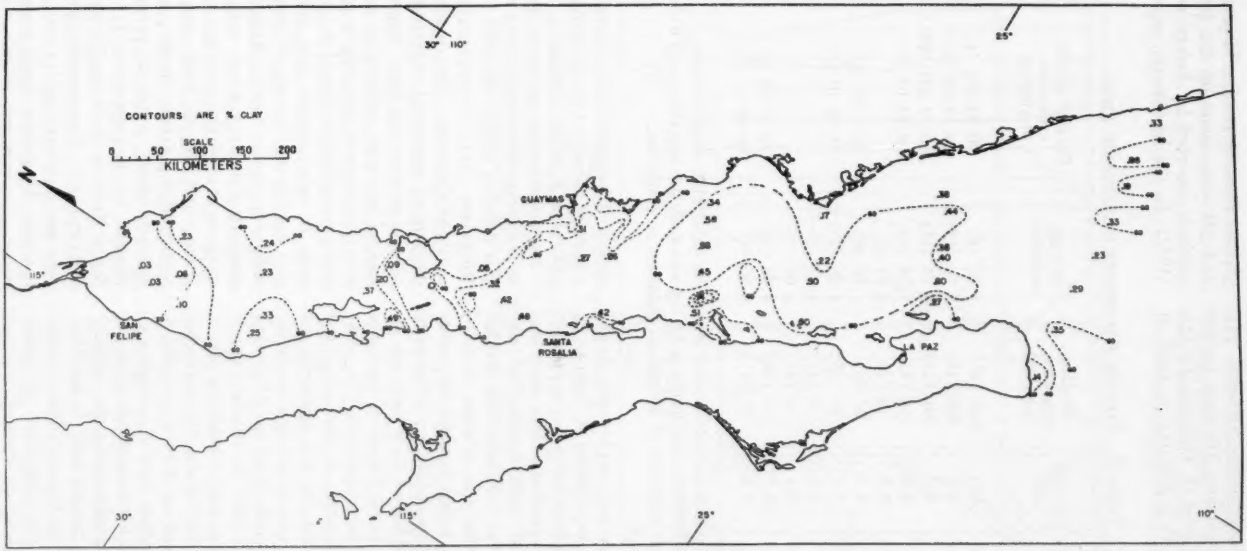

FIGURE 12.—DISTRIBUTION OF ORGANIC NITROGEN (MICRO-KJELDAHL) IN SURFACE SEDIMENTS AS COMPARED WITH CONTOURS OF PERCENTAGE OF CLAY

made analyses for carbonate, nitrogen, pH, Eh, and sulfur constituents. His data for one core were used for Figure 13. This core, 16–223, was 3.73 m long with a penetration depth of 5.18 m. As soon as the core was brought aboard ship 30-cm sections were placed in linen bags, and as much of the interstitial water as possible was squeezed out. A portion of this water was immediately titrated iodimetrically for dissolved sulfide ion. The remainder was divided into two portions. One was acidified with 10 per cent acetic acid, boiled to expel all sulfide ion, and stored; this procedure was followed in order to prevent additions to sulfate ion by oxidation of sulfide during the rest of the cruise before sulfate could be determined. The other part was stored untreated. At the end of the cruise the treated sample was analyzed for sulfate and chloride ions, sulfate by a conductometric titration with barium nitrate (Anderson and Revelle, 1947) checked by standard gravimetric determinations, and chloride by standard titration with silver nitrate. The untreated samples were analyzed for chloride ion; this is unaffected by oxidation during storage and served as a standard for computing sulfate ion in the untreated samples using the sulfate/chloride ratio of the treated ones. In addition, analyses of the mud for ferrous sulfide or other insoluble sulfides (by collection of gases liberated during boiling of strongly acidified mud suspensions) and for molecular sulfur (by extraction with carbon tetrachloride) yielded negative results. Measurements of Eh and pH were made on the fresh core using methods reported by Emery and Rittenberg (1952). In the laboratory, carbonate ion was measured gasometrically (Grippenberg, 1934), and total nitrogen was measured by the standard micro-Kjeldahl method.

TABLE 2.—AVERAGE PARAMETERS OF SEDIMENT TYPES

Sediment type	Per cent area	Median diameter (microns)	Sorting coefficient	Ratio of quartz–orthoclase–plagioclase	Per cent nitrogen
Gravel and sand	0.3	2940 (4)*	1.73 (4)	90–20–10† (1)	..
Sand	6.1	320 (15)	2.74 (15)	89–33–10 (9)	0.094 (3)
Silty sand	4.3	101 (13)	2.74 (13)	110–29–10 (10)	.041 (3)
Clayey sand	0.2	164 (3)	7.74 (3)	108–40–10 (3)	..
Silt	0.1	16 (2)	2.37 (2)	..	..
Sandy silt	1.1	47 (8)	1.88 (8)	51–8–10 (6)	.144 (1)
Clayey silt	2.8	10 (25)	4.36 (25)	73–33–10 (7)	.207 (5)
Clay	2.5	1 (3)	3.93 (3)	..	.291 (2)
Sandy clay	0.1	6 (1)	2.08 (1)	..	.358 (1)
Silty clay	80.1	3 (54)	4.49 (54)	219–59–10 (6)	.412 (22)
Sand-silt-clay	2.4	22 (9)	7.59 (9)	190–42–10 (5)	.236 (5)

* Numbers in parentheses indicate number of samples on which average is based.

† Numbers 90–20–10 indicate that quartz is 4.5 times as abundant as orthoclase or 9 times as abundant as plagioclase and that orthoclase is 2 times as abundant as plagioclase.

Organic nitrogen exhibits a general decrease in percentage with depth in the cores (Fig. 13); this parallels results obtained by Emery and Rittenberg (1952) in sediments of basins off southern California. This is evidently an indication of continued regeneration of buried organic matter with time. Regeneration is indicated by large volumes of an inflammable gas that escaped, forming a porous blistery texture near the bottoms of the cores when they were brought aboard ship. Similar textures also were found in cores of somewhat similar sediments from Santa Barbara Basin in southern California where mass-spectrometer analyses showed the chief gas to be methane (Emery and Hoggan, 1958). Other products of regeneration, carbon dioxide, ammonia, and orthophosphate, must be prominent, as indicated by measurements in sediments of Santa Barbara Basin by Rittenberg, Emery, and Orr (1955). Regeneration of organic matter near the surface is due to activity of aerobic bacteria. At greater depth anaerobic sulfate-reducing bacteria are effective, as revealed by the presence of abundant hydrogen sulfide. Indicative also of change from aerobic con-

ditions in a thin layer at the surface to anaerobic conditions at depth is the decrease of oxidation-reduction potential from positive values at the surface to strongly negative ones at depth.

Miscellaneous Properties

Comparison with the *Rock-color chart* (National Research Council, 1948) shows that most of the fine-grained sediment is light olive gray

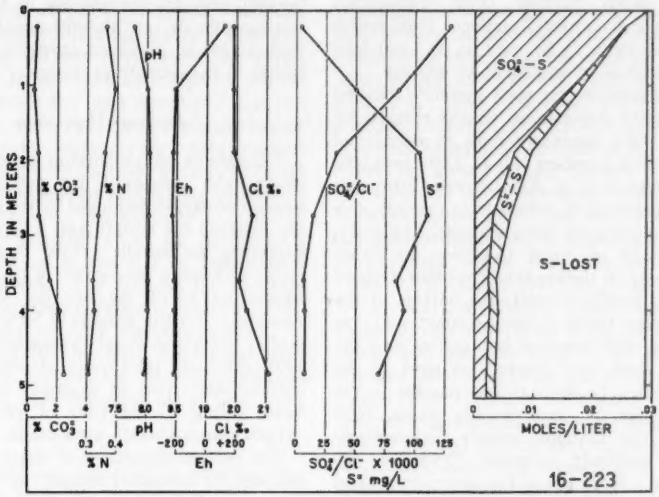

FIGURE 13.—SOME PROPERTIES OF DIATOMACEOUS MUD IN A CORE

Core 16-223 from 626 m in Sal si Puedes Basin was collected on 9 December 1940. Analyses by S. C. Rittenberg. Sample depths in the core have been multiplied by the ratio of penetration depth to core length (518/373) in order to obtain *in situ* depths. On the right is the depth distribution of sulfate-sulfur and sulfide-sulfur computed from analyses of $SO_4^=/Cl^-$ ratio and Cl ‰. The decrease with depth of the total of both forms is a measure of the amount of sulfur that diffused into overlying water.

When dissolved sulfate and sulfide ions are computed as mols per liter of interstitial water (Fig. 13), the sulfur exhibits a marked decrease in abundance with depth. If steady-state conditions held throughout the period of deposition of the core, or if sediment now at a depth of 5 m was originally like that now at the surface, then much of the sulfate must have been regenerated to hydrogen sulfide. Negative results in tests for acid-soluble sulfides and molecular sulfur show that important regeneration products do not exist in these sediments. The hydrogen sulfide that remains in the interstitial water is, however, only a small fraction of the amount originally formed; therefore most of the hydrogen sulfide must have diffused upward to the overlying water. This process is similar to that discovered for ammonia regenerated from organic nitrogen in sediments of Santa Barbara Basin off southern California (Rittenberg, Emery, and Orr, 1955).

(5Y 6/2) or olive brown (5Y 4/3) when rewetted after drying during long storage. Sediments at the north end of the gulf are generally somewhat lighter than those at the south. Where diatoms are abundant the sediment tends to be browner than elsewhere; some samples are dusky yellow (5Y 5.5/4). The coarser-grained sediment, sand, and sand and gravel have a wide range of color depending on their composition.

Grain specific gravities of the diatomaceous muds are as low as 2.18 gm/cc and average 2.35 because of the abundance of the light mineral opal that constitutes the diatom frustules. Fresh cores from the gulf as elsewhere present a sharp decrease in water content near the surface and a more gradual decrease at depth. Even after partial drying and resulting shrinkage, the near-surface parts of the cores of diatomaceous muds have porosities as great as 60 per cent by volume and the deeper parts about 35 per cent (computed from grain specific

gravity and bulk density measured for dried lumps coated with lacquer). When completely dried, the top parts have bulk densities as low as 0.8 gm/cc and can float on water. The low bulk density and high porosity of the diatomaceous muds parallel these well-known properties of diatomite (Bramlette, 1946) which permit diatomite to be used as an insulating material and as an absorbent for liquids.

Sediments having the most abundant diatoms are laminated down to all depths reached by the cores. The laminae consist of alternating light and dark members (Pl. 2). Light members are concentrations of diatoms with little clay or silt, whereas dark members are mainly clay and silt but contain some diatoms. The members may be of equal thickness, or either member may be thicker than the other. Graded bedding is locally present; the bottom of the light member forms a sharp contact with the underlying dark member but grades into the overlying dark one. Diatoms in most of the light members lie more or less parallel to the bedding, but in exceptionally thick light members the diatoms, mostly *Coscinodiscus* sp., are randomly oriented. Typically, the diatoms in a layer are of the same species and size. Where mixtures of species do occur, the diatoms are usually large.

In order for a laminated deposit of this nature to form, there must be either an alternation in the type of material brought to the area of deposition, or else a periodic flooding of the depositional area with one of the materials being deposited. The sharp bottom and gradational top of the diatomaceous member indicate that periodically there is a sudden increase followed by a long attenuation in the supply of diatoms relative to inorganic sediments. The presence of some diatoms throughout the sediment indicates that they are always present in the surface water, and some are constantly settling to the bottom.

Numerous accounts of diatom blooms (Fig. 7) support the evidence from the sediments. The cycle of organic-inorganic deposition is thought to be annual. Northwesterly winds starting in October and November blow the surface water near Tiburón and Angel de la Guarda islands southward so that it is replaced by subsurface water. A supply of nutrients is brought to the surface by upwelling and mixing, and in December and January phytoplankton blooms begin. Blooms are likely to originate periodically in different places until the northwesterly winds cease in April and May. During and immediately after the blooms, the number of diatoms falling to the bottom is very great. Later, when nutrients are largely exhausted from surface waters, diatom production is greatly reduced.

Preservation of the laminations is made possible only by the absence of benthic burrowing animals, an absence required by the replacement of dissolved oxygen by hydrogen sulfide in the interstitial waters.

Rate of Deposition

The rate of phytoplankton growth during a bloom was measured by determining the amount of oxygen produced by the phytoplankton between the surface and a depth of 40 m. According to Revelle (1950) these measurements indicate a production of organic matter amounting to 2 mg/cm²/day dry weight. Assuming that the weights of SiO_2 and organic matter are about equal (Vinogradov, 1953, p. 146), the daily production of silica is also 2 mg/cm²/day. This is probably a maximum figure owing to the time of year that the oxygen measurements were made.

The rate of deposition of detrital sediment can also be estimated roughly on the basis of its supply. Before being diverted the Colorado River annually discharged about 18×10^9 m³ of water and 180 million tons of sediment past Yuma (U. S. Bureau of Reclamation, 1952; Gould, 1954) and thence to the gulf. According to data prepared by the Secretary of Hydraulic Resources of Mexico (Personal communication) and to estimates by Tamayo (1949) the smaller streams along the east side of the gulf annually discharge water amounting to 19.5×10^9 m³. If the discharges of sediment by the Colorado River and the smaller streams were proportional to their discharges of water, the total weight of sediment reaching the gulf via streams would have been about 375 million tons each year. If the sediment had been deposited evenly throughout the entire gulf, the rate would have been about 180 mg/cm²/year, but most of it must have been deposited on the submarine parts of the Colorado delta north of Angel de la Guarda Island. Since the diversion of the Colorado River its contribution to the gulf has been reduced to only about 8 million tons per year, and the rate of deposition of detrital sediments must consequently have been reduced.

If one diatom member and one clay-silt member of the laminae represent deposition for a year, the annual rate of deposition can be computed more exactly for the areas of lami-

nated diatomaceous mud. Measurements of the laminae made on thin sections show that their thickness generally decreases with depth in the cores, in accordance with the increased compaction at depth shown by decreased water content and porosity. Average measurements of laminae in the top meter of sediment, corrected for 40 per cent shortening during coring and 18 per cent shrinkage on drying, are 0.92 mm for the light layers and 0.53 mm for the dark ones. This figure is almost exactly the same as that obtained by a field count of 200 layers in a 7-inch section of core, when the latter is corrected for shortening caused by coring operations (Revelle, 1950). At an average dry-bulk density of the surface sediment of 1.00 gm/cc the rate of deposition is 145 mg/cm²/year. The rate for the diatomaceous members then averages about 92 mg/cm²/year and that for the clay-silt member, 53 mg/cm²/year. On this basis the longest cores adjusted for compaction at depth reached laminae that were deposited about 7500 years ago.

Conclusions and Geological Significance

Origin of Gulf

In 1910 Botsford suggested that the gulf owes its origin to erosion by the Colorado River; however, the subsequent surveys that revealed its great depth and many basins effectively rule out this possibility. Synclinal folding is also inadequate as an explanation because of the presence on the peninsular side of steep scarps and of westerly dipping strata. An origin by faulting seems to be the only acceptable one, considering the seismic activity, position of known faults, presence of straight scarps, position and nature of basins, and the relationship of the gulf to known faults in California. The general form suggests that the gulf occupies the western side of a westward-tilted fault block that has been fragmented by many secondary faults.

Initiation of the gulf trough in the Mesozoic is suggested by its close relationship to the San Andreas fault, believed to have been in existence during the Jurassic (Hill and Dibblee, 1953), and to the intrusion of the peninsular batholith during the Middle Cretaceous (Larsen, 1954). Cenozoic transgression of the sea into the trough is indicated by Eocene marine sediments near the end of the peninsula and Oligocene to Early Miocene ones nearly as far north as Carmen Island (Anderson, 1950). During the Middle Miocene the peninsula was elevated and eroded. Volcanic activity began with the deposition on land of flows and of pyroclastics that thin and become finer-grained both eastward and westward of the gulf-peninsula shore line. By Pliocene time shallow seas invaded almost the entire length of the gulf and left deposits along much of the peninsula (Wilson, 1948) and on most of the islands (Durham, 1950; Natland, 1950). Early Pliocene marine sediments are known in Imperial Valley near the Salton Sea (Dibblee, 1954), but before Middle Pliocene the delta of the Colorado River separated Imperial Valley from the present gulf (Longwell, 1954), so that subsequent deposition in Imperial Valley was of terrestrial origin (Buwalda and Stanton, 1930; R. E. Arnal, 1957, Ph.D. Dissertation, Univ. Southern Calif.). Late Pliocene seas extended as far north as Angel de la Guarda Island and probably even to the delta. Pronounced tectonic activity was accompanied by intermittent volcanic outbursts and the formation of many ore deposits (Wisser, 1954). Subsidence and development of the gulf, uplift of the peninsula, and formation of numerous fault blocks, both in the gulf and on the peninsula, characterize this epoch. From Early Pliocene, the peninsula of Baja California existed as a barrier between the gulf and the Pacific Ocean, so that the fauna of Imperial Valley—Gulf of California—is a tropical one, whereas that from the Pacific side of the peninsula and from southern California is warm temperate (Durham, 1950).

Throughout the Pleistocene, diastrophic activity continued as indicated by movements along faults and by numerous Pleistocene terraces and shell deposits high above sea level (Beal, 1948; Wilson, 1948; Noble, 1950; Ives, 1951). Frequent seismic shocks and the presence of recent fault scarps indicate that the region is still in the formative stage. Sediments have been able to keep up with subsidence only at the mouth of the Colorado River, where at least 6000 m of deltaic sediments are present.

Since Dana's first use of the term "geosynclinal" in 1873, the word geosyncline has been used in many ways—in structural, physiographic, and stratigraphic senses. For the present purpose the definition proposed by Kay (1951, p. 107) will be used: "A geosyncline is a surface of regional extent subsiding deeply during the accumulation of succeeding surficial rocks." The area of the delta fits this definition in its area, depth, and sediments. Sediments

north and south of the delta are not so thick, and those to the south are deep-water types. Although the structural and physiographic continuity is evident, the supply of sediment at the south has been inadequate to keep up with subsidence. Thus the whole Imperial Valley—Gulf of California trough must be considered a geosyncline. According to Kay's (1951) classification it might be considered an epieugeosyncline ("deeply subsiding troughs with limited volcanism associated with rather narrow uplifts and overlying deformed and intruded eugeosynclines"); however, the pre-Late Miocene eugeosynclinal sediments deposited before the main period of subsidence are rather minor. Thus, on the basis of Miocene-Recent history, the gulf is best considered a taphrogeosyncline ("sediment-filled deeply depressed rift blocks, bounded by one or more high angle faults").

Lithofacies of Gulf

Before an adequate comparison can be made between sediments of the gulf and rocks in the geologic column, it is necessary to consider what the sediments would be like after lithification. Compaction should affect primarily the fine-grained argillaceous sediment, converting it to shale, siltstone, and claystone. Coarse material should be cemented to form sandstones and conglomerates. On this basis a lithofacies map can be made of the rock types presumed to result from the lithification of sediments now in and near the gulf. In constructing the chart, near-shore areas from which samples were not available were assumed to have sand bottoms. Surrounding land areas where rock is not exposed were assumed to be covered by sand and gravel. On the basis of their high clay and feldspar content, most of the sands deposited in the gulf should form graywackes and subgraywackes according to Pettijohn's classification (1957, p. 291). Locally, sand along the sides of the gulf should form arkose. Limestone should be absent from most of the area with the exception of shell and algal limestones in a few coastal zones. The general facies based on present sediments will be two large areas of shale separated by sandstone and flanked by shallow-water sandstones and continental sandstones and conglomerates (Fig. 14).

According to Pettijohn's (1957, p. 638–644) concept of the tectonic control of sedimentation, the first sediments deposited in a geosyncline are likely to belong to the orthoquartzite-carbonate or the euxinic-black shale facies. Next is expected the Flysch facies of interbedded shale and graywacke and finally the molasse facies of subgraywackes and protoquartizites, largely nonmarine. There is no record in the gulf of either pre-Flysch facies and it is doubtful that they exist. The Flysch facies is well represented throughout most of the gulf with its widespread silty clays that should lithify to shale. Interbedded are feldspathic sands emplaced probably by turbidity currents that should form beds of graywacke. Some sediments that will be shales are euxinic in that hydrogen sulfide is present in interstitial waters although absent in overlying waters; this euxinic character is independent of the nature of detrital sediments brought to the gulf, and instead it is almost certainly the result of partial regeneration of organic matter produced in the overlying waters. Abundant diatom tests, indicative of high phytoplankton production relative to contribution of detrital sediments, should form highly siliceous shales—a unique characteristic of gulf sediments and one not typical of ancient geosynclines. The molasse facies is also represented in the gulf in the area of the Colorado delta which has built to above sea level so that continental sands relatively low in feldspar content form discontinuous sand bodies. Eventually, if subsidence were to cease, the deltaic molasse sediment would spread atop the deep-water Flysch facies but would not necessarily be separated from the Flysch by a period of intense orogenesis, as has been considered necessary in other and ancient geosynclines. In short, although the sediments of the gulf fit theories of tectonic control, the climate and areas of provenance appear to have exerted a greater control on them than has tectonism.

Diatomaceous Muds

The most distinctive sediment of the gulf is the diatomaceous mud found in the middle third. This closely resembles impure forms of diatomite of the Late Miocene Valmonte formation of the Palos Verdes Hills near Los Angeles. A sample of diatomite having nearly the same content of diatoms and calcium carbonate as the muds was found to have a closely similar grain-size distribution (Table 3). The diatoms in the Valmonte formation are more comminuted than are those of the gulf, and most are a fibrous type similar to *Thalassiothrix*, whereas most of those in the mud are whole *Coscinodiscus*-type forms. Both diatoms

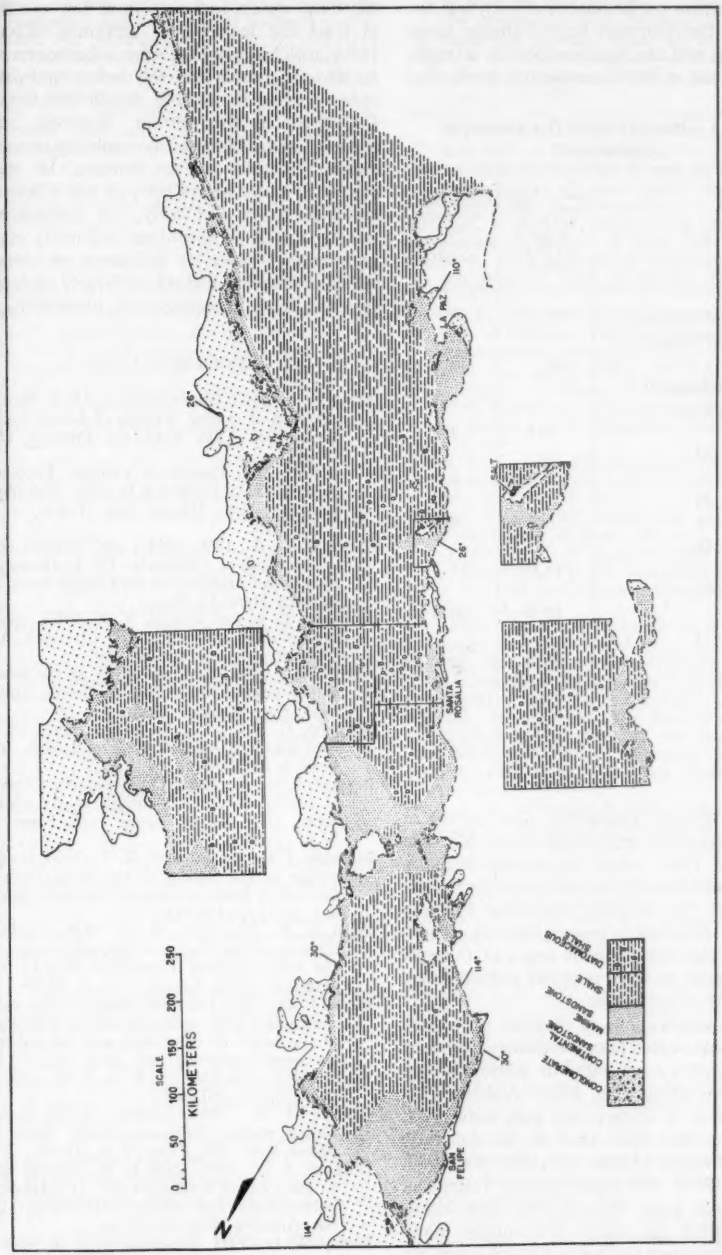

FIGURE 14.—PROBABLE LITHOFACIES TO BE EXPECTED OF PRESENT SURFACE SEDIMENTS

ceous sediments are laminated (Pl. 2), but the laminae of the diatomite have a greater range of thickness and are more continuous laterally than are those of the diatomaceous muds. The

TABLE 3.—PROPERTIES OF DIATOMACEOUS SEDIMENTS

	Gulf of California (Lat. 27° 16.3′; Long. 111°51.7′; 1496 m)	Valmonte diatomite, Late Miocene, Los Angeles
Percentage of diatoms	58	60
Percentage of calcium carbonate	23	25
Weight percentage of grains (microns)		
62	6.4	2.0
31	5.0	3.6
16	5.7	8.4
8	5.0	11.8
4	17.9	20.3
2	16.5	20.6
	43.5	33.3
	100.0	100.0

rhythmic type of lamination also occurs in porcelaneous and cherty shales of the Miocene (Bramlette, 1946), where its presence suggests seasonal variations in sedimentation like those of the gulf. In no sense can these Miocene strata be considered geosynclinal in origin. Similarly, the diatomaceous muds of the gulf do not appear to have required a geosyncline as their site of deposition.

Great concentrations of diatoms in ancient sediments have often been ascribed to abundant supplies of silica contributed by volcanic action or by rivers (Bramlette, 1946). Although the concentration of silica in the gulf water even at depth is less than that of the Colorado River—10 versus 14 ppm SiO_2 (Revelle, 1950; Howard, 1954)—the much greater volume of incoming sea water than of river flow means that upwelled sea water can supply many hundred times more silica to diatoms than can the rivers. The amount of silica in solution in the deep waters increases from the mouth to at least the region near Guaymas (Revelle, 1950), which shows that silica is being removed by diatom growth near the surface and partly redissolved as the organic debris falls through the water to the bottom. However, much silica is lost by burial of incompletely dissolved diatom frustules in the bottom. In effect, silica-rich water enters the gulf and silica-poor water leaves it. Evidently, the diatomaceous muds, as well as the other sediments of the gulf, cannot serve as indicators of tectonic sedimentation but instead are largely controlled by climatic and oceanographic phenomena.

REFERENCES CITED

Allen, W. E., 1923, Observations on the surface distribution of marine diatoms of Lower California in 1921: Calif. Acad. Sci. Proc., v. 12, p. 437–442

—— 1938, The Templeton Crocker Expedition to the Gulf of California in 1935: The phytoplankton: Am. Micros. Soc. Trans., v. 57, p. 328–335

Anderson, C. A., 1950, 1940 E. W. SCRIPPS cruise to the Gulf of California. Pt. I. Geology of islands and neighboring land areas: Geol. Soc. America Mem. 43, 54 p.

Anderson, L. J., and Revelle, R. R., 1947, Apparatus for rapid conductometric titrations: Anal. Chemistry, v. 19, p. 264–269

Beal, C. H., 1948, Reconnaissance of the geology and oil possibilities of Baja California, Mexico: Geol. Soc. America Mem. 31, 138 p.

Botsford, C. W., 1910, Geological notes on the west coast of Mexico: Eng. and Min. Jour., v. 89, p. 223–224

Bramlette, M. N., 1946, The Monterey formation of California and the origin of its siliceous rocks: U. S. Geol. Survey Prof. Paper 212, 57 p.

Buwalda, J. P., and Stanton, W. L., 1930, Geologic events in the history of the Indio Hills and the Salton Basin, southern California: Science, n. s., v. 71, p. 104–106

Cupp, E. E., and Allen, W. E., 1938, Planktonic diatoms of the Gulf of California obtained by the Allan Hancock Expedition of 1937: Allan Hancock Pacific Exped., v. 3, p. 61–99

Dana, J. D., 1873, On some results of the earth's contraction from cooling including a discussion of the origin of mountains and the nature of the earth's interior: Am. Jour. Sci., v. 5, p. 423–443, 474–475; v. 6, p. 6–14, 104–115, 161–172, 304, 381–382

Dibblee, T. W., 1954, Geology of the Imperial Valley region, California: Calif. State Div. Mines Bull. 170, Chap. 2, p. 21–28

Durham, J. W., 1950, 1940 E. W. SCRIPPS cruise to the Gulf of California. Pt. II. Megascopic paleontology and marine stratigraphy: Geol. Soc. America Mem. 43, 216 p.

Emery, K. O., 1954, Source of water in basins off southern California: Jour. Marine Research, v. 13, p. 1–21

Emery, K. O., and Dietz, R. S., 1941, Gravity coring instrument and mechanics of sediment coring: Geol. Soc. America Bull., v. 52, p. 1685–1714

—— 1950, Submarine phosphorite deposits off California and Mexico: Calif. Jour. Mines and Geology, v. 46, p. 7–15

Emery, K. O., and Hoggan, D., 1958, Gases in marine sediments: Am. Assoc. Petroleum Geologists Bull., v. 42, p. 2174–2188

Emery, K. O., and Rittenberg, S. C., 1952, Early diagenesis of California basin sediments in relation to origin of oil: Am. Assoc. Petroleum Geologists Bull., v. 36, p. 735–806

Gilbert, J. Y., and Allen, W. E., 1943, The phytoplankton of the Gulf of California obtained by the E. W. Scripps in 1939–1940: Jour. Marine Research, v. 5, p. 89–110

Goode, J. P., 1943, Goode's school atlas: New York, Rand McNally & Co., 286 p.

Gould, H. R., 1954, Sedimentology: Lake Mead Comprehensive Survey of 1948–1949: U. S. Depts. of Interior and Navy, p. 211–366

Grim, R. E., Dietz, R. S., and Bradley, W. F., 1949, Clay mineral composition of some sediments from the Pacific Ocean off the California coast and the Gulf of California: Geol. Soc. America Bull., v. 60, p. 1785–1808

Grippenberg, Stina, 1934, A study of the sediments of the north Baltic and adjoining seas: Fennia, v. 60, 231 p.

Gutenberg, B., and Richter, C. F., 1949, Seismicity of the earth: Princeton, N. J., Princeton Univ. Press, 273 p.

Hanna, G. D., 1927, Geology of the west Mexican islands: Pan-Am. Geologist, v. 48, p. 1–24

Hill, M. L., and Dibblee, T. W., Jr., 1953, San Andreas, Garlock, and Big Pine faults, California: Geol. Soc. America Bull., v. 64, p. 443–458

Howard, C. S., 1954, Physical and chemical characteristics of the inflowing water: Lake Mead Comprehensive Survey of 1948–1949: U. S. Depts. of Interior and Navy, p. 157–173

Ives, R. L., 1951, High sea levels of the Sonoran shore: Am. Jour. Sci., v. 249, p. 215–223

Kay, M., 1951, North American geosynclines: Geol. Soc. America Mem. 48, 143 p.

Larsen, E. S., Jr., 1954, The batholith of southern California: Calif. State Div. Mines Bull. 170, Chap. 7, p. 25–30

Longwell, C. R., 1954, History of the Lower Colorado River and the Imperial Depression: Calif. State Div. Mines Bull. 170, Chap. 5, p. 53–56

Marine Research Committee, 1958a, Physical and chemical data, CCOFI cruise 5702 (MLR 93) 6–26 February 1957: Scripps Inst. Oceanography, p. 14–47

Marine Research Committee, 1958b, Physical and chemical data, CCOFI cruise 5708 (MLR 99) 9–27 August 1957: Scripps Inst. Oceanography, p. 223–250

Milner, H. B., 1952, Sedimentary petrography: 3d ed., London, Thos. Murby and Co., 666 p.

Munk, W. H., 1941, Internal waves in the Gulf of California: Jour. Marine Research, v. 4, p. 81–91

National Research Council, 1948, Rock-color chart: Washington, D. C., 6 p.

Natland, M. L., 1950, 1940 E. W. Scripps' cruise to the Gulf of California. Pt. IV. Report on the Pleistocene and Pliocene Foraminifera: Geol. Soc. America Mem. 43, 56 p.

Noble, J. A., 1950, Manganese on Punta Concepción, Baja California, Mexico: Econ. Geology, v. 45, p. 771–785

Ordóñez, E., 1936, Principal physiographic provinces of Mexico: Am. Assoc. Petroleum Geologists Bull., v. 20, p. 1277–1307

Osorio Tafall, B. F., 1943, El mar de Cortés y la productividad de sus aguas: Anales de la Escuela Nac. de Ciéncias Biol., v. 3, p. 73–118

Pettijohn, F. J., 1957, Sedimentary rocks: 2d ed., New York, Harper & Bros., 718 p.

Reiche, P., 1950, A survey of weathering processes and products: Univ. N. M. Pub. Geology, no. 3, 95 p.

Revelle, R., 1950, 1940 E. W. Scripps cruise to the Gulf of California. Pt. V. Sedimentation and oceanography: survey of field observations: Geol. Soc. America Mem. 43, 6 p.

Rittenberg, S. C., Emery, K. O., and Orr, W. L., 1955, Regeneration of nutrients in sediments of marine basins: Deep-Sea Research, v. 3, p. 23–45

Roden, G. I., 1958, Oceanographic and meteorological aspects of the Gulf of California: Pacific Sci., v. 12, p. 21–45

Shepard, F. P., 1948, Submarine geology: New York, Harper & Bros., 348 p.

—— 1950, 1940 E. W. Scripps cruise to the Gulf of California. Pt. III. Submarine topography of the Gulf of California: Geol. Soc. America Mem. 43, 32 p.

—— 1954, Nomenclature based on sand-silt-clay ratios: Jour. Sed. Petrology, v. 24, p. 151–158

Slevin, J. R., 1923, Expedition of the California Academy of Sciences to the Gulf of California in 1921: Calif. Acad. Sci. Proc., v. 12, p. 55–72

Sverdrup, H. U., 1940, The Gulf of California: Preliminary discussion of the cruise of the "E. W. Scripps" in February and March, 1939: 6th Pacific Sci. Cong. Proc., v. 3, p. 161–166

Sverdrup, H. U., and staff, 1943, Oceanic observations of the Scripps Institution in 1939: Rec. Observations Scripps Inst. Oceanography, v. 1, p. 65–160

Sykes, G., 1937, The Colorado delta: Carnegie Inst. Wash. Pub. 460, 193 p.

Tamayo, J. L., 1949, Geografía general de México, Tomo II: México, D. F., 583 p.

Tarbet, L. A., 1951, Imperical Valley: Am. Assoc. Petroleum Geologists Bull., v. 35, p. 260–263

Townsend, C. H., 1901, Dredging and other records of the U. S. Fish Commission Steamer "Albatross" with bibliography relative to the work of the vessel: U. S. Fish Comm. Rept. for 1900, p. 387–562

Twenhofel, W. H., and Tyler, S. A., 1941, Methods of study of sediments: New York, McGraw-Hill Book Co., Inc., 183 p.

U. S. Bureau of Reclamation, 1952, Report of river control and investigations, lower Colorado River basin, calendar years 1950 and 1951: Special Pub., 98 p.

U. S. Navy Hydrographic Office, 1951, Sailing directions for the west coasts of Mexico and Central America: 9th ed., Pub. 84, 305 p.

Vinogradov, A. P., 1953, The elementary composi-

tion of marine organisms: New Haven, Conn., Sears Found. for Marine Research, Yale Univ., 647 p.

Wilson, I. F., 1948, Buried topography, initial structure and sedimentation in the Santa Rosalia area, Baja California, Mexico: Am. Assoc. Petroleum Geologists Bull., v. 32, p. 1762–1807

—— 1955, Geology and mineral deposits of the Boleo copper district, Baja California, Mexico: U. S. Geol. Survey Prof. Paper 273, 134 p.

Wisser, E. H., 1954, Geology and ore deposits of Baja California: Econ. Geology, v. 49, p. 44–76

DEPARTMENT OF OCEANOGRAPHY, OREGON STATE COLLEGE, CORVALLIS, OREGON; DEPARTMENT OF GEOLOGY, UNIVERSITY OF SOUTHERN CALIFORNIA, LOS ANGELES 7, CALIF.

MANUSCRIPT RECEIVED BY THE SECRETARY OF THE SOCIETY, FEBRUARY 9, 1959

ALLAN HANCOCK FOUNDATION CONTRIBUTION No. 239

BULLETIN OF THE GEOLOGICAL SOCIETY OF AMERICA
VOL. 71, PP. 1011-1026, 4 FIGS. JULY 1960

CHEMICAL COMPOSITION OF SANDSTONES

By G. V. Middleton

Abstract

The author has collected 168 chemical analyses from the literature. All analyses with less than 5 per cent Al_2O_3 ("quartzite" clan) were removed. The remaining analyses were divided on a tectonic basis into three clans; taphrogeosynclinal, eugeosynclinal, and others (mainly exogeosynclinal). Histograms for the seven major oxides and variation diagrams for K_2O/Na_2O and alkalies/Al_2O_3 indicate that the tectonic associations group together clans of chemical analyses which differ significantly from each other. The eugeosynclinal graywackes especially differ from other sandstones by their low K_2O/Na_2O ratio, which is correlated with the presence of basic volcanic detritus. Arithmetic and geometric means for the seven major oxides for the four clans are as follows (given to two significant figures):

	Taphrogeosynclinal		Eugeosynclinal		Exogeosynclinal		"Quartzites"		Average Arith.
	Geom.	Arith.	Geom.	Arith.	Geom.	Arith.	Geom.	Arith.	
SiO_2	83	80	71	69	79	73	93	87	78
Al_2O_3	11	10	14	13	12	11	3.3	3.1	8.7
Fe_2O_3 (total iron)	2.0	2.5	4.9	5.4	3.6	4.2	1.5	3.8	4.1
MgO	0.24	0.53	2.2	2.5	1.2	1.8	0.34	0.69	1.4
CaO	0.89	2.8	2.7	4.4	2.4	6.9	0.37	3.8	4.6
Na_2O	0.72	1.3	3.1	3.2	0.83	1.1	0.31	0.48	1.4
K_2O	2.9	3.2	1.8	2.0	1.5	1.9	0.82	1.3	1.9

CONTENTS

TEXT

Page
Introduction 1011
Chemical characteristics of the main sandstone clans 1015
The average sandstone 1020
Appendix: list of analyses 1021
References cited 1025

ILLUSTRATIONS

Figure Page
1. Alkalies–alumina histograms 1014
2. Alkalies–alumina variation diagrams 1019
3. K_2O–Na_2O variation diagrams 1020
4. Histograms for eight major oxides in the four sandstone clans 1022

TABLES

Table Page
1. Average compositions of sandstone clans. 1015
2. Average compositions of sandstones from the literature 1016
3. Composition of the average sandstone ... 1017

Introduction

The author has collected 168 analyses of sandstones from the literature. The analyses are grouped into four sandstone clans; the basis of the classification is primarily structural rather than petrographical or geochemical. The average chemical composition differs significantly from clan to clan, and the reason for these differences is discussed.

The author wishes to express his thanks to R. E. Jones and D. M. Shaw for criticism and discussion of this paper. This paper contains results of work preliminary to a project on the petrography and geochemistry of graywackes

which is being supported by grants from the Geological Survey of Canada.

SELECTION OF ANALYSES: Most of the analyses come from Europe (especially Great Britain, France, and Switzerland) and America. In order to avoid undue bias, the author did not include analyses of Pleistocene and Recent sediments in this study. Glacial deposits are rare in the geological column, and yet many analyses of Pleistocene glacial sediments are available. Many recent sediments must be greatly influenced by being reworked from glacial deposits and are therefore also excluded.

No composite analyses or averages were used. Except for the sandstone dikes of Shasta County, California, which are not normal sediments, all analyses which gave values for alkalies and alumina have been accepted. Since many analyses of building stones do not give values for alkalies, they have been rejected. This means that the analyses used are not very strongly biased toward those sandstones which are economically valuable. The analyses used probably include too many unusual varieties, especially those with cements of unusual types. These analyses were not excluded, however, because the main part of the sandstone is probably not unusual. Unusual cement will not greatly affect the averages provided they are calculated on a geometric rather than on an arithmetic basis.

Some of the older analyses are probably not accurate. In some cases inaccurate analysis is rather strongly suggested (*e.g.*, analysis 147 has total alkalies in excess of alumina), but since it is difficult to determine without introducing personal bias which of the older analyses are not reliable, no analysis has been rejected because of suspected inaccuracy. Eight major oxides were studied, and their distribution is shown in histograms (Fig. 4). Neither CO_2 nor combined water were considered because relatively few analyses give accurate determinations: many analyses merely record "loss on ignition". The sources of the analyses are given in the Appendix.

PREVIOUS WORK: Earlier studies of the geochemistry of sandstones include averages calculated by Clarke (1924), Tyrrell (1933), and Pettijohn (1957). Mackie (1900) in his chemical and petrographic study of Torridonian, Devonian, and Permo-Triassic sandstones in the Elgin area, Scotland, remarked upon the preferential removal of lime, magnesia, and soda during weathering and the consequently high K_2O/Na_2O ratio in sandstones. Kennedy (1951) in a comparative study of Torridonian and Moinian sediments argued that the chemical differences between these two groups result from sedimentary differentiation within a single sedimentary group. He showed that the increase in silica and decreases in alumina and in K_2O/Na_2O ratio in the Moines as compared with Torridonian are similar to chemical variation observed by Barth (1938) within the Sparagmite group of Southern Norway and ascribes the variation to a progressive increase in the "residual" component of the sedimentary rocks as the distance from the source area increases.

Apart from brief discussions by authors of the general role played by sandstones in the geochemical cycle and a few studies of minor elements in sandstones (*e.g.*, Murray and Adams, 1958), little attention has been paid to the chemical composition of sandstones.

GROUPING OF ANALYSES: A number of problems beset any geochemical study of sandstones. The chemical characteristics of sandstones depend upon (1) the geological processes acting before and during deposition, and (2) diagenetic processes acting after the deposition of the sand. The latter include compaction, cementation, and removal of minerals by intrastratal solution. The diagenetic factors are subject to erratic variation, so that it is generally agreed that sandstones should be classified primarily on the basis of characteristics which reveal the provenance or transportational and depositional history of the rock.

For this study, however, it was decided not to group the sandstones according to their petrographic or geochemical characteristics, nor according to the local nature of the ancient environment in which they were deposited, but according to the broader tectonic setting of the basin in which they were deposited. The primary basis of grouping is therefore structural.

Such a grouping of sandstones corresponds closely to Krynine's classification. However, instead of Krynine's three groups of detrital rocks (Krynine, 1948, p. 136), four clans are recognized. This follows Krynine's most recent remarks upon the classification of sandstones (Krynine, 1956). Krynine's classification of sediments is primarily tectonic, yet, as he remarks (1942, p. 542), "... the fundamental difference between various regional diastrophic types is *mineralogical* and hence to a large extent chemical." This being the case, the different tectonic associations should include groups of sediments which show distinct chemical variation series, although transitional

types may be expected and certain chemical types may be common to two or more tectonic associations.

The writer attempted a grouping based on tectonics (1) because a large number of the analyses are not accompanied by a satisfactory petrographic description of the rock, so that a petrographic classification would be impossible; and (2) because he wished to test the hypothesis that a tectonic classification would group together clans of analyses which differed significantly.

All sandstones with Al_2O_3 <5 per cent were first separated into a clan called "quartzites". This was done largely for convenience and because ratio diagrams, such as Al_2O_3/alkali diagrams, would be needlessly complicated by the inclusion of analyses of sandstones which contained very little besides quartz and a cement.

The remaining sandstones were then distributed into clans according to the following tectonic classification:[1]

(1) taphrogeosynclinal or postorogenic graben sandstones

(2) eugeosynclinal including also epieugeosynclinal sandstones

(3) exogeosynclinal and other sandstones.

The exogeosynclinal group is the least well defined and probably includes some sandstones from miogeosynclines and autogeosynclines. Probably some of the sandstones here grouped as quartzites properly belong tectonically to one of the other three groups.

It is *not* suggested that rocks of any particular composition, mineralogical or chemical, are restricted to a particular tectonic setting. Nevertheless, it is suggested that the evidence presented in this paper confirms Krynine's statement quoted heretofore. Most of the analyses grouped as "quartzites" were described as such in the literature and came from stable shelf, miogeosynclinal, autogeosynclinal, or exogeosynclinal sites: most of those grouped as eugeosynclinal were described as graywackes (or high-rank graywackes); most of those grouped as taphrogeosynclinal were described as arkoses or feldspathic sandstones; and most of those grouped as exogeosynclinal were described as sandstones or low-rank graywackes.

The incorrect grouping of a few sandstone analyses, which may have resulted from the present author's ignorance of the correct tectonic setting or as a result of the consequences of forcing sandstones into a somewhat inflexible grouping, will not, however, seriously affect the generalizations made. A far more serious criticism, in the author's opinion, would be the inadequacy of the sample which was available.

The following paragraphs show how the analyses have been grouped. Numbers refer to entries in the Appendix. Query marks indicate that insufficient information is available to determine the tectonic setting with certainty.

QUARTZITES: 1, 2, 3, 4, 5, 6, 7, 19, 25, 26, 42, 47, 53, 54, 56, 59, 63, 66, 69, 71, 72, 73, 78, 79, 92, 93, 94, 95, 96, 97, 98, 128, 130, 131, 138, 139, 140, 141, 147, 148, 152, 155, 156, 158, 159, 160, 161, 162, 163, 164, 165, 166, 167, 168

TAPHROGEOSYNCLINAL: 18, ? 21, ? 23, 24, 38, 49, 60, 104, 105, 106, 107, 108, 109, 110, 111, 136, 137, 142, 143, 144, 145, 146, 149, 150, 151, 153, 154, ? 157

EUGEOSYNCLINAL: 11, 12, ? 22, ? 40, ? 43, 44, 45, ? 50, ? 57, ? 61, 64, 67, 68, 80, 81, 82, 83, 84, ? 85, ? 86, ? 87, 88, 89, 90, 91, 100, 101, 102, 103, 112, 113, 114, 115, 120, 121, 122, 123, 124, 125, ? 134, ? 135

EXOGEOSYNCLINAL: 8, 9, 10, 13, 14, 15, 16, ? 17, ? 20, 27, 28, 29, 30, 31, 32, 33, 34, 35, 36, 37, ? 39, ? 41, ? 46, ? 48, ? 51, ? 52, ? 55, 58, ? 62, ? 65, 70, 74, 75, 76, 77, ? 99, 116, 117, 118, 119, ? 126, ? 127, ? 129, ? 132, ? 133

FACTORS INFLUENCING CHEMICAL COMPOSITION: The common cementing agents are carbonates and silica. Hence the abundances of SiO_2, CaO, and MgO are practically valueless for any indication of the prediagenetic history of the rock. It may be, however, that certain types of sandstones more commonly have certain types of cements than other types.

Another factor is introduced by the presence or absence of cement. The original porosity of sandstones is about 20–30 per cent, and consequently the percentage weight of any oxide other than one contained in the cement will be reduced by about 25 per cent if a cement is introduced before compaction. Hence little importance can be ascribed to the weight per cent of any oxides, as quoted in the chemical analysis, without correcting for the introduction of cement. Such a correction is very difficult to make. Even in the case of a carbonate cement, it is not known whether some of the carbonate may not have been present as rock or fossil fragments rather than as introduced cement. The exact composition of the carbon-

[1] Most geologists will recognize the grouping that the author is attempting to achieve, which corresponds roughly to Krynine's groups or series (1948) or clans (1956), to Pettijohn's consanguineous associations or facies (1957), and to Dapples, Krumbein, and Sloss' lithologic associations (1948).

ate is also not known. In the case of silica a correction is not possible without a detailed petrographic investigation of the rock.

Hence it is clear that ratios between oxides must be studied in preference to actual weight per cent.

The contents of Fe_2O_3 and FeO in sandstones depend upon a number of factors. Iron may be present in a sandstone (1) in allogenic (terrigenous) minerals such as iron oxides, sulfides or carbonates, clay minerals, micas, and chlorite; (2) in rock fragments—these are mainly of two types, (a) sedimentary, including shales and siltstones and their low-grade metamorphic derivatives, and (b) volcanic, especially basic volcanic rocks; (3) in jasper (ferruginous chert); (4) in authigenic (orthochemical) sulfides, carbonates, or hydrated oxides; and (5) in glauconite. The presence of iron in a sandstone is therefore controlled primarily by its provenance but also by the chemical conditions which prevailed in the basin of deposition and in the sediment during diagenesis, particularly during the early stages of diagenesis. A further factor is the intensity and duration of weathering of the source materials prior to deposition. In general, the more intense and prolonged the weathering, the more iron will pass into solution and therefore will not be deposited in a sandstone.

Alumina and alkalies occur in sandstones in: clay minerals; micas; feldspars; glauconite; argillaceous or micaceous rock fragments; and volcanic rock fragments. Further consideration of the forms listed shows that both alkalies and alumina occur essentially in two main groups of minerals: (1) clay minerals, micas, and chlorites, and (2) feldspars. None of these minerals are commonly quantitatively important as authigenic minerals, although traces of authigenic feldspar and mica are not rare. Hence, if a chemical investigation of sandstones is to be independent of diagenetic factors, it may be based upon ratios between Al_2O_3 and alkalies or between individual pairs of oxides.

The clay mineral-mica group has a lower $K^{+1} + Na^{+1}/Al^{+3}$ ratio (atomic ratio about 0.15–0.5:1) than the feldspar group (atomic ratio about 0.5–1:1). If, therefore, there are two series of sandstones, one characterized by high feldspar content and relatively low content of clays and micas (the arkoses) and the other characterized by a relatively low content of feldspars and high content of clays, micas, chlorites, and argillaceous rock fragments (the graywackes) as maintained by Krynine (1948), with relatively few transitional types, then a histogram for the ratio alkalies/Al_2O_3 might show a bimodal distribution (Fig. 1). In order to avoid confusion by quartz-rich sandstones, only those sandstones containing more than 5.0 per cent Al_2O_3 were selected. Glauconitic sandstones were also excluded.

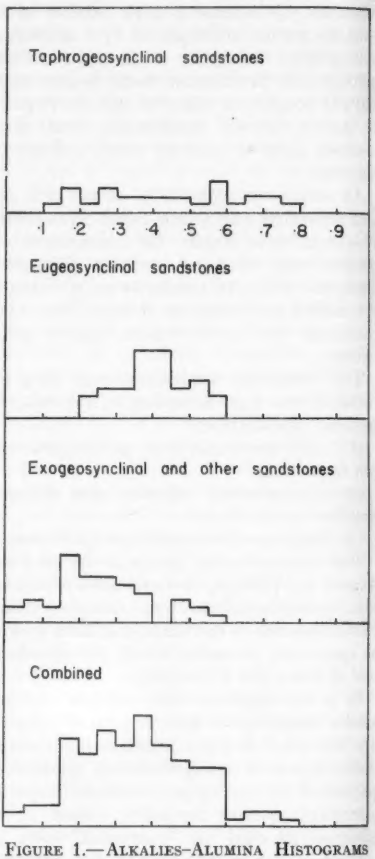

FIGURE 1.—ALKALIES–ALUMINA HISTOGRAMS

The histograms show the distribution of the ratio alkalies/alumina for the taphrogeosynclinal, eugeosynclinal, and exogeosynclinal clans, and for the three clans combined. Note that the histogram for the combined clans shows a very broad maximum, suggesting bimodality. There is a clear distinction in modal ratios between the eugeosynclinal and exogeosynclinal clans.

The resulting histogram is inconclusive

It shows a slight bimodality which cannot be considered significant in view of the inadequate sampling. The histograms for individual sandstone clans are also plotted. Comparison of these shows that the lower maximum in the combined histogram is due mainly to the abundance of exogeosynclinal sandstones, whereas the higher maximum is a composite of the eugeosynclinal and taphrogeosynclinal sandstones.

TABLE 1.—AVERAGE COMPOSITIONS OF SANDSTONE CLANS

Averages for SiO_2 and Al_2O_3 are grouped arithmetic means; averages for other elements are grouped geometric means. Numbers in parentheses are ungrouped arithmetic means.

	Taphrogeosynclinal	Eugeosynclinal	Exogeosynclinal and others	"Quartzite"
SiO_2	77.12 (77.10)	65.67	68.43	(83.11)
Al_2O_3	9.85	12.73	10.23	(2.96)
Fe_2O_3	1.82 (2.40)	4.52 (5.09)	3.10 (3.89)	1.33 (3.64)
MgO	0.22 (0.51)	2.03 (2.40)	1.07 (1.71)	0.30 (0.66)
CaO	0.83 (2.68)	2.51 (4.20)	2.08 (6.40)	0.33 (3.62)
Na_2O	0.67 (1.24)	2.86 (3.04)	0.72 (1.00)	0.28 (0.46)
K_2O	2.68 (3.05)	1.65 (1.87)	1.31 (1.75)	0.73 (1.28)
TOTAL	93.19 (96.83)	91.97 (95.00)	86.94 (93.41)	89.04 (95.73)
Recalculated to 100 per cent				
SiO_2	82.75 (79.62)	71.40 (69.12)	78.71 (73.25)	93.34 (86.82)
Al_2O_3	10.57 (10.17)	13.84 (13.40)	11.77 (10.95)	3.32 (3.09)
Fe_2O_3	1.95 (2.48)	4.92 (5.36)	3.56 (4.16)	1.49 (3.80)
MgO	0.24 (0.53)	2.21 (2.53)	1.23 (1.83)	0.34 (0.69)
CaO	0.89 (2.77)	2.73 (4.42)	2.39 (6.85)	0.37 (3.78)
Na_2O	0.72 (1.28)	3.11 (3.20)	0.83 (1.07)	0.31 (0.48)
K_2O	2.88 (3.15)	1.79 (1.97)	1.51 (1.87)	0.82 (1.34)
TOTAL	100.00 (100.00)	100.00 (100.00)	100.00 (99.98)	99.99 (100.00)

CHEMICAL CHARACTERISTICS OF THE MAIN SANDSTONE CLANS

Tables 1–3 show the compositions of sandstones.

"QUARTZITE" CLAN: Quartzites have been defined arbitrarily herein as sandstones containing less than 5.0 per cent Al_2O_3. Theoretically, a sandstone with 5.0 per cent Al_2O_3 might consist of a pure quartz sand with up to 30 per cent argillaceous matrix; practically, such a situation appears to be rare. Almost all sandstones with 5 per cent alumina contain a fair proportion of rock fragments and/or feldspar in addition to argillaceous material. Most of the analyses included in this group are of rocks described as quartzites, protoquartzites, and quartz sandstones.

Some of the sandstones grouped in the quartzite clan are found in miogeosynclines and other noncratonic settings. As a result of the arbitrary definition of quartzites the classification used here departs to some extent from a true tectonic classification.

Sandstones described as glauconitic were also included in the quartzite clan even if the Al_2O_3 content exceeded 5.0 per cent. One exception to this rule was made: for the purposes of comparison two glauconitic Molasse[2] sandstones were included with most of the other Molasse sandstones in the exogeosynclinal clan. Glauconite is an authigenic mineral of unusual chemical composition, so that glauconitic sandstones are easily recognized

[2] Molasse is used in this paper in a stratigraphic sense to refer to certain groups of sandstones found in Switzerland and adjacent areas (*cf.* Appendix). The same applies to the usage in the explanation of Figures 2 and 3 of the term Flysch.

from their chemical analyses. In general they have a high alkalies/Al_2O_3 ratio and high K_2O/Na_2O ratio, but unlike the arkoses they have a high total iron/alkalies ratio. Glauconite usually indicates slow deposition, and hence cratonic setting; however, glauconitic sandstones are also found in extracratonic environments (*e.g.*, in the Molasse).

TABLE 2.—AVERAGE COMPOSITIONS OF SANDSTONES FROM THE LITERATURE

	1	2	3	4	5	6
SiO_2	78.66	84.86	68.1	64.7	76.37	93.16
TiO_2	0.25	0.41	0.7	0.5	0.41	0.03
Al_2O_3	4.78	5.96	15.4	14.8	10.63	1.28
Fe_2O_3	1.08	1.39	1.0*	1.5	2.12	0.43
FeO	0.30	0.84	3.4	3.9	1.22	
MgO	1.17	0.52	1.8	2.2	0.23	0.07
MnO	tr	tr	0.2	0.1	0.25	
CaO	5.52	1.05	2.3	3.1	1.30	3.12
Na_2O	0.45	0.76	2.6	3.1	1.84	0.39
K_2O	1.32	1.16	2.2	1.9	4.99	
H_2O+	1.33	1.47	2.1	2.4	0.83	0.65
H_2O-	0.31	0.27		0.7		
P_2O_5	0.08	0.06	0.2	0.2	0.21	
CO_2	5.04	1.01	..	1.3	0.54	2.01
SO_3	0.07	0.09	..	0.4	..	..
SrO	tr	none	..	..	..	..
BaO	0.05	0.01	..	..	..	..
Li_2O	tr	tr	..	..	..	..
S				0.2		
TOTAL	100.41	99.86	100.00	101.0	100.94	101.14

1. Composite analysis of 253 sandstones (Clarke, 1924, p. 547)
2. Composite analysis of 371 sandstones used for building purposes (Clarke, 1924, p. 547)
3. Average graywacke (Tyrrell, 1933) (30 analyses)
4. Average graywacke (Pettijohn, 1957) (23 analyses)
5. Average arkose (Pettijohn, 1957) (5 analyses)
6. Average quartzite (Pettijohn, 1957) (8 analyses)

* Corrected from 3.4, as originally given (probably a misprint)

TAPHROGEOSYNCLINAL SANDSTONE CLAN: The tectonic setting of this clan is the taphrogeosyncline (Kay, 1951), possibly also including some zeugogeosynclines, or the intracratonic fault basin (Krumbein and Sloss, 1953). The sediments are also frequently called postorogenic since they usually occur in fault basins formed in association with an orogenic belt but after the main period of folding and metamorphism. Many of the arkoses are found in this setting, but certain analyses of rocks named arkose do not fit the sedimentary-tectonic framework of this clan (*cf.* analyses nos. 22, 40 in the Appendix). These examples can also be clearly distinguished by their chemical characteristics, and they belong properly to the group of high-rank or eugeosynclinal graywackes. On the other hand, many of the sandstones included in this clan would not be petrographically described as arkoses but as feldspathic sandstones; a few so-called arkoses are also found in the exogeosynclinal clan.

The variation diagrams (Figs. 2, 3) show that the taphrogeosynclinal clan is characterized by high K_2O/Na_2O ratio (very rarely less than 1.00) and by high alkalies/Al_2O_3 ratio. The common red, obviously iron-stained or cemented sandstones in this clan are actually much poorer in iron than the graywackes. The reason is that the average granite, granodiorite, or feldspathic gneiss (from which arkoses are derived) contains relatively little iron (usually about 1.5–2.5 per cent).

The arkoses (as commonly petrographically defined) occur almost exclusively within the arkose clan. Their chemical composition distinguishes them from the other main group of highly feldspathic sediments, the high-rank graywackes which occur almost exclusively in the eugeosynclinal clan. Comparison of the distribution diagrams for K_2O/Na_2O (Fig. 3) shows that there is practically no overlap of the fields for the two clans; relatively little overlap is observed in the diagrams for alkalies/Al_2O_3 (*cf.* Figs. 2, 3). This observation supports Krynine's view and invalidates Gilbert's contention (1955, p. 295) that it is incorrect to contrast graywackes with arkoses. It should be noted, however, that Gilbert chose feldspar content as his criterion of whether or not a rock is arkosic. Defining an arkose only on this basis neglects completely a fundamental difference between two important clans of sandstones. Contrary to Gilbert's opinion, the term graywacke is not necessarily defined on a textural basis, but may be defined on the basis of mineralogy. Many exogeosynclinal graywackes are relatively well sorted and would undoubtedly be called quartzites but for the presence of many dark fine-grained rock fragments. Recently an attempt has been made by Pettijohn (1957, p. 301–314), using the criterion of clay content, to class as graywackes (as opposed to subgraywackes) only those graywackes which are also turbidites (Kuenen, 1957). The author believes that this is a valid point of view, but that it excludes from the graywackes many rocks to which geologists have consistently given the name in the past. Furthermore, it is very doubtful whether Pettijohn's proposed mineralogical classification is effective in separating turbidites from other types of sandstones (*cf.* Krynine, 1956).

TABLE 3.—COMPOSITION OF THE AVERAGE SANDSTONE

	1	2	3
SiO_2	77.96	84.30	77.89
Al_2O_3	9.17	5.12	8.74
Fe_2O_3	3.65	1.51	4.06
MgO	1.22	1.25	1.40
CaO	4.59	5.92	4.57
Na_2O	1.22	0.48	1.41
K_2O	2.18	1.41	1.92
TOTAL	99.99	99.99	99.99

1. Average prepared from arithmetic averages in Table 1, weighted as follows: taphrogeosynclinal:eusynclinal:exogenosynclinal:"Quartzite" = 32.5:10:35:22.5.

2. Clarke's composite (Table 2, analysis 1) recalculated to seven major elements for comparison.

3. Average prepared from arithmetic averages in Table 1, weighted according to the relative abundance of analyses used in this study.

EUGEOSYNCLINAL CLAN: These sandstones are in fact (although not necessarily by definition) the graywackes of Pettijohn (1957). As far as the author knows they are most commonly although not invariably turbidites. They are distinguished by their occurrence in folded mountain belts and by their association with volcanic rocks, radiolarian cherts, graptolitic shales, and intrusive(?) serpentines. No distinction is made herein between the eugeosynclines and epieugeosynclines of Kay (1951). The analyses probably include relatively few epieugeosynclinal sandstones.

The sandstones in this clan have one chemical characteristic which clearly sets them off from all other sandstones (except probably for a few noneugeosynclinal volcanic sandstones)—they have a K_2O/Na_2O ratio of less than 1.0 (*See* Fig. 3). This characteristic needs further investigation. Pettijohn (1943; 1949) noted the low K_2O/Na_2O ratio of graywackes (high-rank graywackes of Krynine, 1948) and remarked that although the composition of a graywacke might be approximated by a mixture of two parts shale with one part arkose, this mixture did not give the right proportions of K_2O and Na_2O. Pettijohn (1949) suggested that incomplete chemical weathering of the source material was responsible.

An analysis of the possible causes of low K_2O/Na_2O ratio suggests the following possible explanations:

(1) The source rocks are soda-rich. The most abundant possible source rocks have average contents of alkalies as shown at the top of the next page.

From this it is clear that the most promising source for abundant Na_2O is basic volcanic rocks, especially in the spilite suite. Spilites, furthermore, are characteristically associated with eugeosynclinal belts. In many cases where the petrography of eugeosynclinal graywackes has been studied, the presence of volcanic debris in these sandstones has been reported.

Rock Type	Na_2O (Per Cent)	K_2O (Per Cent)	K_2O/Na_2O Ratio	Source of Averages
Precambrian granite	3.24	4.50	1.39	Daly (1933, p. 9)
Alkaline granite	4.55	4.20	0.92	Daly (1933, p. 10)
Quartz diorite	3.37	2.10	0.62	Daly (1933, p. 15)
Granodiorite	3.70	2.75	0.74	Daly (1933, p. 15)
Rhyolite	3.34	4.58	1.37	Daly (1933, p. 9)
Andesite	3.58	2.04	0.57	Daly (1933, p. 16)
Basalt	3.11	1.52	0.49	Daly (1933, p. 15)
Spilite	4.93	0.73	0.15	Sundius (1930)
Shale	1.83	3.73	2.04	Shaw (1956, p. 929)
Mica schist	2.00	3.43	1.71	Shaw (1956, p. 929)
Granite gneisses	3.0–3.5	2.5–3.0	0.85 (approx.)	Lapadu-Hargues (1946, p. 28

Other volcanic sandstones which possibly may not be truly eugeosynclinal (*e.g.*, the Mt. Diablo sandstones from California which are epieugeosynclinal?) show very close chemical similarities to the eugeosynclinal graywackes.

(2) Regional soda metasomatism. This explanation cannot be lightly dismissed in view of the body of opinion which explains the closely associated spilite suite of volcanic rocks in this way. However, the author rejects this hypothesis because there is practically no petrographic evidence to support a theory of regional metasomatism of graywackes.

(3) Incomplete weathering of the source rocks (Pettijohn, 1949). Since Na_2O is removed from rocks during weathering at least as rapidly as K_2O and commonly more rapidly (*cf.* Leith and Mead, 1915; Goldich, 1938), and since potassium feldspars are believed to be more resistant to weathering than plagioclase feldspars, it appears that the source rock for graywackes must have at least as low a K_2O/Na_2O ratio as they have, however incomplete the weathering. Evidence in favor of this hypothesis, as opposed to the hypothesis of basic volcanic provenance, is fairly convincing in some cases. Petrographic studies of some eugeosynclinal graywackes show practically no evidence for basic volcanic provenance but strong evidence for high-grade metamorphic or granite gneiss provenance. An example is the Rensselaer grit (Dale, 1893; Balk, 1953). Also it is clear from the figures given that the abundant quartz diorite-granodiorite plutonic association is sufficiently rich in soda to be a suitable source for graywackes in which the K_2O/Na_2O ratio is not too low. This is particularly apparent if some of the K_2O in plutonic rocks is concentrated not in the relatively stable potassium feldspars but in the unstable mineral biotite. It must be remembered that a low K_2O/Na_2O source-rock ratio is required to offset the effect, in the derived graywacke, of clay materials and argillaceous rock fragments.

The writer concludes that the peculiar characteristics of high-rank graywackes are a result of a partial volcanic (spilitic) provenance, combined with rapid erosion and little chemical weathering. Petrographic evidence supports this hypothesis in many cases (*e.g.*, Tanner graywacke, Harz, Germany, Helmbold, 1952; Barmouth grit, North Wales, Matley and Wilson, 1946, p. 31; Taveyanna sandstone, Switzerland (Flysch), Niggli and Niggli, 1952, p. 244; Franciscan graywacke, California, Gilbert, 1955, p. 303; Knife Lake graywacke, Minnesota, Grout, 1933, p. 995; Archean graywacke, Kirkland Lake, Ontario, Todd, 1928, p. 19–20).

The important differences between high-rank graywackes and low-rank graywackes and arkoses suggest the advisability of a revision of existing petrographic classifications to make this distinction more evident on a petrographic level. This might be achieved by distinguishing between potassium and plagioclase feldspars and between argillaceous or metamorphic and volcanic rock fragments.

The high content of iron may be attributed to derivation from basic volcanic rocks (with an average total iron of over 13 per cent Fe_2O_3) and argillaceous rocks (with an average total iron of about 7 per cent Fe_2O_3). The provenance, rapid erosion, and deposition in generally deep, poorly oxygenated waters all contribute

the low Fe_2O_3/FeO ratio. The alkalies/$_2O_3$ ratio is lower than that of arkoses as a sult of the abundance of argillaceous mate-ls both as rock fragments and as clay atrix. As indicated by Figure 1, there is little

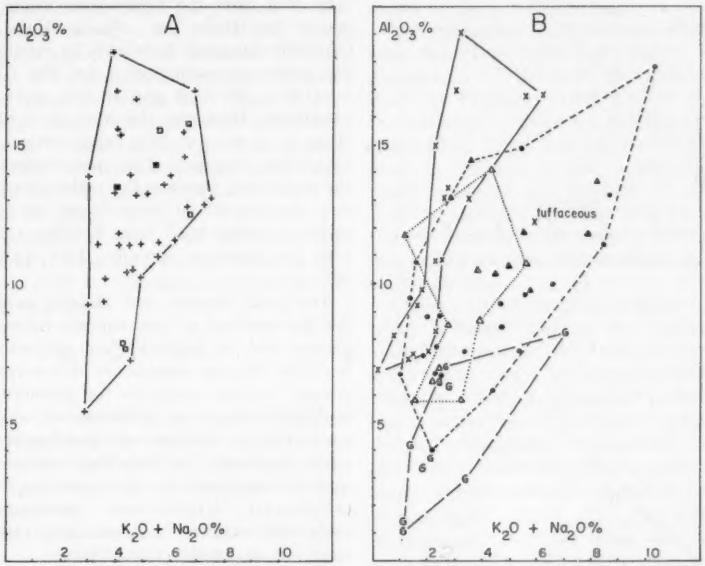

FIGURE 2.—ALKALIES–ALUMINA VARIATION DIAGRAMS

A shows the distribution of values for the eugeosynclinal sandstones. Open squares indicate sandstones om the Flysch of Switzerland, and solid squares indicate sandstones from the Macigno of Italy. B shows e distribution of values for the Molasse (open triangle), Coal Measures (cross), taphrogeosynclinal (solid rcle and solid triangle), and glauconitic (G) sandstones. Within the taphrogeosynclinal clan, the Torri-nian sandstones are indicated by the solid triangle. Notice the wide range of variation within a formation most as large as within-clan variation).

The Coal Measure sandstones form a well-defined subgroup of the exogeosynclinal clan. The Molasse ndstones are intermediate in character between the Coal Measure sandstones and the majority of the phrogeosynclinal sandstones. Note that the distinction between taphrogeosynclinal and Coal Measure ndstones becomes clearer at higher values of alumina.

The glauconitic sandstones form a clearly defined group rich in alkalies.

idence to support a belief that there is a ear separation between sandstones with ldspar and a few clay materials or chlorite arkoses), and sandstones rich in clay and loritic materials. An opposite opinion. owever, is not clearly supported either, nce other factors may produce the observed istribution of elements (*e.g.*, the diagenetic eakdown of feldspars).

The characterization of eugeosynclinal gray-ackes by their basic volcanic provenance is lly in accordance with Kay's views (1951) n the nature of the source lands for eugeosyn-linal sediments. However, in most cases it may be noted that the provenance is mixed, both volcanic and metamorphic or sedimentary rocks being common in the source area.

EXOGEOSYNCLINAL CLAN: This is tectonically the least well-defined clan; lack of precise definition is indicated by the greater and more irregular variation in chemical composition shown by the histograms. For this reason the discussion which follows deals with subgroups, which appear to be somewhat more clearly defined.

The characteristic tectonic setting, with sediments spreading away from the deformed eugeosyncline and exterior miogeosyncline, across the old interior miogeosyncline and craton, is shown in many cases, notably for the group of Coal Measure sandstones from the Carboniferous of Belgium and for the group of Molasse sandstones.

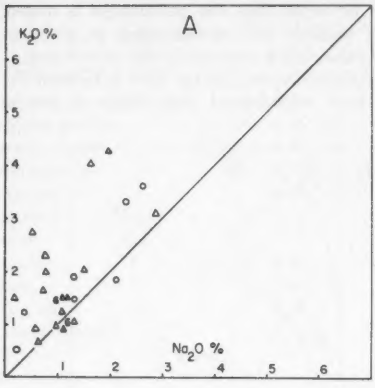

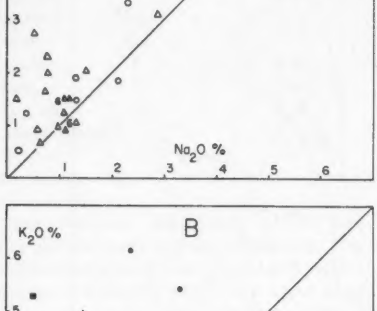

FIGURE 3.—K_2O–Na_2O VARIATION DIAGRAMS

A shows the distribution for some exogeosynclinal sandstones (Molasse indicated by open circle or by letter G if glauconitic, Coal Measures indicated by open triangle). B shows the distribution of taphrogeosynclinal sandstones (solid circles and squares) and eugeosynclinal sandstones (crosses and open squares). Torridonian sandstones are indicated by solid squares and the Swiss Flysch sandstones by open squares. Notice the wide variation within formations.

Note the rare occurrence of K_2O/Na_2O ratios of less than 1.0 in any clan other than the eugeosynclinal. The only members of the eugeosynclinal clan with high K_2O/Na_2O ratios are one of the Precambrian graded beds from Finland (analysis 134) and one of the Knife Lake Precambrian graywackes (analysis 102).

It must be admitted, however, that many sandstones were included in this clan for want of a better group to put them in, and that the averages given for this clan are therefore unsatisfactory.

The most abundant types represented by published analyses are the Coal Measure sandstones. These sandstones (Figs. 2, 3) are characteristically low-rank graywackes (*i.e.*, poor in feldspar), with a few feldspathic types. They are clearly distinguished from eugeosynclinal graywackes by their high K_2O/Na_2O ratio and from the taphrogeosynclinal sandstones by their low alkalies/Al_2O_3 ratio. Generally speaking there is little overlap with the taphrogeosynclinal clan (*cf.* Fig. 3), particularly if the total iron/alkalies ratio is also considered. However, the Molasse sandstones (Figs. 2, 3) seem to be a group with intermediate characteristics. This may indicate that the distinction between the taphrogeosynclinal and exogeosynclinal clans is not as clear as might be understood from Krynine (1948, p. 136: *See*, however, Krynine, 1956, paragraph 10).

The Coal Measure and Molasse sandstones are intermediate in iron content between the arkoses and the eugeosynclinal graywackes. A few Coal Measure sandstones have a very high content of iron owing to the presence of an authigenic siderite or pyrite cement which was precipitated at the time of deposition or during early diagenesis. The fairly high content of iron may be explained by the metamorphic and sedimentary (argillaceous) provenance of most coal measures and relatively rapid erosion, transportation, and burial.

In spite of the fact that the exogeosynclinal sandstones might be expected to be derived from folded eugeosynclinal rocks, the volcanic provenance is not apparent, and the dominant provenance appears to be low-grade metamorphic or sedimentary rocks.

THE AVERAGE SANDSTONE

Average sandstones have been computed for each of the four different clans. In view of the inadequate sampling and somewhat dubious method of classification into clans, no great significance can be attached to the averages given. It was felt that what was of most interest was some indication of the "typical" (= modal) composition of the three clans with Al_2O_3 >5 per cent. As suggested by Ahrens (1954a and b) for some minor elements, and as is indicated for five of the major elements in this study (Fe_2O_3, MgO, CaO, Na_2O, K_2O—*cf.* Fig. 4), the percentage weight of the oxides tends to follow a log-normal distribution more closely than a normal distribution. Under these circumstances it is felt that the geometric

or logarithmic) mean is a more significant average than the arithmetic mean. For SiO_2 and Al_2O_3 the dispersion is relatively small, so that the distribution approximates to normal. Consequently there is little difference between the arithmetic and geometric means (for example, for taphrogeosynclinal sandstones the geometric mean for SiO_2 is 76.46 per cent and the arithmetic mean is 77.10 per cent) and the arithmetic means are therefore used for these two oxides (*cf.* Table 1).

For other oxides, the arithmetic mean may be up to ten or more times as great as the geometric mean. The arithmetic mean is far more influenced by a few very high values than is the geometric mean.

The geometric means were computed for grouped data, using the groupings shown in the histograms (Fig. 4). The mean is given by the following equation:

$$\log \bar{X} = \frac{\Sigma(f \cdot \log X)}{N}$$

where $\bar{X}$ is the geometric mean, X is the geometric midpoint of the interval, f is the number of analyses falling in the interval, and N is the total number of analyses used in computing the mean.

The geometric mean of a log-normal distribution is identical with the mode, whereas the arithmetic mean is commonly far removed from the mode. Thus, the arithmetic mean gives a very poor idea of the composition of a "typical" member of the clan.

Arithmetic means have been computed, however, because it is not possible to use geometric means for calculating crustal abundance of the elements. The arithmetic means have also been used to calculate two "average sandstones" on the basis of two different weightings (Table 3).

For the first average the analyses were weighted according to the estimates of the relative abundance of the different sandstone clans given by Krynine (1948, p. 156), and for the second average the weighting follows the relative abundance of analyses used in this study. The analyses used fall into groups as shown at the foot of this page.

The estimates of abundance which result from this study agree more closely with the abundances of different petrographic types given by Pettijohn (1957, p. 293) than with the abundances given by Krynine. However, it should be noted that the four clans are defined on different criteria in this study than those employed by Krynine or Pettijohn. Also the sampling bias may well result in the relative abundance of analyses giving a poor estimate of the true relative abundances of the sandstone clans.

Clarke's (1924) composite analysis (Table 2), which is usually cited as the "average sandstone," is recalculated to 100 per cent for the seven major oxides for comparison (Table 3). Probably Clarke's composite contained too high a proportion of quartzites. Owing to their detailed stratigraphic subdivision and wide areal extent, sediments on the craton are commonly overrepresented in museum collections of sedimentary rocks. An overrepresentation of quartzites (including those with calcareous cement) would explain why Clarke's composite is relatively poor in Al_2O_3 and Fe_2O_3 and rich in CaO.

Appendix: List of Analyses

The references given for the analyses are to the publication from which the analysis was first collected. In many cases this is not the original publication of the analysis.

1. Glauconitic quartz sand, Thanetian (Tertiary) of Mons-en-Baroeul, France (Cayeux, 1929, p. 46)

Clan	Number of Analyses	Percentage	Abundances (Per Cent)	
			(Krynine, 1948)	(Pettijohn, 1957)
Quartzite	57	34	22.5	approx. 30
Nonglauconitic	48	29	..	..
Glauconitic	9	5	..	..
Arkose	27	16	32.5	approx. 15
High-rank graywacke	41	24	10	..
Low-rank graywacke	43	26	35	..
Glauconitic	2	1	..	..

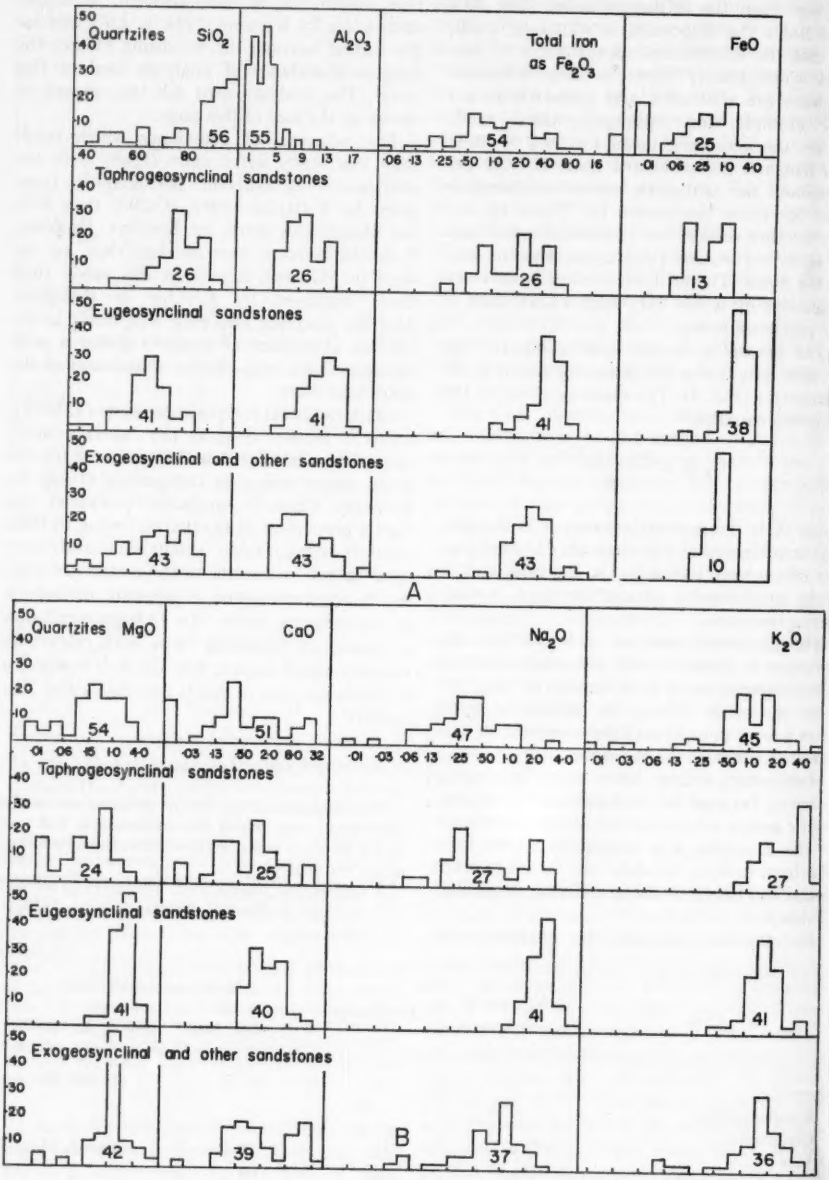

FIGURE 4

(*See foot of next page*)

2. Sand with opaline cement, Cenomanian of Bracquegnies, Belgium (Cayeux, 1929, p. 130)
3. Sand with opaline cement (glauconitic) Thanetian (Tertiary) of Angre, Belgium (Cayeux, 1929, p. 130)
4. Sand with chalcedony cement, Ypresian (Tertiary) of Mont Panisel, Belgium (Cayeux, 1929, p. 132)
5. Quartzite of Fontainebleau, France (Cayeux, 1929, p. 142)
6. Quartzite of Beauchamp, France (Cayeux, 1929, p. 142)
7. Calcareous quartzite of Fontainebleau, France (Cayeux, 1929, p. 155)
8. Molasse, Aquitanian (Tertiary) of Belmont, Switzerland (Cayeux, 1929, p. 161)
9, 10. Molasse, Burdigalian (Tertiary) of Voreppe, France (glauconitic) (Cayeux, 1929, p. 163)
11, 12. Macigno (Tertiary), Italy (Cayeux, 1929, p. 171)
13, 14. Coal Measure sandstone, north of Charleroi, Belgium (Cayeux, 1929, p. 176)
15. Hornu and Wasmes sandstone (Coal Measures), Belgium (Cayeux, 1929, p. 176)
16. Grand Hornu sandstone (Coal Measures), Belgium (Cayeux, 1929, p. 176)
17. Fonjoine sandstone, France (Cayeux, 1929, p. 178)
18. Lison arkose (Permian), France (Cayeux, 1929, p. 182)
19. Glauconitic and phosphatic sandstone, Aptian, Boulonnais, France (Cayeux, 1929, p. 191)
20. Sandstone with cement of organic matter, Landes, France (Cayeux, 1929, p. 193)
21. Arkose (Precambrian) Laize valley, France (Cayeux, 1929, p. 202)
22. Graywacke(?) (Cambrian) Omonville-La-Rouge, France (Cayeux, 1929, p. 207). This rock is described by Cayeux as an arkose but contains only 10 per cent orthoclase and has much paragonite matrix.
23. Arkose of Fépin (Lower Devonian), Belgium (Cayeux, 1929, p. 210)
24. Arkose (Triassic), Saint-Léger-du-Bois, France (Cayeux, 1929, p. 212)
25, 26. Titaniferous sandstone, Orge valley, France (Cayeux, 1929, p. 219)
27, 28, 29, 30. Hornu and Wasmes sandstones (Coal Measures), ?Belgium (Cayeux, 1929, p. 227)
31. Coal Measure sandstone, north of Charleroi, Belgium (Cayeux, 1929, p. 227)
32. Grande Bouillon sandstone (Coal Measures), ?Belgium (Cayeux, 1929, p. 227)
33, 34, 35. Stephanian sandstones (Coal Measures), ?Belgium (Cayeux, 1929, p. 232)
36. Woodkirk blue stone (Coal Measures), near Wakefield, England (Trueman, 1954, p. 21)
37. Pennant sandstone (Carboniferous), Craig yr erg quarry, South Wales (Trueman, 1954, p. 21)
38. "Buntsandstein" (sandstone with 19 per cent feldspar, 11 per cent micas) (Correns, 1949, p. 379–380)
39. "Spiriferensandstein" (sandstone with 6 per cent feldspar) (Correns, 1949, p. 379–380)
40. "Arkose" (sandstone with 20 per cent plagioclase, 3 per cent orthoclase, 3 per cent micas, 4 per cent serpentine, 16 per cent clay minerals) (Correns, 1949, p. 379–380)
41. Sandstone, Hummelstown, Pennsylvania (Clarke, 1924, p. 547)
42. Ferruginous sandstone, Hunstanton, England (Clarke, 1924, p. 547). This is probably a quartzite and is classed as such in spite of the fact that it has slightly more than 5 per cent alumina.
43. Miocene sandstone, Mt. Diablo, California (Clarke, 1949, p. 547)
44. Graywacke, Hurley, Wisconsin (Clarke, 1949, p. 547)
45. Barmouth grit (Cambrian), North Wales (Phillips, 1881, p. 21)
46. Yoredale sandstone (Carboniferous), Shalk Beck, Cumberland, England (Phillips, 1881, p. 21)
47. Millstone grit (Carboniferous), Brigham, Cumberland, England (Phillips, 1881, p. 21)
48. Lower Coal Measures sandstone, Spinkwell quarry, Bradford, England (Phillips, 1881, p. 21)
49. Bunter sandstone (Triassic), Bootle Well, Liverpool, England (Phillips, 1881, p. 21)
50. Graywacke, Neranleigh series, Queensland, Australia (David, 1950, v. 1, p. 224)
51. Triassic sandstone, Hawkesbury series, Pyrmont, Sydney, Australia (coal-bearing) (David, 1950, v. 1, p. 443)
52. Feldspathic sandstone, Middle series (Triassic) Midlands area, Tasmania, Australia (coal-bearing and tuffaceous) (David, 1950, v. 1, p. 443)
53. Oligocene sand, Rosental, Germany (Niggli *et al.*, 1930, p. 55)

FIGURE 4.—HISTOGRAMS FOR EIGHT MAJOR OXIDES IN THE FOUR SANDSTONE CLANS

The histograms for each of the four clans are plotted on the same scale for comparison. The scale on the abscissa is geometric for all oxides except SiO_2 and Al_2O_3. The ordinate scale is in percentage of total number of analyses used to compute the histogram. This number is inscribed within each histogram, since in some of the analyses used not all the oxides were determined. Note that the eugeosynclinal clan forms the least dispersed group, with a clear approximation to log-normal distribution for most oxides. The greater dispersion for other clans may be partly explained by the variation introduced by the presence in some cases of authigenic cement (which is almost invariably absent in the eugeosynclinal sandstones). The clearly bimodal distribution of CaO in the "quartzite" and exogeosynclinal clans results from a calcite cement.

54. Greensand (glauconitic), New Jersey (Niggli *et al.*, 1930, p. 56)
55. Dolomitic marly sand, Raceville, New York (Niggli *et al.*, 1930, p. 56)
56. Marly sand, Arroyo del Cerro, California (Niggli *et al.*, 1930, p. 56)
57. Chico sandstone (Upper Cretaceous), Mt. Diablo, California (Niggli *et al.*, 1930, p. 57)
58. "Arkose", Molasse (Tertiary), Unterägeri, Kt. Zug., Switzerland (Niggli *et al.*, 1930, p. 57)
59. Berea sandstone (Mississippian), Ohio (Niggli *et al.*, 1930, p. 58)
60. Bunter sandstone (Triassic), Niederhessen, Germany (Niggli *et al.*, 1930, p. 58)
61. Chico sandstone, Mt. Diablo, California (Niggli *et al.*, 1930, p. 58)
62. Marly sandstone, St.-Gingolph, Genfersee, Switzerland (Niggli *et al.*, 1930, p. 59)
63. Glauconitic sandstone (Lower Cretaceous), Sevelen, Rheintal, Switzerland (Niggli *et al.*, 1930, p. 59)
64. Taveyannaz sandstone, Flysch (Tertiary), Dürrenberg, Kiental, Switzerland (Niggli *et al.*, 1930, p. 59)
65. Sandstone, Helvetic Nappe, Merligen, Thuner See, Switzerland (Niggli *et al.*, 1930, p. 253)
66. Calcareous quartzite, Flysch (Tertiary), Steinbruch Guber, Alpnach-Dorf, Switzerland (Niggli *et al.*, 1930, p. 254)
67. Altdorfersandstein, Flysch (Tertiary), Altinghausen, Kt. Uri, Switzerland (Niggli *et al.*, 1930, p. 254)
68. Flysch (Tertiary), Matt, Sernftal, Switzerland (Niggli *et al.*, 1930, p. 254)
69. Calcareous glauconitic quartzite, Brisischichten (Lower Cretaceous), Switzerland (Niggli *et al.*, 1930, p. 254)
70. Lower Süsswassermolasse (Tertiary), Gränichen, Burghalde, Kt. Aargau, Switzerland (Niggli *et al.*, 1930, p. 262)
71. Glauconitic sandstone, Niederischichten (Albian) Unter Rafis, Rheintal, Switzerland (Niggli *et al.*, 1942, p. 47)
72. Glauconitic sandstone, Gamser Schichten (Gargasian), Buchserberg quarry, near Buchs, Switzerland (Niggli *et al.*, 1942, p. 47)
73. Quartzite (Triassic), Tatschis, west Tamins, Switzerland (Niggli *et al.*, 1942, p. 47)
74. Molasse, Burdigalian (Tertiary) (Niggli *et al.* 1942, p. 48)
75. Molasse, Helvetian (Tertiary) (Niggli *et al.*, 1942, p. 48)
76. Upper Süsswassermolasse (Tertiary), Dettenberg, near Eschenmosen, Switzerland (Niggli *et al.*, 1942, p. 50)
77. Molasse (Tertiary), Altishofen, Bohrloch, Switzerland (Niggli *et al.*, 1956, p. 75)
78. Quartz sand (Rhaetic), Erschwil, Switzerland (Niggli *et al.*, 1956, p. 77)
79. Glauconitic sandstone (Gargasian), Bucherserberg, Switzerland (Niggli *et al.*, 1956, p. 69)
80. Paleozoic graywacke, Mungo River, New Zealand (Pettijohn, 1957, p. 306)
81. Archaen graywacke, Manitou Lake, Ontari Canada (Pettijohn, 1957, p. 306)
82. Eocene graywacke, Olympic Mountai Washington (Pettijohn, 1957, p. 306)
83. Keewatin graywacke, Casummit Lak Ontario, Canada (Pettijohn, 1957, p. 306)
84. Kulm graywacke, Steinbach, Frankenwal Germany (Pettijohn, 1957, p. 306)
85. Rensselaer graywacke, 1½ miles east Spencertown, New York (Balk, 1953, p. 824
86. Rensselaer graywacke, one-quarter of a m west of Kendall Pond, New York (Balk, 195 p. 824)
87. Rensselaer graywacke, lens in chlorito quartz-chlorite schist, 1½ miles east-southea of Center Berlin, New York (Balk, 1953, 824)
88. Aure graywacke (Miocene), Papua (Pettijoh 1957, p. 306)
89. Cretaceous graywacke, Papua (Pettijoh 1957, p. 306)
90. Archean graywacke, Kirkland Lake, Ontari Canada. Sylvanite mine (Todd, 1928, p. 20)
91. Archaen graywacke, Kirkland Lake, Ontari Canada. Lake Shore mine (Todd, 1928, p. 2
92. Lorrain quartzite (Huronian) (Pettijoh 1957, p. 298)
93. St. Peter's quartzite (Ordovician) (Pettijoh 1957, p. 298)
94. Mesnard quartzite (Precambrian) (Pettijoh 1957), p. 298)
95. Tuscarora quartzite (Silurian) (Pettijoh 1957, p. 298)
96. Oriskany quartzite (Devonian) (Pettijoh 1957, p. 298)
96. Oriskany quartzite (Devonian) (Pettijoh 1957, p. 298)
97. Berea quartzite (Mississippian) (Pettijoh 1957, p. 298)
98. Sioux quartzite (Precambrian) (Pettijoh 1957, p. 298)
99. Graywacke, Stanley shale (Carboniferous) near Mena, Arkansas (Pettijohn, 1957, p. 319
100. Graywacke phase of the Rove formation (Animikie, Precambrian), Loon Lake, Minne sota (Grout, 1933, p. 997)
101. Knife Lake graywacke (Precambrian), Knif Lake, Minnesota (Grout, 1933, p. 997)
102. Knife Lake graywacke, Jordan Lake, Minne sota (Grout, 1933, p. 997)
103. Knife Lake graywacke, South of Tower Minnesota (Grout, 1933, p. 997)
104. Arkose, Torridonian (Precambrian) nea Bernera, Glenelg, Scotland (Kennedy, 1951, p 257)
105. Arkose (Torridonian) Beinn na Seamraig grit north shore, Loch na Dal, Skye, Scotland (Kennedy, 1951, p. 257)
106. Arkose (Torridonian) Kinloch, Skye, Scotland (Kennedy, 1951, p. 257)
107. Arkose (Torridonian), Kinloch beds, head o Loch na Dal, Skye, Scotland (Kennedy, 1951, p. 257)

108. Portland arkose (Triassic), Connecticut (Pettijohn, 1957, p. 324)
109. Torridonian arkose (Pettijohn, 1957, p. 324)
110. Arkose, Lower Old Red Sandstone, Scotland (Pettijohn, 1957, p. 324)
111. Sparagmite arkose (Precambrian) (unmetamorphosed), Engerdalen region, Norway (Pettijohn, 1957, p. 324)
112. Timiskaming graywacke (Precambrian), near Porcupine Lake, Ontario, Canada (H. G. MacPherson, 1958, p. 76)
113. Tanner graywacke (Carboniferous-Devonian) (coarse-grained), Harz, Germany (Helmbold, 1952)
114. Tanner graywacke, medium-grained (Helmbold, 1952)
115. Tanner graywacke, fine-grained (Helmbold, 1952)
116, 117. Molasse (Tertiary), Couvet, Val-de-Travers, Switzerland (Niggli *et al.*, 1930, p. 286)
118, 119. Molasse (Tertiary), Montier, Switzerland (Niggli *et al.*, 1930, p. 288)
120. Franciscan graywacke (?Jurassic), Piedmont, California (Taliaferro, 1943, p. 136)
121. Franciscan graywacke, Sulphur Bank, California (Taliaferro, 1943, p. 136)
122. Franciscan graywacke, Carbona quadrangle, California (Taliaferro, 1943, p. 136)
123. Franciscan graywacke, Mt. Diablo, California (Taliaferro, 1943, p. 136)
124, 125. Taveyannazsandstein, Flysch, Diablerets, Switzerland (Niggli and Niggli, 1952, p. 231)
126. Dakota sandstone (Cretaceous) Minnesota (Merrill, 1903, p. 516)
127. Berea sandstone (Mississippian) Ohio (Merrill, 1903, p. 516)
128. Quartzite, Siskowit Bay, Wisconsin (Merrill, 1903, p. 516)
129. "Quartzite", Pipestone, Minnesota (Merrill, 1903, p. 516)
130. Quartzite, Hinckley, Minnesota (Merrill, 1903, p. 516)
131. Quartzite, near Fort Snelling, Minnesota (Merrill, 1903, p. 516)
132. Sandstone, Fond du Lac, Minnesota (Merrill, 1903, p. 516)
133. Sandstone, Jordan, Minnesota (Merrill, 1903, p. 516)
134. Coarse-grained, light-colored portion of varve (Archaen), Finland (Simonen and Kuovo, 1951, p. 101)
135. Coarse-grained base of megavarve (Archaen), Finland (Simonen and Kuovo, 1951, p. 101)
136. Jotnian arkose (Precambrian), Köyliö, Muurunmäki, Finland (Simonen and Kuovo, 1955, p. 63)
137. Jotnian arkose, Köyliö, Tuiskula, Finland (Simonen and Kuovo, 1955, p. 63)
138. Lauhavouori quartzite, Tiiliharju, Finland (Simonen and Kuovo, 1955, p. 79)
139, 140. Ogallala formation (Pliocene), Kansas (W. W. Rubey, T. P. Hill, and D. A. Welsh, 1954, unpub. MS., U.S. Geol. Survey, p. 5)
141. Paskapoo sandstone (Tertiary), Calgary, Alberta (Parks, 1916, p. 218)
142. Torridonian arkose (Precambrian), Torridon, Scotland (Mackie, 1900, p. 58)
143. Torridonian arkose, Glen Banaisdale, Scotland (Mackie, 1900, p. 58)
144. Middle Old Red Sandstone ("Lower" ORS of Mackie), Tarradale, Black Isle, Scotland (Mackie, 1900, p. 58)
145. Middle Old Red Sandstone, Red Crags, Fochabers-on-Spey, Scotland (Mackie, 1900, p. 58
146. Matrix of conglomerate, Middle Old Red Sandstone, Tynet, Scotland (Mackie, 1900, p. 58)
147. Matrix of conglomerate, Middle Old Red Sandstone, Achenroath, Scotland (Mackie, 1900, p. 58)
148. Upper Old Red Sandstone, Scaat Craig, Scotland (Mackie, 1900, p. 59)
149. Upper Old Red Sandstone, Kings Steps, Nairn, Scotland (Mackie, 1900, p. 59)
150, 151. Upper Old Red Sandstone, Newton, Elgin, Scotland (Mackie, 1900, p. 59)
152. Upper Old Red Sandstone, Rosebrae, Elgin, Scotland (Mackie, 1900, p. 59)
153. Upper Old Red Sandstone, Bishopmill, Elgin, Scotland (Mackie, 1900, p. 59)
154. Upper Old Red Sandstone, Oakbrae, Elgin, Scotland (Mackie, 1900, p. 59)
155. "Reptiliferous sandstone" (Permo-Trias), Cuttieshillock, Scotland (Mackie, 1900, p. 59)
156. "Reptiliferous sandstone" (Permo-Trias), Spynie, Scotland (Mackie, 1900, p. 59)
157. "Reptiliferous sandstone" (Permo-Trias), Findvassie, Scotland (Mackie, 1900, p. 59)
158. "Reptiliferous sandstone" (Permo-Trias), Covesea, Scotland (Mackie, 1900, p. 59)
159. "Reptiliferous sandstone" (Permo-Trias), Greenbrae, Scotland (Mackie, 1900, p. 59)
160. Quartzite (Cambrian, Revinian), near Fépin, Belgium (Reade and Holland, 1898, p. 293)
161. Quartzite (Lower Devonian), near Fépin, Belgium (Reade and Holland, 1898, p. 293)
162, 163, 164. Bunter sandstone (Triassic) with baryte cement, Bidston Hill, Liverpool, England (Moore, 1898, p. 252)
165, 166, 167, 168. Bunter sandstone (Triassic), or iron concretion in sandstone, Prenton Hill, Liverpool, England (Moore, 1898, p. 244)

References Cited

Ahrens, L. H., 1954a, The log-normal distribution of the elements (a fundamental law of geochemistry and its subsidiary): Geochim. Cosmochim. Acta, v. 5, p. 49–73

—— 1954b, The log-normal distribution of the elements (2): Geochim. Cosmochim. Acta, v. 6, p. 121–131

Balk, R., 1953, Structure of graywacke areas and Taconic Range, east of Troy, New York: Geol. Soc. America Bull., v. 64, p. 811–864

Barth, T., 1938, Progressive metamorphism of Sparagmite rocks of southern Norway: Norsk. Geol. Tidsskr., Bd. 18, H. 1, p. 54–65

Cayeux, Lucien, 1929, Les roches sedimentaires de France; Roches siliceuses: Paris, Imprimerie Nationale, 696 p.

Clarke, F. W., 1924, The data of geochemistry: U. S. Geol. Survey Bull. 770, 841 p.

Correns, C. W., 1949, Einführung in die Mineralogie; Kristallographie und Petrologie: Berlin, Springer, 414 p.

Dale, T. N., 1893, The Rensselaer grit plateau in New York: U. S. Geol. Survey Ann. Rept. 1891–1892, Pt. II, p. 297–340

Daly, R. A., 1933, Igneous rocks and the depths of the earth: 2d ed., New York, McGraw-Hill Book Co., 598 p.

Dapples, E. C., Krumbein, W. C., and Sloss, L. L., 1948, Tectonic control of lithologic associations: Am. Assoc. Petroleum Geologists Bull., v. 32, p. 1924–1947

David, T. W. E., 1950, The geology of the Commonwealth of Australia: London, E. Arnold & Co. (v. I, 747 p.; v. II, 618 p.; v. III, maps)

Edwards, A. B., 1947a, The petrology of the Miocene sediments of the Aure trough, Papua: Royal Society Victoria Proc., v. 60 (n.s.), p. 123–148

—— 1947b, The petrology of the Cretaceous graywackes of the Purari Valley, Papua: Royal Soc. Victoria Proc., v. 60 (n.s.), p. 163–171

Gilbert, C. M., 1955, Sedimentary rocks, p. 251–384 *in* Williams H., Turner, F. J., and Gilbert, C. M., Petrography: San Francisco, W. H. Freeman, 406 p.

Goldich, S. S., 1938, A study in rock-weathering: Jour. Geology, v. 46, p. 17–58

Grout, F. F., 1933, Contact metamorphism of the slates of Minnesota by granite and gabbro magmas: Geol. Soc. America Bull., v. 44, p. 989–1039

Helmbold, R., 1952, Beitrag zur Petrographie der Tanner Grauwacken: Heidelberzer Beit. Miner. und Petrog., Bd. 3, H. 4, p. 253–288

Kay, Marshall, 1951, North American geosynclines: Geol. Soc. America Mem. 48, 143 p.

Kennedy, W. Q., 1951, Sedimentary differentiation as a factor in the Moine-Torridonian correlation: Geol. Mag. v., 88, p. 257–266

Krumbein, W. C., and Sloss, L. L., 1953, Stratigraphy and sedimentation: San Francisco, W. H. Freeman, 497 p.

Krynine, P. D., 1942, Differential sedimentation and its products during one complete geosynclinal cycle: 1st Congr. Panamericano Ing. Minas y Geologia, tomo 2, Geologia, Pt. I, p. 537–561

—— 1948, The megascopic and field classification of sedimentary rocks: Jour. Geology, v. 56, p. 130–165

—— 1956, Alice in graywackeland (Abstract): Jour. Sed. Petrology, v. 26, p. 188–189

Kuenen, Ph. H., 1957, Sole markings of graded graywacke beds: Jour. Geology, v. 65, p. 231–258

Lapadu-Hargues, P., 1946, Sur l'existence et la nature de l'appart chimique dans certaines séries cristallophylliennes: Bull. Soc. Géol. France, 5th ser., v. 15, p. 255–310

Leith, C. K., and Mead, W. J., 1915, Metamorphic geology: New York, Henry Holt

Mackie, W., 1900, Seventy chemical analyses of rocks (chiefly from the Moray area): Geol. Soc. Edinburgh Trans., v. 8, p. 33–61

Macpherson, H. G., 1958, A chemical and petrographic study of Precambrian sediments: Geochim. Cosmochim. Acta, v. 14, p. 73–92

Matley, C. A., and Wilson, T. S., 1946, The Harlech dome, north of the Barmouth estuary: Geol. Soc. London Quart. Jour., v. 102, p. 1–35

Merrill, G. P., 1903, Stones for building and decoration: 3d ed., New York, John Wiley, 551 p.

Moore, C. C., 1898, The chemical examination of sandstones from Prenton Hill and Bidston Hill: Geol. Soc. Liverpool Proc., v. 8, p. 241

Murray, E. G., and Adams, J. A. S., 1958, Thorium, uranium and potassium in some sandstones: Geochim. Cosmochim. Acta, v. 13, p. 260–269

Niggli, P., and Niggli, E., 1952, Gesteine und Minerallagerstätten; zweiter Band, Exogene Gesteine und Minerallagerstätten: Switzerland, Basel, 557 p.

Niggli, P., de Quervain, F., and Winterhalter R. U., 1930, Chemismus schweizerischer Gesteine: Beiträge zur Geologie der Schweiz, Geotech. Ser., Lf. 14, 389 p. Nachtrag 1: de Quervain, F., and Friedlaender, C., 1942, Beiträge zur Geologie der Schweiz, Geotech. Ser., Lf. 20, 108 p. Nachtrag 2: de Quervain, F., and Jenny, V., 1956, Beiträge zur Geologie der Schweiz, Geotech. Ser., Lf. 34, 103 p.

Parks, W. A., 1916, Report on the building and ornamental stones of Canada; vol. IV, Provinces of Manitoba, Saskatchewan and Alberta: Canada Dept. Mines, Mines Branch, Rept. No. 388, 333 p.

Pettijohn, F. J., 1943, Archean sedimentation: Geol. Soc. America Bull., v. 54, p. 925–972

—— 1949, 1957, Sedimentary rocks: New York, Harper Bros., 1st ed., 526 p.; 2d ed., 718 p.

Phillips, J. A., 1881, On the constitution and history of grits and sandstones: Geol. Soc. London Quart. Jour., v. 37, p. 6–28

Reade, T. M., and Holland, P., 1898, The phyllades of the Ardennes compared with the slates of North Wales: Geol. Soc. Liverpool Proc., v. 8, p. 274–293

Shaw, D. M., 1956, Geochemistry of pelitic rocks. Part III, Major elements and general geochemistry: Geol. Soc. America Bull., v. 67, p. 919–934

Simonen, A., and Kuovo, O., 1951, Archaean varved schists north of Tampere in Finland: Géol. Soc. de Finlande, Compte Rendues, p. 93–114

Simonen, A., 1955, Sandstones in Finland: Bull. Comm. Géol. Finlande, v. 168, p. 57–87

Sundius, N., 1930, On the spilitic rocks: Geol. Mag., v. 67, p. 1–17

Taliaferro, N. L., 1943, Franciscan-Knoxville problem: Am. Assoc. Petroleum Geologists Bull., v. 27, p. 109–219

Todd, E. W., 1928, Kirkland Lake gold area: Ontario Dept. Mines Ann. Rept., v. 37, Pt. 2, p. 1–167

Trueman, A. E., *Editor*, 1954, The coalfields of Great Britain: London, Edward Arnold, 396 p.

Tvrrell, G. W., 1933, Greenstones and graywackes: Finland Géol. Comm., B. no. 102, p. 24–26

HAMILTON COLLEGE, MCMASTER UNIVERSITY, HAMILTON, ONTARIO, CANADA

MANUSCRIPT RECEIVED BY THE SECRETARY OF THE SOCIETY, FEBRUARY 6, 1959

BULLETIN OF THE GEOLOGICAL SOCIETY OF AMERICA
VOL. 71, PP. 1027-1062, 8 FIGS., 3 PLS. JULY 1960

PETROLOGY AND STRUCTURE OF THE COCKEYSVILLE FORMATION (PRE-SILURIAN) NEAR BALTIMORE, MARYLAND

BY PHILIP W. CHOQUETTE

ABSTRACT

The Cockeysville formation near Baltimore, Maryland, is a sequence of intricately folded carbonate-rich metasedimentary rocks about 750 feet thick and of pre-Silurian age (Wasserburg *et al.*, 1957). The formation lies near the base of the Glenarm series, which mantles five elongated domes of Precambrian (?) basement gneiss at the eastern edge of the Piedmont Province. Sediments and gneissose phases of the domes were regionally metamorphosed to about the amphibolite facies as defined by Eskola *et al.* (1939).

Crystalline metadolomite, calc-schist, and calcite marble constitute most of the Cockeysville. Local breakdown of dolomite accompanied the formation of diopside-quartz-tremolite calc-silicate marble and was marked by a "retrograde" paragenetic sequence of diopside to tremolite to talc.

Calcite marble, which occurs in distinct layers and discordant masses associated with calc-schist and phlogopite-calcite metadolomite, is believed to have had a multiple origin. Mineral assemblages and rock associations suggest that some of the marble formed syntectonically from argillaceous limestone, quartzose limestone, and argillaceous dolomite (dedolomitization); other calcite marble may have recrystallized from essentially pure limestone. Discordant masses of calcite marble formed in part by replacement of dolomite or argillaceous limestone and locally dilated their enclosing rocks; some of these masses may have begun crystallizing from limestone; all show coarse nondirectional fabric suggestive of a late tectonic or post-tectonic origin.

Metasomatism in the recrystallizing sediments was evidently restricted to aureoles around basic and granitic dikes. Such intrusions are rare, and in general the marbles are chemically similar to sedimentary carbonate rocks. Tourmaline, apatite, and scapolite, which are minor but widespread, can reasonably be attributed to recrystallization with little or no addition of material.

Metamorphic grade remains essentially constant throughout the area mapped by the writer. Various facies of the Cockeysville marble, however, can be assigned on the basis of their mineral assemblages to any one of several metamorphic subfacies; local variations of CO_2 pressure, H_2O pressure, and bulk composition may be largely responsible for these variations.

Structural elements in the carbonate rocks—minor fold axes, lineations, cross-joints, and foliation—closely reflect corresponding structural elements of the gneiss domes, and this parallelism diminishes with distance from the domes. The minor folds show a crude variation in intensity and type with distance from the domes.

CONTENTS

TEXT

	Page
Introduction	1028
Regional setting	1028
Previous work and scope of this report	1030
Acknowledgments	1030
Stratigraphy of the Cockeysville formation	1031
Structural geology	1032
Regional structure	1032
Structure of the carbonate rocks	1032
Structural relations to the gneiss domes	1032
Foliation	1035
Primary structures and textures	1035
Minor folds	1036
Linear structures	1037
Petrography and petrogenesis	1038
Calc-schist	1038
Metadolomite	1039
General statement	1039
Chemical composition	1039
Texture and mineralogy	1039
Structural behavior	1039
Calc-silicate marble	1039
General statement	1039
Petrography	1042
Origin of the calc-silicate marble	1042
Calcite marble	1044
Introduction	1044
Petrography	1045
Origin of the calcite marble	1048

Page

Summary and conclusions: metamorphism of the Cockeysville sediments 1049
Structural behavior 1049
Role of metasomatism 1050
Metamorphic intensity 1050
References cited 1051

ILLUSTRATIONS

Figure Page

1. Index map showing location and generalized geologic setting of map area in eastern Maryland 1030
2. Measured section showing location of Cockeysville-Wissahickon contact 1032
3. Generalized cross joints and linear elements in the Cockeysville area 1033
4. Statistical diagrams of structural elements in marbles, southwest half of Phoenix anticlinorium 1034
5. Crumpling and boudinage in flexure folds. 1036
6. Flowage folds 1037
7. Partly discordant bodies of calcite marble. 1047
8. Plot of per cent dolomite vs. per cent calcite plus phlogopite in five representative metadolomites 1048

Plate Facing page

1. Folding in Cockeysville marble 1034
2. Photomicrographs of Cockeysville marble. 1035
3. Geologic map of the Cockeysville area, Maryland 1052

TABLES

Table Page

1. Stratigraphy of the Glenarm series and associated rocks in the Cockeysville area, Maryland 1029
2. Modal analyses of carbonate rocks from the Cockeysville formation 1040
3. Chemical analyses of Cockeysville metadolomite, calc-silicate rocks, and marble of intermediate composition; chemical analyses of dolomitic sediments 1043
4. Comparison of features of calcite marble lenses and other discordant bodies found in metadolomite and in calc-schist 1046

Introduction

Regional Setting

The Cockeysville formation (Mathews and Miller, 1905) is part of a thick sequence of carbonate and detrital metasedimentary rocks (Table 1), the Glenarm series, which underlies much of the Piedmont Province along a belt extending from Virginia into southeastern Pennsylvania (Fig. 1). In the area mapped by the writer the Glenarm metasedimentary rocks rest with possible unconformity on four elongated domes of Precambrian (?) basement rocks known in the literature as Baltimore gneiss (Williams, 1892).

Both the Glenarm series and the basement gneiss have been folded along northeast-trending axes and regionally metamorphosed to about the lower amphibolite facies as defined by Eskola *et al.* (1939). Metamorphic grade remains essentially constant throughout the map area but is reported to decrease from Baltimore west and northwest across the Piedmont (Knopf and Jonas, 1929b, p. 102; Cloos and Hietanen, 1941, p. 136).

Regional deformation and metamorphism were accompanied by the syntectonic emplacement of granitic plutons (Knopf and Jonas, 1929b) and swarms of granitic pegmatites. The pegmatites, most of which are too small to show at map scale (Pl. 3), were introduced mainly into the borders of the gneiss domes, the base of the Glenarm, and along formation contacts within the Glenarm.

At least one premetamorphic (?) lamprophyre dike intrudes the Cockeysville (Choquette, 1957, Ph.D. thesis, The Johns Hopkins Univ., p. 70–72) and may be related to a complex of serpentine peridotite and pyroxenite partially exposed in the map area.

Seven or more Triassic (?) diabase dikes, recording a second and much later period of basic intrusive activity, cut across the entire sequence of metamorphic and plutonic rocks Dikes and pre-Triassic (?) rocks alike are overlapped a few miles southeast of the Cockeysville area by Cretaceous and Tertiary sedimentary rocks and are locally mantled by alluvium and terrace gravels.

Absolute ages have not been established for either the basement complex or the Glenarm series, owing to the lack of fossils and the uncertain stratigraphic relations between the Glenarm series and known Paleozoic rocks to the west. Although some writers have tentatively assigned the metasedimentary rocks to the Precambrian (Knopf and Jonas, 1923; 1929b), many now believe they are of Early Paleozoic age (Cloos, 1948; Swartz, 1948). The age question is of considerable importance in working out the tectonic history and stratigraphy of the region and has been reviewed by Swartz (1948, p. 1506–1512).

Despite the lack of information about absolute age, however, recent A^{40}/K^{40} age determinations (Wasserburg *et al.*, 1957) have

TABLE 1.—STRATIGRAPHY OF THE GLENARM SERIES AND ASSOCIATED ROCKS IN THE COCKEYSVILLE AREA, MARYLAND

Age		Lithologic Unit	Thickness (feet)	Reference
Triassic (?)	Post-Glenarm intrusives	Diabase dikes	—	—
Late Ordovician-Early Silurian		Pegmatite dikes and sills	—	—
Pre-Silurian (?)		Lamprophyre dikes(s)	—	—
Pre-Silurian	Glenarm series	Peters Creek formation (not exposed in map area)	0–3000 0–4000	Knopf and Jonas (1929b) Swartz (1948)
		Wissahickon formation: mica schist, garnet-mica schist, staurolite-kyanite-garnet mica schist with interlayered metaquartzite and paragneiss; biotite paragneiss at base, metadolomite exposed near base at one locality (Top not exposed)	0–2000 0–3500 0–2250	Mathews and Miller (1905) Knopf and Jonas (1929b) Swartz (1948)
		Cockeysville formation: metadolomite, calc-schist, calc-gneiss, calcite marble; calc-silicate marble in upper part of formation, locally; a few thin layers of metaquartzite and graphite schist	0–2300 0– 400 0– 500 0– 750	Mathews and Miller (1905) Knopf and Jonas (1929b) Swartz (1948) Choquette (1957, Ph.D. thesis, The Johns Hopkins Univ.)
		Setters formation: biotite paragneiss, sericite metaquartzite, some garnet mica schist; basal part injected by concordant pegmatites	0–1000 0– 750 0–1000 0–1000	Mathews and Miller (1905) Knopf and Jonas (1929b) Swartz (1948) Choquette (1957, Ph.D. thesis, The Johns Hopkins Univ.)
		UNCONFORMITY?		
Precambrian (?)	Basement complex	Baltimore gneiss: microcline augen gneiss; biotite-oligoclase migmatite, amphibolite schist, mica schist, and feldspathic gneiss near top; quartz monzonite and granodiorite near center of Towson and Chattalonee domes, may be younger intrusives (Base not exposed)		

established that Glenarm sediments were deposited at least as long ago as the Early Silurian. Radiometric ages of micas from the Cockeysville and Setters formations and of microcline and muscovite from syntectonic pegmatites introduced into the Glenarm series date the regional metamorphism of the Glenarm at about 350 ± 20 m. y. ago.

Previous Work and Scope of This Report

Literature dealing with the Glenarm and basement complex in this part of the Piedmont includes geologic maps of the Baltimore region (Williams, 1892; Knopf and Jonas, 1929a; Cloos and Broedel, 1940); regional stratigraphic studies (Mathews and Miller, 1905; Miller, 1905, Ph.D. thesis, The Johns Hopkins Univ.; Knopf and Jonas, 1929b); structural investigations of the gneiss domes (Broedel, 1937; Stefansson, 1943, Ph.D. thesis, The Johns Hopkins Univ.); and a description of the economic geology, rock types, and inferred paleogeography of the Cockeysville formation (Miller, 1905, Ph.D. thesis, The Johns Hopkins Univ.).

Little attention has been focused on the structure and petrogenesis of the metasedimentary rocks near Baltimore, however. This report is an attempt to fill partially the need for such studies and deals with one unit of the Glenarm series at and near its type locality. The writer has remapped the Cockeysville area and has subdivided the carbonate rocks where possible. New data are presented that have a bearing on several petrologic problems connected with the Cockeysville and to some extent with the Glenarm series as a whole. Specifically, the problems are: (1) origin of calcite marble and calc-silicate rocks in the formation; (2) relative roles of sedimentary composition, metasomatism, metamorphic differentiation, intensity of deformation, and other factors during metamorphism of the carbonate sediments; (3) structural behavior of the marbles and their structural relations to the gneiss domes; and (4) metamorphic grade.

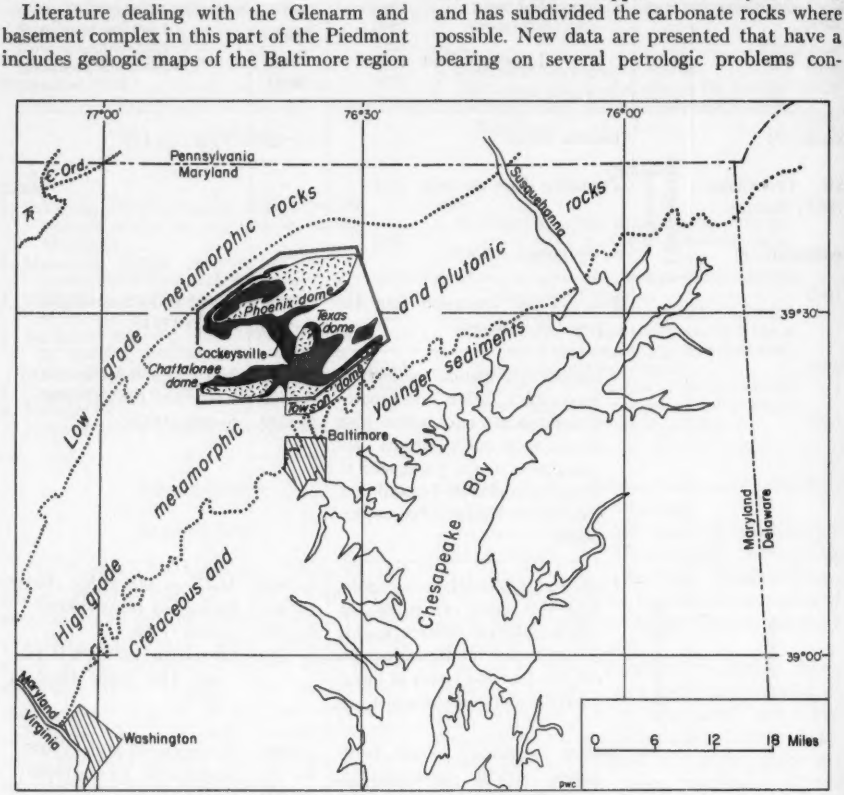

FIGURE 1.—INDEX MAP SHOWING LOCATION AND GENERALIZED GEOLOGIC SETTING OF MAP AREA IN EASTERN MARYLAND

Cockeysville formation underlies area shown in gray.

ACKNOWLEDGMENTS

I am indebted to The Johns Hopkins University for scholarships and assistantships in support of graduate work and of research for

this report, and to The Geological Society of America for a supporting grant from the Penrose Bequest. I wish to thank A. C. Waters, whose advice, critical suggestions for improvement of the manuscript, and ideas were invaluable; and Ernst Cloos, who suggested a study of the Cockeysville formation, pointed out geologic problems involved and made possible the research.

The time and assistance given by the following men are greatly appreciated: F. J. Pettijohn, Olcott Gates, and C. A. Hopson of The Johns Hopkins University offered suggestions about the field work and interpretations; G. R. Stevens of Lafayette College accompanied me in the field several times and made structural data available; Pierre Sauve of the Quebec Department of Mines and Gilles Allard of Petrobras discussed petrographic aspects of the work.

R. D. Proctor of the White Pigment Company, Proctor, Vermont, kindly allowed the publication of data collected while I was temporarily employed by that company. I am indebted to R. Dana Russell and other personnel of The Ohio Oil Company for time and use of facilities to complete the text and illustrations for this report.

Stratigraphy of the Cockeysville Formation

Stratigraphic units within the Cockeysville have not been distinguished because of complex folding, a rarity of sedimentary structures, and a scarcity of both surface exposures and subsurface data. Instead, an attempt has been made to outline by means of an outcrop map the areal distribution of six major rock types that make up almost the entire formation: (1) calc-schist,[1] (2) phlogopite-calcite metadolomite, (3) quartz metadolomite, (4) calc-gneiss, (5) calcite marble, and (6) calc-silicate marble. At only two places in the area is calcite marble thick enough to form a mappable unit; generally it occurs in layers or lenses less than 10 feet thick, interlayered with calc-schist or phlogopite-calcite metadolomite. Calc-silicate marble seems to be restricted in occurrence to quartz metadolomite, in which it occurs as small nests, pods, and discontinuous layers.

Despite the uncertainty about detailed stratigraphy, a few general observations seem justified:

(1) The Cockeysville formation shows an apparent change in over-all composition from north to south and southwest across the map area. Metadolomite and interlayered calcite marble make up an estimated 80 per cent of the formation from the north side of the Phoenix anticlinorium southeast to Loch Raven Reservoir. South and southwest of an arbitrary line connecting Lutherville and Glenarm, Maryland, however, calc-schist interlayered with metadolomite and calcite marble evidently constitute most of the Cockeysville. This broad change in lithology is believed to represent a relict sedimentary facies change, from interbedded dolomite and limestone in the north to calcareous shale and associated limestone and dolomite in the south and west.

(2) The carbonate rocks are most impure near the base and top of the formation. The basal unit of the Cockeysville, where it is partially exposed along the southeast flanks of the Texas domes, is quartz-rich diopside-tremolite calc-gneiss (Table 2, modes 7, 8). This calc-gneiss overlies Setters metaquartzite and garnet-mica gneiss and underlies Cockeysville metadolomite; it may therefore represent a relict transition for noncarbonate to carbonate sedimentation.

The Cockeysville-Wissahickon contact is also gradational (Fig. 2) at the one locality where it is exposed, 2 miles east of Pikesville, Maryland. The fine-grained tourmaline-bearing paragneiss exposed at this locality has been chosen arbitrarily as the basal unit of the Wissahickon because it evidently persists throughout the area, and its lower contact (though poorly accessible for close study) appears to be one of slight unconformity. Moreover, aplite sills and pegmatite dikes occur close to this lower contact, as they do

[1] In this report the Cockeysville rocks are referred to as carbonate rocks or marbles, but particular varieties are defined as follows:

Calcite marble: medium- to very coarse-grained marble, white to grayish or bluish white, nondolomitic, and composed of 85 per cent calcite or more.

Metadolomite: fine- to medium-grained marble, white to pale pinkish tan or pale bluish gray, and generally composed of 85 per cent dolomite or more; calcite ranges in amount from 0 to 20 per cent; the term was suggested by Brooks (1954).

Calc-schist and calc-gneiss: fine- to medium-grained marble, light gray, bluish gray, or tannish purple, and devoid of dolomite; micas and other minerals besides calcite constitute 50 per cent or more of the rock; the calc-shists are mica-rich and conspicuously foliated; the calc-gneisses are quartz-rich and massive or gneissose.

Calc-silicate rocks: medium- to very coarse-grained rocks, white to pale gray, with or without traces of dolomite, and rich in diopside, quartz, tremolite, calcite, and locally talc, in varying proportions.

along the contact between the Setters formation and the basement complex.

(3) Thickness estimates of the Cockeysville (Table 1) give no more than an order of magnitude, for the formation's stratigraphic thickness

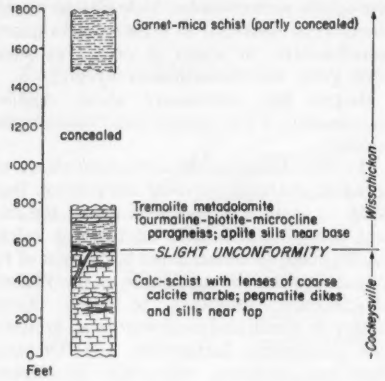

FIGURE 2.—MEASURED SECTION SHOWING LOCATION OF COCKEYSVILLE-WISSAHICKON CONTACT

Lower 800 feet exposed in two quarries 2 miles east of Pikesville, Maryland; upper 250 feet partially exposed south of the quarries.

has been modifed to an unknown but probably considerable degree by minor folding. The writer's estimate of 750 feet for the maximum thickness is based on two partially exposed sections, one located 1–1½ miles northwest of Butler, Maryland, and the other along a road parallel to Gunpowder Falls, 3½ miles east-northeast of Towson, Maryland. Horizontal distances across the formation outcrop belt in these two areas were averaged and divided by three. The writer's estimate is thus no more than an approximation, and at least a 30 per cent error is probable.

The Cockeysville pinches out laterally along the gneiss domes at six localities in the area. The reason for these pinch outs is uncertain, but they occur within such short distances that they may be structural rather than stratigraphic, perhaps mainly because of flowage induced by differential movement over the gneiss domes. Direct evidence that the carbonate rocks were extremely mobile lies in the flowage and drag folds found at almost every outcrop in the area. A deep well at Lutherville, Maryland, near a major normal fault has provided indirect evidence: the well passed through 3000 feet of marble, an abnormally thick section (Broedel, 1937, p. 182) probably due to repetition by minor folding.

STRUCTURAL GEOLOGY

Regional Structure

The main structural elements in the Cockeysville area are three northeast-trending major folds: (1) a gently southwest-plunging anticlinorium in the north (the Phoenix structure); (2) a composite, discontinuous anticlinal fold along the south edge of the area, formed by the Texas and Chattalonee domes; and (3) a broad synclinorium of Cockeysville and Wissahickon extending across the center of the area between the two anticlinal uplifts. The domes are in most places steep-sided, as Broedel concluded (1937, Pl. 32). The central synclinorium, even though its form is locally obscured by isoclinal minor folds in the carbonate rocks, appears to be shallow and may be essentially flat-bottomed between the Chattalonee and Phoenix structures.

This picture is complicated by the Texas dome, a steep-sided mass of microcline augen gneiss which straddles the inferred axis of the synclinorium. The dome is bounded on its west side by a high-angle normal fault whose southern extension abruptly cuts off the Towson dome.

Trends of minor crinkle axes in the Wissahickon schist (G. R. Stevens, 1955, personal communication) and of foliation in the Cockeysville formation suggest that the western half of the central synclinorium may be cross-folded along north-trending axes, possibly as a reflection of the north-trending Texas dome.

Structure of the Carbonate Rocks

Structural relations to the gneiss domes.—Several features indicate that the gneiss domes probably controlled the symmetry and intensity of deformation in the carbonate rocks. Cross joints, foliation, monor fold axes, and small-scale linear elements (Fig. 3) in the marbles along the borders of the domes parallel closely the corresponding structural elements within the domes as compiled by Broedel (1937) and locally by the writer. This parallelism decreases with distance from the domes, however, as is evident in the carbonate rocks immediately southwest of Loch Raven Reservoir and north-northwest of Texas, Maryland. The parallelism is most conspicuous along the axis of the Phoenix anticlinorium (Fig. 4; Pl. 3),

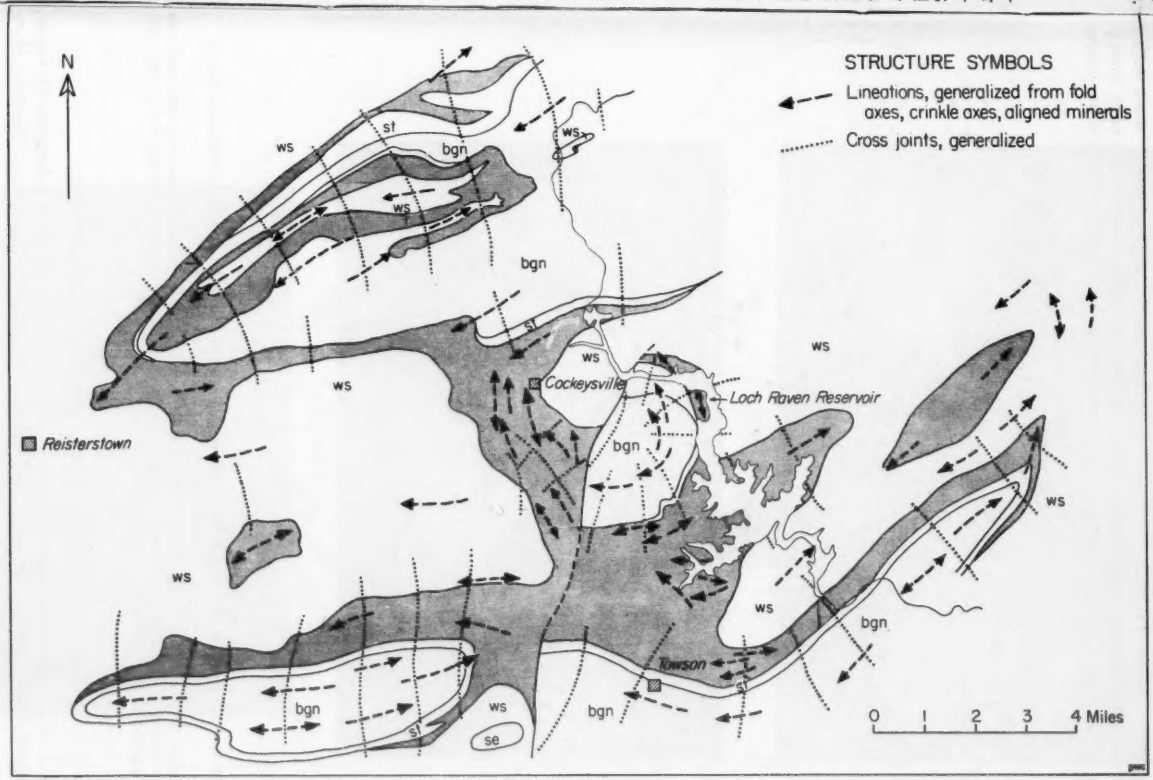

FIGURE 3.—GENERALIZED CROSS JOINTS AND LINEAR ELEMENTS IN THE COCKEYSVILLE AREA

Lineations are based on minor fold axes, axes of small crenulations, and aligned minerals, single or aggregated. Structures of gneiss domes are in part generalized from Broedel (1937, Pl. 32).

where minor structures reflect closely the symmetry of the major structure.

The relationship between gneiss domes and intensity of carbonate rock deformation is inferred from both direct and indirect evidence. Direct evidence is provided by minor folds in the marbles; these are generally open throughout most of the central anticlinorium, whereas

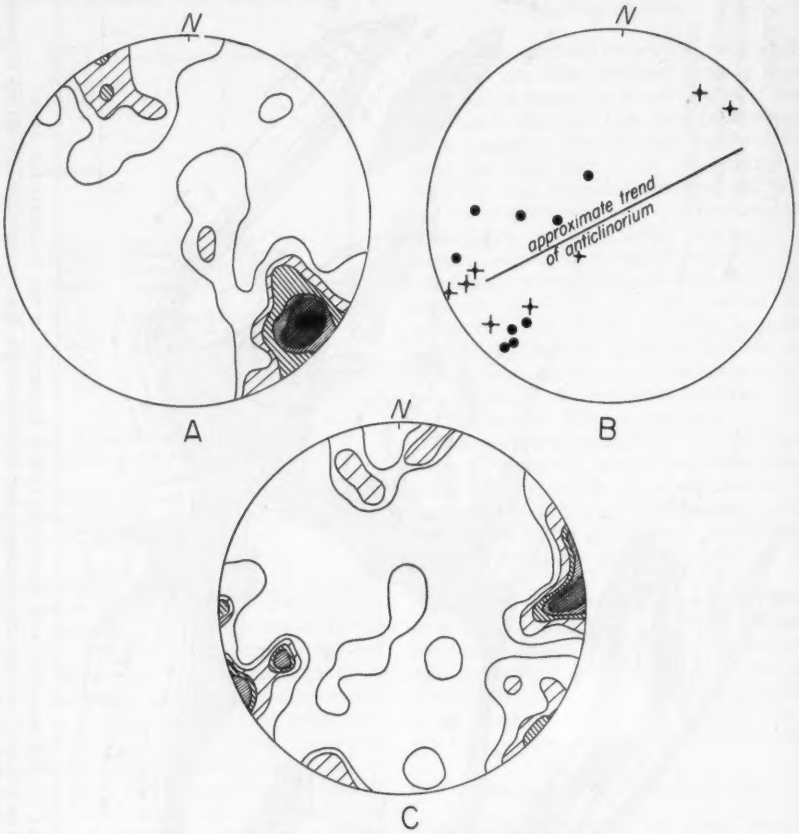

FIGURE 4.—STATISTICAL DIAGRAMS OF STRUCTURAL ELEMENTS IN MARBLES, SOUTHWEST HALF OF PHOENIX ANTICLINORIUM

A. foliation, 97 poles, contour intervals 20-13-11-5-3-1 per cent. B. lineations, minor fold axes and axes of crinkles (crosses), and aligned minerals (dots). C. joints, 50 poles, contour intervals 8-6-4-2-1 per cent. Equal-area projections of the lower hemisphere.

PLATE 1.—FOLDING IN THE COCKEYSVILLE MARBLE

FIGURE 1.—Tight laminar flowage folds in calc-schist. Dark-gray material is phlogopite-rich marble, white is calcite marble. Hammer near top of photo gives scale. Quarry is 2 miles east of Pikesville, Maryland.

FIGURE 2.—Flexure folds in interlayered metadolomite and calcite marble. Metadolomite layers stand out as ridges on the outcrop. Note hammer for scale. A quarter of a mile southwest of Belfast, Maryland.

FIGURE 3.—Folded remnants of metadolomite. Remnants, bordered unevenly by coarse phlogopite, (dark gray), occur in relatively pure calcite marble, and dip steeply toward the observer. Quarry at Texas, Maryland.

FIGURE 1

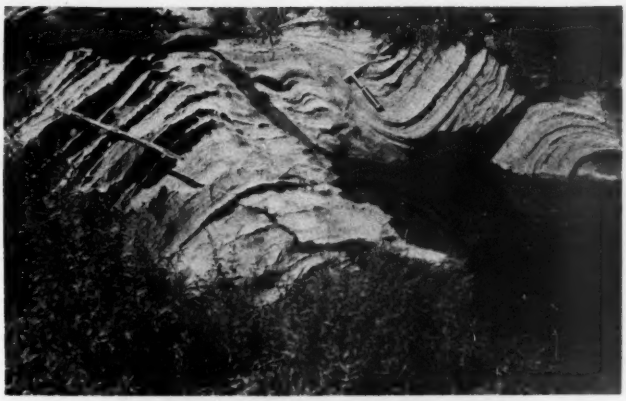

FIGURE 2

FIGURE 3

FOLDING IN THE COCKEYSVILLE MARBLE

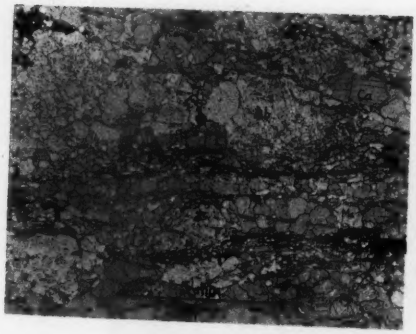

FIGURE 1

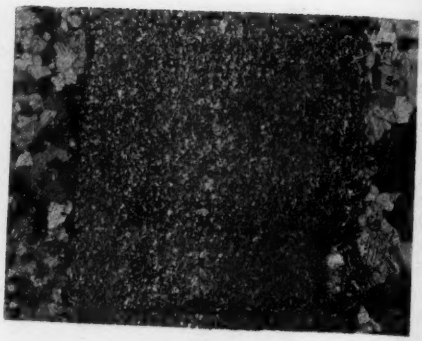

FIGURE 2

FIGURE 3

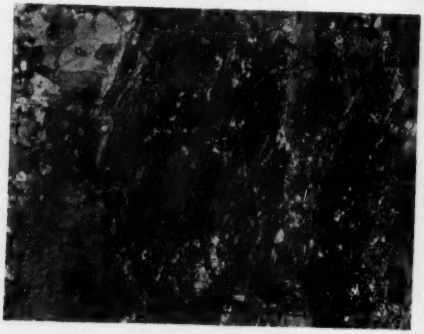

FIGURE 4

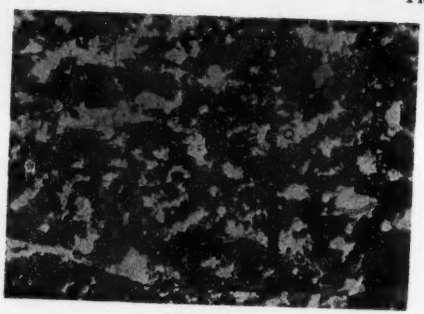

FIGURE 5

PHOTOMICROGRAPHS OF COCKEYSVILLE MARBLE

in steeply dipping marbles close to the domes the folds are most commonly isoclinal, tightly appressed, and locally drawn out into slender, pointed apices. Isoclinal folds are particularly common along the flanks of the Towson and Chattalonee domes (Pl. 1, fig. 1). Indirect evidence of the relationship may lie in the distribution of syntectonic pegmatites. Pegmatites intruding the Cockeysville are restricted almost entirely to steeply dipping, tightly folded marble close to gneiss domes. Their distribution may be only an indication of intense intrusive activity connected with pegmatization within the domes, but their confinement to strongly deformed marbles seems to be more than a coincidence.

Foliation.—Most of the carbonate rocks possess a marked foliation expressed as compositional layering and/or directional fabric. As a rule the foliation probably reflects sedimentary bedding, because foliation parallels formation contacts and parallels boudined layers of metadolomite, metaquartzite, and graphite schist. In places, however, the metamorphic foliation clearly transects bedding. Some of the layers of calcite marble exposed in a commercial quarry at Texas, Maryland, for example, display a gently and uniformly dipping foliation but contain badly contorted relics of metadolomite as well as discontinuous layers and streaks of dark-gray graphitic and pyritic marble (Fig. 6B), which record intense minor folding later masked during recrystallization and replacement. Bedding is also obscure in some of the steeply dipping carbonate rocks along the flanks of gneiss domes where calc-schist and calcite marble occur as alternating streaks, thin lenses, and V-shaped wisps in isoclinal laminar-slip flowage folds (Fig. 6A, D).

Calcite, dolomite, phlogopite, and muscovite in preferred orientation impart the directional fabric. Tabular calcite crystals and short tabular dolomite crystals show a rather diffused but noticeable orientation; their long axes are parallel to foliation. In general the calcite orientation is strong in layered calcite marble and relatively weak in impure marbles where calcite constitutes only a minor fraction of the rock. Certain discordant masses of calcite marble in the Cockeysville (Fig. 7; Table 4) tend as a group to have directionless fabric and are interpreted as having formed in an esssentially static state.

That most of the recrystallization was syntectonic is attested to by the preferred orientation of carbonates and micas and also by S-shaped trains of ultrafine inclusions (sericite, ?graphite, rarely tourmaline needles and unidentified globular opaques) in strongly oriented albite porphyroblasts in some of the calc-schists.

Although only one *S* plane is conspicuously developed in the Cockeysville marbles, at least two pronounced *S* planes, foliation and a fracture cleavage, occur regionally in the Wissahickon and Setters formations (Broedel, 1937, p. 185). This difference appears to reflect the more limited capacity of the carbonate rocks to transmit stress, a property which is also evident from the fact that the minor folds so abundant in the Cockeysville do not appear to have affected the upper or lower surface of the formation.

Primary structures and textures.—Very few primary structures or textures are recognizable. Most of the carbonate rocks were completely recrystallized and consist of metamorphic mineral assemblages in which grain diameters average about 0.5–2 mm. Although the form

PLATE 2.—PHOTOMICROGRAPHS OF COCKEYSVILLE MARBLE

FIGURE 1.—Calc-schist, phlogopite-rich (Ph) layer. Muscovite (Ms), phlogopite, pyrite (Py), and quartz (Q) tend to be segregated into discrete layers separated by calcite- (Ca) rich layers. The large porphyroblast is albite (Ab). Ordinary light.

FIGURE 2.—Graphite schist showing probable relict graded bedding. Base of layer is pyritic (Py); proportions of graphite (Gr) and of mica increase upward (toward right) as grain size decreases. Adjoining rock is scapolite-rich (Sc) calcite (Ca) marble.

FIGURE 3.—Metadolomite. Chiefly dolomite (Do), calcite (Ca), phlogopite (Ph), and quartz (Q) with traces of pyrite (Py). Calcite marble commonly associated with this type of metadolomite. Ordinary light.

FIGURE 4.—Tremolite-rich calc-silicate rock. Tremolite (Tr) porphyroblast encloses remnants of diopside (Di); both are partly altered to felts of talc (Ta), microcrystalline calcite, and quartz. Aggregate of dolomite (Do) and calcite (Ca) is interpreted as unsilicated portion of parent dolomite. Ordinary light.

FIGURE 5.—Diopside-quartz calc-silicate. Diopside (Di) occurs in large sieved porphyroblasts partially replaced by mosaics of quartz (Q). Genetically related quartz-rich metadolomite on strike occurs in outcrops nearest the calc-silicate. (*See* Table 2, mode 22.) Ordinary light.

and probable original composition of beds can be inferred from certain relatively competent layers such as metadolomite and metaquartzite, rock of probable sedimentary character has been found at only one locality in the area: an abandoned quarry near Maryland 143, 1½ miles northeast of Warren, Maryland, where a lens of coarse calcite marble (Fig. 7) contains what is interpreted as a sedimentary remnant of aphanitic white limestone.

Probable relict graded bedding has been identified at several places, however, in layers 2–8 cm thick of dark-purple, very fine-grained graphite schist (Pl. 2, fig. 2; Table 2, mode 6). The graded bedding is inferred from a tendency of these layers to show a decrease in grain size, decrease in amounts of quartz and feldspar, and increase slightly in graphite, pyrite, and sericite content from bottom to top. Top directions determined from the graded (?) beds correspond with those determined by stratigraphic and structural criteria.

Minor folds.—An almost infinite variety of minor folds occur in the carbonate rocks, but for descriptive purposes these folds can be grouped arbitrarily in two categories: (1) flexure folds and (2) flowage folds. The flowage folds can be subdivided into (a) folds produced by penetrative laminar flow along closely spaced subparallel planes, as interpreted by the writer, and (b) folds apparently due to nonlaminar flowage. The flowage folds are most abundant in steeply dipping marble close to the domes, whereas the flexure folds are the predominant type in most of the central synclinorium. Type 2b resembles the type of flowage fold described by Bain (1931); folds of this kind are particularly common within thick layers of calcite marble, which evidently was the least competent of any of the carbonate rocks during deformation. The laminar flowage folds, type 2a, occur only in steeply dipping marble close to the gneiss domes. The writer interprets them as products of intense shearing of the carbonate rocks along the domes in directions chiefly parallel to formation contacts and to the borders of the domes.

Characteristics of the minor folds upon which these generalizations are based are summarized below:

(1) *Flexure folds* (Fig. 5; Pl. 1, fig. 2)
- Generally open, little apical thickening of layers
- Marked directional fabric in the limbs and weakly directional or directionless fabric in the crests of folds
- Crumpling, minor faulting, and boudinage of relatively competent layers (*e.g.*, metadolomite, graphite schist, metaquartzite); some flowage of incompetent material (*e.g.*, calcite marble, calc-schist)

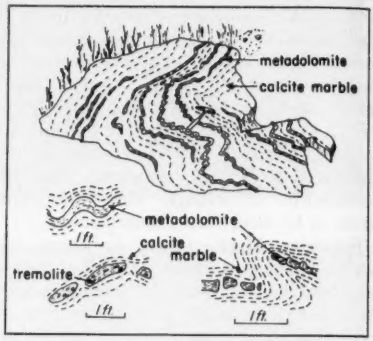

FIGURE 5.—CRUMPLING AND BOUDINAGE IN FLEXURE FOLDS

Foliation generalized by dashed lines. Outcrop at top sketched from photograph; hammer shows scale.

- Symmetry elements of minor flexure folds related systematically to major folds, a conclusion based on detailed structure of parts of the Phoenix anticlinorium in minor folds, lineations in *b*, and cross joints in *ac;* foliation planes in minor folds statistically contain major fold axes (Fig. 4)
- Wave-length order: 10^0–10^4 cm
- Occurrence: mainly in marbles dipping about 40°–50° or less, in the broad axial part of the central synclinorium

(2) *Flowage folds*

(a) *Laminar flowage folds* (Fig. 6A, C, D; Pl. 1, fig. 1)
- Generally isoclinal, tightly appressed and drawn out into peaked crest; layers greatly thickened in crests; rocks involved commonly found as thin lenses, schlierenlike streaks, pointed hook-shaped forms
- Marked and rather uniform directional fabric parallel to axial planes; folds accentuated by micas arranged en echelon, each parallel to axial planes
- Few differences in relative competency apparent between rock types involved; little or no boudinage, systematic crumpling, or offsetting of layers; lateral and vertical lithologic and mineralogic gradations common
- Little systematic relationship between symmetry elements of minor and major folds; minor fold axes generally parallel

to formation contacts and foliation, however

Wave-length order: less than 10^2 cm

Occurrence: mainly in steeply dipping marbles (about 40°–50° or more), close to formation contacts on immediate flanks of the gneiss domes

(b) *Nonlaminar (?) flowage folds* (Fig. 6B)

Generally isoclinal, drawn out into sharp crests with much apical thickening

Axial planes bent, oriented inconsistently but roughly parallel to foliation; folds accentuated by zones of graphitic and pyritic marble or by strung-out clusters of phlogopite

Fold axes oriented inconsistently with respect to major fold axes

Directional fabric, usually strong, roughly parallel to axial planes of minor folds, but not consistently so

Wave-length order: 10^0–10^3 cm

Occurrence: generally within calcite marble layers 10 cm or more thick; some folds affect several layers of differing composition; prevailing dip of foliation ranges from nearly horizontal to vertical

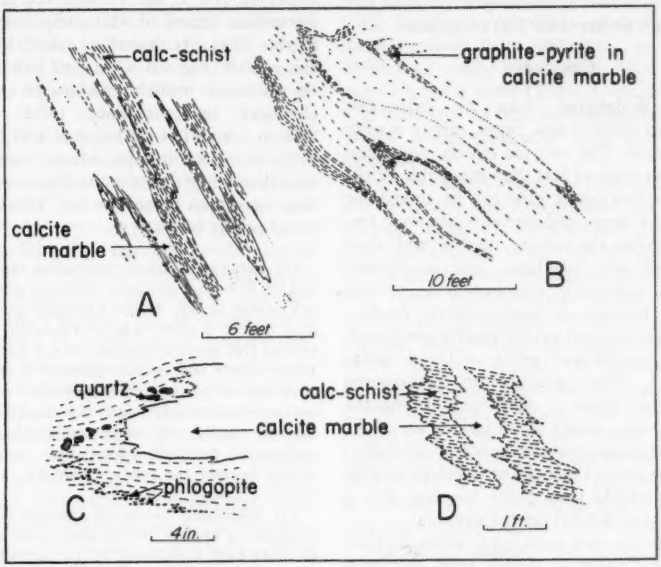

FIGURE 6.—FLOWAGE FOLDS

Folds in A, C, and D interpreted as products of laminar flowage parallel to axial planes of folds; folds in B apparently due partly to nonlaminar movement. Aligned phlogopites (generalized as dashed lines) suggest flowage directions. Calcite marble in C has essentially directionless fabric.

Linear structures.—Several kinds of linear elements are found in the carbonate rocks. In this paper they are referred to the directions *a*, *b*, and *c*, as modified from Cloos (1946, p. 6); *b* is the fold axis, *a* is perpendicular to *b*, and *c* is normal to the foliation *ab*. The major lineations are:

parallel to *b*: long axes of tremolite and diopside porphyroblasts;
strings of pyrite cubes;
axes of minor undulations in layers;
axes of crinkles;
long axes of boudins (?);

parallel to *a*: long axes of thin pods of vein quartz.

Lineations in *b* are by far the more common type. The orientation of boudined fragments of layers can be clearly discerned at only a few localities, where the long axes of the boudins parallel flexure fold axes, perhaps as a result of stretching along *a* around the fold axes. Porphyroblasts of tremolite and diopside commonly contain planes of phlogopite inclusions that lie aslant to the foliation of the surrounding rocks; orientation of these inclusions suggests that the porphyroblasts became oriented chiefly by rolling in the foliation, *ab*.

Systematically oriented linear elements in the Cockeysville appear to be restricted in occurrence to flexure folds, in which erratic mass flowage is presumed to have been minor during the deformation.

Petrography and Petrogenesis

Calc-Schist

Marble designated here as calc-schist includes two distinct rock types, calcite marble and calc-schist. The two are closely associated and occur in units of less than mappable thickness. A few individual units can be traced the length of the larger exposures in the area, but in most places the calcite marble and calc-schist interfinger, interlense, and intergrade. Calc-schist commonly contains pods, lenses, and small patches of coarse calcite marble.

The calc-schist and calcite marble are purple or tannish purple and white or bluish white respectively. They weather to rust-colored outcrops that have a distinctive corrugated appearance as a result of variations in calcite content and consequent differences in solubility. The volume ratio of calc-schist to calcite marble is highly variable from place to place but is estimated as about 3/1 on the average.

Although the two rock types differ in bulk composition (Table 2, modes 1–5), the main difference is in the ratio of calcite to noncarbonate minerals; the mineral species are similar. Both rocks contain dark-brown phlogopite (*e.g.*, X/Y = pale yellowish tan, Z = reddish brown; biaxial (−), 2V = 7°–10°; $n_x = 1.607 \pm 0.002$, $n_y = 1.604 \pm 0.002$) and dark-brown or black tourmaline which in thin section is pleochroic from pale yellow to deep reddish brown. Muscovite, microcline, and plagioclase occur in both rocks and appear to be characteristic only of those varieties of calcite marble that are found with calc-schist; calcite marble in other lithologic associations lacks all three minerals. In a sense, then, the calc-schist and calcite marble are concentrations of the same minerals into carbonate-poor and carbonate-rich layers.

This segregation is evident on a microscopic as well as megascopic scale. In detail the calc-schist consists of alternating paper-thin partings of phlogopite-apatite-tourmaline-sphene-pyrite and of calcite-quartz-feldspar. All gradations exist between these two apparent end types, but the two assemblages are generally distinct (Pl. 2, fig. 2).

It is not clear whether or not any appreciab metasomatism accompanied the metamorphis of the sediments that gave rise to calc-schist The discontinuous form of composition layers, the intense minor folding that is local apparent (Pl. 1, fig. 1), and the large part discordant lenses of extremely coarse calci marble that are found at some localities i calc-schists (Fig. 7B, C) are all indications tha the sediments probably underwent considerabl chemical reorganization. Other evidenc though somewhat ambiguous and subject t more than one interpretation, suggests whe considered together that metasomatic change may have been rather limited. This evidence noted briefly below:

(1) Concentrations of tourmaline and phlogopit locally line the contacts between mica-rich an calcite-rich layers. At one unusually good exposur in a quarry 2 miles east of Pikesville, Maryland several thin granitic pegmatites cut the calc-schis Border zones and contact aureoles of these pegma tites are in places tourmaline-rich, suggesting contact-metasomatic source for tourmaline in the marbles nearby, and yet no perceptible gradients in amount of tourmaline have been noted in calc schists beyond the contact aureoles, which rarely exceed a foot in thickness.

(2) Apparently the small amounts of boron and phosphorus present in the tourmaline and apatit that are both ubiquitous in the calc-schists (Table 2, modes 1–4) could have been provided by the sediments themselves; published analyses (Rankama and Sahama, 1950, p. 491) show boron contents of about 0.005–0.015 per cent in limestones and dolomites and about 0.05 per cent in shales and these figures are of the same order of magnitude as those estimated for the calc-schists.

(3) Water content in the calc-schists ranges between about 3 and 8 per cent, amounts not excessive for argillaceous limestones, which are inferred to have been the parent sediments.

(4) Scapolite in the marble (Table 2, modes 1, 2) has the properties of a calcic variety near Me 70 in composition (Winchell, 1933, p. 293–294).[2] Scapolite of such composition could reasonably have developed from limestone during "normal regional metamorphism," according to some authorities, without the addition of material to its lattice (Turner and Verhoogen, 1951, p. 492).

On the basis of these features, the writer believes that the metasomatism which accompanied recrystallization of Cockeysville sediments to calc-schists was of local extent and

[2] Uniaxial (−), or biaxial (−) with 2V = 0°–5° in strained crystals; colorless, moderately low relief, two cleavages at 90°, maximum birefringence 0.038–0.040

robably of negligible importance in deter-ining the mineralogical make-up of the arbles.

Metadolomite

General statement.—Metadolomite makes up uch of the Cockeysville formation and occurs roughout the map area. Despite its abun-ance, however, it shows little variation in omposition from place to place (Table 2, odes 9–14; Table 3, analyses A–C, 9–14). The etadolomite can be subdivided arbitrarily, cording to slight differences in composition d because of two mutually exclusive rock sociations, into two types: (1) phlogopite-alcite metadolomite, associated with calcite arble; and (2) quartz metadolomite, with hich calc-silicate marble occurs but not alcite marble. The first type of metadolomite sually consists of 2 per cent quartz or less, p to 4 per cent phlogopite, and as much as 0 per cent calcite. Quartz metadolomite ontains 3–10 per cent quartz but little or no hlogopite or calcite except in aureoles around orphyroblasts of tremolite or diopside.

Physical properties of the two rock types eflect these differences in mineralogy. The hlogopite-calcite metadolomites are typically an or pinkish tan where fresh. They weather eadily, because of the soluble calcite, to rayish-brown, punky, friable rock or to pale-an dolomite sand. The quartz metadolomites re typically bluish white or grayish white and elatively insoluble. They weather to hard, rab-gray, knobby outcrops because of an bundance of quartz and scattered tremolite nd diopside porphyroblasts.

The metadolomites appear to be little odified metamorphic equivalents of slightly rgillaceous dolomite. This conclusion is based on (1) their chemical composition, (2) their extural and mineralogical uniformity, (3) their structural behavior, and (4) their relation-hips with associated marbles. The first three eatures are discussed here; the fourth is deferred to sections of this report dealing with calcite marble and calc-silicate rocks.

Chemical composition.—A comparison of published and calculated analyses[3] of Cockeysville metadolomite with published analyses of sedimentary carbonate rocks shows that these marbles differ little from dolomite in bulk composition. The CaO/MgO ratios lie in the same range, 1.25–1.85, and water, CaO, MgO, and CO_2 are present in comparable amounts. Only locally, in tremolite- and diopside-rich rocks derived from dolomite, are chemical differences really substantial: SiO_2 is higher and CO_2 much lower (Table 3, analyses 14–16). The majority of the metadolomites compare closely with calcareous and noncalcareous dolomite.

Texture and mineralogy.—The metadolomites are uniformly medium-grained, for the most part (Pl. 2, fig. 3). Variations in grain size are local and are due to patches of coarse-grained calcite and to scattered silicate porphyroblasts. The main constituents—calcite, dolomite, quartz, and phlogopite—occur in statistically uniform distribution throughout the rocks, which seldom consist of compositionally different layers or zones and very rarely contain exotic minerals. Textural and mineralogical consistency such as this could reasonably result from recrystallization of the sediments with little metasomatism but would seem improbable if a profound chemical reorganization had accompanied the recrystallization.

Structural behavior.—Metadolomite layers have apparently been deformed as competent materials in those folds not formed primarily by flowage. Most of the layers are laterally persistent; folded layers have been crumpled, boudined, or offset (Fig. 5); their fabric is directional and their recrystallization was apparently syntectonic. If the sediments underwent any notable chemical changes during metamorphism, the changes must have occurred early during or before folding in order for individual units of metadolomite to maintain their identity during deformation, and the fabric should record a period of early recrystallization. No such record is apparent in the rocks.

Calc-Silicate Marble

General Statement.—Porphyroblasts of tremolite and diopside are found in most of the metadolomite. In general they are sparsely distributed and make up about 2 per cent or

[3] The percentages of MgO, CaO, and CO_2 calculated from modal analyses probably are not accurate to less than 5 per cent, for both calcite and dolomite in metamorphic rocks depart in composition from their ideal formulas (Goldsmith, Graf, and Joensuu, 1955; Graf and Goldsmith, 1955; Harker and Tuttle, 1955). Analyzed calcites from calcite-dolomite marble in the Grenville series of northern New York, for example, contain as much as 6 mol per cent $MgCO_3$ (Goldsmith, Graf, and Joensuu, 1955, p. 223).

TABLE 2.—MODAL ANALYSES OF CARBONATE ROCKS FROM THE COCKEYSVILLE FORMATION

	1	2	3	4	5	6	7	8	9	10	11	12	13	14	15	16	17	18	19	20	21	22	23	24	25
Calcite	40.7	6.2	35.0	90.2	71.1	1.2	38.0	49.4	16.3	1.6	13.6	3.2	1.3	5.1	28.7	8.3	8.2	11.3	—	—	—	94.5	90.6	98.3	78.0
Dolomite	—	—	—	—	—	—	—	—	78.0	93.8	83.0	95.2	96.6	68.4	7.0	18.0	—	—	—	—	—	—	1.6	—	—
Quartz	22.0	24.8[a]	20.3	4.0	7.2	41.3	34.8	14.6	1.9	0.8	1.9	0.6	—	3.2	6.8	5.5	3.3	10.4	23.3	29.5	55.6	4.2	1.8	4.0	19.6
Phlogopite	10.6	31.6	13.1	1.0	10.5	11.1	tr.	1.6	3.6	1.0	1.5	0.6	2.0	0.7	0.2	0.7	—	0.2	0.1	—	tr.	0.8	5.5	0.4	1.7
Muscovite	—	—	23.9	2.8	5.6	10.7	—	—	—	—	—	—	—	—	—	—	—	—	—	—	—	—	—	—	—
Tremolite	1.1	2.2[b]	—	—	—	—	9.2	7.4	—	—	—	—	—	3.1	51.7	4.2	16.1	4.8	0.8	1.7	5.3	—	—	—	—
Diopside	0.1	2.4	—	—	—	—	4.0	14.4	—	—	—	—	—	19.5	1.5	63.3	72.4	73.3	75.6	68.8	39.1	—	—	—	—
Talc	—	—	—	—	—	—	—	—	—	—	—	—	—	—	2.6	—	—	—	—	—	—	—	—	—	—
Microcline	11.4	17.6	2.3	0.3	2.2	4.3	0.3	0.2	—	—	—	—	—	—	1.5	—	—	—	—	—	—	—	—	—	—
Plagioclase	tr.	2.2	1.5[c]	0.7	0.6[d]	1.0	0.5	0.2	—	—	—	—	—	—	—	—	—	—	0.2	—	—	—	—	—	0.2[f]
Myrmekite	0.4	—	—	—	—	—	—	—	—	—	—	—	—	—	—	—	—	—	—	—	—	—	—	—	—
Scapolite	10.8	10.0	—	—	—	—	4.1	4.1	—	—	—	—	—	—	—	—	—	—	—	—	—	—	—	—	—
Chondrodite (?)	—	—	—	—	—	—	—	0.5	—	—	—	—	—	—	—	—	—	—	—	—	—	—	—	—	—
Monticellite	—	—	—	—	—	—	3.3	0.9	—	—	—	—	—	—	—	—	—	—	—	—	—	—	—	—	—
Clinozoisite	—	—	—	—	—	1.8	0.1	—	—	—	—	—	—	—	—	—	—	—	—	—	—	—	—	—	—
Serpentine minerals	—	—	—	—	—	0.8	—	—	—	—	—	—	—	—	—	—	—	—	—	—	—	—	—	—	—
Cordierite	—	—	—	—	—	—	—	—	—	—	—	—	—	—	—	—	—	—	—	—	—	—	—	—	—
Apatite	tr.	tr.	0.2	0.2	—	0.2	—	—	—	—	—	—	—	—	—	—	—	—	—	—	—	—	—	—	—
Sphene	0.5	0.4	0.5	tr.	0.1	0.6	0.7	0.8	—	—	—	—	—	—	—	—	—	—	—	—	—	0.1	0.1	0.2	0.1
Tourmaline	tr.	tr.	tr.	tr.	—	0.4	0.2	0.1	—	—	—	—	—	—	—	—	—	—	—	—	—	—	—	—	—
Zircon	—	—	tr.	—	—	0.6	—	—	—	—	—	—	—	—	—	—	—	—	—	—	—	—	—	—	—
Graphite	—	0.4	1.7	0.3	0.5	22.9	4.0	4.9	—	—	—	—	—	—	—	—	—	—	—	—	—	—	—	—	—
Pyrite	2.4	2.2	1.5	0.5	1.1	3.1	0.8	0.9	0.2	2.8	—	0.4	0.1	tr.	—	—	—	—	—	—	—	0.4	0.4	1.1	0.4
Magnetite	—	—	—	—	—	—	—	—	—	—	—	—	—	—	—	—	—	—	—	tr.	—	—	—	—	—
Other	—	—	—	—	1.1[e]	—	—	—	—	—	—	—	—	—	—	—	—	—	—	—	—	—	—	—	—
Total	100.0	100.0	100.0	100.0	100.0	100.0	100.0	100.0	100.0	100.0	100.0	100.0	100.0	100.0	100.0	100.0	100.0	100.0	100.0	100.0	100.0	100.0	100.0	100.0	100.0

[a] May include some untwinned albite
[b] An 10–12
[c] An 8–10
[d] An 24
[e] Cordierite, talc (?), leucoxene (?)
[f] An 4 plus microcline

1. Calc-schist, 1 foot from contact with pegmatite, 3½ miles east-northeast of Towson, Maryland
2. Calc-schist, 2 miles northeast of Towson, Maryland

[a] May include some untwinned albite
[b] An 10–12
[c] An 8–10
[d] An 24
[e] Cordierite, talc (?), leucoxene (?)
[f] An 4 plus microcline

1. Calc-schist, 1 foot from contact with pegmatite, 3½ miles east-northeast of Towson, Maryland
2. Calc-schist, 2 miles northeast of Towson, Maryland
3. Calc-schist, quarry 2 miles east of Pikesville, Maryland
4. Calcite marble interlayered with calc-schist, quarry 2 miles east of Pikesville, Maryland
5. Calcite marble, stream bed 1½ miles southwest of Ruxton, Maryland
6. Graphite schist, quarry 2 miles north-northeast of Marriotsville, Maryland (in Howard County, south of map area)
7. Calc-gneiss, unmottled, 4 miles north-northeast of Towson, Maryland, near State highway 144
8. Calc-gneiss, slightly mottled by calcite, 3 miles north-northwest of Towson, Maryland
9. Metadolomite interlayered with calcite marble, 3½ miles southwest of Butler, Maryland, near State highway 128
10. Metadolomite relic in calcite marble quarry at Texas, Maryland
11. Metadolomite interlayered with calcite marble, Ruxton, Maryland
12. Metadolomite, 2 miles southeast of Butler, Maryland
13. Metadolomite, 12 feet from contact with diabse dike, ¾ mile southwest of Butler, Maryland
14. Diopside metadolomite, 1¾ miles northeast of Towson, Maryland
15. Calcite-tremolite transition rock, 1½ mile north-northeast of Towson, Maryland
16. Dolomitic calc-silicate rock, ½ mile north-northeast of Stevenson, Maryland, along State highway 130
17. Tremolite-diopside calc-silicate rock, 1 mile north of Glenarm, Maryland
18. Calcitic quartz-diopside calc-silicate rock, 2½ miles east-northeast of Towson, Maryland
19. Quartz-diopside calc-silicate rock, 1¼ miles northeast of Stevenson, Maryland
20. Quartz-diopside calc-silicate rock, 1½ miles north-northeast of Glenarm, Maryland
21. Diopside-quartz calc-silicate rock, 2 miles northwest of Ruxton, Maryland
22. Calcite marble interlayered with metadolomite, 3½ miles southwest of Butler, Maryland, near State highway 128
23. Calcite marble interlayered with metadolomite, 1¼ miles west of Stevenson, Maryland
24. Calcite marble interlayered with metadolomite, 2½ miles northeast of Towson, Maryland, on shore of Loch Raven Reservoir
25. Calcite marble interlayered with metadolomite, 2¼ miles southwest of Butler, Maryland

less of the rocks. At many localities, however, metadolomite is studded with porphyroblasts in such abundance that the silicates coalesce to the virtual exclusion of carbonate minerals. Such calc-silicate marble occurs in irregular nests and pods and in tabular zones elongated in the foliation along certain layers of metadolomite. Rarely is the form of these occurrences visible in three dimensions. Calc-silicate marble is restricted in its occurrence to quartz metadolomite in the upper part of the Cockeysville; concentrations of silicate minerals of this type have not been observed in the more common calcite-phlogopite metadolomite, which contains little or no quartz (Table 2, modes 9–13).

Textural and chemical features of the calc-silicate marbles, in the absence of directly traceable sedimentary source rocks, indicate that the calc-silicate marbles recrystallized from sediments ranging in composition from quartz dolomite to dolomitic chert or chert-rich dolomite and suggest that the dedolomitization (Teall, 1903) did not involve metasomatic changes other than CO_2 loss and possible SiO_2 enrichment.

Petrography.—Diopside in the silicate-rich zones occurs as stubby porphyroblasts. Some of these are pseudomorphed by tremolite filled with small inclusions of calcite and quartz; other diopsides are fresh and essentially free of inclusions. In hand specimen they range from pale gray to medium greenish gray, and under the microscope they are essentially colorless (Pl. 2, figs. 4, 5).

Tremolite occurs in two forms, as pseudomorphs after diopside and as stellate or fibrous aggregates of slender prismatic crystals. Like the diopsides, they are generally pale (light gray, cream, or light greenish gray in hand specimen and colorless in thin section). Both minerals are Mg-rich varieties which probably contain little or no iron.

At a few localities, fibrous tremolite and stubby diopside occur side by side in the same outcrop, within a few centimeters of each other. In a given outcrop, both show the same orientation in many places, either parallel or askew to foliation, and contain rotated or unrotated planes of phlogopite inclusions. The two minerals appear to have had essentially contemporaneous origins.

An aureole composed mainly of coarse calcite and deficient in quartz relative to the host rock usually surrounds each porphyroblast of tremolite. Diopside porphyroblasts generally lack such aureoles but are surrounded by quartz-poor aureoles about 1–3 mm wide; the diopsides that are partly altered to tremolite and contain inclusions of calcite and quartz are commonly surrounded by aureoles somewhat richer in calcite than the surrounding metadolomite. Calcite-rich, quartz-poor aureoles show a crude tendency to vary directly in width according to the size of tremolite porphyroblasts; whether or not a similar variation accompanies variations in the degree of alteration of the diopsides is not known, however.

Some calc-silicate marbles consist chiefly of diopside that is partly altered to tremolite along the traces of cleavages and fractures. Small inclusions of strain-free calcite and quartz occur in or close to the altered patches. Textural relations of this kind are found in the rock analyzed in mode 17 (Table 2).

Other calc-silicates, such as those of modes 19–21 (Table 2), are essentially pure diopside-quartz rocks; they consist of irregular, interlocking diopside porphyroblasts as much as 2 inches long that show various stages of replacement by mosaics of clear, unstrained quartz (Pl. 2, fig. 5).

Talc has formed locally as an alteration product from both tremolite and diopside (Pl. 2, fig. 4) and occurs as felts of microcrystalline flakes along fractures and cleavages in the porphyroblasts. Tiny crystals of quartz and calcite occur in and near the talc felts. Talc alteration is generally more extensive in diopsides than in tremolites.

Modal analyses 14-21 (Table 2) are fairly representative of the mineralogical range between quartz metadolomite and carbonate-free calc-silicate marble, even though the rocks they represent were taken from different localities. Partial chemical analyses calculated from these modes, if the carbonates are considered to approximate pure calcite and pure dolomite (*see* footnote 3), show progressive enrichment in SiO_2 and loss of CO_2 in the series metadolomite to calc-silicate marble. Despite this change, the CaO/MgO ratios of these rocks all approximate that of pure dolomite (Table 3, G).

Origin of the calc-silicate marble.—It is reasonable to assume that the calc-silicate marble, like the individual porphyroblasts of tremolite that occur in metadolomite, formed essentially from dolomitic sediments. This opinion is based on the restricted occurrence of calc-silicate marble, the relict patches of

TABLE 3.—CHEMICAL ANALYSES OF COCKEYSVILLE METADOLOMITE, CALC-SILICATE ROCKS, AND MARBLE OF INTERMEDIATE COMPOSITION; CHEMICAL

TABLE 3.—CHEMICAL ANALYSES OF COCKEYSVILLE METADOLOMITE, CALC-SILICATE ROCKS, AND MARBLE OF INTERMEDIATE COMPOSITION; CHEMICAL ANALYSES OF DOLOMITIC SEDIMENTS

	A	B	C	9	10	11	12	13	14	15	16	17	18	19	20	21	D	E	F	G
SiO_2	0.44	5.57	3.88	2.2	0.8	2.2	0.7	—	17.0	39.9	44.0	53.6	54.1	64.6	67.5	77.9	7.96	3.24	24.92	—
Al_2O_3	1.22	0.40	1.24	n.d.	n.d.	n.d.	n.d.	n.d.	n.d.	n.d.	n.d.	n.d.	n.d.	n.d.	n.d.	n.d.	1.97	0.17	1.82	—
Fe_2O_3	n.d.	n.d.	n.d.	n.d.	n.d.	n.d.	n.d.	n.d.	n.d.	n.d.	n.d.	n.d.	n.d.	n.d.	n.d.	n.d.	0.14	0.17	0.66	—
FeO	tr.	n.d.	0.32	n.d.	n.d.	n.d.	n.d.	n.d.	n.d.	n.d.	n.d.	n.d.	n.d.	n.d.	n.d.	n.d.	0.56	0.06	0.40	—
MgO	20.87	20.30	20.41	18.3	21.6	18.8	21.1	21.6	19.8	16.1	17.1	17.6	14.2	14.7	13.7	9.3	19.46	20.84	14.70	21.9
CaO	30.73	29.08	30.06	31.7	29.8	32.7	30.9	30.1	29.1	25.1	26.8	25.4	26.1	20.5	18.4	11.8	26.72	29.58	22.32	30.4
MnO	1.22	n.d.	0.02	n.d.	n.d.	n.d.	n.d.	n.d.	n.d.	n.d.	n.d.	n.d.	n.d.	n.d.	n.d.	n.d.	0.07	—	—	—
Na_2O	n.d.	n.d.	n.d.	n.d.	n.d.	n.d.	n.d.	n.d.	n.d.	n.d.	n.d.	n.d.	n.d.	n.d.	n.d.	n.d.	0.42	—	0.04	—
K_2O	n.d.	n.d.	n.d.	0.8	0.6	0.3	0.1	0.4	n.d.	n.d.	n.d.	n.d.	n.d.	n.d.	n.d.	n.d.	0.12	—	0.03	—
$H_2O\pm$	n.d.	n.d.	n.d.	0.5	0.5	0.2	0.1	0.2	0.1	1.2	1.2	0.3	1.0	0.2	0.4	1.0	0.63	0.30	0.78	—
FeS_2	n.d.	n.d.	0.06	n.d.	n.d.	n.d.	n.d.	n.d.	n.d.	n.d.	n.d.	n.d.	n.d.	n.d.	n.d.	n.d.	—	—	—	—
CO_2	45.85	44.26	43.93	44.7	46.1	45.1	47.1	46.8	33.8	15.1	11.2	3.1	4.6	—	—	—	41.13	45.54	33.82	47.7
Other	n.d.	n.d.	n.d.	n.d.	n.d.	n.d.	n.d.	n.d.	n.d.	n.d.	n.d.	n.d.	n.d.	n.d.	n.d.	n.d.	1.22	—	0.64	—
Total	100.33	99.61	99.92	98.2	99.4	99.3	100.0	99.1	99.8	97.4	100.0	100.0	100.0	100.0	100.0	100.0	100.40	99.90	100.13	100.0
CaO:MgO	1.47	1.43	1.48	1.72	1.39	1.74	1.41	1.39	1.47	1.56	1.57	1.44	1.84	1.38	1.34	1.26	1.37	1.42	1.52	1.39

A. Cockeysville metadolomite, locality unknown. T. E. Whitfield, analyst (*in* Knopf and Jonas, 1929b, p. 165)

B. Cockeysville metadolomite, locality unknown. E. A. Schneider, analyst (*in* Knopf and Jonas, 1929b, p. 165)

C. Cockeysville metadolomite, locality unknown. W. F. Hunt, analyst (*in* Knopf and Jonas, 1929b, p. 165)

9–21. Cockeysville metadolomite (9–13), calc-silicate rocks (17–21), and rocks of intermediate composition (14–16): partial analyses recalculated from modes 9–21 of Table 2. *See* Table 2 for locality and petrographic description.

D. Niagaran dolomite, Silurian, Illinois. D. F. Higgins, analyst (*in* Pettijohn, 1957, p. 418)

E. "Knox" dolomite, Cambro-Ordovician, Alabama, W. F. Hillebrand, analyst (*in* Pettijohn, 1957, p. 418)

F. Cherty dolomite, Niagaran group, Silurian, Ohio. D. Schaaf, analyst (*in* Pettijohn, 1957, p. 418)

G. Ideal dolomite

metadolomite that are found in some occurrences (Pl. 2, fig. 4), and the small pods and nests of tremolite and/or diopside clusters in quartz-rich metadolomite.

The mineral associations suggest that five over-all reactions may have operated during recrystallization of the dolomitic rocks:

(1) dolomite + 2 quartz $\rightleftharpoons$ diopside + 2 CO_2 (Weeks, 1956, p. 259)
(2) 5 dolomite + 8 quartz + water $\rightleftharpoons$ tremolite + 3 calcite + 2 CO_2 (Bowen, 1940, p. 239)
(3) 5 diopside + water + 3 CO_2 $\rightleftharpoons$ tremolite + 3 calcite + 2 quartz (after Bowen, 1940, p. 243)
(4) 3 diopside + water + 3 CO_2 $\rightleftharpoons$ talc + 3 calcite + 2 quartz
(5) 3 tremolite + 2 water + 6 CO_2 $\rightleftharpoons$ talc + 6 calcite + 4 quartz.

Because examples of progressive metamorphism are not present in the Cockeysville, it is difficult to substantiate these reactions except by inference. Reactions (1) and (2) are inferred from the presence of calcite aureoles around tremolites and partially tremolitized diopsides, yet not adjacent to fresh diopsides. Reaction (3) is likely to have occurred because of the common association of diopside, tremolite, calcite, and quartz in textural relations which indicate that the last three are alteration products from diopside. The two talc reactions, (4) and (5), are based on the obvious alteration of both tremolite and diopside to felts of talc, calcite, and quartz.

Whether or not stoichiometric amounts of the reacting minerals—reactions (1) and (2)—were present in the dolomitic sediments is uncertain. In many places it is clear that if porphyroblastic growth did proceed according to these reactions, considerable transfer of material must have accompanied the recrystallization; the dolomite/quartz ratio necessary to drive reactions (1) and (2) to completion would have been about 1/2, whereas the usual ratio in the metadolomites is about 8/1 or more. Moreover, if a rock such as that analyzed in mode 21 of Table 2 (*see* Pl. 2, fig. 3) recrystallized from a sediment according to reaction (1), silica must have been added at the sites of recrystallization; about 65 per cent by weight of quartz is required to convert a pure dolomite-quartz sediment into a pure diopside rock by this reaction, yet the calc-silicate rock in this case is devoid of dolomite and contains more than 55 per cent quartz.

Recrystallization to metadolomite and to calc-silicate marble does not appear to have made significant differences in CaO/MgO ratios (Table 3, analyses A–C, 9–21), as studies of carbonate rocks in the Grenville series have also shown (Engel and Engel, 1953); during formation of the calc-silicates, chemical changes other than CO_2 loss and SiO_2 enrichment seem to have been rather local and probably of limited extent.

Two aspects of the petrology of the calc-silicate rocks seem particularly interesting. First is the evident contemporaneity of tremolite and diopside in places. Second is the occurrence of apparently retrograde paragenetic sequences: diopside altering to tremolite, diopside to talc, and tremolite to talc; in a few cases all three alterations occur in one thin section. Reversals of these sequences have not been noted in the calc-silicate marbles, however. Such alterations might have resulted from (1) a decrease in rock pressure at constant temperature or a decrease in temperature at constant pressure (Bowen, 1940; Tilley, 1948); (2) differences in reaction rates under either of the conditions just suggested; or (3) local variations in the amounts and partial pressures of water (Yoder, 1952) and/or carbon dioxide. However, appreciable variations in temperature or total rock pressure at a given time within rock volumes of the order of a few cubic inches are difficult to imagine. In rocks under high confining pressure and consequently having low permeabilities, local variations in CO_2 pressure and H_2O pressure might have existed which impelled the different alterations. In many places metadolomites contain only scattered silicate porphyroblasts, and these porphyroblasts are fringed by rather sharply defined aureoles rich in calcite or poor in quartz; these features seem to support the idea of poor fluid transmissibility and local partial pressure gradients.

Calcite Marble

Introduction.—One of the most intriguing petrologic problems in the Cockeysville formations concerns the occurrence and origin of calcite marble. This marble occurs in layers, attenuated lenses, thick and partly discordant lenses, podlike masses, plugs, thin irregular dikes, and small patches (Figs. 6, 7; Pl. 1, figs. 1, 3). Generally the layers or discordant masses are thin; few exceed 3–5 feet in thickness, and the average thickness of layers is about 5–20

cm. Two areas, however, one near Texas, Maryland, and the other about 1 mile east of Reisterstown, Maryland, are underlain by units of calcite marble 50 feet thick or more.

Calcite marble is most abundant in association with metadolomite; it is moderately abundant in sequences of calc-schist (Pl. 2, fig. 1) and in a few exposures occurs in laterally gradational relationship with layers of calc-gneiss.

The calcite marble appears to have originated in more than one way. Irregular masses formed in part by replacing adjacent rocks, but some evidently began to form from limestone and eventually dilated and also replaced adjoining relatively calcite-poor rocks. Some irregular masses formed in part during the dissociation of dolomite in rocks they replaced; major products of dedolomitization in such cases appear to have been calcite and phlogopite. Possibly some layered calcite marble formed during the differentiation of recrystallizing argillaceous limestone (calc-schist) or quartzose limestone (calc-gneiss). Although much of the layered calcite marble appears to have been syntectonic, many of the discordant masses clearly formed during a late tectonic or post-tectonic stage in the metamorphism.

Petrography.—Several properties generally characterize the calcite marble regardless of its occurrence or form:

(1) The marble is medium- or coarse-grained and pure white to bluish or grayish white where fresh; it weathers to massive, gray, bosslike outcrops of distinctive appearance. It generally consists of 90 per cent or more $CaCO_3$ and, locally, as in an operating quarry at Texas, Maryland, contains more than 99 per cent $CaCO_3$ (James Campbell, 1955, personal communication).

(2) The marble is almost invariably devoid of dolomite (the mineral), even where closely associated with metadolomite (Table 2, modes 22–25).

(3) As a rule the calcite marble is distinctly coarser-grained than other marble in the formation; grain size ranges between about 0.5 mm and 10 cm and averages about 1–3 cm. Marked lateral and vertical changes in grain size and fabric are common, in many places within a single outcrop a few feet long.

(4) Mineralogically, the calcite marble closely resembles the rocks it is associated with, as indicated in Table 4 and detailed in Table 2. (*Compare* modes 4–5 with modes 22–25.) The resemblance is reflected in number and species of minerals and even in the optical properties of two particular minerals, tourmaline and phlogopite; for example, calcite marble interlayered with richly micaceous layers in calc-schist contains a dark-brown Fe-rich phlogopite, whereas the phlogopite in marble associated with metadolomite is a pale Mg-rich variety (*e.g.*, X/Y = colorless, Z = pale yellowish brown; biaxial (−), 2V = 5°–7°; $n_x = 1.595 \pm 0.002$, $n_y = 1.592 \pm 0.002$), which is optically similar to that in the metadolomite.

Characteristic of the calcite marble are concentrations of coarse minerals which, like the mineral constituents disseminated through this marble, tend to vary according to the mineralogy of associated marbles; thus muscovite and microcline are found only in calcite marble that occurs in calc-schists, and tremolite and diopside, both of which have a porphyroblastic habit in metadolomite, occur as large isolated porphyroblasts only in calcite marble associated with metadolomite.

Other properties of calcite marble in the Cockeysville show a relation to the form in which the marble occurs and are therefore discussed under separate headings.

DISCORDANT MASSES: Features of the discordant masses are summarized in Table 4 and illustrated diagrammatically in Figure 7. The characteristics which seem to bear most directly on petrogenetic interpretation are the irregular shapes of the lenses, the locally deflected and locally transected country rocks, the isotropic fabric within discordant masses, and the inclusions of associated rocks (Fig. 7D). Because of their fabric, which generally contrasts sharply with the strongly directional fabric of enclosing rocks, these discordant masses appear to have been of late tectonic or post-tectonic origin. The relics, as well as the crosscutting relations and gradational borders (Fig. 7D), indicate that in part the calcite marble formed at the expense of enclosing rocks. One large lens (Fig. 7A) may have begun recrystallizing from rather pure limestone, however; it contains a thin, wispy inclusion (relic?) of white, microcrystalline limestone (?), a rock unknown anywhere else in the area mapped.

Most of the irregular lensoid masses (Fig. 7A, B, C) show pinch-and-swell structure. By analogy with a genetic interpretation of structurally similar granitic pegmatites (Ramberg, 1952, p. 252, 256), these masses may owe their shapes to dilation of the enclosing rocks. This interpretation, if correct, would explain the way in which foliation of adjacent rocks is not only transected but locally deflected around irregularities in the borders of these lenses. An alternative interpretation, that the deflected foliation is due not to dilation but to differential movement of adjacent rocks along

the lenses, seems weakened by the directionless fabric in the lenses, which strongly suggests crystallization in an essentially static environment.

mica-rich layers. In general, the thinner layers are mineralogically quite homogeneous, but in quarries at Texas a thick mass of calcite marble

TABLE 4.—COMPARISON OF FEATURES OF CALCITE MARBLE LENSES AND OTHER DISCORDANT BODIES FOUND IN METADOLOMITE AND IN CALC-SCHIST

Features	Calcite marble associated with	
	Metadolomite	Calc-Schist
Form; contact relations	Irregular lenses, dikes, plug-shaped offshoots; borders irregular, contacts sharp or gradational, foliation of adjacent rocks deflected around or replaced by protrusions of calcite marble; border concentrations of coarse phlogopite (locally with tremolite diopside quartz)	Irregular lenses; borders irregular, contacts sharp or gradational, foliation of adjacent rocks deflected or cut off by protrusions of calcite marble; no conspicuous concentrations of silicate minerals along borders
Texture and fabric	Very coarse-grained; crystals up to 6–10 cm long; fabric isotropic	Very coarse-grained; crystals up to about 8 cm long; fabric isotropic
Mineralogy	Calcite Quartz Mg-phlogopite Mg-tourmaline Pyrite (Rarely sphene, apatite)	Calcite Quartz Fe-phlogopite Muscovite Fe-tourmaline Pyrite Graphite Microcline Plagioclase Sphene Apatite Biotite (rare)
Mineral zoning	Common; quartz and tourmaline concentrated near borders; phlogopite concentrated at borders	Rare; tourmaline and pyrite locally concentrated near borders
Other	Relics of metadolomite; relic of limestone (one example known)	Rare; one probable relic of calc-schist known

LAYERED CALCITE MARBLE: In contrast to the discordant masses, layers of calcite marble generally possess a strongly directional fabric, except locally in the crests and troughs of minor folds. The layers rarely show mineral zoning; phlogopite concentrations occur along some contacts with metadolomite but as a rule are discontinuous or lacking. Individual layers commonly persist with uniform thickness along the length of an outcrop, but many layers, particularly those associated with calc-schist, pinch and swell, bifurcate, and intergrade with

contains abundant remnants of metadolomite and scattered, isolated remnants or segregations (?) of metaquartzite. Some of the metadolomite remnants are crumpled and boudined, show frayed and gradational margins, and appear to have been first folded and then partially replaced by calcite marble. Many of these relics are bordered by thick concentrations of coarse phlogopite (Pl. 1, fig. 3).

Mineralogically most of the layered calcite marbles resemble the discordant masses of marble. At Texas, Maryland, however, the

calcite marble contains an unusually large assemblage of at least 22 minerals, most of which occur as segregations 1–70 cm in maximum dimension. Levey (1946, p. 274–275) identified fuchsite, purple fluorite, galena, sphalerite, rutile, talc, green diopside, margarite, molybdenite, wollastonite, and chrysotile in calcite marble exposed in a quarry operated by Harry T. Campbell Sons and Company at Texas. The writer has also noted Mg-tourmaline, Mg-phlogopite, sericite, chlorite, tremolite, grayish-white diopside, sphene, apatite, scapolite, pyrite, chalcopyrite, pyrrhotite, and limonite.

Calcite marble associated with metadolomite commonly contains isolated porphyroblasts of tremolite and diopside and encloses clusters of coarse phlogopite similar in size and optical properties to phlogopite that borders remnants of metadolomite.

OTHER OCCURRENCES OF CALCITE MARBLE: Varieties of metadolomite that are rich in calcite and phlogopite commonly contain small patches of calcite rimmed by coarse phlogopite. Like the mica in isolated clusters, this phlogopite optically resembles that in the enclosing rocks. Thickness of the phlogopite rim tends to vary with the size of the calcite patch. Mica-rich borders such as these seem to characterize only the patches in metadolomite; calcite-rich patches in calc-schist generally lack such borders.

Calc-gneiss in the Cockeysville formation (Table 2, modes 7, 8) generally has a mottled appearance because of calcite-rich, phlogopite-rimmed patches. These patches show a variety of shapes and sizes that would seem to preclude the possibility that they were originally limestone fragments or biotic constituents, unless these were greatly distorted and enlarged during metamorphism. In one exposure at Texas, Maryland, unmottled calc-gneiss grades

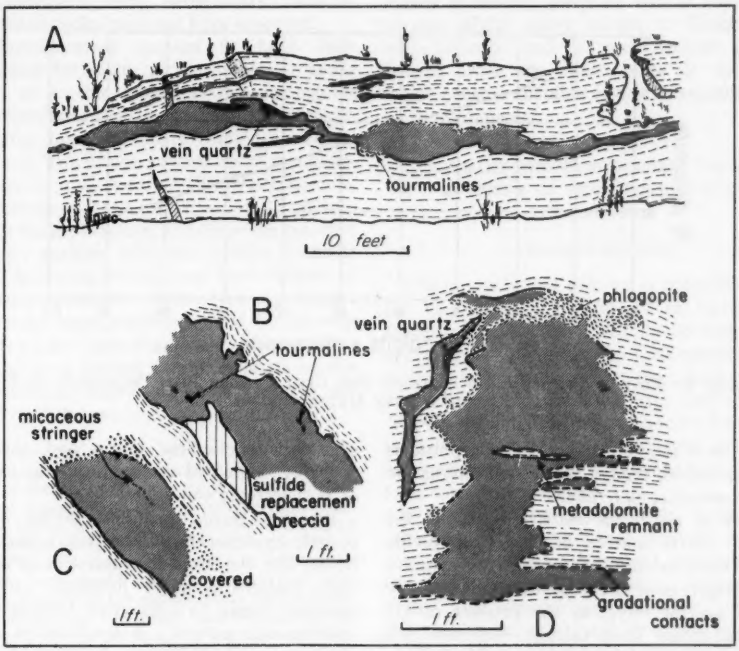

FIGURE 7.—PARTLY DISCORDANT BODIES OF CALCITE MARBLE

Marble is enclosed by metadolomite (A, D) or calc-schist (B, C) and contains inclusions interpreted as unreplaced remnants (in A toward right end of lens, not shown); possibly the micaceous stringer in C; and in D). Sulfide replacement breccia (B) composed largely of calcite and quartz in matrix of pyrite and chalcopyrite.

laterally into a mottled zone which in turn grades into coarse marble containing thin streaks of disseminated graphite and pyrite (?); distance of transition is about 5 feet. Whether this is a relict sedimentary facies pite, which can be interpreted as "impurities" that were either expelled to the margins of the calcite marble or left there as lag products. Finally, the discordant masses, though enclosed by foliated, layered marble, have es-

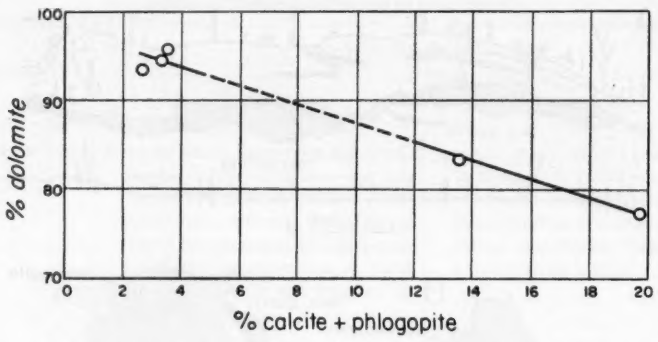

FIGURE 8.—PLOT OF PER CENT DOLOMITE VS. PER CENT CALCITE PLUS PHLOGOPITE IN FIVE REPRESENTATIVE METADOLOMITES

change or a consequence of metamorphism is not established, though the second alternative seems somewhat more likely.

Origin of the calcite marble.—Little of the layered calcite marble in the Cockeysville shows characteristics that are clearly diagnostic of its origin; most could be interpreted in any one of several ways, as the product of (1) recrystallization from calcium carbonate-rich limestone in limestone-dolomite and limestone-calcareous shale sequences; (2) syntectonic replacement by calcite; or (3) the syntectonic differentiation of originally homogeneous sediments into alternating calcite-rich and calcite-deficient layers.

Many of the discordant masses do display features that suggest reasonable genetic interpretations. The large, irregular lenses of calcite marble that occur in sequences of calc-schist and of metadolomite (Fig. 7) clearly formed in part by replacement: protrusions of these lenses transect as well as deflect adjacent rocks, contain indistinct, remnantlike inclusions of these rocks (at two localities), and—where associated with metadolomite—locally contain clusters of coarse magnesian phlogopite and isolated porphyroblasts of tremolite and diopside that are typical of the metadolomite. Moreover, calcite marble in these masses grades imperceptibly into metadolomite or is fringed by thick concentrations of silicates, especially phlogosentially directionless fabric and therefore probably originated under static late tectonic or post-tectonic conditions.

Whether these discordant bodies formed entirely by replacement, however, is uncertain. Some, like the large irregular lens (Fig. 7A) that contains a small limestone inclusion, probably began to form from limestone and subsequently grew by a combination of replacement and dilation(?). Irregular dikes of calcite marble with gradational contacts and inclusions of wall rock testify to the ability of such newly crystallizing marble to digest other rocks.

Relations in other regions suggest that some calcite marble in the Cockeysville is a "purified" end product of the metamorphism of impure, quartzose, moderately magnesian limestone. Normally, calc-gneiss occurs as the interpreted metamorphic equivalent of such limestone (Table 2, modes 7, 8), but in places calc-gneiss grades through calcite-mottled and streaked marble into white, coarsely crystalline calcite marble. This kind of transition resembles cases described by Bain (1934) from Vermont, in which dark, organic, and aphanitic limestone grades regionally into calcite marble through calcite-mottled, partially recrystallized limestone. Near Bancroft, Ontario, Chayes noted that Grenville limestone locally grades into coarse, pure calcite marble through transition zones of marble that contain "sill-like bands"

of relict chert or fine-grained limestone (Chayes, 1942, p. 457). Unfortunately, metamorphic intensity in the Cockeysville area was relatively high and appears to have been rather uniform, and transitions from sedimentary into recrystallized rocks have not been observed.

Dedolomitization appears to have been responsible for some calcite marble. Irregular masses of marble which marginally replace metadolomite evidently formed in this manner. The large mass of calcite marble at Texas, Maryland, also encloses remnants of metadolomite, shows gradational or silicate-rich borders, and contains isolated concentrations of phlogopite, tremolite, diopside, and other less common minerals; analogy with the smaller irregular masses indicates that it may have formed in part from dolomite. Other features suggest that calcite marble which formed in this way represents the end stage of a process that operated to a limited extent in much of the recrystallizing dolomite: These features are summarized below:

(1) Coarse-grained patches of calcite rimmed by coarse phlogopite are common in the metadolomites. Width of the phlogopite rim tends to vary directly with the size of the patch. The patches have directionless fabric and range in cross-sectional shape from circular to highly irregular and branchlike. If these patches represented recrystallized sedimentary features, they should logically display the same directional fabric as the metadolomite around them; in the absence of this fabric, and because of the mineralogy of the patches, the patches are interpreted as the results of dedolomitization, in which calcite and phlogopite formed as by-products from the dissociation of dolomite in the presence of water, potash, alumina, and silica.

(2) In five representative metadolomites for which modal analyses were run, an apparently straight-line inverse relationship exists between per cent of dolomite and per cent of calcite plus phlogopite (Fig. 8). This relationship suggests that the calcite and phlogopite may have formed in part as dolomite dissociated. Modal analyses recalculated in terms of chemical composition, which compare fairly closely with published chemical analyses of representative metadolomites (Table 3, analyses A–C, 9–13), show that the metadolomites are close to pure dolomite in composition; this tends to support the hypothesis that calcite and phlogopite in these marbles formed during the dissociation of dolomite. Texture, however, does not indicate whether or not the dolomite was earlier than its suggested by-products.

(3) Calcites in the metadolomites, in patches enclosed by metadolomite, and in calcite marble, are typically clouded with inclusions, whereas dolomite crystals are clear and essentially free of inclusions (Pl. 2, fig. 3). Tilley (1920, p. 452–453) considered that turbidity of calcite grains in this kind of occurrence indicated the formation of calcite by dissociation of dolomite. Negative support for this suggestion is the fact that calcites occurring in Cockeysville calc-schists, which contain little magnesium and are lacking in dolomite, are typically free of inclusions.

The group of features described above give reason to believe, therefore, that at least some of the calcite which occurs in Cockeysville metadolomite and in some calcite marble formed from the constituents of dolomite, which became unstable during recrystallization of the sediments.

Summary and Conclusions: Metamorphism of the Cockeysville Sediments

Structural Behavior

The intensity and pattern of deformation in the carbonate rocks appears to have been closely controlled by proximity to and shape of four gneiss domes in the Cockeysville area. This relation is inferred from the trends of cross joints, lineations, minor fold axes, and foliation (Figs. 3, 4) and also from a tendency for minor folds in the marble to change from predominantly flexure folds to predominantly flowage folds toward the domes.

Evidently the carbonate rocks transmitted only a part of the stress that produced regional deformation of the basement complex and Glenarm series near Baltimore; although the Setters and Wissahickon formations both display a systematic and mutually parallel fracture cleavage transecting the foliation, the carbonate rocks lack this cleavage (perhaps in part because of their relatively low mica content). Moreover, despite the extensive development of minor folds in the marbles, the upper and lower surfaces of the Cockeysville, judging from the surface configuration of their traces as inferred from outcrops and topographic expression, do not appear to be greatly complicated by minor folds; hence the minor folding is believed to have been largely intraformational.

Linear elements of the marbles generally lie parallel to *b*, the minor fold axes, and statistically parallel to the major fold axes (Fig. 4). Most of these lineations are consistently oriented only in minor folds that were produced mainly by bending rather than flowage; they are of five kinds: (1) axes of crinkle folds, (2) axes of wavelike undulations in the foliation, (3) long axes of boudined fragments, (4) long axes of tremolite and diopside porphyroblasts, and (5) strings of pyrite crystals. Vein quartz blebs locally lie in the foliation normal to *b*.

Recrystallization of the carbonate sediments was chiefly syntectonic, and only one *S* plane, the foliation, is prominently developed. Some discordant masses of coarse calcite marble probably formed during the last stages of deformation, however, and may in some cases have been post-tectonic.

Role of Metasomatism

Additive metasomatism appears to have been limited chiefly to narrow aureoles around pegmatites, and appreciable amounts of CO_2 must have been released during the formation of calc-silicate marble and calcite marble from dolomites, but several features suggest that the addition of material was local in scale and relatively negligible in determining the mineralogy of the marbles. The evidence is threefold:

(1) Scapolite is absent from all the rocks except calc-gneiss and some calc-schist (Table 2). At one locality its occurrence may be related to a nearby pegmatite, but elsewhere in the area such a relationship is not apparent, and the scapolite is a calcic variety that might have developed from carbonate sediments during normal regional metamorphism. Similarly, tourmaline and apatite, both of which are widely but sparsely distributed in the Cockeysville, occur in amounts such that their boron and phosphate could have been provided by the sediments themselves (Table 2).

(2) Chemical analyses (Table 3) indicate that metadolomites in the Cockeysville probably recrystallized from sediments that ranged from essentially pure dolomite to slightly argillaceous and calcareous dolomite, siliceous dolomite, or dolomitic chert. Recrystallization appears to have been accompanied by negligible changes in bulk composition except for the loss of CO_2 to a limited extent.

(3) Pegmatite intrusions, which are surrounded by narrow tourmaline-rich contact-metasomatic aureoles, are few and seem to be restricted largely to the upper and lower Cockeysville, close to formation contacts (Pl. 3). Lack of mineral gradients near these pegmatites indicates that their contact effects probably did not extend much more than a few inches to a few feet beyond their margins.

Metamorphic Intensity

As a group, the Cockeysville marbles can be placed arbitrarily somewhere in the lower amphibolite facies as defined by Eskola *et al.* (1939), perhaps near the boundary with the epidote amphibolite facies. According to a more recent facies classification (Fyfe, Turner, and Verhoogen, 1958, p. 199–237), the marbles would be assigned to the staurolite-quartz and sillimanite-almandine subfacies of the newly defined almandine amphibolite facies. These decisions concerning facies are based on the absence of chlorite from outcrops of the Cockeysville[4] and in the Wissahickon schists; the ubiquitous occurrence of phlogopite; the virtual absence of wollastonite; and the common occurrence of both tremolite and diopside.

Few minerals in the carbonate rocks appear to be reliable indices of metamorphic grade. Plagioclase, for example, has an average composition of about An 10–25 but ranges from An 4 (in a calc-schist) to An 84 (in a calcite marble); its composition seems to have been a function of bulk rock composition as much as temperature and rock pressure. Dolomite and quartz reacted locally with or without water to form tremolite or diopside, yet coexist in many places. Wollastonite has been reported at one locality, in calcite marble (?), but has not been noted elsewhere. Although calcite and quartz may be stable together throughout the pressure-temperature range of the amphibolite facies (Ramberg, 1952) and may coexist under P–T conditions of the granulite facies (Turner and Verhoogen, 1951, p. 475), Harker and Tuttle (1956, p. 249) have suggested that wollastonite may form at temperatures as low as 350° C.

The occurrence of diopside and tremolite may provide the best index of metamorphic grade in the Cockeysville; the two occur locally within a few inches of each other, and diopsides are commonly altered to tremolite. Ramberg (1952, p. 152) suggested that the conditions under which tremolite reacts with calcite and quartz to form diopside may be valid boundary conditions between carbonate rocks of the epidote amphibolite and the amphibolite facies.

Common mineral assemblages in the carbonate rocks and their associated noncarbonate rocks are the following:

Calcareous assemblages (Cockeysville):

- Calcite-quartz-phlogopite(-muscovite)-microcline-oligoclase
- Calcite-quartz-phlogopite
- Calcite-quartz-tremolite-diopside-graphite (-scapolite)
- Dolomite-calcite-quartz-phlogopite
- Dolomite-calcite-quartz-tremolite(-diopside)

[4] Small amounts of chlorite were noted in water-well cuttings of the Cockeysville, but chlorite has not been observed in outcrops of marble and is believed to be a superficial alteration product from phlogopite.

Diopside-quartz-calcite-tremolite(-talc)
Diopside-quartz(-tremolite)
Tremolite-diopside-calcite-quartz-dolomite-(-talc)

Basic assemblage (Wissahickon):

Andesine-epidote-hornblende

Pelitic assemblages (Setters, Wissahickon):

Quartz-graphite-phlogopite-muscovite-microcline
Quartz-microcline-biotite-oligoclase
Quartz-muscovite-biotite-oligoclase
Muscovite-biotite-quartz-oligoclase-garnet
Muscovite-biotite-quartz-oligoclase-kyanite-(-garnet-staurolite)

Despite the increase in intensity of deformation toward the gneiss domes, a corresponding increase in metamorphic grade is not apparent. Diopside and tremolite occur in about equal amounts in either quartz metadolomite or phlogopite-calcite metadolomite throughout the area. Calcite and quartz coexist in marble adjacent to and at considerable distances from the domes. Phlogopite remains unaltered in all the rocks regardless of their proximity to the domes. Calc-silicate marbles are developed chiefly in the southern half of the area, just north of the Towson and Chattalonee domes, but their occurrence seems to be related to composition of the sediments rather than to metamorphic intensity. The writer therefore concludes that metamorphic grade is essentially constant throughout the area of study.

References Cited

Bain, G. W., 1931, Flowage folding: Am. Jour. Sci., ser. 5, v. 22, p. 503–530

—— 1934, Calcite marble: Econ. Geology, v. 29, p. 121–139

Bowen, N. W., 1940, Progressive metamorphism of siliceous limestone and dolomite: Jour. Geology, v. 48, p. 225–274

Broedel, C. H., 1937, The structure of the gneiss domes near Baltimore, Maryland: Md. Geol. Survey Rept., v. 13, p. 149–187

Brooks, H. K., 1954, The rock and stone terms limestone and dolomite: Am. Jour. Sci. v. 452, p. 755–760

Chayes, F., 1942, Alkalic and carbonate intrusives near Bancroft, Ontario: Geol. Soc. America Bull., v. 53, p. 449–512

Cloos, E., 1946, Lineation, a critical review and annotated bibliography: Geol. Soc. America Mem. 18, 122 p.

—— 1948, Structures of basement rocks of Pennsylvania and Maryland and their effect on overlying structures (Abstract): Am. Assoc. Petroleum Geologists Bull., v. 32, p. 2162

Cloos, E., and Broedel, C. H., 1940, Geologic map of Howard County, Maryland: Md. Geol. Survey

Cloos, E., and Hietanen, A., 1941, Geology of the 'Martic overthrust' and the Glenarm series in Pennsylvania and Maryland: Geol. Soc. America Special Paper 35, 207 p.

Engel, A. E. J., and Engel, C. G., 1953, Compositional evolution of a major marble unit, Grenville series, northwest Adirondack Mountains, New York (Abstract): Geol. Soc. America Bull., v. 64, p. 1417–1418

Eskola, P., *et al.*, 1939, Die Entstehung der Gesteine: Berlin, Springer, 344 p.

Fyfe, W. S., Turner, F. J., and Verhoogen, J., 1958, Metamorphic reactions and metamorphic facies: Geol. Soc. America Mem. 73, 259 p.

Goldsmith, J. R., Graf, D. L., and Joensuu, O. I., 1955, The occurrence of magnesian calcites in nature: Geochim. et Cosmochim. Acta, v. 7, p. 212–250

Graf, D. L., and Goldsmith, J. R., 1955, Dolomite-magnesian calcite relations at elevated temperatures and CO_2 pressures: Geochim. et Cosmochim. Acta, v. 7, p. 109–129

Harker, R. I., and Tuttle, O. F., 1955, Studies in the system CaO-MgO-CO_2—Part 2, Limits of solid solution along the binary join $CaCO_3$-$MgCO_3$: Am. Jour. Sci., v. 253, p. 274–282

—— 1956, Experimental data on the P_{CO_2}-T curve for the reaction, calcite + quartz ⇌ wollastonite + carbon dioxide: Am. Jour. Sci., v. 254, p. 239–256

Knopf, E. B., and Jonas, A. I., 1923, Stratigraphy of the crystalline schists of Pennsylvania and Maryland: Am. Jour. Sci., ser. 5, v. 5, p. 40–62.

—— 1929a, Geologic map of Baltimore County, Maryland: Md. Geol. Survey

—— 1929b, Geology of the crystalline rocks: Md. Geol. Survey Baltimore County Rept., p. 97-199

Levey, H., 1946, Minerals of the H. T. Campbell quarry of Texas, Maryland: Rocks and Minerals, v. 21, p. 274–275

Mathews, W. H., and Miller, W. J., 1905, Cockeysville marble: Geol. Soc. America Bull., v. 16, p. 347–366

Pettijohn, F. J., 1957, Sedimentary rocks: 2d ed., N. Y., Harper and Brothers, 718 p.

Ramberg, H., 1952, The origin of metamorphic and metasomatic rocks: Chicago, Univ. Chicago Press, 315 p.

Rankama, K., and Sahama, Th. G., 1950, Geochemistry: Chicago, Univ. Chicago Press, 912 p.

Swartz, F. M., 1948, Trenton and sub-Trenton of outcrop areas in New York, Pennsylvania and Maryland: Am. Assoc. Petroleum Geologists Bull., v. 32, p. 1493–1595

Teall, J. J. H., 1903, On dedolomitization: Geol. Mag., v. 10, decade 4, p. 513–514

Tilley, C. E., 1920, The metamorphism of the Precambrian dolomites of southern Eyre Peninsula, South Australia: Geol. Mag., v. 57, p. 449–462, 492–500

—— 1948, Earlier stages in the metamorphism of siliceous limestones and dolomites: Mineralog. Mag., v. 28, p. 272–276

Turner, F. J., and Verhoogen, J., 1951, Igneous and metamorphic petrology: N. Y., McGraw-Hill Book Co., 602 p.

Weeks, W. F., 1956, A thermochemical study of equilibrium relations during metamorphism of siliceous carbonate rocks: Jour. Geology, v. 64, p. 245–270

Wasserburg, G. J., Pettijohn, F. J., and Lipson, J., 1957, A^{40}/K^{40} ages of micas and feldspars from the Glenarm series near Baltimore, Maryland: Science, v. 126, p. 355–356

Williams, G. H., 1892, Geology of Baltimore, Maryland, and its vicinity: Am. Inst. Mining and Eng. Guidebook, p. 77–124

Winchell, A. N., 1933, Elements of optical mineralogy—*Part 2:* Descriptions of minerals: 2d ed., N. Y., John Wiley & Sons, 459 p.

Yoder, H. S., Jr., 1952, The MgO-Al_2O_3-SiO_2-H_2O system and the related metamorphic facies: Am. Jour. Sci., Bowen Volume, pt. 2, p. 569–627

THE OHIO OIL CO., P.O. BOX 269, LITTLETON, COLO.

MANUSCRIPT RECEIVED BY THE SECRETARY OF THE SOCIETY, NOVEMBER 17, 1958

BULLETIN OF THE GEOLOGICAL SOCIETY OF AMERICA
VOL. 71, PP. 1053-1066, 5 FIGS. JULY 1960

BIOGEOCHEMICAL PROSPECTING FOR MANGANESE IN NORTHEAST TENNESSEE

By F. Donald Bloss and Robert L. Steiner

Abstract

Samples of mature leaves and second-year twigs were collected from 36 chestnut oaks (*Quercus prinus L.*) growing above two areas of subsurface manganese mineralization in northeast Tennessee. Of the metals determined to be most abundant in ore specimens and concentrates from the general area (*i.e.*, manganese, iron, barium, cobalt, and nickel in decreasing order of abundance), all but cobalt were readily determinable spectrochemically in the ashes of leaves and twigs. The average values (weight per cent) for the tree samples collected as well as for soil specimens from the 1-foot depth at each tree locale were:

	Mn	Ba	Fe	Ni
Twig ash	3.8	1.01	0.24	0.017
Leaf ash	3.8	0.36	0.35	0.014
Nearby soil	0.29	0.04	6.9	<0.001

Two areas were sampled; one, the Hutchens property, was later developed into an economic ore body. The manganese bodies of the second, the Rominger property, proved to be too low in over-all concentration to be of economic value. Significantly, the samples from the Hutchens area more frequently exceeded the average values for manganese barium, and nickel given in the preceding table than did those from the Rominger area. Although nickel was not detectable in the surface soil, the appearance of nickel in excess of average in chestnut-oak leaf and twig ash was confined almost exclusively to the Hutchens area, particularly to the trees most closely overlying the subsurface manganese ore body. Nickel in chestnut-oak leaf and twig ash thus seemed to be a fairly reliable guide to ore, apparently acting as a pathfinder for manganese.

CONTENTS

TEXT

	Page
Introduction	1054
Acknowledgments	1054
Experimental methods	1054
Sampling methods	1054
Preparation of samples	1054
Methods of spectrographic analyses	1055
Ore composition	1056
Analyses of soil and trees overlying manganese bodies	1060
Comparison of tracts sampled	1060
Distribution of manganese	1061
Distribution of barium	1061
Distribution of nickel	1061
Distribution of cobalt	1065
Distribution of iron	1065
Background values for chestnut-oak leaves	1065
Conclusions	1065
References cited	1065

ILLUSTRATIONS

Figure	Page
1. Map showing location of the Blue Spring mine area, Tennessee	1055
2. Approximate thickness, depth below surface, and areal distribution (as interpreted from drill-hole data) of the subsurface manganese bodies of the Rominger tract (upper diagram) and the Hutchens tract (lower diagram)	1057
3. Areal distribution of the manganese contents of soil, leaf ash, and twig ash with respect to the subsurface manganese bodies (ruled) of the Rominger tract (up-	

Figure Page

per diagram) and of the Hutchens tract (lower diagram) 1062
4. Areal distribution of the barium contents of soil, leaf ash, and twig ash with respect to the subsurface manganese bodies (ruled) of the Rominger tract (upper diagram) and of the Hutchens tract (lower diagram) 1063
5. Areal distribution of the nickel contents of leaf and twig ash with respect to the subsurface manganese bodies (ruled) of the Rominger tract (upper diagram) and of the Hutchens tract (lower diagram) 1064

TABLES

Table Page

1. Spectrographic conditions during analyses 1055
2. Wave lengths of the emission lines used in determining the elements present 1056
3. Ore analyses 1056
4. Metal content of chestnut oaks and soils in and around areas of manganese mineralization 1058
5. Location and metal contents of six chestnut oaks far from area of manganese mineralization 1061

Introduction

Prospecting for manganese in northeastern Tennessee has been limited for the most part to those areas of the residual clay overlying the Shady dolomite (Cambrian) where "float ore" is present near the surface. The methods used (test pits, tunnels, and auger or churn drilling) are relatively slow and expensive and, consequently, large areas remain unprospected. Furthermore, prospecting by surface indications is not feasible where the residual clay of the Shady dolomite is veneered by gravel. A biogeochemical method, particularly if deep-rooted plants were involved, therefore, appeared to be a possible method of prospecting for manganese in the area.

An investigation was therefore conducted of the metal contents of the leaf and twig ash of the chestnut oak (*Quercus prinus L.*), one of the few deep-rooted trees which is well distributed areally in Carter and Johnson counties, sites of Tennessee's principal manganese districts. Chestnut-oak leaf and twig samples (as well as soil samples for comparison) were collected from two adjacent mineralized areas in the general vicinity of Blue Spring mine (Fig. 1).

Acknowledgments

The work reported herein was made possible by the interest and co-operation of Dr. Isabel H. Tipton of the Physics Department of the University of Tennessee. Dr. R. E. Shanks of the Botany Department of the University of Tennessee gave valuable assistance in tree identification. Mr. R. U. Butler of the Virginia Iron, Coal and Coke Company generously made available maps and ore samples. Ore samples were analyzed for iron and manganese by Mr. Zaney Taylor and Mrs. Rhoda Taylor in the laboratory of the Virginia Iron, Coal and Coke Company. Mr. Stuart Maher and Mr. C. P. Findlayson of the Tennessee Division of Geology kindly collected the leaf samples reported on in Table 5.

The writers wish to thank Prof. H. E. Hawkes of the Division of Mineral Technology of the University of California and Prof. Harry V. Warren and Dr. R. E. Delavault of the University of British Columbia for reviewing the manuscript and offering constructive suggestions. All opinions expressed, however, are the responsibilities of the writers.

Experimental Methods

Sampling Methods

Mature leaves and 2-year-old twigs were collected from the peripheral branches of the lowest large limb of those chestnut oaks having a base diameter between 1 and 2 feet. Leaf maturity was determined by leaf size as compared with the largest leaves of the branch. Twig samples were cut from a section of the twig between the first- and second-year growth scars. Within 5 feet of each tree sampled, soil samples were collected (when possible) from the 1-foot depth.

Samples of milled ore were kindly provided by the Virginia Iron, Coal and Coke Company. In addition, one sample of "hard" manganese ore was collected from the Blue Spring Mine.

Preparation of Samples

The leaf and twig samples were washed in distilled water and then dried in fused silica dishes for 16 hours at 110° C. The dried samples were then ashed in a muffle furnace at 450° C. for 20 hours. The soil and ore samples were dried and crushed and sieved to isolate the −100 mesh fraction.

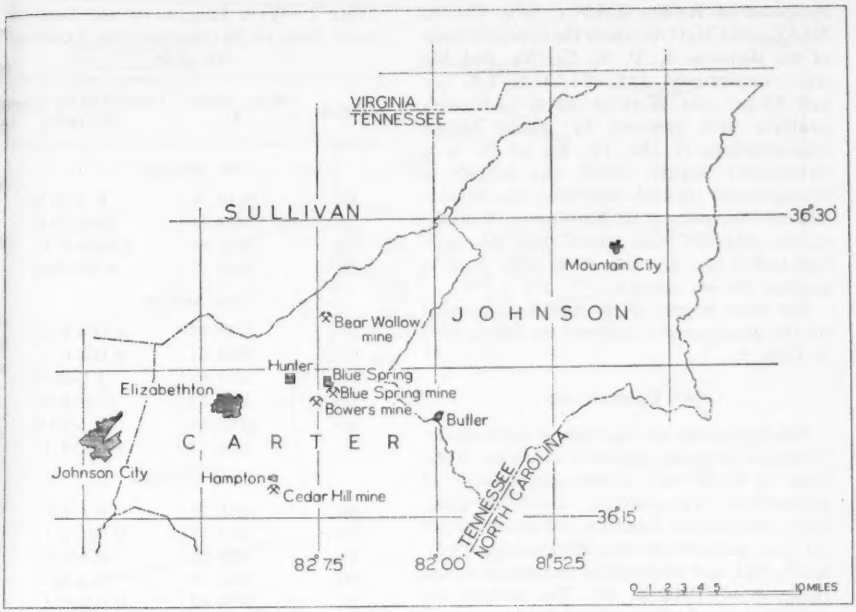

FIGURE 1.—MAP SHOWING LOCATION OF THE BLUE SPRING MINE AREA, TENNESSEE

TABLE 1.—SPECTROGRAPHIC CONDITIONS DURING ANALYSES

	Ore samples	Soil samples	Leaf and twig samples
Sample electrode*	3/16" by 1½" with cavity 0.1470" diameter and 2 mm deep	Same	Same
Counter electrode	⅛" by 1½" flat end	Same	Same
Sample charge	10 mg of a mixture containing 2 parts ore and 8 parts graphite powder	4 mg soil mixed with 16 mg graphite powder	5-mg sample mixed with 10 mg graphite powder†
Slit width	0.02 mm	0.02 mm	0.02 mm
Excitation	10 amp D.C.	10 amp D.C.	5 amp D.C.
Burning time	15 sec.	40 sec.	To completion (60–70 sec.)
Film	Eastman I-L	Eastman I-L	Eastman SA-2

* Electrodes and graphite powder were National Special Spectroscopic Graphite
† Graphite powder contained 600 ppm of Pd as the internal standard

Methods of Spectrographic Analyses

A 1.5-m grating Bausch and Lomb spectrograph having a dispersion of 15 Å/mm in the first order and 7.5 Å/mm in the second order was used in conjunction with a custom-built direct-current power supply of 300 volts potential. The sample electrode was arced (as the anode) with the center portion of the 8-mm arc gap focused on the grating. Spectrographic conditions are summarized in Table 1.

Working curves for the leaf and twig analyses were prepared by adding known concentrations of Mn, Ba, and Ni to a synthetic-plant matrix

composed of K_2CO_3, KH_2PO_4, SiO_2, $CaCO_3$, Na_2CO_3, and MgO, in which the concentrations of the elements K, P, Si, Ca, Na, and Mg were, respectively, 23.9, 4.1, 18.0, 7.2, 3.5, and 3.0 per cent. Working curves for the soil analyses were prepared by adding known concentrations of Mn, Fe, Ba, or Ni to a natural-clay matrix, which was actually a homogeneous residual clay from the Mascot dolomite formation of the Knox group. Working curves prepared from "Spex" mix standards (Mitteldorf and Landon, 1956) were used to analyze the ore samples.

The wave lengths of the emission lines used for the spectrographic analyses are summarized in Table 2.

Table 2.—Wave Lengths of the Emission Lines Used in Determining the Elements Present

Element	Wave length Å	Concentration range (Per cent)
	Ore Analysis	
Ba	6110.78	0.1–10.0
Co	3453.51	0.05–10.0
Li	6707.84	0.0005–0.1
Ni	3414.77	0.05–10.0
	Soil Analysis	
Ba	6141.72	0.004–0.4
Co	3453.51	0.004–0.4
Fe	5455.61	1.0–20.0
Mn	4823.52	0.01–1.0
Mn	6016.64	0.1–10.0
Ni	3414.77	0.001–0.1
	Plant Analysis	
Ba	3071.59	0.1–4.0
Co	3453.51	0.001–0.1
Fe	3024.03	0.1–4.0
Mn	3022.75	0.4–10.0
Ni	3050.82	0.001–0.1

Ore Composition

The manganese ore minerals of northeastern Tennessee generally consist of (1) dense, hard, black or bluish-black nodules (or veinlets) of psilomelane, cryptomelane, occasional pyrolusite, and in some localities, hollandite and/or (2) soft, noncoherent concentrations of pyrolusite, wad, and unidentified manganese oxides (King *et al.*, 1944, p. 49). The nodules are embedded (and the soft varieties may be

Table 3.—Ore Analyses

	% Mn*	% Fe	% Ba	% Co	% Ni	% Li	Description†
a	38.3	14.9	1.7	.16	<.05	.025	Blue Spring Mine 3-4-57 No. 1
b	34.4	21.7	1.3	.10	<.05	.018	Blue Spring Mine 3-4-57 No. 2
c	40.7	7.2	0.8	.11	<.05	.010	Blue Spring Mine 2-27-57
d	40.8	10.0	1.5	.18	<.05	.016	Blue Spring Mine 2-26-57
e	52.7	2.0	0.16	.30	.10	.075	Blue Spring Mine solid chunk
f	36.0	8.3	0.95	.18	.08	.025	Blue Spring Mine hand washed
g	38.6	4.2	1.1	.20	.06	.005	Blue Spring Mine fines (from f)
h	38.0	14.3	1.5	.10	<.05	.004	Bowers Mine 6-5-56 No. 1
i	42.3	4.7	1.2	.10	<.05	.008	Bowers Mine 6-5-56 No. 2
j	39.2	13.6	1.0	.05	<.05	.002	Bear Wallow Mine 7-11-57
k	41.6	9.0	1.6	.08	<.05	.001	Bear Wallow Mine 2-12-57
l	42.3	9.1	1.8	.09	<.05	.014	Cedar Hill Mine 10-5-56 No. 1
m	40.8	11.5	1.4	.09	<.05	.011	Cedar Hill Mine 10-5-56 No. 2
n	44.6	9.4	0.5	.06	<.05	.0005	Cedar Hill Mine 12-6-56
o	42.4	9.1	1.0	.09	<.05	.010	Cedar Hill Mine 10-6-56
p	37.2	8.5	0.6	.08	<.05	.0005	Cate Property—Hampton
q	40.6	8.9	1.8	.10	<.05	.006	Car** No. 16313 3-21-57
r	40.2	10.1	1.2	.09	<.05	.011	Car** No. 16135 4-12-57
Av....	40.6	10.0	1.2	.12	<.055	.013	

* Mn and Fe determinations by Zaney Taylor and Rhoda Taylor of the Virginia Iron, Coal And Coke Company (except for samples e, f, and g)

† Mine locations shown in Figure 1

** Composite sample from railroad freight car

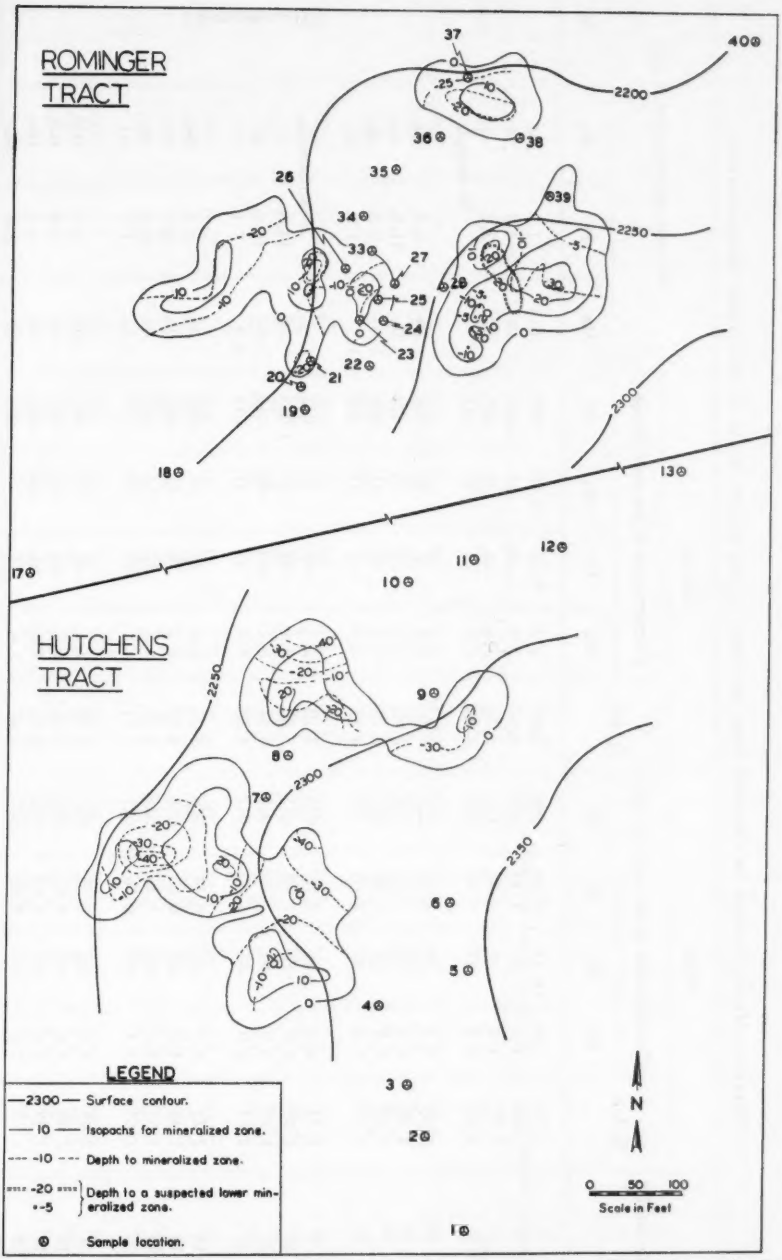

FIGURE 2.—APPROXIMATE THICKNESS, DEPTH BELOW SURFACE, AND AREAL DISTRIBUTION (AS INTERPRETED FROM DRILL-HOLE DATA) OF THE SUBSURFACE MANGANESE BODIES OF THE ROMINGER TRACT (UPPER DIAGRAM) AND THE HUTCHENS TRACT (LOWER DIAGRAM)
Locations of chestnut oaks sampled are marked by circles.

TABLE 4.—METAL CONTENT OF CHESTNUT OAKS AND SOILS IN AND AROUND AREAS OF MANGANESE MINERALIZATION

Sample locale*	Twigs					Leaves					Per cent concentration in soils			
	% Ash	Concentration in per cent (in ash)				% Ash	Concentration in per cent (in ash)							
		Mn	Fe	Ba	Ni		Mn	Fe	Ba	Ni	Mn	Fe	Ba	Ni
1	2.51	1.6	0.15	0.80	.004	5.95	2.3	0.34	0.46	.007	.015	2.3	.04	
2	2.16	4.6	.26	1.10	.015	4.87	3.4	.32	.22	.010	.01	3.3	.11	
3	1.97	4.4	.15	0.80	.011	5.54	3.4	.23	.21	.005	.02	3.3	.11	
4	1.81	5.3	.55	1.50	.031	6.85	4.1	.43	.44	.024	No Sample			
5	2.20	7.3	.22	0.70	.025	5.18	4.8	.32	.29	.024	.26	9.8	.04	
6	1.86	6.4	.25	1.70	.036	5.30	4.9	.20	.48	.029	1.0	11.0	.14	
7	1.94	5.3	.22	2.30	.037	5.78	5.2	.42	.51	.036	1.0	9.8	.08	
8	2.12	5.0	.24	1.60	.021	4.85	4.7	.43	.45	.033	1.1	11.0	.06	
9	1.54	4.4	.38	1.70	.035	3.10	3.8	.60	.40	.032	No Sample			Less than 0.001
10	1.60	9.0	.47	1.90	.075	5.82	5.4	.30	.52	.035	.78	14.0	.07	
11	1.25	6.9	.90	2.30	.062	4.64	5.4	.36	.86	.040	.94	14.0	.07	
12	2.52	5.0	.30	1.00	.012	5.38	5.0	.29	.41	.016	1.0	7.1	.07	
13	2.22	4.5	.16	0.74	.008	6.21	4.6	.25	.26	.008	.04	3.7	.04	
14	1.46	4.2	.24	0.65	.012	4.75	4.2	.28	.15	.006	.26	6.7	.06	
15	1.65	5.4	.36	1.15	.030	3.76	4.6	.37	.33	.029	.09	8.5	.01	
16	2.63	3.5	.13	0.76	.011	4.44	4.4	.26	.47	.017	.26	5.9	.04	
17	2.98	1.4	.16	0.55	.007	5.70	2.1	.22	.24	.007	.01	4.2	.028	
18	2.60	3.0	.19	0.62	.016	5.78	3.0	.25	.28	.012	.01	2.4	.029	
19	2.49	3.8	.26	0.62	.014	6.12	3.8	.62	.28	.010	.31	3.3	.060	
20	1.75	2.9	.16	0.98	.007	3.40	3.6	.34	.25	.004	.02	3.0	.027	
21	1.28	3.0	.19	0.90	.014	4.11	3.6	.32	.32	.010	.12	4.6	.033	
22	1.96	3.6	.35	1.10	.020	4.55	3.4	.41	.38	.007	.48	6.9	.038	

21	1.28	3.0	.19	0.90	.014	4.11	3.6	.32	.32	.010	.12	4.6	.033	
22	1.96	3.6	.35	1.10	.020	4.55	3.4	.41	.38	.007	.48	6.9	.038	
23	1.82	4.2	.18	1.05	.013	4.21	3.9	.47	.25	.013	.25	7.6	.020	
24	3.08	3.0	.19	0.84	.003	5.05	3.8	.42	.50	.008	.11	6.6	.023	
25	2.04	2.7	.26	0.60	.014	5.50	3.6	.48	.42	.009	.12	10.2	.025	
26	2.73	3.3	.21	0.60	.007	5.80	4.0	.24	.41	.008	.19	8.2	.014	
27	2.24	1.7	.20	0.94	.013	5.25	4.5	.31	.36	.010	.14	11.2	.014	
28	2.23	3.2	.18	0.72	.007	4.28	3.7	.45	.30	.008	.17	15.0	.016	
33	2.30	2.6	.12	0.66	.005	5.78	3.7	.21	.30	.008	.05	6.0	.017	
34	2.58	3.3	.19	0.66	.004	5.00	3.4	.28	.27	.007	.04	4.3	.022	
35	2.38	2.6	.13	0.80	.009	4.20	2.6	.25	.23	.006	.07	4.5	.028	
36	2.06	2.2	.15	0.70	.004	4.02	3.0	.44	.44	.003	.03	5.2	.034	
37	1.68	1.7	.20	0.95	.006	3.25	1.7	.36	.25	.007	.03	4.7	.013	
38	2.58	1.8	.13	0.92	.005	5.68	1.7	.24	.44	.007	.10	4.3	.016	
39	2.36	3.2	.14	0.80	.012	6.31	4.3	.47	.29	.009	.60	9.8	.020	
40	3.10	2.3	.19	0.75	.005	5.66	2.0	.38	.28	.005	.12	3.6	.025	
Average.....	2.16	3.8	.24	1.01	.017	5.06	3.8	.35	.36	.014	.29	6.9	.04	<0.001

Less than 0.001

* Sample locales 1–13, 17–28, 33–40 shown in Figures 2–5

dispersed) in a waxy, yellow, structureless clay which is locally called "buckfat". Limonite is a common associate of the manganese minerals and is often intimately intermixed.

Chemical and spectrochemical analyses of ore minerals and ore concentrates (Table 3) indicate manganese and iron are the major elements present. Barium is next in abundance. Of the minor elements, cobalt, nickel, and lithium are most abundant. Of these, cobalt is present in the greatest amounts, being determinable in all 18 samples. Nickel was determinable in only 3 samples.

Unfortunately, few analyses of the minor elements in the manganese ore of Northeast Tennessee are available for comparison. King *et al.* (1944) report cobalt in manganese ore concentrates from the Butler district (Proffitt prospect), the Shady Valley district (Scott prospect), the Stoney Creek district (Blue Spring mine), and the Embreeville district (Bumpass Cove). In this last locale, their analyses of the hard manganese oxides (p. 263–264) showed 0.14 per cent cobalt and 0.13 per cent nickel. At the Blue Spring mine the present writers found, in addition to cobalt, determinable amounts of nickel in three of seven samples (Table 3). The writers suspect that cobalt and, to a lesser extent, nickel occur more frequently in the manganese ore of northeast Tennessee than has been reported heretofore.

Lithium, because of the intensity of its 6707 Å line, was determinable in all samples analyzed spectrochemically. The amounts present in the ore, however, appear inconsequential.

The manganese ores throughout northeastern Tennessee appear to be mixtures of the soft, noncoherent and of the hard, nodular varieties. The chemical analyses of the milled ore samples from particular locales substantiate this mixed nature since (1) no obvious relationship between barium and manganese contents exists, and (2) the ratio of barium to manganese is far below that expectable if psilomelane were the sole ore mineral.

Analyses of the ore had thus indicated that manganese, iron, barium, cobalt, and, to a lesser extent, nickel were sufficiently widespread (in significant amounts) to serve as indicator elements in northeast Tennessee. Therefore, the distribution of these particular elements in trees and soils overlying known but undeveloped zones of subsurface manganese mineralization were studied to test their possibilities as indicators.

Analyses of Soil and Trees Overlying Manganese Bodies

Spectrographic analyses were made of the leaves, twigs, and surrounding soil of 36 chestnut oaks growing on undisturbed ground overlying several subsurface bodies of manganese, the presence, location, and attitude of which had been determined previously from drill-hole data. Chestnut-oak sites Nos. 1–13 overlie two irregular manganese bodies (Fig. 2, lower diagram) near and on a property known as the Hutchens tract. Three unplotted locales, Nos. 14–16, were located along an access road (for a drill rig) leading northeastward along the 2200-foot contour from the Hutchens tract to the Rominger tract, a distance of about one-quarter of a mile. No manganese of note was encountered in the drill holes along this road. Within the Rominger tract, however, three irregular bodies of manganese had been blocked out from the drill-hole data (Fig. 2, upper diagram). Locations 17–28 and 33–40 of the chestnut oaks sampled are shown relative to these three subsurface bodies. Outside the areas marked off as manganese-ore bodies in Figure 2, the drill holes had encountered no significant manganese mineralization; it was assumed therefore that these intervening areas were barren (although possibly a small body of manganese may have escaped detection).

Results of the analyses are summarized in Table 4.

The manganese mineralization appears reflected in the chemical composition of the trees of the area. Their leaf ash, for example, averages 3.8 per cent manganese, 0.35 per cent iron, 0.36 per cent barium, and 0.014 per cent nickel. In contrast, six chestnut oaks of the same species far from the manganese district average 2.1 per cent manganese, 0.36 per cent iron, 0.22 per cent barium, and 0.005 per cent nickel (Table 5). Thus, leaf ash from the manganese district appears significantly higher in manganese, barium, and nickel, three elements which are evidently locally concentrated in the ore.

Comparison of Tracts Sampled

The Hutchens tract and the Rominger tract appeared comparable in topography, stratigraphy, and vegetation. The Hutchens tract, during the year following the geochemical sampling, was developed into an economic ore body of manganese, whereas the Rominger

tract was not, chiefly because its concentration of manganese was too low. The writers thus fortunately could compare the geochemical data for an economic ore body with those from a manganese body which appeared not up to ore grade.

TABLE 5.—LOCATION AND METAL CONTENTS OF SIX CHESTNUT OAKS FAR FROM AREA OF MANGANESE MINERALIZATION

	Per cent metal in leaf ash				Tree location	Underlying formation
	Mn	Fe	Ba	Ni		
1	3.0	0.47	0.26	0.006	On Missionary Ridge, ¼ mile N. of Chickamauga Lake	Copper Ridge dolomite (Cambrian)
2	2.4	0.36	0.25	0.004		
3	2.8	0.41	0.30	0.005		
4	1.7	0.38	0.26	0.005	Near Red Bank, Tennessee	Knox dolomite, undivided (Cambro-Ordovician)
5	1.4	0.27	0.13	0.004		
6	1.3	0.28	0.13	0.004		
Average...	2.1	0.36	0.22	0.005		

DISTRIBUTION OF MANGANESE

For the 36 analyses of Table 4, the manganese content averaged 3.8 per cent for both leaf and twig ash. If the average ash percentages of the leaves and twigs are accepted as 5.06 per cent and 2.16 per cent, respectively, the manganese content of the leaves prior to ashing averages 0.19 per cent, whereas that of the twigs averages only 0.08 per cent. The average manganese content of the soil samples is 0.29 per cent.

The geographic variation of manganese in the soil and in chestnut oaks overlying the manganese bodies of the Hutchens and Rominger tracts is presented in Figure 3. As may be seen from the conventions used on the maps, the manganese content of soil, leaf ash, and twig ash is, for the Hutchens tract (Fig. 3, lower diagram) above the average for at least two of these materials, except for samples 1, 2, 3, and 9. Of these, locales 1, 2, and 3 are located uphill as well as relatively distant from the mineralized areas. For sample 9, however, no soil sample had been obtained.

For the Rominger tract (Fig. 3, upper diagram), the situation was reversed; there were only two places wherein two of the three categories exceeded the average in manganese content, namely samples 23 and 39, each located directly above a subsurface body of manganese.

DISTRIBUTION OF BARIUM

The average barium content of twig ash (Table 4) was 1.01 per cent, whereas that of leaf ash was only 0.36 per cent. Prior to ashing therefore, the average barium content of the twigs was 0.022 per cent, whereas that of the leaves was 0.018 per cent, the differential being thereby narrowed. For the soils sampled, the average barium content was 0.04 per cent.

The distribution of barium in soil, twig ash, and leaf ash for the two tracts is shown in Figure 4. For the Hutchens tract (Fig. 4, lower diagram) an above-average content of barium exists for at least two of the three materials analyzed at all stations except 1, 3, 5, and 13. Of these, stations 1 and 13 are most distant from the subsurface bodies of manganese.

On the other hand, for the Rominger tract (Fig. 4, upper diagram), only one locality, station 22, was above the average in at least two of three categories, and only stations 23, 24, 25, 26, 36, and 38 possessed above-average barium contents in one category. Stations 22–26 cluster directly over one subsurface manganese body.

DISTRIBUTION OF NICKEL

Nickel was present in small but determinable amounts in the manganese ore but in the soil (at shallow depths near the trees) was below 0.001 per cent. It is determinable, however, in the leaf and twig ash of the chestnut oaks, perhaps being absorbed by tree roots in contact with the ore at depth. Although to the writers' knowledge nickel is not known to play any specific role in the physiology of trees, the

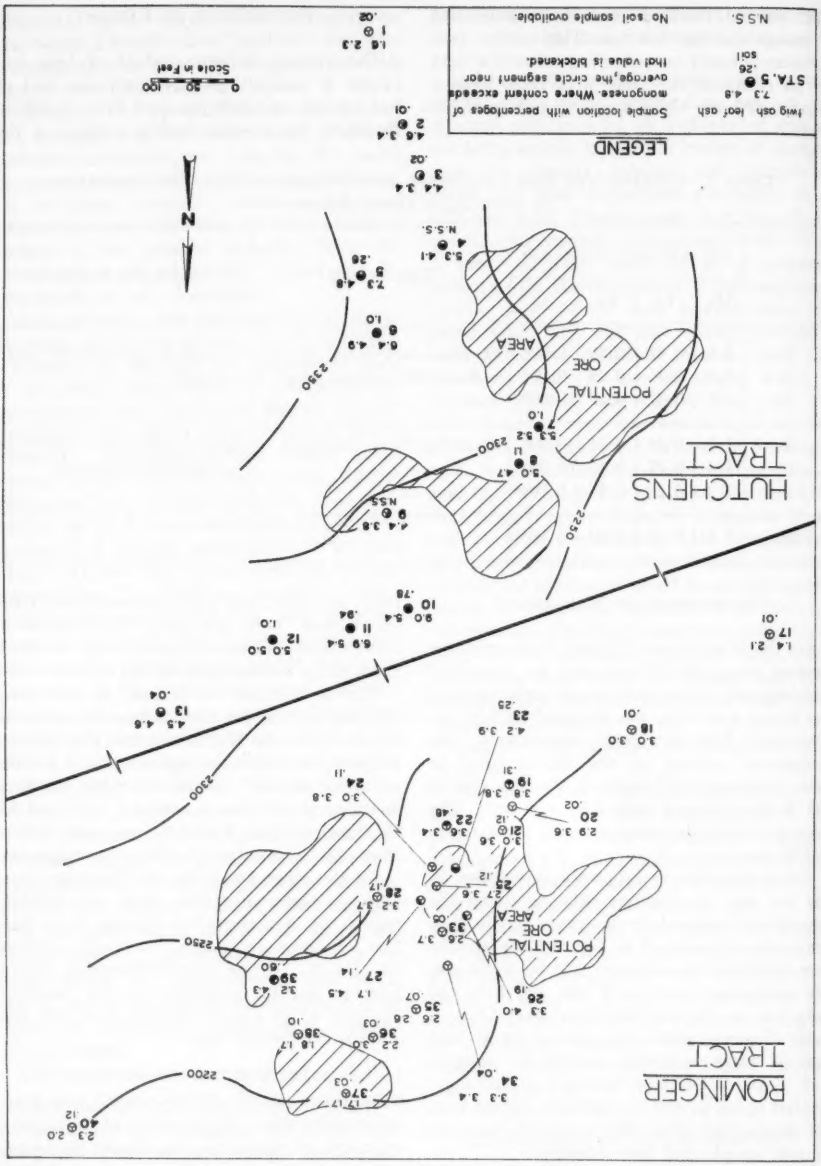

FIGURE 3.—AREAL DISTRIBUTION OF THE MANGANESE CONTENTS OF SOIL, LEAF ASH, AND TWIG ASH WITH RESPECT TO THE SUBSURFACE MANGANESE BODIES (RULED) OF THE ROMINGER TRACT (UPPER DIAGRAM) AND OF THE HUTCHENS TRACT (LOWER DIAGRAM)

average nickel content of leaf and twig ash (Table 4) was 0.014 and 0.017 per cent, respectively. For leaves and twigs prior to ashing it would therefore average 0.0007 and 0.0004 per cent respectively. As for the manganese and iron, the leaves prior to ashing contained more nickel, on the average, than did the twigs.

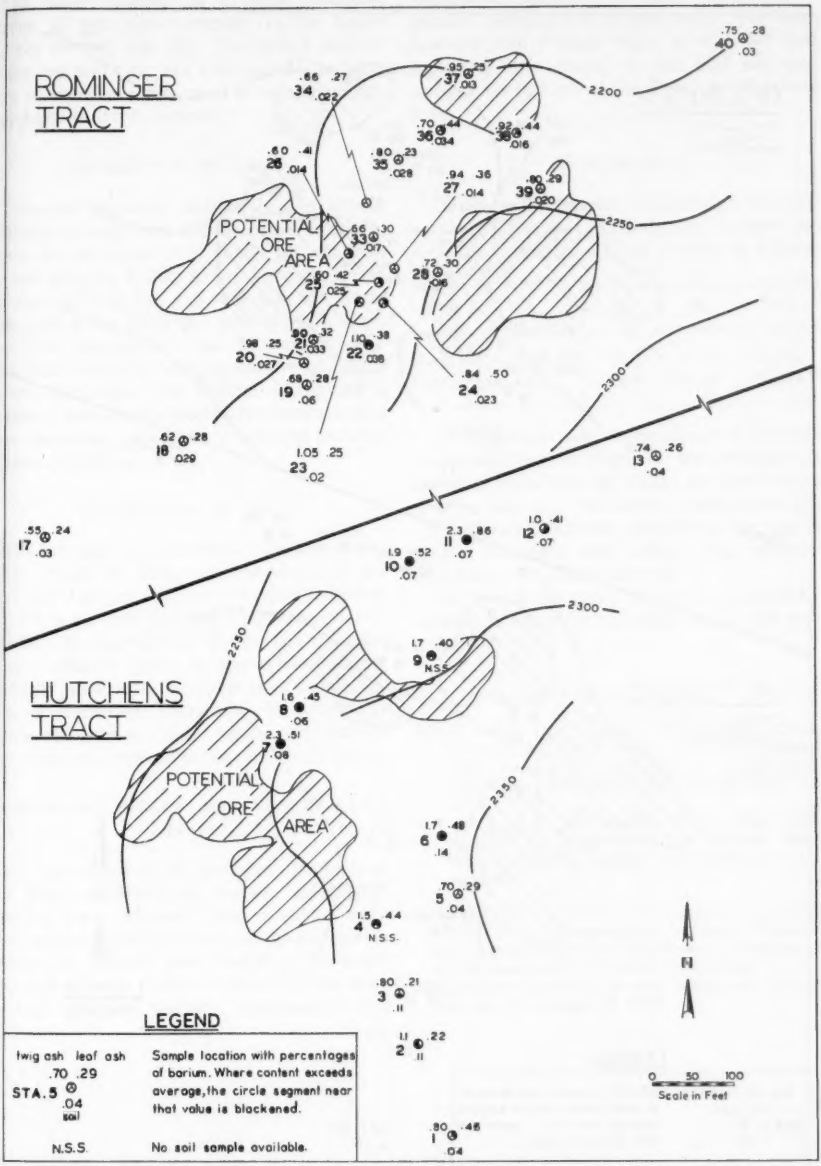

FIGURE 4.—AREAL DISTRIBUTION OF THE BARIUM CONTENTS OF SOIL, LEAF ASH, AND TWIG ASH WITH RESPECT TO THE SUBSURFACE MANGANESE BODIES (RULED) OF THE ROMINGER TRACT (UPPER DIAGRAM) AND OF THE HUTCHENS TRACT (LOWER DIAGRAM)

In the Hutchens tract (Fig. 5, lower diagram) only localities 1, 2, 3, and 13 are below average in nickel content for both leaf and twig ash—again these are the sites most distant from the mineralized areas. All stations nearer were above average for both leaf and twig ash. By contrast, in the Rominger area (Fig. 5, upper diagram), all samples were, with the exception

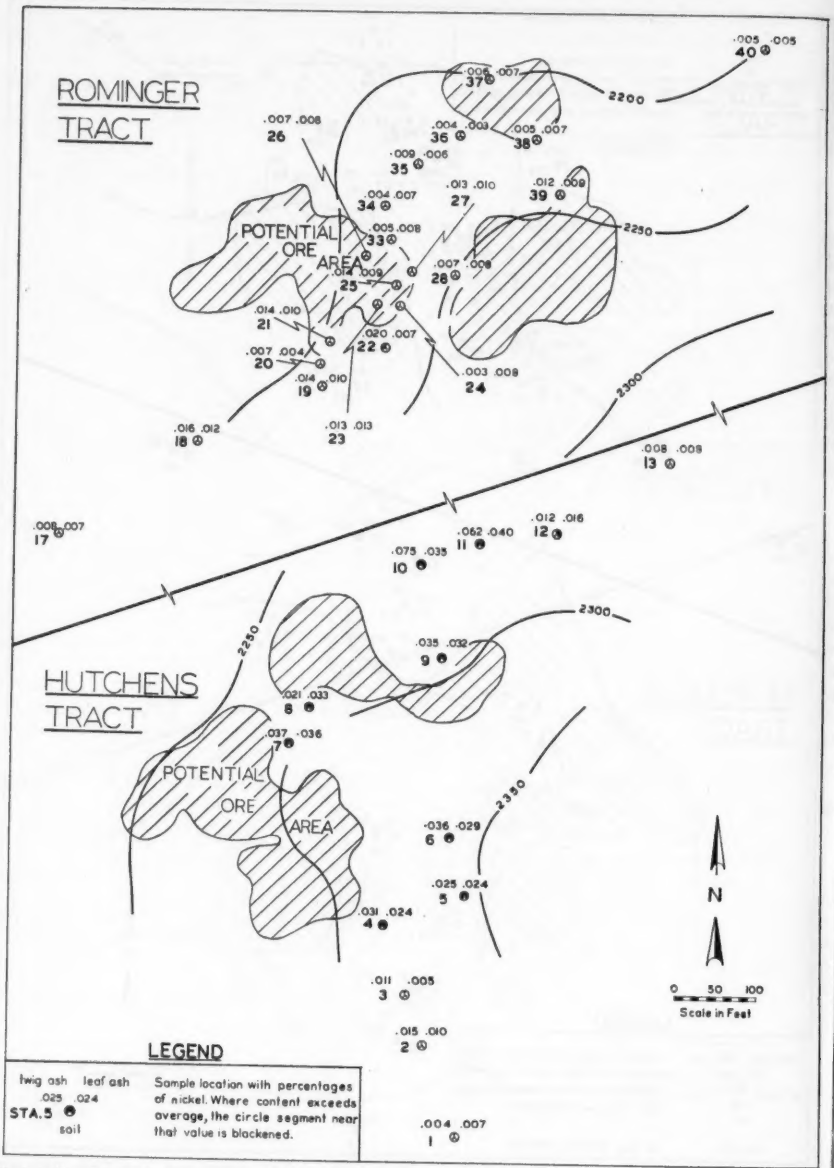

FIGURE 5.—AREAL DISTRIBUTION OF THE NICKEL CONTENTS OF LEAF AND TWIG ASH WITH RESPECT TO THE SUBSURFACE MANGANESE BODIES (RULED) OF THE ROMINGER TRACT (UPPER DIAGRAM) AND OF THE HUTCHENS TRACT (LOWER DIAGRAM)

of 22, below average as to nickel content; station 22 was above average in the nickel content of twig ash only. The nickel content of the leaf and twig ash thus appears to have been an excellent indicator of ore-grade manganese deposits in this instance.

Distribution of Cobalt

Although generally present in the ore in amounts greater than nickel, cobalt was also below its detection limit (0.004 per cent) in the soil samples. Unlike nickel, however, it was not detectable in leaf and twig ash, the detection limit being 0.001 per cent. Cobalt, thus, has little promise for use in geochemically detecting subsurface manganese ore in northeastern Tennessee. The striking differential in uptake of cobalt and nickel by the trees sampled does, however, present an interesting problem in plant physiology.

Distribution of Iron

The average iron contents of the leaves and twigs (Table 4) were, respectively, 0.35 per cent and 0.24 per cent for the ashed materials and 0.018 per cent and 0.005 per cent prior to ashing. The distribution of iron did not offer a very reliable guide to the mineralization, probably because of the ubiquity of iron in the soils of northeast Tennessee. Above-average values did tend to cluster nearer the blocked-out areas of mineralization for both areas.

Background Values for Chestnut-Oak Leaves

For contrast with the averages (Table 4) of the Rominger-Hutchens sample suite, leaf samples were collected from chestnut oaks growing about 200 miles south of the manganese district on residual soils overlying the Knox dolomite. Results (Table 5) show this new suite of leaf samples contains significantly less manganese, barium, and nickel than the comparable Rominger-Hutchens suite. For iron, however, the average value of 0.36 per cent compares very closely to the 0.35 per cent average for leaf ash of the Rominger-Hutchens suite.

Conclusions

(1) Of the 36 chestnut oaks sampled, the average weight per cent of manganese, barium, and nickel in the twig and leaf ash was as follows:

	Mn	Ba	Ni
Twig ash	3.8	1.01	0.017
Leaf ash	3.8	0.36	0.014

(2) Chestnut oaks in northeast Tennessee containing two or more of the elements in excess of these average values are likely to be growing near or over bodies of manganese ore.

(3) Cobalt, although present in the ore in greater amounts than nickel, was not detectable in the plant material.

(4) Nickel appeared to be a particularly reliable indicator of manganese ore in the area studied.

References Cited

King, Philip B., Ferguson, Herman W., Craig, Lawrence C., and Rodgers, John, 1944, Geology and manganese deposits of northeastern Tennessee: Tennessee Div. Geology Bull. 52, 275 p.

Mitteldorf, A. J., and Landon, D. O., 1956, Semiquantitative spectrochemical analysis using Spex standards: Applied Spectroscopy, v. 10, p. 12–14

Department of Geology, Southern Illinois University, Carbondale, Illinois; Department of Geology and Geography, University of Tennessee, Knoxville, Tennessee

Manuscript Received by the Secretary of the Society, November 24, 1958

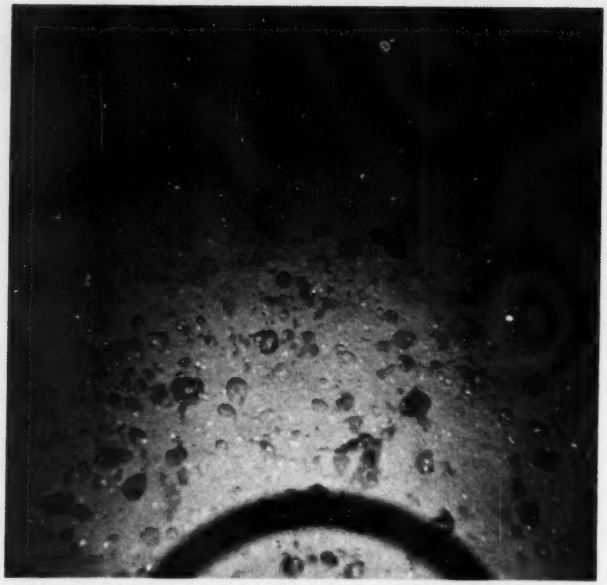

FIGURE 1.—Manganese nodules resting on red clay; no visible evidence of biological activity. Field coverage: about 2 square meters. Station No. 10, Southwestern Pacific Basin; depth 4770 meters.

FIGURE 2.—Manganese nodules or coated rocks resting on calcareous ooze. A visible wormlike organism is near the large nodule in the right foreground. Field coverage: about 2 square meters. Station No. 11, Southwestern Pacific Basin; depth 4560 meters.

PHOTOGRAPHS OF DEEP SEA FLOOR

BULLETIN OF THE GEOLOGICAL SOCIETY OF AMERICA
VOL. 71, PP. 1067-1074, 1 FIG., 5 PLS. JULY 1960

PHOTOGRAPHIC STUDY OF SOME DEEP-SEA FLOOR ENVIRONMENTS IN THE EASTERN PACIFIC

By Carl J. Shipek

Abstract

A number of ocean-floor environments in the Eastern Pacific have been investigated with the U. S. N. Electronics Laboratory Deep-Sea Camera, Type III. Fourteen ocean stations were occupied from the R/V Baird which participated in the Scripps Institution of Oceanography Expedition "Downwind." Nine successful lowerings to depths in excess of 4500 m along a track between San Diego, California, and Valparaiso, Chile, yielded a number of photographs of scientific interest. Analysis of these photographs has revealed that: certain areas of the Pacific sea floor are covered with surface concentrations of manganese; biological, chemical, and physical forces are acting continuously to form, change, and disrupt the microrelief and character of deep pelagic sediments; and the camera has proven useful as a scientific tool to conduct rapid surveys of the sediment–water interface for information on the character and distribution of geological, biological, chemical phenomena.

The rate of accumulation of pelagic sediments is closely related to the chemical formation of manganese nodules to account for the existence of widely distributed and exposed quantities of such free minerals on the sea floor.

CONTENTS

TEXT

	Page
Introduction	1067
Acknowledgments	1069
Description and operation of camera equipment	1070
Detection and significance of microrelief in deep-sea sediments	1070
Definition	1070
Physical processes	1070
Biological processes	1071
Chemical processes	1072
A look into the problem of manganese formation and sediment accumulation	1072
Conclusions	1074
References cited	1074

ILLUSTRATIONS

Figure	Page
1. Distribution of main types of pelagic sediments in Eastern and Southeastern Pacific Ocean showing "Downwind" deep-camera stations	1068

Plate	Facing page
1. Photographs of deep-sea floor	1067

	Following page
2. NEL Type III deep-sea camera	
3. Photographs of deep-sea floor	1072
4. Photographs of deep-sea floor	
5. Photographs of deep-sea floor	

TABLES

Table	Page
1. Bottom relief and sediment at deep-camera stations—S.I.O. Cruise "Downwind"	1069

Introduction

In co-operation with the Scripps Institution of Oceanography, "Downwind" Expedition to the Eastern and Southeastern Pacific in 1957–1958, the U. S. Navy Electronics Laboratory, San Diego, California, undertook a program of ocean-floor investigations with a special deep-sea camera. A series of stations was occupied from the R/V Baird, one of the two vessels making the cruise. Fourteen lowerings in depths of water ranging from 1320 to 4754 m were made between San Diego, California, and Valparaiso, Chile. Figure 1 shows the locations of the stations and the general distribution of main types of pelagic sediments in the eastern and southeastern Pacific.

Red clays and calcareous and siliceous oozes were photographed and cored as a part of an extensive program of bathymetric surveying, geological and biological sampling, chemical determinations of sea water, and geophysical measurements of substrata. Because the deep-camera lowerings on "Downwind" constituted

one of the first co-ordinated attempts to sample visually the widely scattered and deep marine features of the Pacific, an effort was made to obtain some new visual information on the relationships between the character of materials that form at the interface and the forces that act upon them.

Significant pictures were initially collected in the Clipperton Fracture Zone south of San Diego where camera station No. 2 showed manganese nodules resting on a siliceous ooze that appears to be slightly rippled. Moving south into the region of the East Equatorial Pacific, stations Nos. 3 and 4 were made in an area of calcareous-siliceous ooze where there was no visible evidence of manganese nodules. The appearance of the bottom indicated strong biological activity by benthos feeders. Station No. 8 in a deep basin of French Polynesia disclosed well-developed manganese nodules which were mantled by discontinuous caps of red clay. At station No. 9 in this same general

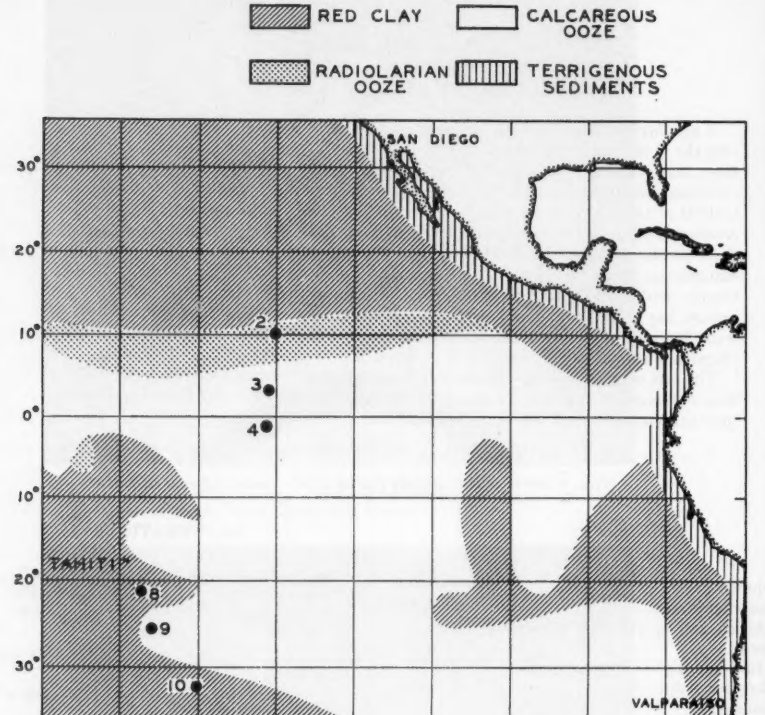

FIGURE 1.—DISTRIBUTION OF MAIN TYPES OF PELAGIC SEDIMENTS IN EASTERN AND SOUTHEASTERN PACIFIC OCEAN

● DOWNWIND deep-camera stations
After Revelle *et al.* (1955)

area, a series of photographs from the upper surface of a seamount disclosed a pattern of well-formed symmetrical ripple marks in a pteropod ooze. South of this region on the northeastern edge of the Southwestern Pacific Basin, station No. 10 showed more manganese nodules resting on a red clay bottom. A calcareous ooze with very large manganese nodules was discovered at station No. 11, on the eastern edge of this basin; but a calcareous ooze about 600 miles to the east at station No. 12 showed no visible evidence of manganese. Station No. 13 disclosed red clay in the northeast section of the Pacific Antarctic Basin, but the photograph obtained was not suitable for printing. No manganese nodules were visible. Arrival in Valparaiso, Chile, terminated the first leg of "Downwind" and the deep-sea photography program.

TABLE 1.—BOTTOM RELIEF AND SEDIMENT AT DEEP-CAMERA STATIONS
S.I.O. Cruise "Downwind"

CAMERA STATN.[1]	REGION	LAT.	LONG.	DEPTH METERS	BOTTOM SEDIMENT	MINOR RELIEF[2]	MICRORELIEF		
							PHYSICAL	BIOLOGICAL	CHEMICAL
2	CLIPPERTON FRACTURE ZONE	10°-25'N	130°-35'W	4712	RADIOLARIAN OOZE	SUBDUED 50 FATH. HILLS	IRREGULAR BETWEEN NODULES		MANGANESE NODULES, LESS THAN 10CM
3	EAST EQUATORIAL PACIFIC	3°-12.5'N	131°-31'W	4440	SILICEOUS OOZE	FLATTISH 20 FATH. HILLS		BENTHIC ANIMALS, PLOW TRAILS LESS THAN 5CM, CHURNING	
4	EAST EQUATORIAL PACIFIC	1°-21'S	131°-33'W	4510	CALCAREOUS OOZE	LOW HILLS		BENTHIC ANIMALS, MOUNDS, TRAILS	
8	FRENCH POLYNESIA	21°-37'S	147°-40'W	4684	RED CLAY	FLATTISH BOTTOM OF TROUGH	RED CLAY CAPS ON NODULES.		MANGANESE NODULES, LESS THAN 20CM
9	FRENCH POLYNESIA	25°-57'S	146°-21'W	1320	CALCAREOUS OOZE (PTEROPOD)	FLATTISH TOP SURFACE OF SEAMOUNT	SYMMETRICAL RIPPLE MARKS 5-10 CM		
10	S.W. PACIFIC BASIN	32°-08'S	140°-30'W	4770	RED CLAY	SUBDUED 50 FATH. HILLS	IRREGULAR BETWEEN NODULES		MANGANESE NODULES, LESS THAN 10CM
11	S.W. PACIFIC BASIN	42°-50'S	125°-32'W	4560	CALCAREOUS OOZE			SMALL WORM, NUMEROUS TRAILS	MANGANESE NODULES, 30 CM AND LESS
12	PACIFIC ANTARCTIC RIDGE	44°-26'S	110°-39.5'W	3180	CALCAREOUS OOZE	150 FATH. HILLS		ANIMAL CHURNING, LESS THAN 5CM	

1. All bottom photographs taken on slopes of 5 per cent or less
2. Copied from shipboard log, Scripps "Downwind" Expedition 1957–1958, dated May 1958

Difficulties imposed by depth of water and adverse sea and weather conditions during some of the lowerings reduced the total number of useful photographs to 25 for the 9 stations which were successful. Eight photographs have been included in this report to illustrate specific marine features, mineral occurrences, and effects of biological and physical activity on bottom sediments. Table 1 gives detailed information on each photograph. All but one were taken in color which allows ready identification of clay, calcareous ooze, and such minerals as nodular manganese. Although it is difficult in underwater color photography to obtain true shades of some sediments because of water absorption, resulting colors help in the detection of details normally lost in black and white photography. Owing to the high cost of color reproduction, only two have been selected for color printing.

ACKNOWLEDGMENTS

The author is grateful to Dr. H. W. Menard of Scripps Institution of Oceanography and Institute of Marine Resources, La Jolla, California, who made this study possible, offered many useful ideas, and reviewed the manuscript. For informative discussions on pelagic sediments, the author thanks Dr. W. Riedel of Scripps Institution. Mr. Max Silverman of Scripps and the officers and crew of the R/V BAIRD provided valuable assistance during the camera lowerings. The author is grateful to Dr. G. H. Curl, Dr. E. L. Hamilton, Mr. E. C. Buffington, and Dr. R. S. Dietz of the U. S. Navy Electronics Laboratory, San Diego, California, for critically reviewing the manuscript. For processing of the film and preparation of enlargements, the author expresses his continuing thanks to the NEL Photographic Section. Miss Peggy Hagar of the Drafting and Standards Section and Mr. G. L. Prible of the Sea Floor Studies Section assisted in the preparation of the illustrations. To Mrs. Dorthy B. Hancks and Mr. Nicholas Nicoloff of the Marine and Special Components Section,

NEL, the author will always be grateful for the engineering and drafting assistance which made the NEL Type III Deep Sea Camera possible. Many thanks are due the members of the Technical Services Division who put forth special effort to construct the camera, which has performed faultlessly for 4 years.

Description and Operation of Camera Equipment

The NEL Type III Deep Sea Camera (Shipek, 1957) was designed especially to photograph closeups of deep-sea floor surfaces. For this reason and because of its portability, it was employed on "Downwind". As a compact unit, it consists of a light-weight metal frame which holds a water-tight aluminum camera case, light source, flash tube, and water-flooded reflector in the proper oblique relationship to the bottom at the moment of exposure. Plate-2 illustrates the various parts of the underwater unit, which, complete, weighs about 80 kg in sea water. It can be safely lowered to depths in excess of 6000 m on a 0.2 cm diameter wire from any standard hydrographic winch. A suspended lead weight from a protected spring-loaded tripping arm actuates the light source and camera upon contact with any interface surface capable of supporting the 4.5 kg lead weight.

A 35 mm spring-wound framing device with an f 2.8, 30 mm wide-angle lens and a 3.18 cm by 3.18 cm alternate camera unit employing an f 6.3, 80 mm wide-view lens were both utilized to photograph about 2 square meters of ocean floor per contact, allowing 15 seconds between exposures for the flash capacitors to recharge, the film to advance, and the camera to change its horizontal location with respect to the bottom. Mechanical lowering troubles, excessive wire angles in deep water, and adverse sea conditions caused a certain amount of deviation from the normal field coverage. Some of the photographs were taken when the camera was in a canted position above the bottom. Between 4 and 6 square meters of visible area is covered in each of these photos. Figures 1 and 2 of Plate 1 represent the normal photographic coverage with this camera.

Black and white Tri-X film rated at a speed of 200 ASA and Super Anscochrome film rated at 100 ASA were used at a pre-set target distance of 2.4 m (1.8 m in water) through a 3.18-cm thick fused quartz look-through port. Two 30-cm coring tubes of 3.8-cm diameter were mounted at the base of the camera frame to obtain representative sediment samples for each lowering.

Detection and Significance of Microrelief in Deep-Sea Environments

Definition

The term "microrelief" has been utilized to explain various degrees of roughness of underwater topographic surfaces. For this report, microrelief defines the very small vertical and horizontal irregularities impressed or formed upon a relatively smooth submarine feature of much larger extent. As such, this relief is measured in centimeters. Microrelief caused by burrowing organisms can be related to churning which may extend deep enough into sediments to change the acoustic properties such as reflectivity even at low frequencies. At higher frequencies, sound scattering would be considerably affected by such microrelief.

The study of microrelief on the deep-sea floor requires the investigation of processes at work in different marine environments. Direct camera examination of the small-scale features, which result from the action of different influences on bottom sediments, offers a method of study where a system of indirect measurements involving the examination of currents by meters, for instance, would be extremely difficult to apply. Three basic types of activities have been detected through the interpretation of numerous photographs. Physical, biological, and chemical forces work together, or separately, at the sediment–water interface to form, alter, or rearrange the surface layers of bottom-forming materials.

Physical Processes

Physical forces in the form of either current or oscillatory wave motion of unknown origin and characteristics are being observed on well-formed ripple marks in the coarser fractions of sediments resting on seamounts and other topographic highs in various regions of the Pacific (Menard, 1952). Shepard (1948), Ladd and Tracey (1949), and others have pointed out that fine sediment does not accumulate on topographic highs because of removal of fines by waves and currents. Figure 1 of Plate 5 shows strong well-formed symmetrical ripples superimposed upon calcareous (pteropod) ooze. A high degree of sorting appears to have taken place through the action of oscillatory water movements working across the upper surface of this seamount. A large percentage of the trans-

portable fines have been removed from the upper surface to the vertical water column where eventual settling will take place in deeper areas such as illustrated by Figure 2 of Plate 4.

Unpublished photographs taken by the writer on the southwest slope of Eniwetok Atoll also show some similar deep ripple marks. Nearly all the bottom photographs taken at 11 stations in an area of 70 square miles showed indications of oscillatory water movements. Two stations each having a depth of 1647 m showed strong ripple marks in calcareous sand which appeared to be crusted over by a darker manganeselike coating.

A photo at station No. 8, in French Polynesia (Pl. 4, fig. 2), revealed possible additional indirect evidence of deep currents or waves. Rounded manganese nodules are resting on and in red clay at 4684 m. Strangely, some of the closely spaced nodules are partially mantled with red clay, while others are covered; still others are entirely clean, with fresh-looking surfaces. This general appearance of such a relatively small area (not more than 5 square meters) proves some form of oscillatory water movement capable of moving fine materials from some of the nodules subsequent to a period of increased sediment accumulation. An alternate process to explain the irregular caps of red clay on the nodules falls within the chemical process of manganese-dioxide formation at the interface and the irregular entrapment of red clay sediments at the same time. Since the exposure of manganese nodules on the bottom indicates good water circulation (Goldberg and Arrhenius, 1958), this is additional indirect evidence of currents even though they may be of only very low velocities.

Biological Processes

Biological activity provides another method by which microrelief can form on the deep-sea floor. Emery (1953) has shown how small burrowing and crawling organisms can disturb and alter bottom materials, thus creating such features as pits, mounds, scratches, and tracks. Bruun *et al.* (1953) have positively identified many organisms living at great depths which are capable of producing such microrelief.

The underwater camera gives additional proof of life in the abyssal benthic areas through direct viewing; it is now possible to observe some of the effects of animal activity on the deep-sea floor. Photographs taken along the survey track of "Downwind" showed both direct and indirect evidence of animal life in depths to 4500 m. Figure 2 of Plate 3 shows a plow trail formed by a benthic crawler similar to a gastropod. Figure 1 of Plate 4 shows pit and mound structures probably resulting from worm action. Spongelike animals, gastropods, and echinoids appear to be numerous in this photograph. Dredge hauls by the CHALLENGER and GALATHEA expeditions in similar regions and depths have yielded many forms of hydroids, sponges, gastropods, pelecypods, worms, holothurians, crinoids, echinoids, ophuroids, and asteroids which are normally benthic dwellers. Figure 2 of Plate 1 shows a wormlike animal on a calcareous ooze in an area with many large manganese nodules. A delicate trail, which is not near the wormlike animal, is clearly visible in the ooze along the margin of a large nodule. Other delicate trails criss-cross the area between the nodules and show that animal activity is ever changing. Calcareous ooze banked up onto one edge of a large nodule shows that burrowing animals are also present. The trails, shallow digging, and the freshness of the manganese-nodule surfaces indicate a low rate of deposition for this area. This in turn results in greater biological activity by fewer species to maintain existence in this sparse environment. A more effective rate of accumulation of pelagic materials would have completely covered the slow-forming manganese surfaces. This photograph was taken near a geological boundary change between red clay and calcareous ooze of *Globigerina* origin. It is likely that surface waters have not been favorable to the production of Foraminifera for along period of time. Figure 2 of Plate 5 shows a churned surface which lacks visible benthic life. Bruun *et al.* (1953) point out that many of the inhabitants of abyssal sediments dwell just below the surface of the bottom where they can strain the sediments for small organisms.

Wave and current action at the interface can also act to disrupt and diminish the magnitude of the microrelief formed by biological activity. Figure 1 of Plate 5, which is an area of well-developed ripple marks, shows no visible evidence of life. The available food materials are probably meager in this area. Periodic or continuous removal of the organic detritus and fine fractions of pteropod ooze by bottom-water movements would tend to make the area inhospitable for bottom life.

Figure 1 of Plate 1 was taken in an area of red clay which appears to be extremely low in organisms and detrital materials. Significant

microrelief in this case appears to result mainly from chemical processes.

Chemical Processes

The third type of microrelief results from chemical action at the sediment–water interface. Goldberg and Arrhenius (1958) have proposed an ion process which utilizes the mineral constituents of sea water to form manganese-dioxide coatings on rocks or around various types of nuclei. Dietz (1955) has explained the formation of manganese dioxide on similar objects by a colloidal suspension and precipitation process. Regardless of the origin, the presence of manganese nodules at the interface constitutes an important method of building up extensive microrelief on the sea floor. Vast areas of the Pacific sea floor are covered with such mineral deposits (Murray and Renard, 1891). Photographs, sampling, and computations indicate that the Southwestern Pacific Basin is covered with manganese nodules and that the weight per unit area is about 1–4 gm/cm^2 using a nodular density of 2.0 gm/cm^3 (Menard and Shipek, 1958). Manganese nodules photographed in the basin varied in form from rounded, cobblelike shapes a few cm across to large, boulderlike masses approximately 50 cm in diameter. Rippled bottoms with manganese-oxide crusts in the Eniwetok area indicate how physical and chemical processes can combine to form microrelief of lasting endurance. Manganese nodules have formed on red clays and on siliceous and calcareous oozes in widespread areas of the Pacific (Pl. 1; Pl. 3, fig. 1; Pl. 4, fig. 2).

Deep-sea photographs from the eastern Pacific help confirm the character of the interface by showing the high transparency of water just above the sea floor. Photographs also reveal that the deep sea floor is normally a firm surface capable of supporting such objects as manganese nodules and various forms of benthic life. The typical abyssal bottom does not appear to have any soupy upper layer of watery sediment.

A Look into the Problem of Manganese Formation and Sediment Accumulation

The photographic investigation of environments in the Southwestern Pacific Basin has confirmed the initial discovery of vast quantities of manganese by the Challenger Expedition. At that time detection of such minerals on the sea floor usually resulted from representative sediment sampling which yielded varying sizes of nodules in cores, grab samples, and dredge hauls (Murray and Renard, 1891). The present deep camera stations along the general track of the earlier Challenger expedition have produced photographic data which permit a new look at the manganese problem. Areal-distribution maps can now be constructed, and density concentration used to estimate potential mining reserves. Since the bulk of the manganese nodules rest at the sediment-water interface (Pl. 1; Pl. 3, fig. 1; Pl. 4, fig. 2), their origin must be closely related to rates of sediment accumulation. Coring in this area reveals that most of the manganese nodules are at the present surface (Menard and Shipek, 1958).

Pettersson (1943) and Buttler and Houtermans (1950) have estimated that manganese accumulates in the ocean at the rate of approximately 1 mm per 1000 years. According to Goldberg and Arrhenius (1958) manganese can probably form at the interface at a much lower accretion rate. Goldberg has estimated this rate to be 1 mm/10^4 years. If published rates of sedimentation for Pacific clays and calcareous and siliceous oozes range from about 1 mm to several cm per 1000 years (Arrhenius, 1952) why are the manganese nodules still so prominently exposed at the interface where they no doubt have formed? One can safely assume that rates of manganese formation and sediment accumulation are being closely controlled by such factors as composition of sea water including

Plate 2.—NEL Type III Deep-Sea Camera

Plate 3.—Photographs of Deep-Sea Floor

Figure 1.—Manganese nodules resting on radiolarian ooze. No visible evidence of biological activity. Field coverage: about 5 square meters. Station No. 2; Clipperton Fracture Zone; depth 4712 meters

Figure 2.—Calcareous-siliceous ooze marked by animal plow trail and possible ripple marks. The large object near the center of the photograph may be a species of gastropod. Field coverage: about 4 square meters. Station No. 3; East Equatorial Pacific; depth 4440 meters

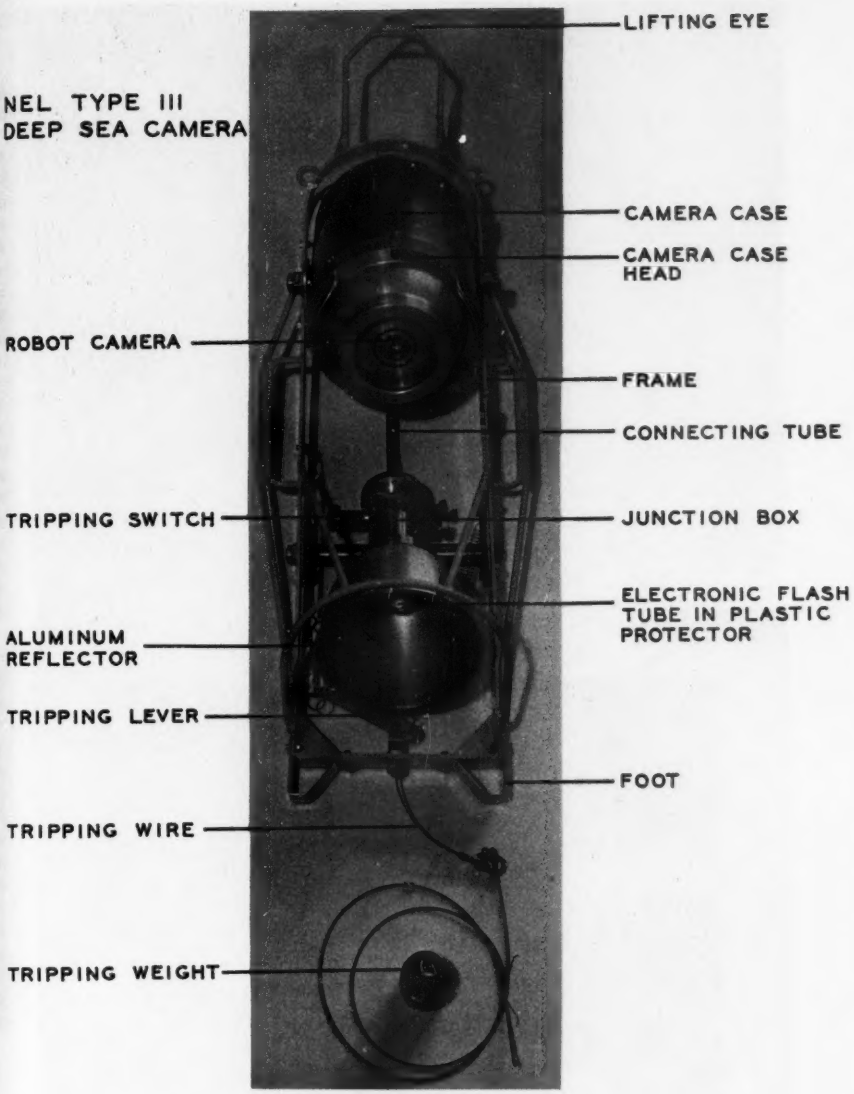

NEL TYPE III DEEP-SEA CAMERA

FIGURE 1

FIGURE 2

PHOTOGRAPHS OF DEEP-SEA FLOOR

FIGURE 1

FIGURE 2

PHOTOGRAPHS OF DEEP-SEA FLOOR

FIGURE 1

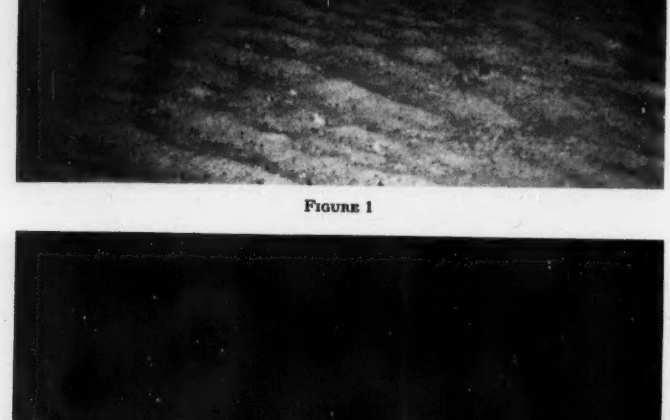

FIGURE 2

PHOTOGRAPHS OF DEEP-SEA FLOOR

supplies of mineral constituents, pelagic sediment accumulation, and the activities of bottom currents or waves. The processes which control the general appearance of the sea floor must be discontinuous and variable throughout geologic time if the suggested sedimentation rates are correct for certain areas. Figure 2 of Plate 4 indicates a local increase in sedimentary activity which is masking nodules which have grown to their present sizes and shapes during a previous period of ineffective sediment accumulation. It is not known if these partially covered nodules are still growing, but fresh-looking surfaces on some of them indicate they are. Although at present the tops of some of the nodules are being covered with red clay, changing rates of accumulation of the clay may cause the formation of alternate layers of manganese and clay in the nodules.

Where sedimentation rates are relatively high (as in an area of calcareous deposition; Pl. 1, fig. 2), why isn't the manganese covered by sediment? Is manganese formed only at the water–sediment interface or can nodules form within the sediments as is implied by the finding of perfectly concentric nodules of manganese dioxide? These and similar questions remain unanswered.

Goldberg (1954) stated "that manganese nodules usually occur in regions of low sedimentation rates, such as topographic highs or seamounts"; also, "that manganese nodules form in areas where the nodules would not be masked by biological contributions or detrital clay constituents falling to the sea floor." Bottom photographs (Pl. 1, fig. 1; Pl. 4, fig. 2) taken in deep areas which are not prominent topographic highs showed many manganese nodules, whereas an adjacent topographic high revealed strong ripple marks with no visible evidence of nodules. The greatest concentrations of manganese appeared at depths in excess of 4500 m on subdued hilly surfaces. The presence or lack of biological life at the deeper stations appeared to have little relation to the presence of manganese. It is not likely that life can occur in great enough quantities in deeper benthic areas to mask the processes of manganese-nodule formation.

Volchok and Kulp (1957) have shown how rates of sedimentation could have tripled in some areas in recent times. The great areal extent of exposed manganese nodules in the Pacific in deeper regions, where present rates of sediment accumulation are supposedly higher (according to the above idea) do not substantiate an increase but instead indicate periods of ineffective sediment accumulation of some length since the origin of the nodules.

It is of course possible that present estimates of the rate of nodule accretion are too low or that the rate is highly variable. It has been shown photographically that deep currents or possible internal wave motions exist in the presence of manganese nodules (Menard, 1952). Goldberg and Arrhenius (1958) have pointed out that the circulation of bottom water is necessary to supply oxygen for the formation of manganese.

Figure 2 of Plate 1 shows large, fresh-looking

PLATE 4.—PHOTOGRAPHS OF DEEP-SEA FLOOR

FIGURE 1.—Calcareous ooze with abundant biological activity. A large plow trail is visible at the right with a possible gastropod disappearing out of the photograph. The mounds in the right foreground were probably formed by burrowing worm action. Several spongelike faunas are visible in the center foreground. Small echinoids are also visible. The general nature of the bottom suggests a considerable amount of churning by unseen burrowing organisms. The identity of the light spots is not known. Field coverage: about 5 square meters. Station No. 4; East Equatorial Pacific; depth 4510 meters

FIGURE 2.—Manganese nodules resting on chocolate-colored clay. Some of the nodules are irregularly covered by clay. No visible evidence of biological activity. Field coverage: about 5 square meters. Station No. 8; region of French Polynesia; depth 4684 meters

PLATE 5.—PHOTOGRAPHS OF DEEP-SEA FLOOR

FIGURE 1.—Calcareous ooze on a topographical high which is ripple-marked by deep-water waves or currents. Coarser fragments have concentrated in the ripple troughs. No visible evidence of biological activity. Field coverage: about 4 square meters. Station No. 9; region of French Polynesia; depth 1320 meters

FIGURE 2.—Calcareous ooze. The irregular pattern of small mounds and depressions suggests active churning by burrowing organisms. Such microrelief is often mistaken for ripple marks. Field coverage: about 4 square meters. Station No. 12; Pacific Antarctic Ridge; depth 3180 meters

nodules resting on a deep calcareous ooze in a region of subdued hills where the rate of sediment accumulation appears to be low and the degree of biological activity relatively high. A photograph taken of calcareous ooze on the Pacific Antarctic Ridge at a much shoaler depth of 3180 m shows no visible evidence of either manganese nodules or biological activity. This would indicate greater sediment accumulation for this latter area.

Since sediment type does not appear to be the direct controlling factor in the formation of manganese nodules, it falls basically upon water composition, rates of pelagic sedimentation, topographic relief, and the magnitude of water circulation to make their origin possible and plausible. In addition, their presence and growth at the sediment–water interface demands extended periods of relatively low or ineffective rates of sediment accumulation for growth to observed sizes. Analysis of dredged manganese nodules (Goldberg, 1954; Mero, 1959) have shown significant percentages of cobalt, copper, and nickel. The chemical relationships employed by both Goldberg and Dietz to explain the origin of manganese nodules are strengthened by the "Downwind" underwater photographs which show large numbers of nodules at the sediment–water interface.

Conclusions

The underwater camera is a useful tool for investigating ocean-floor environments, mineral occurrences, and the natural processes which influence bottom sediments.

Observed ripple marks on topographic highs and possibly physically disturbed red clays at greater depths have established the presence of deep currents or oscillatory wave motion of significant but unknown velocities. Photographs show that physical, biological, and chemical forces are acting at the deep sediment–water interface to create measurable microrelief. It is noteworthy that water movements are more common on the dep-sea floor than previously imagined.

Manganese nodules have been detected primarily on subdued topographic areas of the Eastern Pacific in depths usually greater than 4500 m. The chemical and physical processes which appear to be responsible for their formation are active at the interfaces of both deep clays and oozes.

Significant percentages of cobalt, copper, and nickel in reported chemical analyses of dredged manganese nodules from the Pacific (Goldberg and Arrhenius, 1958; Mero, 1959) give added economic importance to these nodules. Their presence in vast quantities at the surface of different deep pelagic sediments suggests that sediment accumulation has been relatively ineffective for long periods of time in some areas and that the accretion of manganese dioxide is actually equal to or greater than published rates of sediment accumulation.

References Cited

Arrhenius, G., 1952, Sediment cores from the East Pacific: Swedish Deep Sea Expedition, 1947–1948 Rept., v. 5, p. 1–227

Bruun, A. F., *et al.*, 1953, The Galathea deep sea expedition (Translation): Macmillan Co., 296 p.

Buttler, H. V., and Houtermans, F. G., 1950, Photographic determination of activity distribution in manganese lumps of deep-sea origin: Nature, v. 37, p. 400–401

Dietz, R. S., 1955, Manganese deposits on the Northeast Pacific sea floor: Calif. Jour. Mines and Geology, v. 51, no. 3, p. 209–220

Emery, K. O., 1953, Some surface features of marine sediments made by animals: Jour. Sedim. Petrology, v. 23, p. 202–204

Goldberg, E. D., 1954, Marine geochemistry 1. Chemical scavengers of the sea: Jour. Geology, v. 62, p. 249–265

Goldberg, E. D., and Arrhenius, G. O. S., 1958, Chemistry of Pacific pelagic sediments: Geochimica et Cosmochimica Acta, v. 13, p. 153–212

Ladd, H. S., and Tracey, J. I., Jr., 1949, The problem of coral reefs: Sci. Monthly, v. 69, p. 297–305

Menard, H. W., 1952, Deep ripple marks in the sea: Jour. Sedim. Petrology: v. 22, p. 3–9

Menard, H. W., and Shipek, C. J., 1958, Surface concentrations of manganese nodules: Nature, v. 182, p. 1156–1158

Mero, John L., 1959, Economics of mining and processing of deep-sea manganese nodules Inst. Marine Resources, Univ. of Calif., Prelim. Rept., 95 p.

Murray, J., and Renard, A. F., 1891, Deep sea deposits: H.M.S. Challenger, Sci. Results, 362 p.

Pettersson, H., 1943, Manganese nodules and the chronology of the ocean floor: Medd. Oceangr. Inst. Goteborg, v. 2B, p. 1–39

Revelle, R. *et al.*, 1955, Pelagic sediments of the Pacific: Geol. Soc. America Special Paper 62, p. 221–236

Shepard, F. P., 1948, Submarine geology: New York Harper and Bros., 348 p.

Shipek, C. J., 1957, NEL Type III Deep sea camera: U. S. Navy Electronics Laboratory Rept. 768, 17 p.

Volchok, H. L., and Kulp, J. L., 1957, The ionium method of age determination: Geochimica et Cosmochemica Acta: v. 11, p. 219–246

U. S. Navy Electronics Laboratory, San Diego, Calif.

Manuscript Received by the Secretary of the Society, June 12, 1959

BULLETIN OF THE GEOLOGICAL SOCIETY OF AMERICA
VOL. 71, PP. 1075-1086, 2 FIGS. JULY 1960

MODELS AND METHODS FOR ANALYSIS OF THE MODE OF FORMATION OF FOSSIL ASSEMBLAGES

By Ralph Gordon Johnson

Abstract

Theoretical aspects of the formation of fossil assemblages are explored for the purpose of obtaining criteria and methods for the reconstruction of circumstances of preservation of shallow-water marine organisms. Models are developed which represent: (1) a death assemblage preserved under conditions of rapid burial; (2) an assemblage preserved *in situ* under conditions of gradual accumulation; and (3) an assemblage composed almost entirely of remains transported to the site of burial.

The histories represented by the models influence the following features of fossil assemblages: faunal composition, morphologic composition, density, disassociation of hard parts, fragmentation, surface condition of fossils, chemical and mineralogical composition of fossils, orientation, dispersion, and the texture and structure of the sedimentary aggregate. The expressions of these features indicate that biological criteria are more indicative of the mode of accumulation than physical criteria.

The stretched-line method of sampling provides a means of obtaining objective and repeatable measures of features of the fossil assemblages in place. It is restricted to sediments in which fossils can be recovered readily. A rank-correlation analysis of 11 samples from the Pleistocene Millerton formation of Tomales Bay, California, is given as an example of a means of evaluating the interrelations of variables measured by the line technique.

CONTENTS

TEXT

	Page
Introduction	1075
Acknowledgments	1076
Formation of fossil assemblages	1076
Possible fates of elements of life and death assemblages	1076
Models of death assemblages	1077
Methods of study	1082
Relationships between measures	1083
Discussion	1083
Selected bibliography	1085

ILLUSTRATIONS

Figure	Page
1. Possible fates of elements of life and death assemblages	1077
2. Inferred relationships of the models	1079

TABLES

Table	Page
1. Relative expressions of features developed under the conditions of the models	1080
2. Rank-correlation coefficients for measures taken in 11 line samples of the Millerton formation of Tomales Bay, California	1084

Introduction

At present we do not know enough about the processes that have acted upon dead organisms to retrace in detail the history of a particular fossil assemblage. Many of these processes (*e. g.*, diagenesis) are not amenable to ordinary methods of study. In the absence of direct knowledge of these processes and their results, reconstructions of the circumstances of preservation have been based upon general assumptions. Several attempts have been made to strengthen the theoretical framework of paleoecology by redesigning and refining these assumptions (recently Boucot, 1953; Miller and Olson, 1955; Olson, 1957). This paper explores the circumstances leading to the preservation of shallow-water marine organisms. Model fossil assemblages are used to examine criteria and methods for reconstruction of the mode of formation of actual fossil assemblages.

In the summer of 1956 the author began a general investigation of the preservability of marine communities. The assemblages of the Pleistocene Millerton formation of Tomales

Bay, California, offer a unique opportunity for evaluation of paleoecological theory and technique. The fauna comprises extant species of which at least 36 per cent are now living in Tomales Bay. The sediments associated with the Millerton fauna resemble closely the sediments of the bay. These circumstances permit a detailed reconstruction of the environment of deposition of the Millerton and the relationships of its fossils to living communities. The reconstructions may then be compared to the conclusions reached by paleontological means. Thus, the theory and methods of paleoecological analysis may be evaluated under as controlled conditions as can normally be achieved with the basic materials of paleontology. The present paper is concerned with the theoretical aspects of this project and is the first in a series dealing with the preservation of the Millerton fauna and the formation of death assemblages in the modern environments of Tomales Bay. While much of what follows is commonly implied in the literature, the detail sought in modern paleoecological studies requires the explicit statement of basic hypotheses so that these may be examined and made amenable to quantification.

Acknowledgments

Financial aid furnished by The Penrose Bequest of The Geological Society of America made possible the field study of the Millerton deposits. Mr. Robert Hessler assisted greatly in the field. Profs. J. Marvin Weller, Robert L. Miller, and Everett C. Olson have consulted with the author throughout this work. Dr. Joel W. Hedgpeth, Director of the Pacific Marine Station, has aided immeasurably in the field both as a stimulating consultant and jovial companion.

Formation of Fossil Assemblages

Possible Fates of Elements of Life and Death Assemblages

Figure 1 shows the possible fates of elements of life and death assemblages pertaining to the formation and preservation of fossil assemblages. The ten cases shown for individuals of a life assemblage[1] at a particular site are variations of four kinds of sequences. An organism may emigrate in the normal course of its existence as a predator or as a planktonic form (case 1). Emigration may result from an unfavorable change in the environment such as a sudden local increase in the amount of sediment deposited, The ability of active animals to detect and avoid unfavorable changes favors the preservation of sedentary forms. If an organism is removed by a predator or currents following death, it cannot contribute to the local death assemblage (case 2). The remaining possibilities for members of a life assemblage result in contributions to a death assemblage but differ in the ultimate disposition of these contributions. Cases 7, 8, and 9 represent the fates of infaunal organisms[2] that die within the sediment. Dying individuals of some infaunal species may emerge from the sediments to perish on the bottom (MacGinitie, 1935). Case 10 represents nonliving parts, such as molts, discarded during a life cycle. Such parts are exposed to the possibilities shown as 3, 4, 5, and 6. Excluding the variations introduced by an infauna, at least four kinds of histories are possible for elements of the exposed death assemblage. Probably the most common history in shallow seas is the destruction of remains by decomposition, mechanical and chemical action, and the action of scavengers; or removal by currents (case 3). The history of particular interest herein is that of an organism which, upon death, enters the exposed death assemblage and persists in some form so that it enters the local buried death assemblage (cases 4, 5, and 6). The period between death and burial is critical as the remains are exposed to a variety of destructive forces. The alteration of an element of a death assemblage depends partially on the length of time it remains exposed and the rates of the biological and physical processes acting upon it. Two dissimilar histories may produce the same net effect upon the same kinds of materials if different periods of exposure are involved.

Remains from other death assemblages may be introduced into the local death assemblage. An element of a buried death assemblage may be reintroduced into the exposed death assemblage by erosion (case 15). Foreign remains may be removed subsequently (case 11) or persist and be included in the local buried

[1] "Life assemblage" as used herein means an assemblage of living organisms, "death assemblage", an assemblage of dead organisms, parts of dead organisms and/or the discarded parts of living organisms. The term "exposed death assemblage" is used for a death assemblage not buried in sediments.

[2] Thorson (1957) has defined the infauna as "... comprising all animals inhabiting the sandy or muddy surface layers of the sea ... *i.e.*, living buried or digging in a substratum."

assemblage (cases 12, 13, 14). Thus, two or more distinctive communities which were separated in life by space and/or time may be mixed after death.

sediments deposited in the area of life and remains introduced into the site of deposition from elsewhere. Additional criteria are required for the assessment of the alteration of a fossil

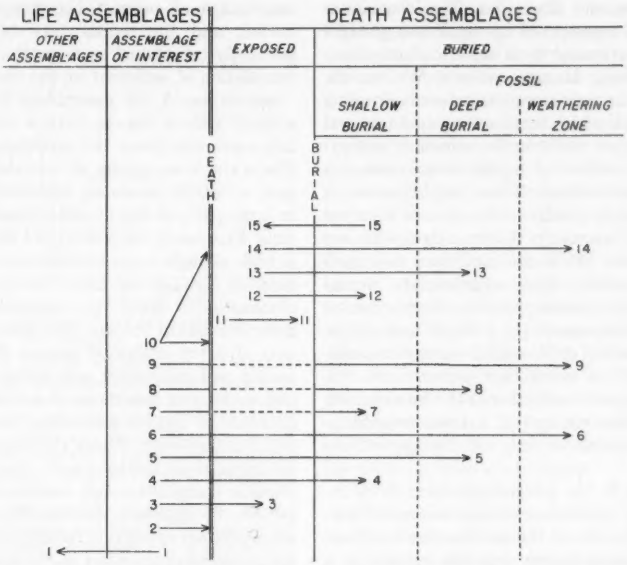

FIGURE 1.—POSSIBLE FATES OF ELEMENTS OF LIFE AND DEATH ASSEMBLAGES

Case 1—emigration; 2—death and immediate removal; 3—remains enter exposed death assemblage but are destroyed or removed; 4, 5, 6—remains enter exposed death assemblage and are buried; 7, 8, 9—remains of infaunal organisms *in situ*; 10—nonliving parts discarded during lifetime; 11—remains from other death assemblages are introduced but destroyed or removed subsequently; 12, 13, 14—remains from other death assemblages are introduced and persist to be buried; 15—buried remains are reintroduced to exposed death assemblage by erosion.

Cases 4, 7, 12—remains are destroyed or removed while buried at a shallow depth; 5, 8, 13—remains are destroyed or removed by diagenetic processes; 6, 9, 14—remains persist and eventually are exposed to weathering.

The remains of organisms that become buried in the sediment may be destroyed or removed while buried shallowly and still under the influence of the local ecosystem (cases 4, 7, 12). They may persist and be more deeply buried only to be destroyed by the physical processes operating within the body of rock (cases 5, 8, 13). Or they may survive and become available for sampling (cases 6, 9, 14). As the death assemblage is brought into the weathering zone, the rate of alteration of the fossils may increase rapidly. This "last-moment" alteration is one of the factors that limits geochemical investigations of primary composition.

The immediate concern here is to develop criteria that will permit distinction between the remains of organisms that are buried in assemblage that has taken place between the time of death and recovery. For studies of evolution, ecology, and geology, the elements not preserved may be as important as or even more important than those that are preserved. Some knowledge of the missing components may be inferred by analogy and the application of principles of ecological integration or by recognition of the physical and chemical effects of organisms upon one another and upon the sediment. The uncertainty inherent in this kind of inferential knowledge constitutes a fundamental limitation of paleontology.

Models of Death Assemblages

A fossil assemblage can contain any proportion of fossils representing different histories.

Each history can produce a wide variety of exposure effects depending upon the rate, effectiveness and period of operation of the processes involved. Thus a broad spectrum of fossil assemblages is possible with regard to mode of accumulation and alteration. The continuum of variation represented by fossil assemblages cannot be expressed by a system of classification recognizing discrete variants. We can obtain a basis for their comparison by constructing special models which feature the environmental conditions that result in the common and extreme combinations of modes of accumulation and exposure effects. These might serve as reference types, similar in function to the type specimen of taxonomy. Three such models are proposed here. While the conditions described are hypothetical, they approximate actual conditions in certain modern environments. The models represent (1) a death assemblage buried at the site of life with a minimum of disturbance, (2) an assemblage intermediate with regard to exposure effects and the introduction of foreign elements; and (3) a death assemblage composed almost entirely of transported remains.

MODEL I: A life assemblage lives in a restricted area of the sea bottom below the low-tide mark but above the maximum wave base. The water mass moves over the bottom at a low velocity which is occasionally raised to erosional competency. The substrate is composed of clastic sediments. Intermittently, small amounts of similar sediments are introduced into the area together with minor amounts of the durable remains of organisms. The abundant and diverse life assemblage consists of soft-bodied organisms and organisms bearing hard parts. Continually and under the conditions of normal mortality, elements of this life assemblage enter the local death assemblage. These decompose; some are buried after varying periods of exposure. Then, suddenly, the entire life assemblage is buried and killed by the rapid introduction of a large amount of sediment not unlike the material of the former substrate. The sedimentary body containing the death assemblage is gradually compacted as a result of further accumulation of sediment at the site.

MODEL II: A life assemblage lives in an environment similar to that described for Model I. Continually and under the conditions of normal mortality, elements of the life assemblage enter the local death assemblage. These decompose; some of the remains are carried away, whereas others of durable composition are buried after varying periods of exposure. In time, the local environment changes and the life assemblage is eventually replaced by another of different composition. The death assemblage of interest becomes more deeply buried, and the sedimentary body becomes gradually compacted as a result of further accumulation of sediment at the site.

MODEL III: A life assemblage lives in a restricted area of the sea bottom below the low-tide mark but above the maximum wave base. The water mass moves at a moderate velocity over a bottom of clastic sediments consisting, in large part, of the durable remains of organisms. Frequently the velocity of the water mass is high enough to move sediment and organic detritus through the area. The hydrodynamic circumstances favor the accumulation of organic remains at the site. The sparse fauna consists of a few epifaunal species of scavengers, boring and encrusting organisms. Continually and under the conditions of normal mortality, elements of this life assemblage enter the local death assemblage. These decompose; some of the remains are carried away, whereas others of durable composition are buried after varying periods of exposure. Eventually, the rate of accumulation of organic remains at the site decreases as changes occur in the source areas of the sediment and debris. In time, the zone containing the high concentration of durable remains is buried and gradually compacted as a result of further accumulation of sediment at the site.

The majority of the elements of a fossil assemblage formed under the conditions of Models I and II will have had a history shown as cases 6 and 9 in Figure 1. The majority of remains brought together as in Model III will have had a history shown as case 14.

The unique feature of Model I is the rapid burial of a life assemblage. Such a history is probably rare in the fossil record. Submarine slumping, storms, or rapid deposition off the mouth of a flooding river might achieve this result. Assemblages resembling those to be expected under the conditions of Model II have been encountered in the superficial sediments of Tomales Bay. At most sites sampled, the death assemblage consisted chiefly of representatives of the local life assemblage. A small fraction of each of the samples, however, consisted of the remains of animals now living elsewhere. The conditions described in Model III probably are more common in shallow water

than those of Model I but less common than those of Model II. Environments in which durable hard parts accumulate under some of the circumstances described in Model III have been encountered in Tomales Bay in channels bordering tidal flats, off wave-eroded shores,

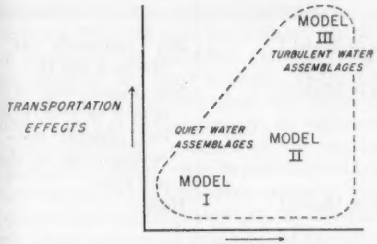

FIGURE 2.—INFERRED RELATIONSHIPS OF THE MODELS

Hypothetical diagram representing the relative alteration of the fossil assemblages resulting from three modes of formation. Model I represents the sudden burial of a life assemblage; Model II, the gradual accumulation and burial of the remains of organisms living at the site of deposition; and Model III, an assemblage comprised almost entirely of transported remains. Exposure effects include degree of abrasion, solution, fragmentation, decomposition, encrustation and boring. Transportation effects include spurious association of species and size sorting. Most fossil assemblages probably occur within the area of the dotted line. Assemblages formed in quiet waters should cluster near Models I and II while those of turbulent water should resemble Model III.

and in very shallow water adjacent to certain beaches. The death assemblages at these sites consist of shells in all states of disintegration. Many complete single valves are present; nearly all show abrasion, boring, and encrustation. Most of the organic sediment, however, consists of riddled and stained angular fragments of shells. Commonly several life assemblages are represented. The inorganic component varies from place to place in composition, size of particles, and proportion to the total sediment. In one area, wave action is eroding fossiliferous Millerton deposits. Off this shore, the fossils of locally extinct Pleistocene species are mingled with the remains of modern forms.

Figure 2 shows the inferred relationships between the model assemblages with regard to exposure and transportation effects. The results of exposure and transportation cannot be sharply distinguished in real circumstances. The introduction or subtraction of elements implies the action of moving water, a principal agent of degradation during local exposure. Introduced elements will contribute previously developed exposure effects to the assemblage. Elements can be subtracted by local destruction as well as by transportation. An assemblage composed largely of exotic elements but exhibiting a miniumum of exposure effects could result from the mass transport of bottom forms and sediments under unusual wave or current action such as might be attained during severe storms. Such assemblages probably are rarely formed in shallow waters. On the other hand, indigenous assemblages can exhibit the entire conceivable range of exposure effects, depending upon the forces in action and the period of time involved. In spite of these complications, Figure 2 provides a medium for viewing a variety of fossil assemblages and a departure point for finding distinguishing features.

The environmental settings and the modes of death and burial specified in the models result in assemblages differing in their relationships to associated sediments and in the degree of exposure effects they exhibit. They should, in theory, influence the following features of the resultant fossil assemblages:

(1) faunal composition
(2) morphologic composition
(3) density of fossils
(4) size-frequency distribution of fossils
(5) disassociation of hard parts
(6) fragmentation of remains
(7) surface condition of fossils
(8) chemical and mineralogical composition of hard parts
(9) orientation of fossils
(10) dispersion of fossils
(11) texture and structure of the sedimentary aggregate.

Table 1 shows the relative expression of these features expected for fossil assemblages formed as in the models. Only the most distinctive or most probable developments of these features are shown.

FAUNAL COMPOSITION: It is expected that many of the species preserved under the conditions of Model I would be associated in death with the species and sediments with which they were associated in life. This is probably also true for Model II assemblages but not for Model III assemblages. By analogy, a faunal list may be translated into collections of modes of life and environmental tolerances. These provide a basis for evaluating the consistency of a particular combination of species with regard to their ecological connotations. For the

TABLE 1.—RELATIVE EXPRESSIONS OF FEATURES DEVELOPED UNDER THE CONDITIONS OF THE MODELS

Only the most distinctive or most probable development is shown.

Feature	Expression		
	Model I	Model II	Model III
Faunal composition	Ecologically coherent assemblage of species	As in Model I	Not necessarily as in Models I and II
Morphologic composition	Delicate structures and heterogeneous shapes and sizes may be preserved. Suites of shapes represented are ecologically consistent.	As in Model I	May consist only of the durable parts of the species present; may be homogeneous in shape and sizes
Density of fossils	Wide range of densities possible	As in Model I	High
Size-frequency distribution	Many species exhibit a size-frequency distribution conforming to an ideal distribution for an indigenous population (Olson, 1957).	Some species as in Model I	Not as in Models I and II
Disassociation	High proportion of articulated remains; disassociated parts represented in appropriate relative numbers for a species	Moderate proportion of articulated remains; disassociated parts as in Model I	Not as in Models I and II
Fragmentation	Low proportion of remains are fragments.	Moderate proportion of remains are fragments.	High proportion of remains are fragments.
Surface condition of fossils	Surfaces of preserved structures as in life.	Various states of wear represented	As in Model II
Chemical and mineralogical composition	No general expectations are warranted by present knowledge in this area.	As in Model I	As in Model I
Orientation	Some species may retain orientation as at time of death.	Majority of fossils oriented with long axis parallel to bedding plane (for exceptions see text)	As in Model II (for exceptions see text)
Dispersion	Articulated remains of some species may retain pattern of dispersion as in life.	Not as in life	As in Model II
Sediment structure and texture	Consistent with inferred tolerances of the fauna and with relatively quiet waters	As in Model I	Not necessarily consistent with inferred tolerances of the fauna; consistent with relatively turbulent waters

ancient fossil record only very broad ecological inferences can be made concerning particular species; other lines of evidence may be necessary in evaluating the ecological homogeneity of ancient assemblages of species. Evidence concerning the composition and sedimentary associations of broadly contemporaneous fossil assemblages can be used to strengthen the analogy.

MORPHOLOGIC COMPOSITION: An assemblage exhibiting delicate structures and heterogeneous shapes and sizes may be preserved under the conditions of Models I and II. Model III assemblages, however, may consist only of the most

durable structures of the species represented and under extreme conditions may consist of elements of similar shape and size. In addition to reflecting exposure effects, the morphologic composition of the assemblage may provide evidence as to the ecological consistency. Shape, growth habit, and shell thickness can serve in this manner for some groups of animals.

DENSITY OF FOSSILS: If assemblages of colonial organisms are excluded, extremely high fossil densities are more probable under the conditions of Model III than for those of Models I and II. Fossil density, as expressed by some convenient measure of the relative proportions of organic remains and sediment, is a function of source (biomass), exposure, rate of deposition, and diagenesis (chiefly compaction). Other sources of evidence are therefore required in order to disentangle the roles played by these factors in any real fossil assemblage.

SIZE-FREQUENCY DISTRIBUTION OF FOSSILS: Under the conditions of Model I, some species should show a size-frequency distribution approximating that of a living population. This result is not probable under the conditions of Models II and III. Further, assemblages of Models I and II should contain forms whose size-frequency distributions conform to those of the complete death assemblage of an indigenous population. This result is not probable under the conditions of Model III. Olson (1957) shows that very precise biological information is required before the size-frequency distributions observed among fossils can be interpreted in these terms.

DISASSOCIATION OF HARD PARTS: Assemblages resulting from the events of Model I would be expected to include a relatively large number of articulated remains. Disassociated skeletal parts would be expected to be represented in appropriate relative numbers in the assemblages resembling Model I. Thus the right and left valves of a species of pelecypod should be present in approximately equal numbers. No such result could be deduced for assemblages resembling Model III. Model II represents assemblages intermediate in these regards. The differences in the strength and means of articulation in different parts of the skeleton and in different organisms complicate attempts to estimate the degree of exposure from the amount of disassociation.

FRAGMENTATION OF REMAINS: The history described for Model III should result in an assemblage of fragments of larger skeletal units. This is certainly the case in the Tomales Bay death assemblages that correspond to Model III. In contrast, a large proportion of the elements of assemblages formed under the conditions of Model I should be unbroken. Model II should result in an assemblage consisting of both broken and unbroken elements. The relative durability of the resistant parts of organisms represented must be considered when assemblages are compared as to fragmentation.

SURFACE CONDITION OF FOSSILS: The surface condition of most of the elements brought together as in Model I should be similar to that in life. The elements of a Model III assemblage, however, might show considerable surface damage as a consequence of wear, collisions in transportation, solution, or the drillings and encrustations of other organisms. Assemblages formed as in Model II would be expected to be intermediate in this regard. Diagenetic processes may also contribute to surface markings or polishing (Pettijohn, 1957, p. 68–72).

CHEMICAL AND MINERALOGICAL COMPOSITION OF HARD PARTS: If primary compositions and diagenetic histories are similar (an unwarranted assumption in most real cases) the chemical and mineralogical composition of elements of a Model III assemblage are likely to be more altered than those of Model I and Model II. At present, our knowledge of the multiple factors involved is insufficient to permit prediction of the geochemical consequences of a specific sequence of events.

ORIENTATION OF FOSSILS: Most of the elements of a Model II or III assemblage would be expected to be oriented with the long axes parallel to the bedding plane where associated with well-sorted sediments of sand size or smaller where the density of the fossils is not high. Under these circumstances, elements may also show a preferred orientation in the plane of bedding in response to a prevailing current direction. A significant proportion of single valves would be expected to be oriented with the concave surfaces downward (Johnson, 1957). When these conditions of sediment and fossil density are not met, interference between shells or between shells and large particles may result in the orientation of the elements at various attitudes. Some of the forms living at the time of rapid burial under the circumstances described for Model I would be expected to retain their primary orientation. Compaction probably would cause some reorientation, but it is not possible to predict the extent without specifying original position, specific features

of the sedimentary aggregate, and the amount of compaction.

DISPERSION OF FOSSILS: Under the conditions described for Model I, the horizontal patterns of dispersion in life may be retained among several species of the death assemblage. No such result could be expected for Models II and III. Life patterns of dispersion are known for only a few marine invertebrates (Connell, 1956; Johnson, 1959). Observation shows that within their general area of habitation, sedentary species are seldom evenly or randomly dispersed. Within the aggregation of individuals, however, random, even, and clustered patterns of distribution have been encountered in different species. The vertical aspect of a life pattern of dispersion in most fossil assemblages is expected to be readily obscured by succession of generations and compaction.

TEXTURE AND STRUCTURE OF THE SEDIMENTARY AGGREGATE: Assemblages of the Model I type would be expected to be associated with sedimentary features consistent with the inferred tolerances of the fauna and with relatively quiet waters. Assemblages arising under the conditions of Model III could be associated with sediments inconsistent with the fauna (*e.g.*, rock-bottom forms associated with sands), and they may exhibit the effects of strong waves or currents. Thus sedimentary features may indicate the ecological consistency of the fauna with respect to the inferred substrate and water movements. Particle size, sorting, and wave and current structures may imply current systems competent enough to effect the transportation of elements to and from the site.

For each of the features of a fossil assemblage it is possible to conceive of circumstances in which a similar expression results from dissimilar histories. Thus compound evidence should be used to determine mode of formation. One inherent weakness of this principle is the tacit assumption that each line of evidence can contribute equally to the strength of a working hypothesis.

The models considered here indicate that biological criteria, such as ecological coherency, are less ambiguous than physical characters. Ecological coherency and size-frequency distribution reflect transportation more directly than exposure effects, which can be developed without transportation. The biological criteria, however, depend on fundamental knowledge which usually is not available. It appears that knowledge of the organization and dynamics of populations of marine organisms (as well as of the physical processes operating on death assemblages) is critical to understanding the nature of fossil assemblages.

In their most distinctive development and taken all together, the features considered here discriminate between assemblages of the Model I and III types. Model II gains its distinctive character, under these conditions, by compromising the differences between the others. As noted previously, real fossil assemblages vary as a continuous series with regard to their suite of characters, so that no set of criteria can delimit all possible variations. It seems possible, theoretically at least, to compare actual fossil assemblages by reference to the extreme development of such features as described here. As knowledge of marine biology increases and the formation of modern death assemblages is studied, the criteria almost certainly will be refined and the number of criteria increased.

METHODS OF STUDY

The principal objective in most paleontological field work is the collection of fossils. Observations upon mode of occurrence of fossils, if made at all, generally are recorded in qualitative terms as supplementary information. For these purposes the field observations of a careful worker may suffice. As attention is focused upon paleoecology, however, systematic and objective observations are required. Fossil assemblages must be compared in the context of their mode of formation. Measures which can be used to reconstruct the history of a fossil assemblage must be developed in connection with studies of modern death assemblages. Only in this way can observational data be substituted for many of the speculations now relied upon to relate measures to events. Many measures appropriate to the features discussed in the preceding section have been in use for some time (*e.g.*, Imbrie, 1955).

Many of the features of interest herein can be observed only in the undisturbed assemblage at an outcrop. Taking samples to the laboratory and breaking down the matrix destroys some of the most important relationships. Careful dissection of block samples is so time consuming as to severely restrict the number of samples that can be used in a particular study. The writer in an investigation of the Pleistocene Millerton formation of Tomales Bay, California, adapted the "stretched-line" method used by plant

ecologists to the sampling of outcrops. In this method a line is stretched across the face of an outcrop, parallel to the planes of bedding. The distance between each fossil encountered along the line is measured. The orientation and state of articulation and preservation are recorded for the entire structure or debris pile represented in part on the sampling horizon. Each specimen is collected, measured, examined for surface features, and identified. From these data a scaled, strip diagram can be constructed showing the distribution and properties of the fossils at the outcrop as sampled along the line. Such a diagram can be used to study the linear pattern of dispersion.

The universe that is sampled in this manner is the face of the outcrop. The number of lines and length of each of them are determined by the objectives of the study and the size and form of the outcrop. In the Millerton study, the zone of interest seldom exceeded 1 m vertically and 3–4 m horizontally. Each line extended the length of the zone, and no more than three lines, randomly place one above the other, were required. As a check on the sampling and the criteria used to select the zone of interest, one narrow zone was sampled throughout its length at four horizons. The data show remarkably good agreement between lines.

The advantages of this sampling procedure are: it provides a means of observing and retaining for study the features of the assemblage as observed in place; it provides a means of treating each outcrop identically; it establishes a context for the precise definition of measures; a relatively large number of features can be measured in a short period of time; and finally, it reduces bias in the collection of fossils.

The disadvantages of this sampling method are, in general, the same as those for the other methods now in use. It is almost entirely restricted to sediments in which fossils can be recovered readily. Care must be taken to sample relatively fresh surfaces in order to avoid, so far as possible, the mechanical effects of weathering. Another disadvantage of the method, as used in the Millerton study, is that the horizontal aspects of the assemblage are overly emphasized. This objection might be overcome by using both vertical and horizontal lines. Many problems also arise in using such samples for statistical inference of the properties of the fossil assemblage in three dimensions. This last weakness certainly is not peculiar to the method of sampling proposed here. The progress of other sciences concerned with somewhat similar problems leads the writer to believe that a satisfactory solution can be achieved.

Relationships Between Measures

If compound evidence is to be used to select the most probable history for a fossil assemblage, it is necessary to know something of the relationships of the several kinds of evidence relied upon. One way of gaining such information from the data provided by line samples can be illustrated as follows. The relationships between 9 variables were studied in 11 line samples of the Millerton formation, involving the occurrence of 607 fossils. These variables were taken as representing some of the features of fossil assemblages that can be influenced by the mode of formation as discussed earlier. The variables studied were line density, percentage of fragments, percentage of articulated remains (pelecypods), percentage of pelecypod valves oriented with concave surfaces downward, median size of sediment, coefficient of sediment sorting, median size of fossils, and coefficient of fossil sorting. The data were analyzed by computing a rank-correlation coefficient for all possible and meaningful combinations (Dixon and Massey, 1951). Thirty-three such combinations were chosen. Table 2 shows that the hypothesis of independence was rejected in only three instances. These were percentage of fragments and shell sorting, percentage of articulated remains and median shell size, and percentage of articulated remains and shell sorting. In the last case a negative relationship is indicated by the test. These results appear reasonable, but more diversified samples are needed before general conclusions can be drawn concerning the interrelationships of the features represented by the measures. An expanded study of this kind is essential to reduce circularity and to evaluate the relative contributions of such evidence in development of hypotheses on mode of formation.

Discussion

A fossil assemblage can have little paleoecological significance if it is not possible to reconstruct, at a high level of confidence, the sequence of events leading to its formation. This contention is supported by the number and nature of the alternative histories possible for elements of life and death assemblages. The geological history of the remains of any organ-

ism is a record of continuous alteration leading to its ultimate destruction as a biological entity. Samples are drawn from assemblages in varying stages of degradation. If these materials are to be used to obtain new knowledge, we must be able to eliminate effects introduced by the mode of formation of fossil assemblages and their subsequent geologic history. This might be accomplished in several ways. We could frame our study so as to employ only those features of a fossil assemblage that can be assumed to have been the least modified (*See* Miller and Olson, 1955 for a more complete discussion of this argument). If we do so, we must concentrate on a very few aspects of the assemblage and have a strong belief in our assumptions. Another approach is to attempt to understand the operation and results of the processes affecting death and fossil assemblages. With such knowledge it may be possible to reduce the inherent bias by recognizing and correcting for its effects in our analysis of data. This approach is potentially the most efficient means of utilizing the fossil record but requires fundamental knowledge in biology and geology which, for the most part, is not now available.

There appear to be three principal sources of bias in the record of an ancient community. These are (1) the selectivity of the destructive processes operating upon death assemblages, (2) the mixing of indigenous and exotic elements in a death assemblage, and (3) the physical and chemical alteration of fossils and enclosing sediment. Direct study of the selective processes operating upon modern death assemblages should provide a basis for more refined interpretations of the discrepancies of the fossil record. In addition, studies on the ecological structure of marine communities are needed for inference of some, at least, of the ecologic roles not represented by fossils. However, since organisms have evolved and physical environments have changed in time, high levels of confidence cannot be placed in explicit inferences concerning those portions of the community that have not been preserved.

TABLE 2.—RANK-CORRELATION COEFFICIENTS FOR MEASURES TAKEN IN 11 LINE SAMPLES OF THE MILLERTON FORMATION OF TOMALES BAY, CALIFORNIA

	%f	%a	%I	%-	mss	css	msf	csf
ld	−0.10	−0.26	−0.55	0.51	0.07	0.31	0.00	0.48
%f	..	†	0.30	−0.16	0.12	0.05	−0.53	0.61*
%a	..	..	0.08	0.24	−0.18	−0.30	0.60*	−0.79*
%I	..	..	..	0.21	0.08	−0.38	−0.18	0.01
%-	..	..	..	..	0.40	0.10	0.31	−0.18
mss	..	..	..	..	..	†	0.30	0.00
css	..	..	..	..	..	..	−0.10	0.28
msf	..	..	..	..	..	..	..	†

* hypothesis of independence rejected at the 5 per cent level of significance

† considered not meaningful

ld—line density; %f—percentage of fragments; %a—percentage of articulated remains; %I—percentage of elements oriented with the long axis parallel to the bedding plane; %-—percentage of pelecypod valves oriented with concave surfaces downward; mss—median size of sediment; css—coefficient of sediment sorting; msf—median size of fossils; csf—coefficient of fossil sorting

The mixing of indigenous and exotic elements can affect both the physical and biological nature of the resultant death assemblages. The implications developed from the models discussed herein are that biological criteria are more indicative of transportation than the physical features. Use of biological criteria requires knowledge of morphology and adaptation, patterns of spatial distribution, size-frequency distributions in stable and unstable populations, and the environmental tolerances and preferences of kinds of marine organisms. The application of such knowledge to ancient communities involves a high degree of uncertainty but the information available from the composition and associations of broadly contemporaneous fossil assemblages can be used to strengthen the chain of analogy.

The bias that results from the physical and chemical alteration of fossils and enclosing sediments can be recognized and corrected only with the aid of supplementary data not

now available. Field and laboratory studies of diagentic processes are greatly needed.

Until supplementary knowledge concerning the sources of bias is available, analysis of the mode of formation and preservation of fossil assemblages must be based upon theoretical foundations. The models proposed here are suggested as devices for comparing actual fossil assemblages in these regards. Their use permits us to relate fossil assemblages as to the general degree of disturbance without specifying, in detail, the causes of disturbance. New methods of study must be developed in the context of both theory and the practical limitations of the outcrop. The "stretched-line" method for obtaining field data is suggested as one effective means of obtaining pertinent data.

Selected Bibliography

Boucot, A. J., 1953, Life and death assemblages among fossils: Am. Jour. Sci., v. 251, p. 25–40

Boucot, A. J., Brace, W., DeMar, R., 1958, Distribution of brachiopod and pelecypod shells by currents: Jour. Sed. Petrology, v. 28, p. 321–332

Connell, J. H., 1956, Spatial distribution of two species of clams *Mya arenaria* L. and *Petricola pholadiformis* Lamarck in an intertidal area: Investigations Shellfisheries Mass., rept. no. 8, p. 15–28

Dixon, W. J., and Massey, F. J., 1951, Introduction to statistical analysis: N. Y., McGraw-Hill Book Co., 370 p.

Imbrie, J., 1955, Biofacies analysis, p. 449–464 *in* Poldervaart, Arie, *Edtior*, Crust of the earth: Geol. Soc. America Special Paper 62, 762 p.

Johnson, R. G., 1957, Experiments on the burial of shells: Jour. Geology, v. 65, p. 527–535

——1959, Spatial distribution of *Phoronopsis viridis* Hilton: Science, v. 129, p. 1221

Ladd, H. S., 1957, Paleoecological evidence, p. 31–66 *in* Ladd, H. S., *Editor*, Treatise on marine ecology and paleoecology, v. 2, Paleoecology: Geol. Soc. America Mem. 67, 1077 p.

MacGinitie, G. E., 1935, Ecological aspects of a California marine estuary: Am. Midland Naturalist, v. 16, p. 629–765

Menard, H. W., and Boucout, A. J., 1951, Experiments on the movement of shells by water: Am. Jour. Sci., v. 249, p. 131–151

Miller, R. L., 1956, Speculation on water currents in a black shale environment (Abstract): Am. Geophys. Union Trans., v. 37, p. 354–355

Miller, R. L., and Olson, E. C., 1955, The statistical stability of quantitative properties as a fundamental criterion for the study of environment: Jour. Geology, v. 63, p. 376–387

Olson, E. C., 1957, Size-frequency distribution in samples of extinct organisms: Jour. Geology, v. 65, p. 309–333

Payne, T. G., 1942, Stratigraphical analysis and environmental reconstruction: Am. Assoc. Petroleum Geologists Bull., v. 26, p. 1697–1770

Pettijohn, F. J., 1957, Sedimentary rocks: 2d ed., N. Y., Harper Bros., 718 p.

Thorson, G., 1957, Bottom communities (sublittoral or shallow shelf), p. 461–534 *in* Hedgpeth, J. W., *Editor*, Treatise on marine ecology and paleoecology, v. 1, Ecology: Geol. Soc. America Mem. 67, 1296 p.

Department of Geology, University of Chicago, Chicago, Illinois

Manuscript Received by the Secretary of the Society, December 9, 1958

BULLETIN OF THE GEOLOGICAL SOCIETY OF AMERICA
VOL. 71, PP. 1087–1108, 12 FIGS., 1 PL. JULY 1960

SUBMARINE TOPOGRAPHY IN THE GULF OF ALASKA

By William M. Gibson

Abstract

A bathymetric chart of the Gulf of Alaska and approaches covering an area of about 800,000 square nautical miles has been prepared from Coast and Geodetic Survey hydrography, 1925–1957, with a view to defining regional physiographic provinces.

The basic data comprise 90 sounding lines across the gulf, 42,000 miles of graphically recorded profiles obtained during the last 5 years, and detailed surveys of 60 seamounts, seaknolls, and ridges. Tentative names are assigned principal features of the sea floor to facilitate discussion.

The bathymetry and illustrated profiles reveal clearly the form of the Aleutian Trench, two submarine mountains, several seamount chains and groups, a ridge and trough province, a 200-mile trench west of Vancouver Island, a great trough paralleling the West Coast, and an inferred fracture zone extending in several wide echelon bands across the gulf.

The submarine topography is discussed in relation to existing theories of earth science and correlated with features previously mapped on the mainland and in the Central Pacific Ocean.

TEXT

	Page
Introduction	1087
Acknowledgments	1088
Surveys	1088
Submarine terminology	1089
Description of the gulf coastal area	1089
General description of the gulf floor	1090
Western and northern margin	1090
General description	1090
Continental shelf	1091
Continental slope	1091
Aleutian Trench	1092
Western floor of the gulf	1093
Eastern margin	1094
Great Trough	1096
Ridge and Trough province	1097
Kodiak Seamount Chain	1100
Mid-Gulf zone	1101
Parker-Bean and Patton-Faris seamount groups	1102
Unimak-Sirius Seamount Chain	1104
Columbia fracture zone	1105
Interpretation	1105
References cited	1107

ILLUSTRATIONS

Figure	Page
1. Great Circle map of structural lineations.	1091
2. Transverse profiles of the Aleutian Trench, Cape St. Elias to Unimak Pass	1092
3. Axial profile, floor of the Aleutian Trench	1093
4. Transverse profiles adjusted normal to axis, Surveyor Deep-sea Channel	1094
5. Transverse profiles of continental slope, eastern margin of Gulf of Alaska	1095
6. Transverse profiles, Baranof Sea Valley	1096
7. Transverse profiles, Moresby Sea Valley	1097
8. Transverse profiles, Explorer Trench	1098
9. Transverse profiles, Ridge and Trough province	1099
10. Transverse profiles, Mid-Gulf zone	1102
11. Profiles along the Patton-Faris Seamount Group	1103
12. Transverse profiles across Parker-Bean and Patton-Faris seamount groups	1104

Plate	Facing page
1. Bathymetric chart showing submarine topography in the Gulf of Alaska and locations of illustrated profiles	1108

Introduction

This study of submarine topography in the Gulf of Alaska and approaches embraces an area of about 800,000 square nautical miles. Although the whole area is referred to as the Gulf of Alaska in this report, the name applies to a more limited northern area.

Knowledge of this region was sketchy until the Coast and Geodetic Survey initiated a program of running deep-sea traverses in 1925. For several years sounding lines were obtained only on the return trip of survey ships after the season's work in waters of western Alaska. In more recent years, because of modern navigation requirements and increased interest of marine biologists, oceanographers, seismologists, and geologists, sounding lines were run on

each crossing. Limited-area surveys of seamounts and other features were also made en route. It is a continuing program.

The Gulf of Alaska was formerly included on Coast and Geodetic Survey Chart 9000 at very small scale, 1:5,000,000; but in 1952 the first edition of Gulf of Alaska Chart 8500 was published at scale 1:2,100,000. The depth-contour interval of 500 fathoms on this larger-scale chart does not, however, reveal the secondary features so important to a study of submarine topography. First details of the gulf topography were presented by Murray in 1941, followed in 1945 by his report on the Aleutian Trench. In 1951 Menard and Dietz presented a comprehensive geological study of the area. This study was based largely on the Coast and Geodetic Survey deep-sea hydrography, supplemented by sounding lines obtained by Navy ships. The results of a joint exploration by the Navy Electronics Laboratory and Scripps Institution of Oceanography in 1951, including the dredging of tops of seamounts and coring the sea floor, were presented by Menard in 1953. In 1955 Menard reported further studies of the Gulf of Alaska.

A considerable accumulation of original ship observations, including graphically recorded profiles of the floor and seamounts, was available for this study. The fathogram profiles are reconstructed in several illustrations presented here, because various scales and vertical exaggerations resulted from the use of several types of echo sounders and also from the effect of different ships' speeds.

Although bathymetric details of this report are considered to be almost complete in certain areas, considerable surveying is still needed to delineate all features in detail. Many sections of the depth contours could rightly be represented by broken lines; solid-line bathymetry is presented with this qualification. An indication of the density of deep-sea sounding lines on which this study is based is given in the index-map inset on Plate 1. Numerous peak depths of seamounts were deleted from copies of the survey sheets used in this study. In recent years, survey information of this nature has not been available for unrestricted publication. A discussion of flat-topped seamounts versus seapeaks is therefore not included in this report. Reference is made to unpublished results of the Chinook and Mukluk expeditions made by scientists of Scripps Institution of Oceanography in 1956 and 1957. Geophysical data collected on these expeditions sponsored by the Office of Naval Research and Bureau of Ships will add materially to existing knowledge of the northeastern Pacific area.

Acknowledgments

The officers and men of the ships and the cartographers in the Washington Office of the Coast and Geodetic Survey have made this work possible, but special credit should accrue to those who set the initial and continuing policy of providing the hydrographic coverage of this great area at little or no extra cost to the Government. Rear Admiral H. A. Karo participated in both the field and office work, encouraged preliminary study, and lent direction and assistance in the presentation.

Inasmuch as the study was made away from the depository of survey records in the Washington Office, valuable assistance at that office was given by G. F. Jordan in the preparation and review of illustrative material.

Surveys

The hydrographic surveys from which the bathymetry on Plate 1 was developed are composed of a continuing accumulation of deep-sea sounding lines obtained en route to and from coastal areas of western Alaska. These reconnaissance surveys have greatly improved in quality in recent years.

The early traverses relied solely on astronomic observations for positioning. Overcast and storms were often experienced on return trips in September, and occasional dead-reckoning courses for long stretches resulted. Depths were ascertained at intervals by sonic reflections read at an instant on a calibrated dial or timed to hydrophone reception. Early improvements in echo sounders were soon reflected in nearly continuous and more reliable soundings. An eventual adjustment of these traverses was contemplated at a later date when the framework of well-controlled lines became established. The very large amount of work required in the analysis of control data in the proposed adjustment is now considered unwarranted. Inadequacies in the early lines do not materially affect small-scale deep-sea charting.

Most traverses and all the limited-area surveys were made in more recent years with benefit of loran positioning and modern recording-type ultrasonic sounders. A large accumulation of well-controlled graphic profiles has resulted. On both outbound and inbound

trips the ships survey seamounts and other features which lie on or adjacent to their traverses. The traverses and limited surveys are planned each year to fill voids in untraversed areas. Lines necessarily converge at the end of the Alaska Peninsula, Kodiak, and Strait of Juan de Fuca. Also, traverses have been concentrated in seamount areas to permit surveys of the features discovered on earlier crossings. These detached surveys have now covered 60 seamounts, ridges, and knolls. Total crossings amount to 90, including the 1957 lines. In the past 5 years 42,000 nautical miles of graphically recorded profiles were obtained in this area by ships of the Coast and Geodetic Survey.

Submarine Terminology

During the exploration and hydrographic development of the Gulf of Alaska and approaches, the names of ships and deceased hydrographers had been assigned to many undersea features. In some cases the names were applied before the form and extent of a feature were adequately known. On the basis of present knowledge some names might be appropriately changed or omitted, as in the case of several peaks rising from a common elevated platform, each having in common usage the name of an early hydrographer. Clarity and simplicity would be furthered if one name were used for the whole structure and the individual peaks named only if their importance warranted.

It is not the scope of this work to change names in current use, but the application of names to currently mapped or previously unrecognized features of the sea floor is necessary to facilitate discussion. New names assigned in this study are in general accord with principles adopted by the International Committee on Nomenclature of Ocean Bottom Features, as given in the minutes of the September 22, 1952, meeting at the International Hydrographic Bureau at Monaco, and in accord with criteria recently established by the Undersea Features Nomenclature Committee at the Navy Hydrographic Office. Since advance approval of a large number of new names by The International Committee, which meets only every 3 years, is not considered practical, those used in this study are tentative.

The agreed general principles are an excellent guide but lack sufficient detail to permit noncontroversial selection. The International Committee has defined a ridge as a long elevation of the deep-sea floor having steeper sides and less regular topography than a rise; seamount is defined as an isolated elevation of the deep-sea floor of about 3000 feet or more and circular or elliptical in form. The term "ridge" has been applied previously to immense structures like the Mid-Atlantic Ridge. Throughout the area of this study are weltlike forms 20–90 miles in length and about 10 miles in width. These structures do not differ greatly from the welts forming the Ridge and Trough Province off the West Coast (Menard and Dietz, 1951, p. 1274). They are termed ridges in this study.

The International Committee favors geographic names over personal names (Wiseman and Ovey, 1954, p. 93), but judgment is required in the application of geographic names derived from continental features to remote submarine forms on the floor of the Gulf of Alaska in a different structural region. Accordingly, new features that cannot be reasonably correlated with an existing geographic name have been assigned appropriate ships' names or names of deceased hydrographers and others identified with exploratory surveys of the region.

Description of the Gulf Coastal Area

The Alexander Archipelago and Vancouver Island stand like guards off the mainland of Canada and Alaska for a distance of 750 miles between Cape Spencer and the Strait of Juan de Fuca. The islands are interspersed throughout a broad and shallow trough lying between the shelf edge and the mainland. The shallow trough, a variation from the usual continental shelf, fringes the entire Gulf of Alaska from Queen Charlotte Sound to Unimak Island. It ends abruptly at the entrance of Queen Charlotte Sound where it intersects the trend of the continental slope at an angle of 45°.

The islands of the Alexander Archipelago are mountainous throughout and are separated by depths to 400 fathoms. A large part of the Behm Canal, which winds around Revillagigedo Island between peaks 2000–4000 feet high, is more than 300 fathoms deep. Clarence Strait and Ernest Sound to the north of Dixon Entrance are 200–350 fathoms deep, as is Sumner Strait. Chatham Strait is 3–8 miles wide, more than 400 fathoms deep in many places, and 200 fathoms deep at Skagway located 200 miles north of the entrance. St. Amand (1957, p. 1351) suggested that this strait is a portion of the great Denali fault curving west and southwest to the Bering Sea.

Northward from Cape Spencer the character of the coastal zone has been modified by recent glaciation, general uplift, and local subsidence (Plafker and Miller, 1957; Miller, 1953; 1957; Jordan, 1958; Gibson, 1958). The rapid recession of ice in the prominent bays is well-known. The area lying between the coast and the Fairweather and Chugach-St. Elias faults is the Gulf of Alaska Tertiary province; high-angle faulting, great uplift, and numerous glaciers are prominent features. The bases of the glaciers lie below sea level and are separated from the sea by a low coastal plain consisting of recent accumulations along the western margin of the ice.

The Gulf of Alaska Tertiary province has a number of other known faults. The Sullivan fault roughly parallels the Chugach-St. Elias fault but turns abruptly seaward toward the Aleutian Trench at Cape Yakataga (Miller, 1957, Sheet 1, Map OM 187 Sheet 1).

An abrupt change in the trend and form of the shore line and continental shelf occurs at Kayak Island. The Copper River delta is fringed on the south by low offlying islands and on the west by northeasterly trending Montague and Hinchinbrook islands which tend to enclose the deep water of Prince William Sound. The coast between Cape St. Elias and Cook Inlet is everywhere deeply indented with deep bays in contrast to the more regular shores and shallow bays along the Gulf of Alaska Tertiary province. Shelikof Strait and Cook Inlet have been inferred to occupy the site of an ancient trench in Mesozoic time (Menard and Dietz, 1951, p. 1277–1279). Kodiak Island and the Alaska Peninsula have deeply indented coasts similar to those of the Kenai Peninsula. The greater width of the continental shelf westward from Cape St. Elias contains a chain of islands including Kayak, Middleton, Kodiak, Chirikof, Trinity, Semidi, and the Shumagins. Many shallow canyons and submarine troughs cross the sound transversely.

Field examinations of the entire coast and adjoining interior made by the U. S. Geological Survey from the Alaska Peninsula opposite Kodiak to Cape Spencer show many alternating geanticlines and geosynclines ranging in age from Triassic to Tertiary (Payne, 1955). They are practically continuous around the great bight of the Gulf of Alaska and include the Yakataga geosyncline, a Tertiary element overlapping the coast and shelf and fronted by the Aleutian Trench. The geosynclines and geanticlines are progressively younger toward the sea.

General Description of the Gulf Floor

The floor of the Gulf of Alaska is in general a fairly smooth plain except where broken by seamounts and ridges and cut by the major Aleutian Trench and minor troughs. It dips westward and southwestward from the eastern margin. The entire floor is traversed from southeast to northwest by echelon lines of seamounts and ridges. Three or four fairly definite lineations cross the Ridge and Trough province transversely and are in turn crossed by transverse structures in the Mid-Gulf zone. Most of the significant features of the sea floor are aligned in trends which converge upon the approaches to Queen Charlotte Sound. Kodiak Seamount Chain and the Ridge and Trough province (Fig. 1) are the principal converging lineations. A slight trough of great width parallels the coast southward from the Queen Charlotte approaches to the Mendocino Seascarp. Explorer Trench, which resembles a great thrust fault, borders the trough for about 200 miles on the west.

The continental slope constitutes a great escarpment that descends from the shelf edge to a base at varying depths along the eastern margin and to the bottom of the Aleutian Trench on the west and north. The base of the escarpment is very irregular in depth on the east and is broken off at Queen Charlotte Sound by a trench and sea valley and off Queen Charlotte Islands by a parallel ridge and trough. The intermittent bench along the northwest wall of the gulf seems to describe in general an old base of the continental slope. The sea floor south of the Alaska Peninsula and Aleutian Trench rises from the bottom of the trench and descends again to the general floor of the gulf, thus describing a feature similar to an anticline. The anticline contains a great variety of superficial forms and is cut by seamount zones.

Some significant features of minor relief have been detected in the hydrography obtained in recent years with recording echo sounders, but further survey work is needed before discussion of minor relief is warranted.

Western and Northern Margin

General Description

The western and northern margin of the Gulf of Alaska comprises: (1) the wide trough or shelf containing Kayak, Middleton, Kodiak, Chirikof, Trinity, Semidi, Shumagin, and Sanak islands;. (2) the shallow troughs ex-

tending across the continental shelf transversely and including Cook Inlet and Shelikof Strait; (3) the continental slope and north slope of the Aleutian Trench including Pamplona Ridge,

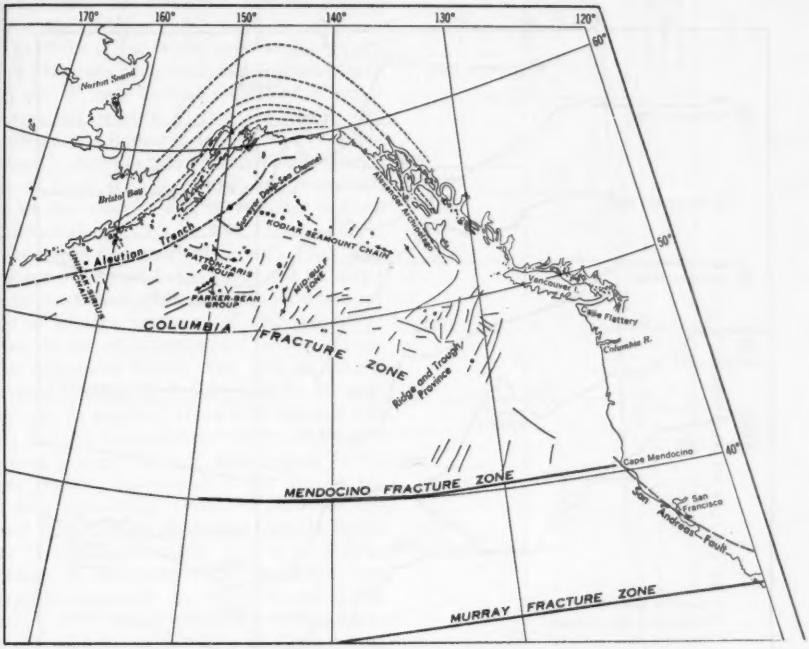

FIGURE 1.—GREAT CIRCLE MAP OF STRUCTURAL LINEATIONS

Shuyak Seamount, Unimak Seamount, a few seaknolls, and numerous steps and benches; (4) the Aleutian Trench with Kodiak Seamount; (5) the southerly slope of the trench with Dall and Derickson seamounts, Surveyor Deep-sea Channel, and the western base of the Patton-Faris Seamount Group; (6) the southerly rise from the Aleutian Trench, which includes many isolated seamounts; seamounts and lesser features associated with the Patton-Faris and Parker-Bean seamount groups, and the Unimak-Sirius Seamount Chain.

Continental Shelf

Detailed discussion of the coastal margin with its broad shelf, islands, and submerged rises and transverse troughs is omitted from this study. The continental shelf is referred to below only where regional considerations are involved.

Continental Slope

The steplike descent of the continental slope and the north slope of the Aleutian Trench is illustrated on the transverse profiles in Figure 2. Most prominent of the steps is the Aleutian Bench first recognized by Murray (1945, p. 775). He described this 20-by-70-mile feature as extending from Unimak Island to the Islands of the Four Mountains, the western limit of the offshore surveys at that time. Subsequent surveys reveal the westward continuity of the bench (Gibson and Nichols, 1953, p. 1178: Gates and Gibson, 1956, p. 143). Profile A6 (Fig. 2) shows that the bench is a smooth level plain 15 miles wide, but it becomes troughlike westward, particularly midway in the Aleutian Arc where a broad trough is flanked seaward by extensive ridges rising more than half a mile above the trough floor. Profile A5 shows the eastern end of the bench broken by Unimak Seamount, a ridgelike structure 10 miles wide and 30 miles long. A very irregular bench of limited extent lies in 1500-fathom depths south of Middleton Island. Shuyak Seamount and

several lesser structures rise from this bench. At the head of the trench south of Cape St. Elias (Profile A1), a prominent seaknoll marks a step, also in 1500-fathom depths. Immediately beyond the head of the trench is an extensive continental slope, superimposed seamounts and seaknolls, and varied depths are indicative of echelon faulting along lines parallel to or slightly converging northeastward toward the axis of the Aleutian Trench.

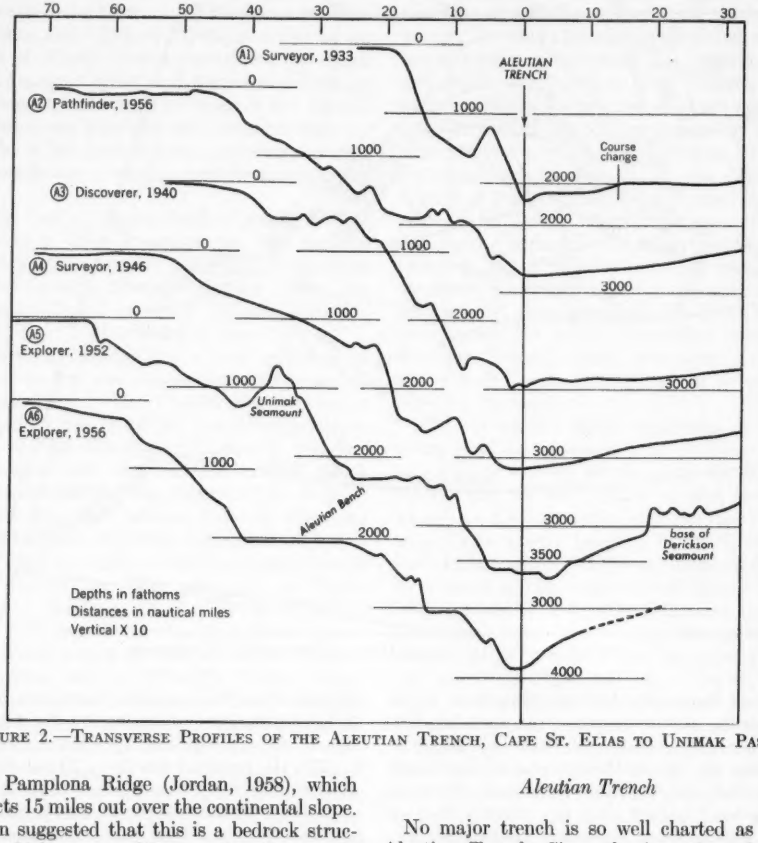

FIGURE 2.—TRANSVERSE PROFILES OF THE ALEUTIAN TRENCH, CAPE ST. ELIAS TO UNIMAK PASS

spur, Pamplona Ridge (Jordan, 1958), which projects 15 miles out over the continental slope. Jordan suggested that this is a bedrock structure which was uplifted and subsequently foundered.

Although the benches lie well above the general level of the gulf floor, they are roughly at a depth of the foot of the continental slope in other sections. In other portions of the continental slope no definite line of demarcation may be seen between the slope and the trench. The Aleutian Bench appears to lie at or near the geographic extension of the axis of the Yakataga geosyncline, a Tertiary tectonic element mapped by the U. S. Geological Survey westward to western Kodiak (Payne, 1955). The more or less troughlike forms of the

Aleutian Trench

No major trench is so well charted as the Aleutian Trench. Since the inception of the Coast and Geodetic Survey's program to explore major bottom features the hydrographic coverage has become almost complete. Unfortunately most of the lines for which fathograms are available crossed the trench at acute angles. Most of the normal crossings were obtained before the advent of recording fathometers. These were specific transverse profiles reported by Murray (1945, p. 765–773). No attempt has been made to illustrate the actual fathograms obtained over the trench and continental slope because of various scale factors and difficulty in comparing profiles run in opposite directions.

Plate 1 shows the Aleutian Trench as an asymetrical depression bordering the foot of the continental slope, and Figure 2 contains six profiles for illustrating the detailed form at widely separated crossings. Figure 2 is intended to supplement the numerous excellent profiles by Murray (1945).

The strike of the trench axis ranges from S. 40° W. between Middleton and Kodiak islands to S. 67° W. near Unimak Seamount. There is an apparent reversal to the east in the area southeast of Middleton Island. The principal changes in direction occur about 60 miles southwest of Cape St. Elias, at Kodiak Seamount, and at the western end of the Patton-Faris Seamount Group.

The trench floor south of Cape St. Elias (Fig. 3) slopes downward to the southwest for about 400 miles at the approximate rate of 4 feet per mile to a point southeast of Chirikof Island where the trench is intersected by the Patton-Faris Seamount Group. The rate of descent increases to about 21 feet per mile for the next 200 miles to depths of about 3700 fathoms and then flattens to general depths of about 3950 fathoms beyond the limit of Figure 3. If the lesser gradient, comparable to the slope of the sea floor east of the trench, is projected up-trench from Unimak Seamount then the raised floor of the trench might be due to a large build-up of sediments. This possibility was originally suggested by Menard and Dietz (1951, p. 1279–1282). Their hypothetical blanket of sediment at the base of Kodiak Seamount (GA-1) is of the same general magnitude as that inferred in Figure 3 of the axial profile of the Aleutian Trench.

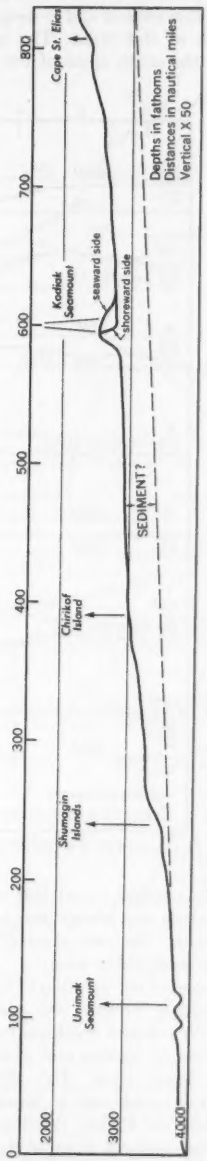

FIGURE 3.—AXIAL PROFILE, FLOOR OF THE ALEUTIAN TRENCH

WESTERN FLOOR OF THE GULF

The floor of the gulf east of Kodiak Island and the Aleutian Trench is a vast plain sloping downward to the axis of the trench from the continental slope on the east. These slopes are traversed by seamount zones but not materially altered in general. The floor flattens between the 2000- and 2200-fathom curves, and in this area major tablemounts and the Surveyor Deep-sea Channel (Gibson, 1958) are found. The latter feature parallels the Aleutian Trench for about 250 miles, then curves west and northwest to intersect the Aleutian Trench at a point about 60 miles southwest of Kodiak Seamount. It is 2–3 miles wide and 500–1000 feet deep over most of its length. Profile B4 (Fig. 4) shows the form of the channel at a point about 5 miles

northwest of Giacomini Seamount. It has a more regular cross section and is deeper southwest and west of this point. The maximum depths are on the south slope of the Aleutian marked by a cluster of seaknolls circumscribed by the 2500-fathom curve, Wildcat and Sirius seamounts. It is also marked by a low western extension of the Parker-Bean Seamount Group.

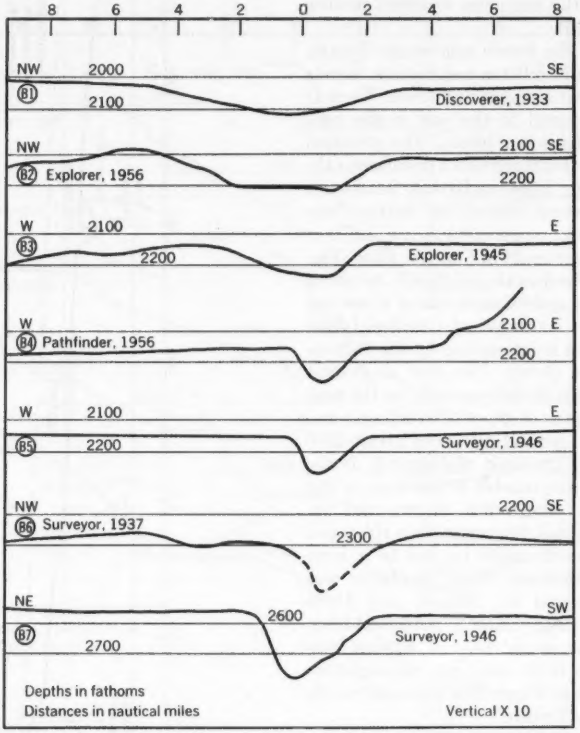

FIGURE 4.—TRANSVERSE PROFILES ADJUSTED NORMAL TO AXIS, SURVEYOR DEEP-SEA CHANNEL

Trench. In the original report this author described the feature as a trough, but subsequent consensus reveals "deep-sea channel" to be a more generally acceptable term.

South and west of the junction of the channel with the Aleutian Trench, the plain of the western gulf floor slopes southward and is extensively broken by groups and chains of seamounts and lesser rises. The Patton-Faris Seamount Group rests on a transverse rise which constricts the trench. Southwest of this constriction the southern slope of the Aleutian Trench culminates in a slight rise. This rise resembles an anticline which continues to the limit of Plate 1 and probably for most of the distance to the end of the trench. It is delineated by a loop of the 2600-fathom curve and is

In addition to the Aleutian Trench rise the western margin of the gulf floor is marked by seamounts along the south slope of the trench. Derickson, Walls, Chirikof, and Dall seamounts are aligned at a distance of 30 miles from the trench axis.

EASTERN MARGIN

The Aleutian Trench is not evident eastward of a line passing south from Kayak Island, although there are slight indications of a submarine canyon traversing the continental slope along the approximate alignment of the axis (Fig. 5). Here the Gulf of Alaska Tertiary province extends about 30 miles back from the coast line between Copper River and Lituya

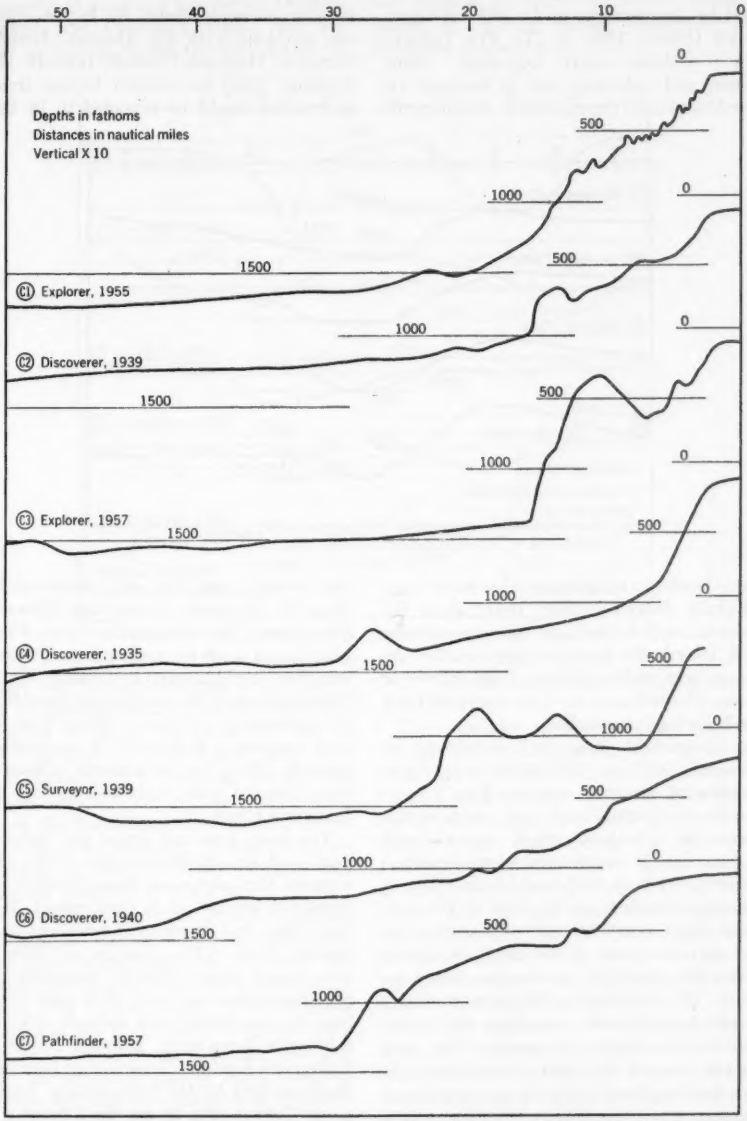

FIGURE 5.—TRANSVERSE PROFILES OF CONTINENTAL SLOPE, EASTERN MARGIN OF GULF OF ALASKA

Bay (Menard and Dietz, 1951, p. 1279; Miller, 1957; Plafker and Miller, 1957). The province is bordered on the east by the Chugach-St. Elias and Fairweather faults and is occupied by a number of glaciers. A low flat coastal area has built up on the seaward side of the glaciers. Pamplona Ridge (Jordan, 1958) and Yakutat Bay are examples of local subsidence in a zone lying roughly on the extended axis of the Aleutian Trench. Middleton Island on the north side of the trench is an example of pulsating emergence in late Pleistocene or Recent time,

marked by five terraces up to 105 feet above sea level (Miller, 1953, p. 17). The Tertiary province contains many high-angle faults, synclines, and anticlines and is featured by deep sediments and general uplift. Assuming its tectonic elements shown by Payne (1955) on the mainland with the Aleutian Trench and Surveyor Deep-sea Channel beneath the sea (Gibson, 1958) an inferred former trench or geosyncline might be expected to lie beneath

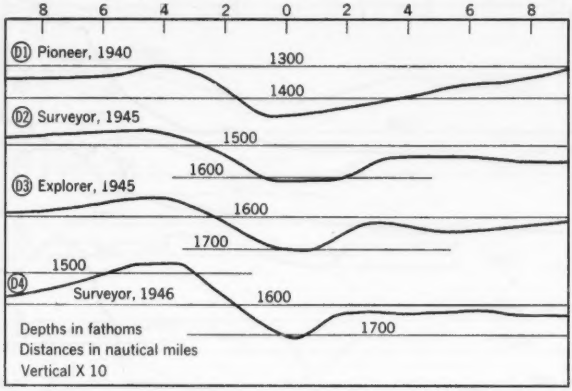

FIGURE 6.—TRANSVERSE PROFILES, BARANOF SEA VALLEY

northern border to continue southwesterly from the Katalla district (Miller, 1957) along the continental shelf to the fault crossing southern Kodiak Island, the province approximates the Yakataga geosyncline (Payne, 1955). Surveyor Deep-sea Channel may mark the southern limit of the Yakataga geosyncline.

The Chugach-St. Elias fault is inferred by St. Amand (1957, p. 1358–1359) to continue southeastward along the coast to form a junction with the Denali fault just south of the entrance to Chatham Strait at a small depression in the continental shelf described by Murray (1941, p. 337) and Heck (1927). A single deep sounding at the foot of the continental slope near the axis of Baranof Sea Valley and due west of the small depression indicates the possibility of a similar deeper depression. The sounding is 300 fathoms deeper than other consecutive soundings and needs substantiation before delineating on the bathymetric chart. St. Amand's inferred submarine fault running along the seaward side of the Queen Charlotte Islands has some very tenuous confirmation from the ridge and trough off Dixon Entrance and the few seaknolls along the margin to the head of Moresby Sea Valley (Fig. 7, profile E1). If a submarine fault existed here it would be buried deeply by sediment except where recent movement might be reflected in the topography.

In view of the general parallelism of the the present coast line and continental slope along the Alexander Archipelago. Queen Charlotte Trough lies between the Queen Charlotte Islands and a rise emanating from Queen Charlotte Sound and marked by Graham Seamount. The steepness of the continental slope here and the probability of heavy silting from glacial melt suggests a great wall of deposition only partially filling the embayment (Queen Charlotte Trough) lying inshore from the Kodiak Seamount Chain.

The long, low, and broad rise forming the northwest side of Baranof Sea Valley (Fig. 6) suggests tectonics more than turbidity-current deposition because of its great extent. Moresby Sea Valley and Explorer Trench cut the continental slope in the entrance of Queen Charlotte Sound where turbidity currents would be expected to flow out along their axes. However, their cross sections favor tectonic origins. The submarine topography between Moresby Sea Valley and Explorer Trench may be a dropped block marked by the two limiting faults. Explorer Trench (Fig. 8) has the form of a thrust fault with a raised escarpment on its east rim similar to that lining the north wall of Mendocino Seascarp ridge.

GREAT TROUGH

The Great Trough (Menard, 1955a, p. 239) lies between the foot of the continental slope

off the coasts of northern California, Oregon, Washington, and Vancouver Island and the east face of the southwest-trending forms of two troughs at Queen Charlotte Sound entrance by cutting across diagonally at a 45-degree angle.

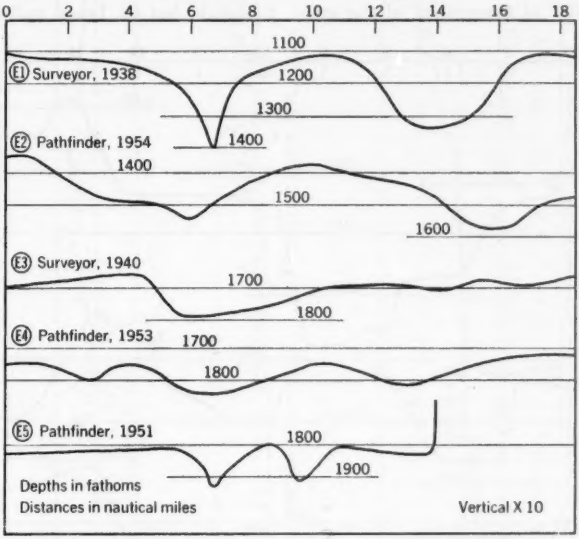

FIGURE 7.—TRANSVERSE PROFILES, MORESBY SEA VALLEY

the Ridge and Trough province (Fig. 9, profile F3). It has a remarkably smooth floor that is indicative of heavy sedimentation and is cut by channels trending south and west (Menard, 1955a, p. 243). Nautical charts of the Coast and Geodetic Survey show prominent terraces in the continental slope which are also cut by submarine canyons. The deep-sea hydrography is not sufficient detailed off the west coast for the mapping of minor relief.

The east limit of the Great Trough is notable for the smooth junction with the continental slope and an initial steep rise of about 400 fathoms followed by a falling off and subsequent steep rise (Fig. 5, profile C7). The bordering topography of the Ridge and Trough province on the west converges upon Heck Seamount lying off the Strait of Juan de Fuca, makes a radical turn left, and ends abruptly in a smooth plain. At this point a long narrow ridge skirts the smooth plain on the east and north, then veers northward along Explorer Trench toward Queen Charlotte Sound, thus forming a border of the Great Trough. The southward prolongation of the axis of the trough occupied by the Queen Charlotte Islands and Hecate Strait coincides with the axis of the Great Trough, although the continental slope separates the

RIDGE AND TROUGH PROVINCE

The northern portion of the Ridge and Trough province (Menard and Dietz, 1951, main plate) included in Plate 1 lies between the Great Trough on the east and Moresby Sea Valley on the west. The latter feature is not a definite border because some less distinct ridge and trough forms are found farther west. Explorer Trench, approximately defining the east border, and Moresby Sea Valley have parallel strikes of about S. 30° W. The province extends to the Mendocino Seascarp on the south, although intersected by ridges and lines of sea mounts trending transversely.

The hydrographic development consists mostly of sounding lines fanning out from the Strait of Juan de Fuca. On account of the divergence of the lines the development becomes weaker with the distance offshore, except for limited-area surveys of numerous seamounts. Most of the larger forms of the gulf floor have been well charted, but more hydrography is needed to develop in detail the minor features of relief. An 80-mile belt extending the approximate width of the province near Queen Charlotte Sound is not sufficiently surveyed to warrant more than general discussion. Moresby

Sea Valley (Fig. 7) lies within the area of insufficient hydrography, but it has been crossed in enough places to define its cross section and continuity.

The complexity of topography of the gulf floor between Eickelberg Ridge and Queen Charlotte Sound precludes portrayal of detailed physiography at the scale of the basic hydrographic sheets and results in excessive generalization at the scale of Plate 1 which is one-third reduction. The importance of this area warrants a complete study, which would best be made at a scale about 6 times that of Plate 1. The importance stems from the convergence upon the approaches of Queen Charlotte Sound of the Queen Charlotte Islands, Hecate Strait lying back of the continental shelf, the Ridge and Trough province, Kodiak Seamount Chain, Queen Charlotte Trough, Moresby Sea Valley, Explorer Trench, the continental slope, and lines of seamounts. The unscrambling of these converging elements may be subject to differences of opinion with regard to details, but the broad pattern seems clear.

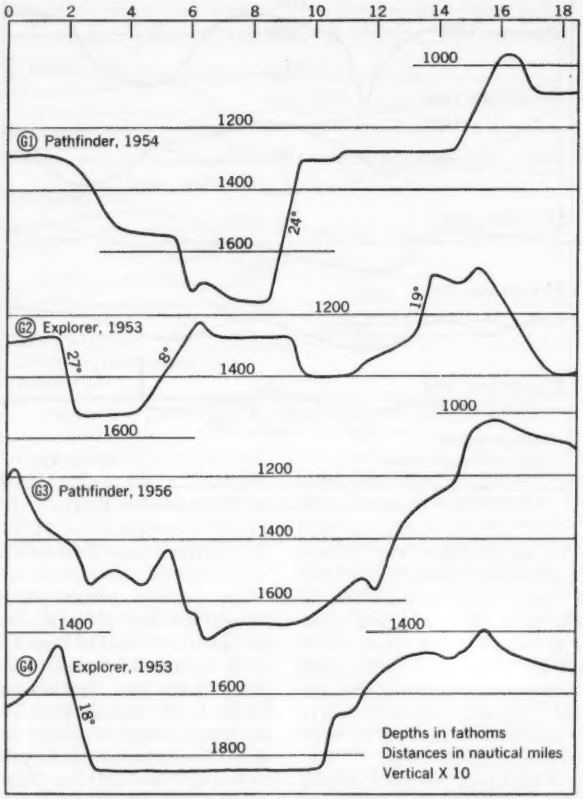

FIGURE 8.—TRANSVERSE PROFILES, EXPLORER TRENCH

The alignment of ridges and troughs (S. 30°W.) is not precise because of many variations due to the interposition of Eickelberg Ridge and numerous seamounts. Most of the linear forms lie to the east of Eickelberg Ridge in a comparatively narrow 60-mile belt, although some lie on either side of the ridge to the north and south. The right-angle bend in the 1700-fathom curve 25 miles southeast of Eickelberg Ridge may represent its merging with one of the linear forms, which then veers to S. 40° W. and continues for 200 miles. The alignment of the ridges and troughs becomes S. 45° W. near the Mendocino Seascarp, and

FIGURE 9.—TRANSVERSE PROFILES, RIDGE AND TROUGH PROVINCE

they are more numerous. The underlying ridges and troughs are not characterized by much relief and are in reality long linear rises with intervening flat sea-floor or shallow troughs. They rise from a gentle plain which slopes downward to the west at the rate of about 2 fathoms per mile (Fig. 9). Explorer Trench and Moresby Sea Valley have definite deeps at their heads near the entrance to Queen Charlotte Sound. There are indications of smaller and shorter features similar to Moresby Sea Valley streaming out from Queen Charlotte Sound. Extensive morainal features that are not adequately surveyed lie close to the foot of the continental slope southeast of Queen Charlotte Sound.

The eastern margin of the Ridge and Trough province contains the Explorer Trench with fringing scarp, a short ridge surmounted by Explorer Seamount, and an extensive low rise running from the entrance of Queen Charlotte Sound parallel to Explorer Trench to a right-angle junction with the southeasterly extension of Eickelberg Ridge, at Warwick Seamount.

Explorer Trench, one of the most striking features of this province (Fig. 8), can be traced for 200 miles from the deep off Vancouver Island S. 30° W. to the east end of Eickelberg Ridge. Indications of its continuance to the southwest require additional confirmation. Its width is 7–10 miles, and the depth below the east scarp ranges from 250 to 725 fathoms. The general sea-floor level is difficult to judge because of the complex topography, but on the west it is estimated to be 100–200 fathoms deeper than that to the east of the scarp. It does not have a graded profile along its axis.

Moresby Sea Valley (Fig. 7) also can be traced for 200 miles, to the west end of Eickelberg Ridge. It is about 50 fathoms deep, 2 miles wide, and has a well-graded profile along its axis.

Heck Seamount is the middle high of a group of three northwesterly trending ridges. The unusual configuration of the group consists of the ends of three low ridges which trend northeastward and abruptly turn northwestward, each terminating in a seamount. The area surrounding and between the three seamounts forms a flat featureless plain of great extent bounded on the east and north by the west scarp of the Great Trough, and on the west by a long narrow scarp rising above the east wall of Explorer Trench. The ridged slopes of Explorer, Stirni, Union, and other seamounts are illustrated in Profile F1 of Figure 9. Heck Seamount has been completely delineated by numerous lines of hydrography, but these lines were run parallel to its axis, and no transverse fathogram is available for determining ridged slopes.

Kodiak Seamount Chain

Kodiak Seamount Chain is featured by a line of great seamounts extending for 650 miles across the Gulf of Alaska without evidence of intervening sea-floor topography that would normally be expected in a fault zone. It is not clear whether the chain comprises two arcs intersecting at Welker Seamount or one long arc accompanied by short shear or tension features. The preferred assumption is that the main fault is marked by Kodiak, Giacomini, Ely, Quinn, Surveyor, Welker, Denson, Hodgkins, Bowie, and Graham seamounts. Shuyak and Dall seamounts seem to be associated with the Aleutian Trench. Although Kodiak Seamount is in the Aleutian Trench its precise alignment with the axis of this zone cannot be disregarded. One secondary lateral shear pattern may be represented by Durgin and Pratt seamounts and another by Brown and Dickins seamounts.

The northwest end of Kodiak Seamount Chain appears to join the Aleutian Trench at Kodiak Seamount, although a 100-mile gap separates it from Giacomini Seamount. Judging by alignment, the southeast end of the chain comprises a seaknoll lying 60 miles southwest of the northwest tip of Vancouver Island, Dellwood Hills, and the rise flanking Queen Charlotte Trough. The first two features seem to be superimposed on the ridges and troughs. The rise emanates from Queen Charlotte Sound and extends northwesterly to Baranof Sea Valley. Its crest is lined with a seaknoll, Graham Seamount, another slight linear rise, and Dickins Seamount. Low saddles tend to separate the latter three features. Bowie, Hodgkins, Denson, and Davidson seamounts rise from the steeper west slope of this flanking rise. The shallow irregular depression lying close to the bases of the seamounts could indicate subsidence due to loading of the crust or scouring through the action of turbidity currents.

The floor along the seamount chain extending northwestward from Brown Seamount is almost devoid of relief and has a slight uniform downslope to Giacomini Seamount. A fault zone such as this is presumed to be might nor-

mally contain a considerable number of significant features of moderate relief on the sea floor in contrast to the apparent evenness. A narrow dikelike form extends from a point about 60 miles southwest of Welker Seamount for more than 100 miles to the northwest. It is about 2 miles wide, 200 fathoms high, and approximately symmetrical. This feature appears to mark the southern limit of Kodiak Seamount Chain. Most of the sounding lines constituting the hydrographic development traverse east-west and should have revealed any existing related structures. However, closer spacing of sounding lines is needed before the lateral extent of the seamount zone is defined.

A wide and shallow trough extends northeastward between Quinn and Surveyor seamounts and into the embayment described by the 2000-fathom curve north of Pratt Seamount. North of the embayment, a slight trough may be traced northeastward for 95 miles. Its existence as a continuous feature needs confirmation from additional traverses and fathograms. Present indications on adjacent sounding lines are soundings ranging from 25 to 115 fathoms below the general floor. The trough appears to be about 2 miles wide, and it may extend up the continental slope toward Alsek Canyon.

Murray (1941, p. 344, 348) illustrated the profiles of the flat-topped seamounts in this zone. Menard and Dietz have studied and reported on them (Menard and Dietz, 1951; Menard, 1955b). The form of the tops of those seamounts that have not been completely surveyed is difficult to judge, for the sounding line may not have crossed the highest point. Almost any profile along slope may show a flattened crest. Fathograms for sounding lines following the crest of a ridge show a definite flat crest. Some of the seamounts have been determined to be flat-topped by numerous sounding lines across the crests, preferably in different directions. Not all seamounts have had this type of development. Welker Seamount has been crossed by only two sounding traverses. Detailed surveys of Pratt, Surveyor, Quinn, and Giacomini seamounts reveal them to be tablemounts. Brown and Denson seamounts have been closely surveyed except for the full extent of their crests.

Mid-Gulf Zone

This zone comprises a variety of submarine forms in various alignments. On the east are Peters, Schoppe, and Whitney ridges with their east-west axes. On the west, Hook Ridge and a parallel westerly chain of seamounts and ridges are aligned in a south-southwesterly direction. West of Whitney Ridge, several ridges and Pathfinder and the Campbell-Scott seamounts have southwesterly axes. Pathfinder and Campbell seamounts were originally reported and illustrated by Nichols (1950).

This area has been traversed by a large number of sounding lines, and many limited-area surveys have been made. Sounding lines have crossed the generally south- to southwest-trending features at right angles in recent years and provide excellent transverse profiles. Some of these crossings are illustrated in Figure 10. Whitney, Schoppe, and Peters ridges are not included because the numerous parallel crossings were made at acute angles to the trend of the ridges.

These easterly ridges may mark a zone of weakness along the southeasterly prolongation of the Parker-Bean Seamount Group. A parallel alignment includes Twin, Scott-Campbell, Pathfinder, and Laskowski seamounts. The Mortons Seamounts are south of this alignment and on a southwesterly extension of a trend marked by the ridge west of Whitney Ridge and minor elevations enclosed by a spur in the 2100-fathom contour.

This southwesterly alignment predominates westward, in the base of Pathfinder Seamount and lesser features 60 miles northeastward. Similarly, Laskowski Seamount and other elevations trending past the east side of Miller Seamount have an alignment transverse to the major seamount zones to the west. Hook Ridge has a comparable trend, which is in part distorted into a north-south alignment. The ridge consists of echelon ridges separated by low saddles and the severely ridged northeastern extensions (Fig. 10, profile J1). The numerous ridges and troughs in this area and 15 miles eastward, delineated from several northwestward sounding lines, strongly suggest southwesterly aligned folds.

The western margin of the Mid-Gulf zone is marked by Miller Seamount. Separated from the Patton-Faris Seamount Group by 100 miles of generally smooth bottom, and having a base with northeasterly trending extensions, it appears to be related with the southwesterly alignments. Additional sounding lines are needed in this area to trace the extent and direction of minor features on the sea floor.

In the extensive area southwestward, low linear rises, depressions, and narrow deep embayments in the depth contours are aligned

in a similar southerly to southwesterly direction. The area does not warrant discussion at this time, however, because the sounding traverses are widely spaced, and future revisions and additions of contours as delineated on Plate 1 are very likely.

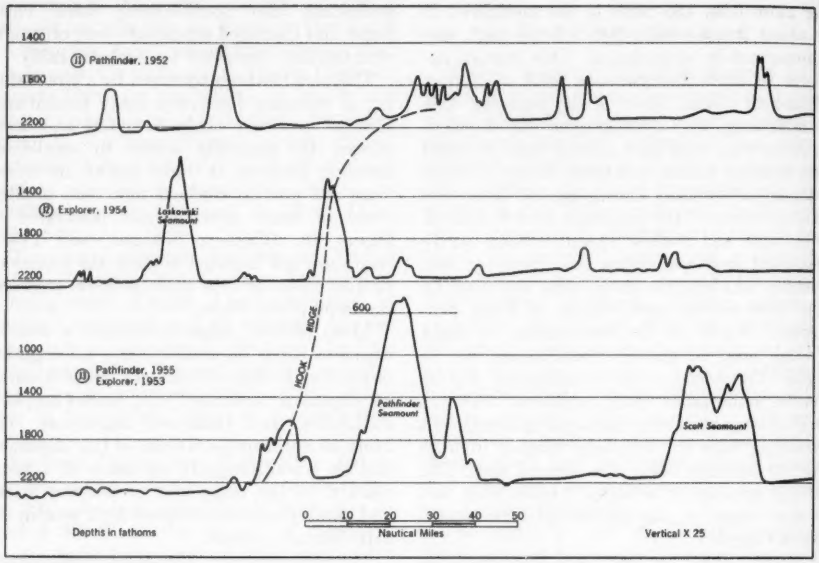

FIGURE 10.—TRANSVERSE PROFILES, MID-GULF ZONE

PARKER-BEAN AND PATTON-FARIS SEAMOUNT GROUPS

The sea floor west of the Mid-Gulf zone slopes down to the south-southwest and down toward the Aleutian Trench to the northwest (Figs. 11, 12). Many of the features of the Gulf of Alaska seamount province are found here (Menard and Dietz, 1951, p. 1270). Murray (1941, p. 351, 354, 359) described individual seamounts from illustrated profiles.

The principal features are found in two parallel seamount zones aligned transverse to the Aleutian Trench. The northerly one, *i.e.*, Patton-Faris Seamount Group, extends 270 miles S. 75° E. from the bottom of the Aleutian Trench opposite Chirikof Island. The southerly, Parker-Bean Seamount Group, extends about 380 miles S. 75° E. from the crest of the southern slope of the Aleutian Trench. Its axis prolonged would contain Laskowski, Pathfinder, Mortons, and Scott-Campbell seamounts which have been described in the Mid-Gulf zone. The Patton-Faris and Parker-Bean seamount groups, which have been described as sub-merged mountains, consist mainly of great seamounts and sea ridges rising from elevated platforms that are separated by and bordered on the north and south by embayments from the Aleutian Trench. Surveyor Deep-Sea Channel, descending the southern slope of the Aleutian Trench, separates the Patton-Faris and Kodiak seamount groups. The poorly defined southern limit of the Parker-Bean seamount group includes many seaknolls and long narrow ridges lying in northeasterly alignments. Hecht Seamount lying in the embayment midway between the two seamount groups is flanked by a shallow depression as is also Bean Ridge and detached Faris Seamount. Deeper depressions lie close to the southern base of the Parker-Bean group. The topography of the two zones suggests extrusions through the crests of underlying rises in the form of seamounts and ridges, followed by partial collapse of the sea floor flanking the extruded structures or by subsidence of the structures due to overloading the crust (Daly, 1951, p. 30).

The Patton-Faris Seamount Group restricts

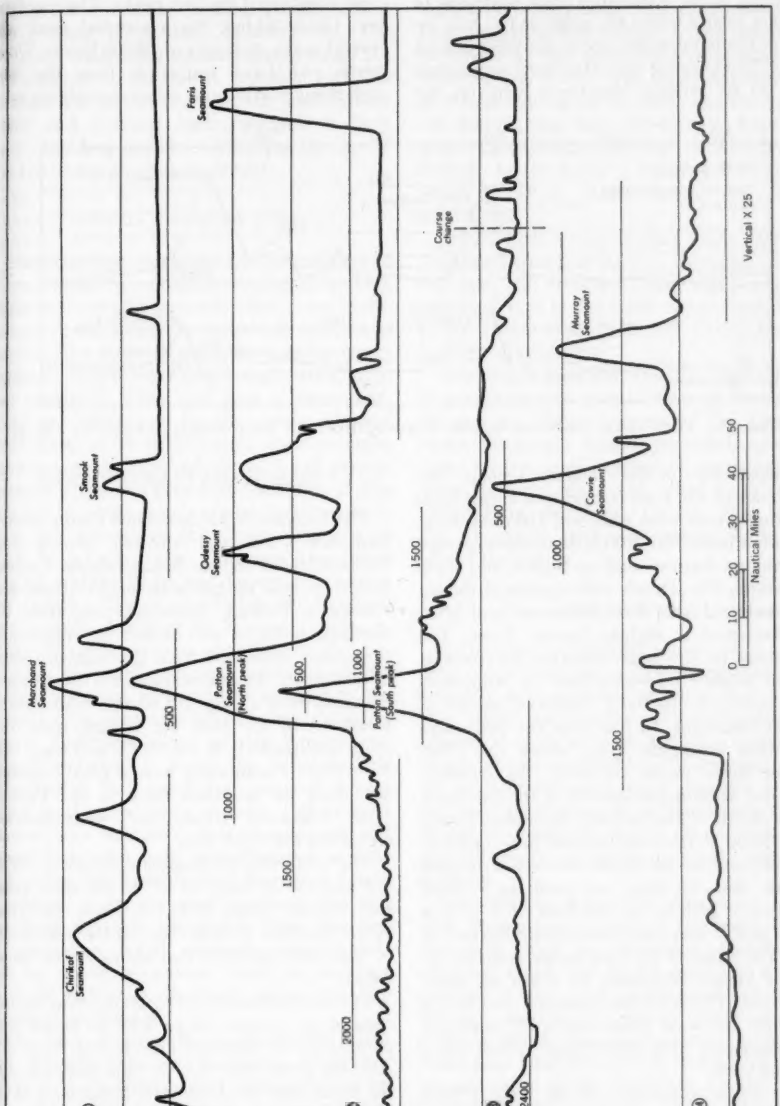

FIGURE 11.—PROFILES ALONG THE PATTON-FARIS SEAMOUNT GROUP

the width of the Aleutian Trench southeast of Chirikof Island where the ridge or rise may be seen in the bathymetry above the 2900-fathom curve. The Chirikof and Marchand seamounts seem to be isolated structures lying on the crest is occupied by four peaks. The southeast rise, Guide Ridge, has a serrated crest with several peaks at depths of 1800 fathoms. Woodworth and Jones seamounts have the same underlying north-south ridges resembling folds

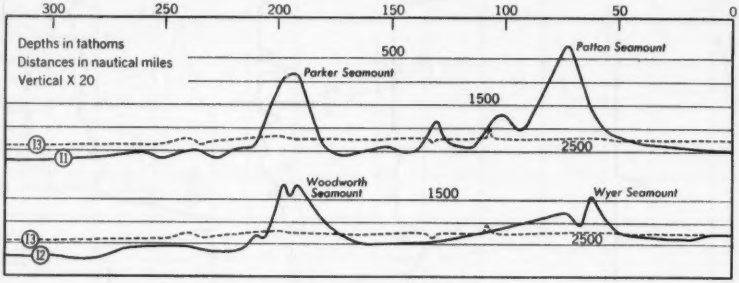

FIGURE 12.—TRANSVERSE PROFILES ACROSS PARKER-BEAN AND PATTON-FARIS SEAMOUNT GROUPS

up-bulged slope of the Aleutian Trench. The remainder of the zone comprises a single large structure 30–40 miles wide and 110 miles long, which lies inside the 2100-fathom curve, except for flanking features such as Smook and Faris seamounts. The 80-mile-wide section of the sea floor eastward from Faris Seamount and Murray Seamount is slightly bowed down. The seamounts on the large structure may consist of two parallel east-west lines of seamounts that have only partially coalesced except at Patton Seamount. In that case the two peaks of Patton Seamount lying above the 1000-fathom curve would represent the partially coalesced western termination of the two lines.

The width of Parker-Bean Seamount Group ranges from 10 miles on the east to 50 miles on the west, and the sill depths between structures indicate that the ridge was built on a raised platform or arch in the sea floor. The arch is folded as if it were compressed from the east or west. The strike of the folds ranges from northeast at Parker Seamount to north at Jones Seamount. The next rise eastward also trends northerly but then turns nearly 90° eastward into alignment with Bean Ridge, which has a serrated crest.

The great seamounts of the Parker-Bean seamount group seem to be structural accumulations overlying the ridged arch, although the possibility exists that the seamounts were compressed and folded with the underlying arch.

The main structure of this zone is marked by two parallel northeasterly trending open folds with intervening troughs. The northwest

UNIMAK-SIRIUS SEAMOUNT CHAIN

The Unimak-Sirius Seamount Chain extends southeast across the Aleutian Trench from Unimak Island and the Sanak Islands. Unimak Island is well dotted with major peaks and volcanoes. Unimak Seamount rises from the northern slope of the trench or continental slope, and Derickson from the southern slope of the trench. Wildcat Seamount is the southern culmination of a long and narrow ridge. Manifestations of the zone are lacking from this point southeasterly to lat. 50° N. and long. 155° W. About 17 seamounts form a gently curving arc along the southern flank of the Parker-Bean Seamount Group and southeastward across the Mid-Gulf zone.

The axis of Sirius Seamount branches off to the south at an angle of 50° to the main zonal axis. It rises about 9000 feet above the crest of the Aleutian Trench rise. All the seamounts of this zone seem to rise above lower linear forms.

Unimak Seamount, 10 by 30 miles in extent, rests on an 8-degree slope with its longer axis parallel to the Aleutian Trench (Fig. 2, profile A5). Its north base lies in 1235 fathoms and the south base in about 2000 fathoms. A deep boxlike canyon extending down the slope from the direction of Sanak Islands borders the seamount on the east, and two other canyons diverge from the west end down the slope toward the bottom of the Aleutian Trench. The form suggests horizontal flow through a horizontal or north-plunging fissure. The ridge containing Derickson Seamount projects into the 3200-

fathom contour of the Aleutian Trench, almost 600 fathoms lower than its south end. The structure comprising Sirius Seamount and the low seaknoll to the north, together with the embayment to the south in the 2600-fathom curve and enclosed basin, suggests a fault zone extending southwesterly from the line of the Derickson-Unimak seamounts.

Columbia Fracture Zone

Assuming that topography of the gulf floor is characterized by north- to northeast-trending ridges and troughs generally, then some explanation of the numerous transverse features is needed. The latter features seem to be superimposed on the ridge and trough topography and consist of ridges and lines of seamounts. They are inferred to be the result of some great stress in the earth's crust, such as might have caused the San Andreas fault and various fracture zones. Sea-floor manifestations of this inferred fracture zone extend northwesterly from the vicinity of the Gorda Seascarp at Cape Mendocino (Fig. 1), across the Great Trough and the Ridge and Trough province to the Aleutian Trench rise. Unlike the fractures to the south described by Menard (1955b, p. 1153) the difference of elevation of the sea floor on the northeast and southwest of the zone is not great and could be ascribed to the general slope. However, the difference on either side of Eickelberg Ridge and the Parker-Bean Seamount Group is about 100 fathoms. This difference is not conclusive, since it occurs where local subsidence is evident. This inferred fracture zone consists of lines of seamounts and ridges in echelon form extending over a wide belt of the sea floor. Kodiak Seamount Chain is inferred to be the most northerly line and the least definitely fractured. Thus, the line of seamounts would represent volcanic outpouring along separated vents in contrast to those farther south which appear to have poured from fissures.

The main fracture transverse to the Ridge and Trough province comprises Eickelberg Ridge and its southeastern and northwestern extensions. Over its 170-mile generally northwestward trend, the fracture is marked by distorted topographic manifestations in the form of abrupt changes in trend, major seamounts, and low saddles. Warwick Seamount on its southeasterly extension rises nearly 10,000 feet to a depth of 250 fathoms. It occurs at an abrupt change in trend and at the southwestern end of an extensive, low transverse rise. Northwest of Eickelberg Ridge, the nearly continuous line of northwesterly trending rises appears to terminate at the southwesterly extension of Moresby Sea Valley. The flanks are depressed as if from loading of the crust, and the numerous flanking rises may be related to transverse or normal faulting of the ridge. Another parallel fracture to the north is believed to be manifested by Heck, Stirni, Union, and Tucker seamounts.

Intermittent seamounts and ridges carry the alignment northwesterly through Peters, Schoppe, and Whitney ridges and across the Mid-Gulf zone at the north end of Hook Ridge to the Parker-Bean Seamount Group and the Aleutian Trench rise.

The Patton-Faris Seamount Group is inferred to constitute two parallel lines of fracture as far east as Miller Seamount. The Unimak-Sirius Seamount Chain projected eastward aligns with a large number of seamounts and seaknolls lying about 150 miles south of the Parker-Bean Seamount Group. The former line appears to mark the most southerly fracture of the zone.

Interpretation

Bathymetry of 800,000 square miles of the deep ocean based on such comprehensive and accurate reconnaissance surveys should provide some confirmation or modification of existing theories of earth science. Comparison of submarine topography with mapping along the contiguous shores should provide correlation and lend direction to further investigations. However, inferences based on physiography are extremely tentative without collateral evidence.

The Aleutian Trench is interpreted as an open geosyncline fringed on the north by an advancing wall of deposition (continental shelf and slope) and on the south by a slight anticline or rise. The northeastern end of the trench, obscured by heavy sedimentation, makes a reverse turn southeastward in general parallelism with the curving tectonic elements mapped back of the coast line by the U. S. Geological Survey (Payne, 1955). Recent and perhaps continuing orogeny is deduced from the pulsating uplift at Middleton Island (Miller, 1953), by general uplift of the Gulf of Alaska Tertiary province and high wave-cut terraces near Lituya Bay (Miller, 1957, personal communication), and by subsidence along the extended axis of the Aleutian Trench at Yakutat Bay and Pamplona Ridge (Jordan,

1958, p. 12). The recent discovery of Surveyor Deep-sea Channel paralleling the Aleutian Trench near the crest of its southeastern slope tends to confirm this possibility. The similarity between Dutoit's (1937, p. 324–326) theoretical marginal geosyncline and moving anticline and the Aleutian Trench and rise is evident. The Aleutian Trench rise would conform to the present position of the moving anticline and the Aleutian Bench to a former one. The fact that the geosynclines and geanticlines are progressively younger toward the sea (Payne, 1955) may tend to confirm Dutoit's theory of sliding continents. In that case the Aleutian Trench rise would have to develop into a far greater feature in order to provide sediments for filling the next foredeep to the southeast. However, conditions seem to be more indicative of a gradual outbuilding of the continental margin than of a sliding mass.

The Alexander Archipelago, occupying a slight trough at the site of a former Cretaceous geosyncline, projected southward beneath the sea coincides with the axis of the Great Trough off the west coasts of Washington, Oregon, and northern California. This trough may mark the site of the geosyncline postulated by Eardley (1951, p. 62–68) as persisting from Silurian to Cretaceous time, and its west bordering ridges and seamounts are remnants of the postulated archipelago constituting sources for volcanic rocks found in the western part of the Cordilleran geosyncline. The continental slope, cutting across at an angle of 45° at Queen Charlotte Sound and tending to separate the two troughs, was more recent. The axes of the Great Trough, Alexander Archipelago, Gulf of Alaska Tertiary province, Chugach-St. Elias fault, Sullivan fault, Aleutian Bench, Aleutian Trench, Aleutian Trench rise, and Surveyor Deep-sea Channel all tend toward parallelism and conform in general with the axes of the tectonic elements mapped along the margins of the land (Payne, 1955).

The deep-sea-floor features comprising the Ridge and Trough province and the Mid-Gulf zone consist mainly of north-northeasterly patterns, and the Columbia fracture zone and Kodiak Seamount Chain consist mainly of transverse northwesterly trends. These orientations happen to agree closely with the axes of the Hawaiian Islands and sunken islands of the Mid-Pacific Mountains at their junction near Necker Island (Hamilton, 1956, p. 38–44). Possibly the same alignments will be found between the Hawaiian Islands and Columbia fracture zone, except for the anomalously trending Mendocino Seascarp. Drag fractures making angles of 8°–15° with the zone of displacement have been produced experimentally by Cloos (1955, p. 244–246) as a result of rotational forces. A model, free to rotate externally and internally to a couple, opened two sets of fractures, one 45°–65° and the other 70°–90° from the direction of pull. The drag fractures would be similar to those of the Kodiak Seamount Chain, and the two sets produced by the couple are similar to the transverse Ridge and Trough and Columbia fracture zones. A common origin or constructional process may be inferred from the close agreement in general form of cross sections of the Hawaiian Islands and Bean and Eickelberg ridges. In each case the ridges may be attributed to fissure eruptions from upwelling and thermal expansion of the hot magma of a subcrustal convection current followed by volcanism through tensional fractures at the crest of the swell, followed by regional and isostatic sinking as indicated by the flanking depressions. However, Bucher (1956, p. 1313), who long postulated the need for surface tension in the mechanism, now believes that deep-seated tension caused by deep earthquakes will create channelways for heat to traverse the earth's crust. In some places, especially in the Mid-Gulf zone, eruptions may have taken place through the crests of folds or through inclined vents along the flanks. Figure 2 shows that the general axis of the Columbia fracture zone falls on the prolongation to sea of the axis of the Coast Range and the San Andreas fault.

St. Amand (1957, p. 1366) pointed out the possibility that the North Pacific basin may have been rotating counter-clockwise for a very long time and quoted a suggestion by Hill and Dibblee of about 225-mile offsets along the San Andreas fault since late Eocene time. No direct confirmation of that movement may be seen in the bathymetry, but there are suggestions of rotational movements. The Bowie, Hodgkins, Davidson, and Denson group comprises four seapeaks in a 75-mile line that are roughly similar to the four seapeaks extending over a 75-mile line northwest of Durgin Seamount. The vents under the latter line are spaced the same as the four seamounts comprising the Surveyor-Giacomini group. The distance between Peters and Whitney ridges, Scott, and Pathfinder seamounts, Sirius to Derickson seamounts and Derickson to Unimak seamounts is about 75 miles. The most likely correlation with a rotational movement would

be between the Durgin-Pratt group and the Surveyor-Giacomini group, if it is real.

Inasmuch as Vancouver Island has risen, subsided, and risen again it is not surprising to find that the Explorer Trench and parallel escarpment lie westward. The relief of the trench and escarpment favors an interpretation of a thrust fault. It is similar in size to the Denali fault of Chatham Strait. Heck Seamount appears to rest in the mid-portion of a great downfaulted block.

The planation of the tops of the tablemounts of the Kodiak seamount province has been attributed primarily to a combination of lowered sea level and local or regional subsidence. During periods of lower sea level crests of the seamounts may have been modified by floating ice islands or a deeply frozen sea in the early stages of volcanism. Riesenberg (1941, p. 366–376) quoted reports of ships in the Antarctic sighting ice islands 50 km long and 500 feet high. The underwater portions of horizontal masses would then have been 3000–4000 feet and deeper if irregular. Extremely large ice islands are known to be moving in the Arctic Ocean. Present currents off the southeast coast of Alaska would tend to carry ice toward the tablemounts. Kreichgauer (Scheidegger, 1958, p. 5) estimated positions of the north pole in Carboniferous time at lat. 35° N., long. 145° W., and in Tertiary time at lat. 51° N., long. 154° W. The latter Tertiary position is about 100 miles southwest of Parker Seamount.

References Cited

Bucher, Walter H., 1956, Role of gravity in orogenesis: Geol. Soc. America Bull., v. 67, p. 1295–1318

Cloos, Ernst, 1955, Experimental analysis of fracture patterns: Geol. Soc. America Bull., v. 66, p. 241–256

Daly, R. A., 1951, Relevant facts and inferences from field geology, p. 23–49 *in* Gutenberg, B., *Editor*, Internal constitution of the earth: New York, Dover Publications, Inc., 439 p.

Dutoit, Alex L., 1937, Our wandering continents: London, Oliver and Boyd, 366 p.

Eardley, A. J., 1951, Structural geology of North America: New York, Harper & Bros., 624 p.

Gates, Olcott, and Gibson, William, 1956, Interpretation of the configuration of the Aleutian Ridge: Geol. Soc. America Bull., v. 67, 127–146

Gibson, William M., 1958, Gulf of Alaska Trough parallels Aleutian Trench: Geol. Soc. America Bull., v. 69, p. 611–614

Gibson, William, and Nichols, Haven, 1953, Configuration of the Aleutian Ridge: Geol. Soc. America Bull., v. 64, p. 1173–1181

Hamilton, E. L., 1956, Sunken islands of the Mid-Pacific Mountains: Geol. Soc. America Me. 64, 98 p.

Heck, N. H., 1927, Some unusual submarine features in the North Pacific: Geog. Rev., v. 17, p. 448–452

Jordan, George F., 1958, Pamplona searidge: Intern. Hydrog. Rev., v. 35, no. 1, p. 3–12

Menard, H. W., Jr., 1953, Pleistocene and Recent sediment from the floor of the Northeastern Pacific Ocean: Geol. Soc. America Bull., v. 64, p. 1279–1294

——1955a, Deep-sea channels, topography and sedimentation: Am. Assoc. Petroleum Geologists Bull., v. 39, p. 236–255

——1955b, Deformation of the Northeastern Pacific basin and the west coast of North America: Geol. Soc. America Bull., v. 66, p. 1149–1198

Menard, H. W., and Dietz, R. S., 1951, Submarine geology of the Gulf of Alaska: Geol. Soc. America Bull., v. 62, p. 1263–1285

Miller, Don J., 1953, Late Cenozoic marine glacial sediments and marine terraces of Middleton Island, Alaska: Jour. Geology, v. 61, p. 17–40

——1957, Geology of the southeastern part of the Robinson Mountains, Yakataga district, Alaska: U. S. Geol. Survey Oil and Gas Inv. Map OM-187

Murray, H. W., 1941, Submarine mountains in the Gulf of Alaska: Geol. Soc. America Bull., v. 52, p. 333–362

——1945, Profiles of the Aleutian Trench: Geol. Soc. America Bull., v. 56, p. 757–782

Nichols, Haven, 1950, New seamount in the North Pacific Ocean: Geog. Rev., v. 40, p. 457–461

Payne, Thomas G., 1955, Mesozoic and Cenozoic tectonic elements of Alaska: U. S. Geol. Survey Misc. Geol. Inv. Map I-84

Plafker, George, and Miller, Don J., 1957, Reconnaissance geology of the Malaspina district, Alaska: U. S. Geol. Survey Oil and Gas Inv. Map OM-189

Riesenberg, Felix, 1941, Cape Horn: London, Robert Hale, 452 p.

St. Amand, Pierre, 1957, Geological and geophysical synthesis of the tectonics of portions of British Columbia, Yukon Territory, and Alaska: Geol. Soc. America Bull., v. 68, p. 1343–1370

Scheidegger, A. E., 1958, Principles of geodynamics: Berlin, Springer-Verlag, 280 p.

Wiseman, John D. H., and Ovey, Cameron D., 1954, Proposed names of features on the deep-sea floor: Deep-Sea Research, v. 2, p. 93–106

101 Wildwood Ave., Piedmont 10, Calif.

Manuscript Received by the Secretary of the Society

Publication Authorized by the Director, Coast and Geodetic Survey

Short Notes

BULLETIN OF THE GEOLOGICAL SOCIETY OF AMERICA
VOL. 71, PP. 1109–1112, 1 FIG., 1 PL. JULY 1960

STRUCTURE ASSOCIATED WITH ROCK CREEP IN THE BLACK HILLS, SOUTH DAKOTA

BY JAMES J. NORTON AND JACK A. REDDEN

Abstract

Many areas of schist in the southern Black Hills, South Dakota, have a thin zone of disintegrated rock that is 4–10 feet below the ground surface and parallel to it. Fresh, undeformed schist overlying this zone has moved downhill in a mass-wasting process since the present surface was formed.

Mass wasting has led to the development of an unusual structure in rocks within a few feet of the ground surface in several places in the Precambrian schists of the southern Black Hills, South Dakota. Although other persons may have seen this structure elsewhere, it does not appear to be well known to geologists, nor are we aware of any previous published description of it. The essential characteristics are shown in Figure 1 by means of a diagram of an exposure at the Dyke Lode pegmatite mine. Photographs at three localities are shown in Plate 1.

The most evident feature is a thin zone of deformed and disintegrated rock (labeled "slip zone" in Fig. 1) 4–10 feet below, and parallel to, a gently sloping ground surface. Both above and below this zone the schist is fresh and relatively unfractured; except for a flexure along each side of the deformed zone, the attitude of the bedding and schistosity in the upper layer is essentially the same as that in the bedrock. The upper layer has shifted downhill, and the disintegrated rock marks a slip zone along which the rock creep took place. During geologic mapping one cannot tell whether an exposure of fresh schist is a true outcrop or whether it overlies a slip zone.

This structure has been observed in about 15 to 20 exposures in prospect pits, mines, and railroad and highway cuts during the course of geologic mapping near Custer and Keystone, South Dakota. It may be much more common than this small number of examples suggests because it has been recognized only where there are vertical artifical exposures.

The lateral extent of this structure ordinarily cannot be determined from the available information. At only a few places is there evidence that it extends for more than 100 feet in any direction. On the other hand, about 2 square miles of gently rolling grasslands near the Crazy Horse monument (Pl. 1, fig. 3) contains enough exposures of this structure to suggest that it underlies nearly all of this area.

The host rock is generally micaceous or thinly laminated schist. It invariably dips steeply and strikes at a large angle to the direction of slope of the ground surface. At most localities the slope of the surface and of the slip zone is 5°–10°; the steepest observed is 22° at the Dyke Lode pegmatite mine (Fig. 1; Pl. 1, fig. 1).

The rock is greatly fractured and weathered at localities where the slip zone is well developed. Most of the larger fragments have a tabular shape controlled by the schistosity and are nearly parallel to the slip zone. Fractures become less abundant above and below the slip zone, and the schistosity gradually assumes its normal attitude in fresh schist. An S-shaped flexure thus formed is the dominant element of the structure in a few places where the displacement apparently is so small that the slip zone is only partly developed.

Even where the slip zone is as well formed as it is at the Dyke Lode, the displacement is not large. A body of pegmatite at the up-slope end of Figure 1 has not been displaced. Only rubble lies above the horizon of slip for a distance of 21 feet from the pegmatite, and the geometry of Figure 1 shows that this distance is the

maximum possible displacement. Planes of schistosity traced through the slip zone show that the displacement is certainly no less than 5 feet and probably exceeds 10 feet.

The immediate cause of this structure is the downhill movement of the upper block under the influence of gravity. The steeply dipping rocks affected by this process are apparently

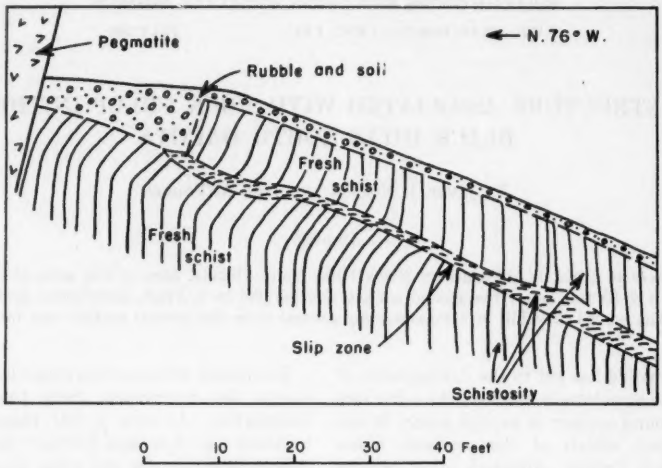

FIGURE 1.—DIAGRAM OF A VERTICAL EXPOSURE SHOWING THE ESSENTIAL FEATURES ASSOCIATED WITH ROCK CREEP, DYKE LODE PEGMATITE MINE, BLACK HILLS, SOUTH DAKOTA

In quartz-mica schist on the north wall of an inclined haulage way. Mine dumps that overlie the soil are omitted. The location is south of the center of the NE ¼ sec. 21, T. 2S., R. 6E., 2.3 miles south-southeast of Keystone, South Dakota.

The parallelism between the slip zone and the existing ground surface indicates that this structure formed fairly recently, but whether or not it is forming at the present time is in doubt. The oldest observed exposures, in prospect pits probably 70 to 80 years old, contain no indication of recent movement. The possibility must be kept in mind that the origin may date from glacial times. Although the Black Hills were not glaciated, they presumably were in a periglacial zone with deep frost action; the depth of alternate freezing and thawing may have been the same as the depth of the slip zone.

so oriented that they have little strength, and the slip zone can develop as a substitute for other structural planes that ordinarily are available for the transport of material during mass wasting. (*Cf.* Balk, 1932, p. 77–78.) Once the slip zone has formed, it must carry water, which facilitates weathering and serves as a lubricant during additional movement.

Aside from these rather obvious conclusions, the mechanisms involved are not entirely apparent. A basic problem is whether a fracture parallel to the surface formed early and the flexure was caused by drag, or whether the slip zone appeared only after the flexure was es-

PLATE 1.—ROCK CREEP AT THREE WIDELY SEPARATED LOCALITIES IN THE SOUTHERN BLACK HILLS, SOUTH DAKOTA

FIGURE 1.—Quartz-mica schist in an area 17 feet wide that is just to the left of the center of the sketch in Figure 1 at the Dyke Lode mine.

FIGURE 2.—Quartz-mica schist in the east wall of the main open pit at the Penobscott gold mine, NE ¼ sec. 11, T. 3S., R. 3 E., about 6½ miles west-northwest of Custer, South Dakota.

FIGURE 3.—An exposure of thin-bedded biotite-garnet schist on the south side of the road to the Crazy Horse monument, SE ¼ NE ¼ sec. 4, T. 3S., R. 4 E., about 4 miles north-northwest of Custer, South Dakota.

FIGURE 1

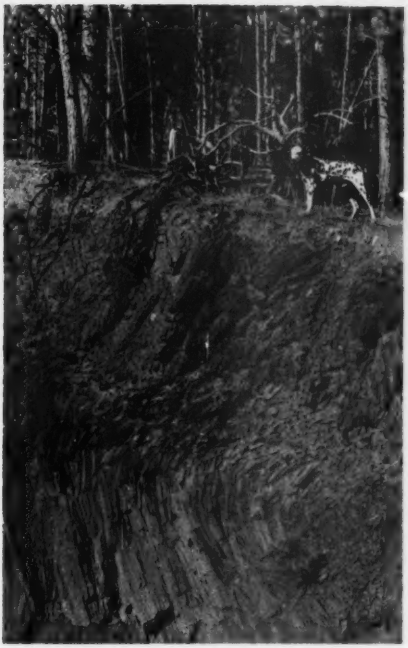

FIGURE 2

FIGURE 3
ROCK CREEP AT THREE WIDELY SEPARATED LOCALITIES IN THE SOUTHERN BLACK HILLS, SOUTH DAKOTA

tablished. If the first step was the fracturing, then it can be loosely described as sheeting, probably formed in response to stresses resulting from erosion and unloading (Billings, 1954, p. 121–123). Regardless of the order, the reason for the relatively constant depth beneath the surface must be a key to the origin. Perhaps the first event in the development of this structure was minute fracturing, at a depth of 5–10 feet, caused by stresses arising from frost action, either under present climatic conditions or at the top of permafrost in a glacial climate. Once a zone of weakness had been established in this way, the upper block could begin to move, and the flexure and slip zone would then form.

References Cited

Balk, Robert, 1932, Geology of the Newcomb quadrangle: N. Y. State Mus. Bull. 290, 106 p.

Billings, M. P., 1954, Structural geology: New York, Prentice-Hall, 514 p.

U. S. Geological Survey, Denver, Colo.; Virginia Polytechnic Institute, Blacksburg, Va.

Manuscript Received by the Secretary of the Society, October 22, 1959

Publication Authorized by the Director, U. S. Geological Survey

BULLETIN OF THE GEOLOGICAL SOCIETY OF AMERICA
VOL. 71, PP. 1113-1120, 8 FIGS., 1 PL. JULY 1960

LATE PLEISTOCENE MARINE TERRACES ON SANTA ROSA ISLAND, CALIFORNIA

BY PHIL C. ORR

Abstract

Three wave-cut platforms with their marine and terrestrial fossil-bearing covers are described and named and are shown to be of late Pleistocene age by means of radiocarbon dating.

Santa Rosa Island (Fig. 1), about 45 miles southwest of Santa Barbara, California, forms a seaward extension of the Santa Monica Mountains that has remained isolated from the mainland since mid-Pleistocene time (Orr, 1956c).

On the northwest coast of the island a series of emerged and submerged marine terraces covers about 13 miles in lateral distance and 1300 feet in height from the continental shelf to the tops of the mountains, recording a long period of sea-level fluctuations, during which at least five submerged (Emery, 1958) and seven emerged wave-cut platforms were formed. Most of these terraces have counterparts on the other islands and the southern California mainland.

The purpose of this paper is to describe two wave-cut platforms and their fossiliferous cover of late Pleistocene age.

For a full understanding of the late Pleistocene history of the fluctuations of sea level, the submerged wave-cut platforms and the older emerged terraces must be considered. Geomorphically, the northwest coast of Santa Rosa Island resembles many parts of the coastal southern California mainland, rather than nearby Santa Cruz Island (Bremner, 1932).

In this paper the terms used follow Bradley (1957, Fig. 2) except for the term "back edge" of Rode (1930, p. 29) and Alexander (1953, p. 11), which is retained in place of "shore-line angle", and for the term "cover" (Davis, 1933) which is used for both marine and nonmarine deposits. A marine terrace may be said to extend from the seaward back edge (shore-line angle) to the next back edge, landward, and to include the seaward sea cliff, or escarpment, the wave-cut platform, and/or the mantle or covering, whether marine or nonmarine (Fig. 3).

Fifty- to 100-foot sea cliffs (Pl. 1, fig. 1) rise from the water line. They are composed of a base of resistant Rincon shales of Miocene age capped by unconsolidated Pleistocene alluvium deposited as alluvial fanglomerates emanating from the canyons which have been cut into an older and higher wave-cut platform at about 250 feet. A similar pair of terraces on the Santa Monica coast have been named by Davis (1933) the "Dume" and the "Malibu". The upper terrace extends about 2½ miles back from the sea and is undoubtedly composed of numerous as yet unstudied wave-cut platforms. In most parts on Santa Rosa Island, the lower terrace is less than 300 yards in width, and it is underlain by three wave-cut platforms. This lower terrace and its wave-cut platforms are the subject of this paper.

The name Santa Rosa Island formation is proposed for the cover on the lower terrace. The exposures of the type locality extend about 4000 yards along the sea cliffs on the northwest coast and are shown in Figure 1. The formation is also found at the mouth of Soledad Canyon, Ranch House Canyon, and from San Augustine to Wreck canyons and between China Camp and Bee Rock on the south coast of the island. On the northwest coast the Santa Rosa Island formation lies unconformably upon the Rincon shale of mid-Miocene age and consists for the most part of buff-colored clays and clay sands; one facies is pure white calcareous eolianite. The three members of the Santa Rosa formation are named from oldest to youngest after the canyons of their type localities: the Garanon, Fox, and Tecolote. Each member has two or more facies (Fig. 2).

Santa Rosa Island is a part of the present Channel Islands group, which, during periods of eustatically fluctuating sea levels, have been repeatedly separated or joined. An under-water profile made by Emery (1958, No. 42) and the writer, directly off the northwest coast of the island, agrees well with other profiles along the southern California coast and islands and indicates a lowering of sea level by at least 400 feet.

As none of these submerged terraces or wave-cut platforms show steep escarpments, they may have been created by rapid fluctuations

Santa Barbara Channel
RADIO POINT
SURVEY POINT
DEER GULCH
ARLINGTON CANYON
CANADA TECOLOTE
CANADA TECOLOTE
CANADA TECOLOTE

and frequent standstills during Wisconsin time, and probably are comparable to the high terraces in Lakes Lahontan and Bonneville, dated by Broecker and Orr (1958). The cover of

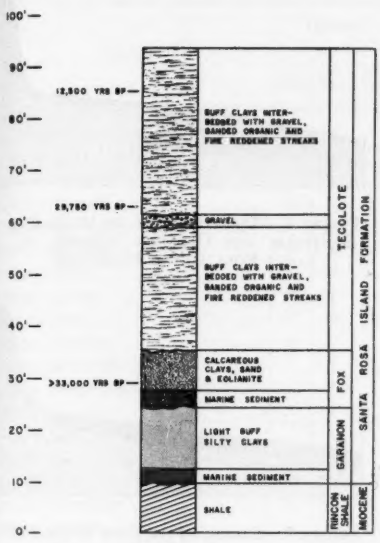

FIGURE 2.—GEOLOGIC COLUMN OF SANTA ROSA ISLAND FORMATION SHOWING RADIOCARBON DATES

the lowest of the emerged terraces on Santa Rosa, comparable to the Dume platform and cover of Davis, is underlain by three wave-cut platforms, the highest of which represents a high sea stand of about 100 feet (Fig. 4) and is probably of Sangamon Interglacial age. This Dume stage is represented on the northwest coast by fossil sea cliffs and escarpments (Pl. 1, fig. 2) rising to the fore edge of the Malibu platform at about 250 feet. The two lower platforms which underlie this terrace are found at 75 feet and 25 feet where the back edge is cut into Miocene Rincon shales of the Saucesian–Zemorrian stage. It is proposed to call the upper, or 75-foot, platform the Fox platform, and the lower, or 25-foot, the Garanon platform. Figure 5 shows the present profile with the three wave-cut platforms and their overlying members of the Santa Rosa Island formation.

The Garanon platform and member with a lower marine and an upper terrestrial facies (Fig. 6) is exposed along the sea cliffs between Jaw Gulch on the west and Tecolote Canyon on the east and is present locally between Survey Point and Arlington Canyon. Almost everywhere the marine deposit is at least 2 feet in thickness and, except for a few isolated erosional channels, appears to be conformable with the overlying terrestrial facies.

The marine facies is in general a light-gray calcareous clay containing fossil bones of whale, sea lion, sea otter, shore birds, and occasional dwarf mammoth as well as organic remains and quantities of "rotted" asphalt exposed along the fore edge of the deposit at an elevation of approximately 16 feet. The marine fauna collected from near the back edge at about 25 feet is a cool-water fauna (Table 1).

It is evident that sea level stood more than 25 feet above present sea level at the back edge of the platform, and then dropped slightly to form a lagoon about 3000 yards in east–west dimension along this section of the coast, perhaps by the formation of a sand bar. Vertebrate remains were trapped here, just as is being done today at the mouths of Arlington and Garanon canyons where small lagoons exist. Sea level continued to drop, as is shown by the terrestrial facies of the Garanon member, which contains the water-worn fragments of *Turritella* and *Ostrea* shells derived from the Miocene sediments, as well as by bones of the dwarf mammoth and of the deer mouse.

With a change in climate, sea level rose rapidly, overflowed the resistant Miocene rocks, and at about 75 feet eroded away the upper portions of the Garanon terrestrial member, forming the 75-foot wave-cut Fox platform.

The Fox platform, as exposed in Garanon Canyon, cuts both Garanon terrestrial alluvium and Miocene Rincon shale (Fig. 7). At the back edge a 25-foot fossil sea cliff is cut into the shale and almost destroys the remnant of the Dume platform. When the sea retreated a shallow marine deposit was left, consisting of calcareous clays containing intertidal marine shells lying on the Fox wave-cut platform where it has been cut into the Miocene. These deposits are found in Garanon Canyon, Gasoline Alley (present head of Fox Gulch), Skull Gulch, Tecolokito Canyon, Tecolote Canyon, and Deer Gulch.

The sea dropped slightly from this stand, and wind-blown calcareous sands were deposited on the marine facies. These sands have been dated (Broecker and Kulp, 1957) at more than 33,000 years B. P.

While it is certain that buff-colored calcareous clays containing root casts and the casts of some fossil trees, snail shells, and calcareous-coated bones of dwarf mammoth followed the

deposition of the basal Fox sands and presumably represented a slightly moister climate accompanied by a lowering of sea level, it is not

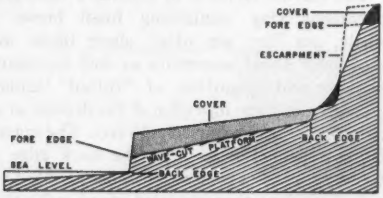

FIGURE 3.—TERMINOLOGY USED IN THIS PAPER

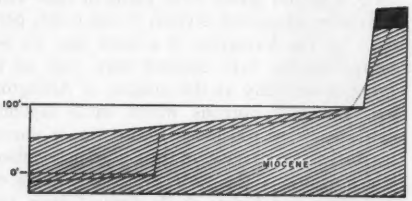

FIGURE 4.—ONE HUNDRED-FOOT SEA STAND OF "DUME" STAGE, 3RD INTERGLACIAL

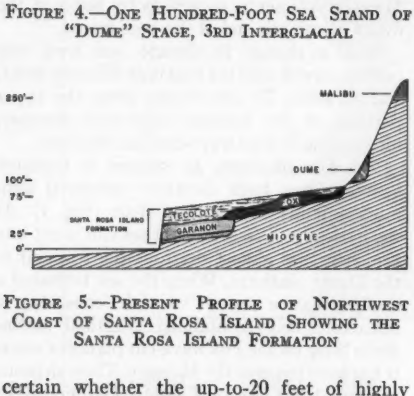

FIGURE 5.—PRESENT PROFILE OF NORTHWEST COAST OF SANTA ROSA ISLAND SHOWING THE SANTA ROSA ISLAND FORMATION

certain whether the up-to-20 feet of highly calcareous eolianite which is deposited against the escarpment is younger than the clays or is contemporaneous with the sands. These beds contain fossil root casts, the fossil land snail *Helminthoglypta ayresiana*, and occasional mammoth bones.

These or similar eolianitic beds disappear to the east and thicken to the west; they reach a maximum thickness of about 50 feet on the higher Malibu terrace.

It would appear that Fox time represents a period of higher-than-present sea stands of about 75 feet to stands below the present. It was followed by a period of erosion which removed the entire Fox series from Skull Gulch

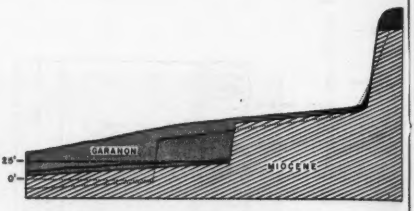

FIGURE 6.—TWENTY-FIVE-FOOT WAVE-CUT PLATFORM AND GARANON MEMBER OF SANTA ROSA ISLAND FORMATION

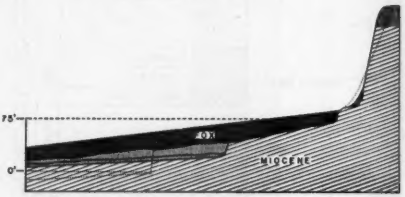

FIGURE 7.—SEVENTY-FIVE-FOOT WAVE-CUT PLATFORM AND FOX MEMBER OF SANTA ROSA ISLAND FORMATION

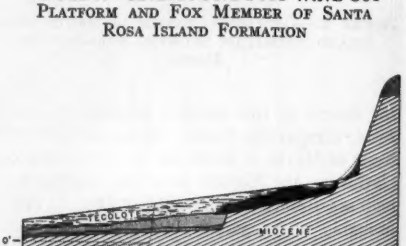

FIGURE 8.—TECOLOTE MEMBER OF THE SANTA ROSA ISLAND FORMATION DURING A PERIOD OF GREATLY LOWERED SEA LEVEL
Dotted lines indicate the present profile

east to Deer Gulch, a distance of about 2000 yards.

There is ample evidence of stream channels cut into the higher Fox beds, but this does not explain the removal of the entire series in this section of the coast. Some marine erosion may have occurred during a possible unrecorded fluctuation of the sea.

The Fox deposition and erosional period was followed by a lowering of sea level and the deposition of the Tecolote member of the

TABLE 1.—INVERTEBRATE FOSSILS FROM THE MARINE FACIES OF THE SANTA ROSA ISLAND FORMATION
Identified by Allyn Smith

Species	Terraces		
	25 Foot	75 Foot	250 Foot
Acanthina spirata punctulata	..	×	..
Acmaea asmi	×	..	..
Acmaea conus	..	×	..
Acmaea digitalis	×	..	..
Acmaea incessa	×	×	..
Acmaea limatula	×	×	..
Acmaea mitra	..	×	..
Acmaea patina	×	×	..
Acmaea pelta	×	×	..
Acmaea persona	×	..	..
Acmaea scabra Eschscholtz	..	×	..
Acmaea scabra Gould	×	×	..
Aletes	..	×	..
Aletes squamigerus	..	×	..
Amphissa columbiana	×	..	..
Amphissa versicolor	×	..	..
Aptyxis luteopicta	×	..	..
Astraea undosa	..	×	..
Balanus tintinnabulum	..	×	..
Bittium	×	..	..
Bittium eschrichtii	..	×	..
Bittium purpureum	×	..	..
Calliostoma	×	..	..
Cardita subquadrata	×	×	..
Conus californicus	×	..	..
Corbula luteola	×	..	..
Crepidula aculeata	..	×	..
Crepidula adunca	×	×	×
Crepidula norrisiarum	..	×	×
Crepidula perforans	..	×	..
Cryptochiton stelleri	×	×	..
Cumingia californica	..	×	..
Cyanoplax hartwegi	..	×	..
Fissurella volcano	×	×	..
Glycymeris subobsoleta	..	×	..
Haliotis cracherodi	×	..	..
Haliotis rufescens	..	×	×
Helminthoglypta ayresiana	×	×	..
Hipponix antiquatus	×	×	..
Hipponix cranioides	×	..	..
Hipponix tumens	×	×	..
Homalopoma carpenteri	×	×	..
Irus lamellifer	..	×	..
Ischnochiton	×	..	..
Lacuna	×	..	..

TABLE 1.—*Continued*

Species	Terraces		
	25 Foot	75 Foot	250 Foot
Littorina planaxis	×	..	..
Littorina scutulata	×	×	..
Lucina californica	×	×	..
Mitra	×	..	..
Mitra idae	..	×	×
Mitrella gausapata	×	×	..
Mopalia muscosa	×	×	..
Mytilus californianus	..	..	×
Ocenebra	×	×	..
Ocenebra circumtexta	×	..	..
Ocenebra foreolata	×	..	..
Ocenebra lurida	×	..	..
Ocenebra lurida aspera	×	×	..
Olivella biplicata	×	×	×
Petaloconchus	×	..	..
Pholadidea penita	..	×	..
Pseudomelatoma	..	×	..
Pseudomelatoma torosa	×	..	..
Saxicava pholadis	..	×	..
Septifer bifurcatus	..	×	..
Siphonaria brannani	×	×	..
Stenoplax conspicuus	..	×	..
Strongylocentrotus drabachiensis	..	×	..
Strongylocentrotus franciscanus	×	×	..
Tegula brunnea	×	..	..
Tegula funebralis	×	×	..
Tegula pulligo	×	..	..
Thais emarginata	..	..	×
Transenella tantilla	×	..	..
Trimusculus reticulatus	×	×	..

Santa Rosa Island formation. The Tecolote member (Fig. 8) consists of buff-colored clays and clay sands, old soil profiles, and thin lenses of subangular gravel composed of Rincon shale. There are many minor unconformities representing stream channeling and at least one major unconformity in which a thick layer of coarse gravel was deposited about midway in the member.

Near the mouths of the major canyons, streaks of charcoal appear, and the earth has been burned to a brick red. Many of these fire areas contain the charred bones of the dwarf mammoth and are attributed to the activities of early man (Orr, 1956b). One such area at the mid-point of the sequence was radiocarbon

dated at 29,700 ± 3000 years B. P. (Broecker and Kulp, 1957).

The beds contain crystallized gypsum roses, especially in the upper section. The perennial streams are heavily mineralized with what is assumed to be dissolved gypsum.

The Tecolote member was deposited during a period of fluctuating sea level in the form of fanglomerates derived from the canyon mouths, and interrupted by channel cutting during periods of higher sea level.

Early writers such as Lawson (1893) and Smith (1902) regarded the emerged terraces of the islands as due to post-Pliocene diastrophism. As a result of the confusion in terminology some writers give the elevation of the cover, while others give the elevation of the wave-cut platform, resulting in apparent differences in the elevation of terraces. Certainly the wave-cut platforms below 100 feet on Santa Rosa Island and the nearby islands and mainland are due to eustatic changes in sea level and not to diastrophism.

Locally, the Santa Rosa Island formation, because of its location on the lowest terrace, its lithology, and its fauna, is probably equivalent, in part at least, to the Santa Cruz Island formation (Chaney and Mason, 1934a), to the Carpinteria formation (Chaney and Mason, 1934b), and to an unnamed formation that is best exposed in the Point Concepcion–Gaviota region but extends intermittently north to Point Sal and east to Santa Barbara.

The Tecolote member is of Wisconsin age, as shown by radiocarbon dates (Fig. 2), ranging from 12,500 years B. P.[1] to beyond 30,000 years B. P. (Orr, 1956a).

Radiocarbon places only a minimum age (>33,000) on the Fox member; since the 30,000 year date is from the mid-Tecolote, the top of the Fox is probably beyond the range of radiocarbon.

The vertebrate fossils are of little help in determining age, as they are unique forms. The invertebrate fossils (Table 1) are of existing species from a cool-water habitat, comparable to that of Point Concepcion-Monterey today, and therefore are of little value. At first thought the cool-water forms suggest glacial conditions, but our knowledge of glacial or interglacial ocean currents and upwelling is incomplete.

It seems likely, therefore, that the higher-than-present wave-cut platforms were the result of either interstadial or interglacial high sea stands during periods of relatively warm climate; as the writer knows of no world-wide evidence to show a higher-than-present interstadial sea stand, he assumes that these wave-cut platforms are of interglacial age and probably reflect fluctuations in sea level during the relatively long Sangamon Interglacial. He therefore assigns a Wisconsin age to the Tecolote member and tentatively a Sangamon Interglacial age to the Fox and Garanon platforms and their members.

[1] Since this was written a preliminary date of 10,400 ± 2000 years B. P. has been measured by Lamont on an insufficient charcoal sample lying in contact with human bone 32 feet below the surface in the Santa Rosa Island formation. This measurement represents the latest date so far secured for coastal Pleistocene deposits, and the earliest date for positive human remains, as distinguished from "evidence" of the presence of man in the Pleistocene on the Pacific Coast.

Acknowledgments

This study is the partial result of 12 seasons of work on Santa Rosa Island, under the leadership of the writer, carried out by the Department of Geology and Anthropology of the Santa Barbara Museum of Natural History, and assisted by the Western Speleological Institute. Among the many people to whom acknowledgment is due are Mr. Ed Vail, representing the owners of the island, who so kindly granted permission to work there; Mr. Harold S. Chase, President of the Santa Barbara Museum of Natural History, and Mr. O. H. Truman, President of the Western Speleological Institute, who have provided funds for the expeditions; Dr. Wallace S. Broecker, Lamont Geological Observatory, who has provided the radiocarbon dates used in the study; Dr. Allyn Smith, California Academy of Sciences, who identified the fossil shells; Wilbur A. Davis, John C. Tyler, Mrs. Louise G. Reid, and Dr. V.

PLATE 1.—NORTHWEST COAST OF SANTA ROSA ISLAND

FIGURE 1.—View showing the "Malibu" terrace in background and the "Dume" terrace with Santa Rosa Island formation in foreground.

FIGURE 2.—Aerial view looking south, with sea cliffs of the Santa Rosa Island formation in foreground, the "Malibu" terrace mid-distance, and the 1000-foot terrace in the distance. Tecolote and Tecolokito canyons in center, Skull Gulch to the right.

FIGURE 1

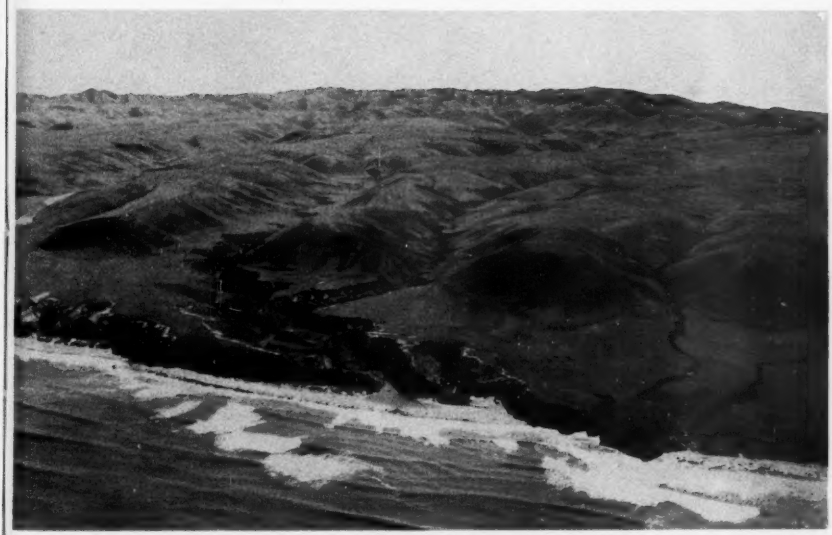

FIGURE 2

NORTHWEST COAST OF SANTA ROSA ISLAND

L. Van
prepara

Bremne
Isla
Sar
no.
Broecke
nat
n. s
Broecke
carl
Bor
100
Chaney,
A
Cal
pale
Was
— 193
posi
tion
Car
79
Davis, W
Mor
Ame
Emery,
terra
ica

L. VanderHoof, who have aided in field work and preparations of maps and manuscript.

References Cited

Bremner, Carl St. J., 1932, Geology of Santa Cruz Island, Santa Barbara County, California: Santa Barbara Mu. Nat. History Occ. Papers, no. 1, p. 5–33

Broecker, W. S., and Kulp, J. L., 1957, Lamont natural radiocarbon measurements IV: Science, n. ser, v. 126, p. 1324–1334

Broecker, W. S., and Orr, Phil C., 1958, Radiocarbon chronology of Lake Lahontan and Lake Bonneville: Geol. Soc. America Bull., v. 69, p. 1009–1032

Chaney, Ralph W., and Mason, Herbert L., 1934a, A Pleistocene flora from Santa Cruz Island, California; *in* Contributions to Pleistocene paleontology of California: Carnegie Inst. Washington Pub. 415-I, p. 1–24

—— 1934b, A Pleistocene flora from the asphalt deposits at Carpinteria, California; *in* Contributions to Pleistocene paleontology of California: Carnegie Inst. Washington Pub. 415-III, p. 45–79

Davis, W. M., 1933, Glacial epochs of the Santa Monica mountains, California: Bull., Geol. Soc. America, v. 44, p. 1041–1133

Emery, K. O., 1958, Shallow submerged marine terraces of southern California: Geol. Soc. America Bull., v. 69, p. 39–60

Lawson, A. C., 1893, The post-Pliocene diastrophism of the coast of southern California: Univ. Calif. Publ., Bull. Dept. Geol. Sci., v. 1, no. 4, p. 115–160

Orr, Phil C., 1956a, Radiocarbon dates from Santa Rosa Island, I: Santa Barbara Mus. of Nat. Hist., Dept. Anthro., Bull. no. 2, p. 1–9.

—— 1956b, Dwarf mammoths and man on Santa Rosa Island: Univ. Utah Anthro. Papers no. 26, p. 74–81

—— 1956c, Radiocarbon, mammoths and man on Santa Rosa Island (Abstract): Geol. Soc. America Bull., v. 67, p. 1777

Orr, Phil C., and Broecker, W. S., 1957, Sea-leve changes on Santa Rosa Island, California (Abstract): Geol. Soc. America Bull., v. 68, p. 1840

Smith, W. S. T., 1902, A topographic study of the islands of southern California: Univ. Calif. Pub., Bull. Dept. Geol. Sci., v. 2, no. 7, p. 179–230

Upson, J. E., 1951, Former marine shore lines of the Gaviota quadrangle, Santa Barbara County, California: Jour. Geology v. 59, p. 415–446

SANTA BARBARA MUSEUM OF NATURAL HISTORY, SANTA BARBARA, CALIF.

MANUSCRIPT RECEIVED BY THE SECRETARY OF THE SOCIETY, JUNE 17, 1959

SANTA BARBARA MUSEUM OF NATURAL HISTORY CONTRIBUTION NO. 1

WESTERN SPELEOLOGICAL INSTITUTE, CONTRIBUTION NO. 15

65. Floo
and
He
66. Stru
Ei
67. Bibl
St
Ne
$6.
Co

1. Stra
2. Pale
3. Evol
4. Geol
5. Stru
8. The
12. Revi
13. Penn
1 fi
14. Brac
15. Tung
16. Eoce
1 fi
18. Line
(Li
21. Origi
25. Evol
26. Bibli
27. Prop
28. Origi
34. Perm
37. Bibli
38. Lowe
39. Sedi
40. Revi
41. Amer
42. Maqu
43. 1940
45. Inte
47. Inte
48. Nort
51. Cata
52. Selec
53. Pale
54. Biost
55. Trilo
1 fi
56. Nort
figs
57. Bibli
61. Strat
$3.0
64. Sunk
65. Hane
66. Ceno
67. Trea
Vo
68. Beek
69. Genu
70. *Fenes*
72. Coas
73. Meta
$4.5
74. Origi
Tut
75. Selec
76. Type
Col
77. Rela
2 pl
78. Moll
$4.5
79. Rock
80. Still
$5.5

65. Floors of the Oceans, I: North Atlantic. Part 1. Physiographic Diagram of the North Atlantic. By Bruce C. Heezen and Marie Tharp. 1958. In color; 54 by 27½ inches. $1.50. Part 2. Text to Accompany Physiographic Diagram. By Bruce Heezen *et al.* 1959. 122 p., 30 pls., 49 figs. $4.50.
66. Structural Conversions in Crystalline Systems and Their Importance for Geological Problems. Wilhelm Eitel. 1958. 178 p., 93 figs., 2 pls. $3.00.
67. Bibliography and Index of Literature on Uranium and Thorium and Radioactive Occurrences in the United States. Part 5. Connecticut, Delaware, Illinois, Indiana, Maine, Maryland, Massachusetts, Michigan, New Hampshire, New Jersey, New York, Ohio, Pennsylvania, Rhode Island, Vermont, and Wisconsin. Margaret Cooper. 1958. 472 p. $6.75. (Also available: Part 1. Ariz., Nev., N. Mex., 25 cents; Part 2. Calif., Idaho, Mont., Wash., Wyo., 25 cents; Part 3. Colo., Utah, 50 cents; Part 4. Mid-Continent, 50 cents)

MEMOIRS

1. Stratigraphy of Western Newfoundland. Charles Schuchert and C. O. Dunbar. 1934. 123 p., 11 pls., 8 figs. $2.40.
2. Paleozoic Plankton of North America. Rudolf Ruedemann. 1934. 141 p., 26 pls., 6 figs. $2.40.
3. Evolution of the Congo Basin. A. C. Veatch. 1935. 183 p., 10 pls., 8 figs. $2.10.
4. Geology in the Coastal Atlas of Western Algeria. R. Van V. Anderson. 1936. 450 p., 19 pls., 2 figs. $4.20.
5. Structural Behavior of Igneous Rocks. By Robert Balk. 1937. 177 p., 24 pls., 38 figs. $4.00.
8. The Universal Stage. By R. C. Emmons. 1943. 206 p., 13 pls., 95 figs. $4.00.
12. Revision of the Upper Cambrian Fauna of New Jersey. B. F. Howell. 1945. 47 p., 8 pls., $1.00.
13. Pennsylvanian Geology of a Part of the Southern Appalachian Coal Field. H. R. Wanless. 1945. 162 p., 40 pls., 1 fig. $3.90.
14. Brachiopoda of the Independence Shale. M. A. Stainbrook. 1945. 76 p., 6 pls., 2 figs. $1.20.
15. Tungsten Mineralization in the United States. P. F. Kerr. 1946. 241 p., 23 pls., 34 figs. $3.50.
16. Eocene Faunas from the Department of Bolivar, Columbia. B. L. Clark and J. W. Durham. 1946. 126 p., 28 pls., 1 fig. $2.10.
18. Lineation: A Critical Review and Annotated Bibliography. Ernst Cloos. 1946. 122 p., 10 pls., 15 figs. Supplement (Literature for 1942–1952), 16 pages, 1953. Reprinted 1957 as one volume, $2.00.
21. Origin and Development of Craters. T. A. Jaggar. 1947. 508 p., 87 pls., 14 figs. $6.00.
25. Evolution of the Horse Brain. Tilly Edinger. 1948. 177 p., 4 pls., 24 figs. $2.00.
26. Bibliographic Index of Permian Invertebrates. C. C. Branson. 1948. 1049 p. $9.50.
27. Propagation of Sound in the Ocean. J. L. Worzel, Maurice Ewing, C. L. Pekeris. 1948. 205 p., 23 pls., 89 figs. $2.75.
29. Origin of Granite (Conference). James Gilluly, *Chairman*. 1948. 139 p., 13 pls., 5 figs. $1.80.
34. Permian Crinoid Calceolispongia. Curt Teichert. 1949. 132 p., 26 pls., 24 figs. $2.50.
37. Bibliography of Fossil Vertebrates, 1939–1943. C. L. Camp, S. P. Welles, and Morton Green. 1949. 371 p., $4.50.
38. Lower Cretaceous Stratigraphy in Southeastern Arizona. Alexander Stoyanow. 1949. 169 p., 27 pls., 2 figs. $2.50.
39. Sedimentary Facies in Geologic History. C. R. Longwell, *Chairman*. 1949. 171 p. $1.75.
40. Revision of the Families and Genera of the Devonian Tetracorals. E. C. Stumm. 1949. 92 p., 25 pls. $2.00.
41. American Permian Nautiloids. A. K. Miller and Walter Youngquist. 1949. 218 p., 59 pls., 39 figs. $3.60.
42. Maquoketa Brachiopoda of Iowa. Y. Wang. 1950. 55 p., 12 pls. $1.40.
43. 1940 E. W. Scripps Cruise to Gulf of California. C. A. Anderson *et al.* 1950. 362 p., 65 pls., 28 figs. $6.50.
45. Interpretation of Ore Textures. E. S. Bastin. 1950. 101 p., 28 figs. $1.75.
47. Interpretation of Aeromagnetic Maps. V. Vacquier *et al.* 1951. 151 p., 14 pls., 83 figs. $2.25.
48. North American Geosynclines. Marshall Kay. 1951. 143 p., 16 pls., 20 figs. $2.00.
51. Catalogue of the Cenozoic Plants of North America through 1950. Robert S. LaMotte. 1952. 381 p., 5 figs. $5.50.
52. Selected Petrogenic Relationships of Plagioclase. R. C. Emmons, *Editor*. 1953. 142 p., 38 figs., 16 pls. $2.00.
53. Paleozoic and Mesozoic Arachnida of Europe, Alexander Petrunkevitch. 1953. 128 p., 58 pls. $3.00.
54. Biostratigraphy of the Maqfi Section, Egypt. L. W. LeRoy. 1953. 73 p., 4 figs., 14 pls. $1.75.
55. Trilobites from the Lower Champlainian Formations of the Appalachian Valley. Byron N. Cooper. 1953. 68 p., 1 fig., 19 pls. $1.75.
56. North American and European Stropheodontids: Morphology and Systematics. Alwyn Williams. 1953. 67 p., 5 figs., 13 pls. $1.50.
57. Bibliography of Fossil Vertebrates. 1944–1948. C. L. Camp, *et al.* 1953. 465 pp. $5.50.
61. Stratigraphy and History of the Moenkopi Formation of Triassic Age. E. D. McKee. 1954. 133 p., 19 figs., 12 pls. $3.00.
64. Sunken Islands of the Mid Pacific Mountains. E. L. Hamilton. 1956. 97 p., 12 figs., 13 pls. $2.50.
65. Handbook of South American Geology. W. F. Jenks, *Editor*. 1956. 378 p., 13 figs., 11 pls. $5.50.
66. Cenozoic Foraminifera from Micronesia. Shoshiro Hanzawa. 1957. 163 p., 12 figs., 41 pls. $4.50.
67. Treatise on Marine Ecology and Paleoecology. Volume 1. Ecology. Joe W. Hedgpeth, *Editor*. 1957. 1296 p. $12.50. Volume 2. Paleoecology. Harry S. Ladd, *Editor*. 1957. 1078 p. $10.00.
68. Beekmantown Group (Lower Ordovician) of Maryland. William J. Sando. 1957. 162 p., 20 figs., 15 pls. $5.00.
69. Genus *Pentremites* and its Species. J. J. Galloway and H. V. Kaska. 1957. 104 p., 5 figs., 13 pls. $2.50.
70. *Fenestella* from the Permian of West Texas. M. K. Elias and G. E. Condra. 1957. 158 p., 17 figs., 23 pls. $3.50.
72. Coastal Sand Dunes of Oregon and Washington. William S. Cooper. 1958. 170 p., 12 figs., 22 pls. $3.50.
73. Metamorphic Reactions and Metamorphic Facies. W. S. Fyfe, F. J. Turner, and J. Verhoogen. 1958. 260 p., 108 figs. $4.50.
74. Origin of Granite in the Light of Experimental Studies in the System $NaAlSi_3O_8$—$KAlSi_3O_8$—SiO_2—H_2O. O. F. Tuttle and N. L. Bowen. 1958. 154 p., 67 figs., 6 pls. $3.75.
75. Selected Bibliographies of Hydrothermal and Magmatic Mineral Deposits. John Drew Ridge. 1958. 200 p. $3.75.
76. Type Specimens of Marine Mollusca Described by P. P. Carpenter from the West Coast (San Diego to British Columbia). K. V. W. Palmer. 1958. 376 p., 35 pls. $7.50.
77. Relation of Ore Deposition to Doming in the North American Cordillera. Edward Wisser. 1960. 118 p., 34 figs., 2 pls. $4.00.
78. Molluscan Faunas of the Flagstaff Formation of Central Utah. Aurèle La Rocque. 1960. 100 p., 2 figs., 4 pls. $4.50.
79. Rock Deformation. David Griggs and John Handin, *Editors*. 1960. 382 p., 40 pls., many line illustrations. $12.00.
80. Stillwater Igneous Complex: A Quantitative Mineralogical Study. Harry H. Hess. 1960. 230 p., 12 pls., 42 figs. $5.50.

Publications of The Geological Society of America

Publications currently in stock may be purchased at prices indicated below, on order accompanied by remittance addres to The Geological Society of America, 419 West 117 Street, New York 27, N. Y. Consult lists on current Bulletins to assured that items of interest are in stock.

BULLETIN

Monthly. Advance subscription, $15 per year; separate number $1.50; back yearly volumes, as available: prior to 1935, $12 per volume; 1935–, $15.00 per volume. Ten-year indexes covering vols. 31–40, 41–50, $1.50 per copy; covering vols. 51– $1.00 per copy.

GUIDEBOOKS FOR ANNUAL MEETING FIELD TRIPS

GUIDES TO SOUTHEASTERN GEOLOGY. (New Orleans). Richard J. Russell, *Editor*. November 1955. $3.00.
GUIDEBOOK FOR FIELD TRIPS. (Minneapolis). G. M. Schwartz, *Editor*. November 1956. $4.00.
GUIDEBOOK FOR FIELD TRIPS. (Atlantic City). Erling Dorf, *Editor*. November 1957. $2.75.
GUIDEBOOK FOR FIELD TRIPS. (Pittsburgh). Field Trip Committee. November 1959. $2.00.

VOLUMES IN ENGINEERING GEOLOGY

APPLICATION OF GEOLOGY TO ENGINEERING PRACTICE, Sidney Paige, *Chairman* (Berkey Volume). By 18 Authors (13 papers 1951, 327 p. $2.75.
ENGINEERING GEOLOGY CASE HISTORIES, P. D. Trask, *Editor*, No. 1, 66 p., 1957. $1.00; No. 2, 48 p., 1958, $1.00; No. 3, 76 p. 1959, $1.00.
TEACHING AIDS AND ALLIED MATERIALS, G. A. Kiersch, *Chairman*, 36 p., 1957. 75 cents.

PENROSE VOLUME

LIFE AND LETTERS OF R. A. PENROSE, JR., H. R. Fairbanks and C. P. Berkey. 1952. 765 p. $4.00.

BIBLIOGRAPHY OF GEOLOGY EXCLUSIVE OF NORTH AMERICA

Annually, 1933–1940; biennially, 1941–1946; annually, 1947–. By Marie Siegrist, Marcia Lakeman, and Mary Grier. Vols. 1– inclusive, $2.50 per volume; Volumes 8–12 out of stock; Volume 13, $3.25; Volume 14, $3.00; Volume 15, $3.00; Volume 1 $4.50; Volume 17, $5.75; Volume 18, $5.50; Volume 19, $7.50; Volume 20, $8.00; Volume 21, $10.00; Volume 22, $10.00.

SPECIAL COLORED MAPS

GLACIAL MAP OF NORTH AMERICA. (Special Paper 60). By Committee on Glacial Map. R. F. Flint, *Chairman*. 1945. $2.00
GLACIAL MAP OF THE UNITED STATES EAST OF THE ROCKY MOUNTAINS. By Committee of National Research Council. R. F. Flint, *Chairman*. 1959. $6.00.
TECTONIC MAP OF CANADA. By Geological Association of Canada. 1950. $1.50.
PLEISTOCENE EOLIAN DEPOSITS OF THE UNITED STATES, ALASKA, AND PARTS OF CANADA. James Thorp and H. T. U. Smith, *Cochairmen*. 1952. $3.00.

ROCK-COLORED CHARTS

Prepared by Committee of National Research Council. $7.00 per set.

TREATISE ON INVERTEBRATE PALEONTOLOGY

Raymond C. Moore, *Editor*

Part D. PROTISTA 3. Chiefly Radiolarians and Tintinnines). By A. S. Campbell and R. C. Moore. 1955. 195 p., 92 figs. $3.00.
Part E. ARCHAEOCYATHA AND PORIFERA. By V. J. Okulitch and M. W. de Laubenfels. 1955. 122 p., 88 figs. $3.00.
Part F. COELENTERATA. By F. M. Bayer *et al.* 1956. 498 p., 358 figs. $7.00.
Part G. BRYOZOA. By Ray S. Bassler. 1954. 253 p., 175 figs. $3.00.
Part L. MOLLUSCA 4 (CEPHALOPODA; AMMONOIDEA). By W. J. Arkell *et al.* 1957. 490 p., 588 figs. $8.50.
Part O. ARTHROPODA 1 (TRILOBITOMORPHS). By 18 authors. 1959. 560 p., 415 figs. $10.50.
Part P. ARTHROPODA 2 (CHELICERATA, PYCNOGONIDA, PALAEOISOPUS). By L. Störmer, A. Petrunkevitch, J. W. Hedgpeth, 1956. 181 p., 123 figs. $3.50.
Part V. GRAPTOLITHINA. By O. M. B. Bulman. 1955. 101 p., 72 figs. $3.00.

SPECIAL PAPERS

1. BIBLIOGRAPHY AND INDEX OF PALEOZOIC OSTRACODA. R. S. Bassler and Betty Kellet. 1934, 500 p., 24 figs. $3.00.
2. FOSSIL CRUSTACEA OF THE ATLANTIC AND GULF COASTAL PLAIN. M. J. Rathbun. 1935. 160 p., 26 pls., 2 figs. $1.50.
3. FOSSIL NON-MARINE MOLLUSCA OF NORTH AMERICA. Junius Henderson. 1935. 313 p. $2.10.
5. GEOLOGY OF SAINT JOHNS, NEW BRUNSWICK. A. O. Hayes and B. F. Howell. 1937. 146 p., 9 pls., 4 figs. $1.50.
7. ATLANTIC SUBMARINE VALLEYS OF THE UNITED STATES AND THE CONGO SUBMARINE VALLEY. A. C. Veatch and Paul A. Smith. 1939. 101 p., 5 charts, 10 pls., 28 figs. $4.80.
11. GEOLOGY AND PALEONTOLOGY OF THE MINGAN ISLANDS, QUEBEC. W. H. Twenhofel. 1938. 132 p., 24 pls., 1 fig. $1.50.
12. TERTIARY FLORA FROM THE RIO PICHILEUFU, ARGENTINA. E. W. Berry. 1938. 149 p., 56 pls., 11 figs. $2.10.
21. PALEONTOLOGY AND STRATIGRAPHY OF THE SILURIAN ROCKS OF THE PORT DANIEL BLACK CAPE REGION, GASPE. S. A. Northrop. 1939. 302 p., 28 pls., 1 fig. $3.00.
28. REVIEW OF THE PELYCOSAURIA. A. S. Romer and L. I. Price. 1949. 538 p., 46 pls., 71 figs. $4.20.
29. PHACOPID TRILOBITES OF NORTH AMERICA. D. M. Delo. 1940. 135 p., 13 pls., $1.20.
33. NUMERICAL STRUCTURE FACTOR TABLES. M. J. Buerger. Reprinted 1953. 119 p., 4 figs. (Cloth bound) $1.50.
37. OZARKIAN AND CANADIAN CEPHALOPODS, Part I, Nautilicones. E. O. Ulrich, Aug. F. Foerste, A. K. Miller and W. M. Furnish. 1942. 157 p., 57 pls., 23 figs. $2.40.
40. HADROSAURIAN DINOSAURS OF NORTH AMERICA. R. S. Lull and N. E. Wright. 1942. 242 p., 31 pls., 90 figs. $2.70.
49. OZARKIAN AND CANADIAN CEPHALOPODS. Part II: Brevicones. E. O. Ulrich, A. F. Foerste, and A. K. Miller. 1943. 240 p., 70 pls., 15 figs. $3.00.
60. GLACIAL MAP OF NORTH AMERICA. By Committee on Glacial Map. R. F. Flint, *Chairman*. 1945. $2.00.
62. CRUST OF THE EARTH. Arie Poldervaart, *Editor*. 1955. 762 p. $6.50.
63. DE NATURA FOSSILIUM, by Georgius Agricola. Translated by M. C. Bandy and J. A. Bandy. 1955. 240 p. $3.00.
64. MARYSVALE, UTAH, URANIUM AREA. Paul F. Kerr *et al.* 1957. 212 p., 21 pls., 106 figs. $6.00.

(*Continued on inside back cover*)